

EGAS



LATVIJAS
UNIVERSITĀTE
ANNO 1919

UNIVERSITY OF LATVIA

47th Conference of the European
Group on Atomic Systems



Riga – Latvia

July 14–17, 2015

Book of Abstracts

Institutional support



Exhibitors



Book of Abstracts



47th Conference of the European
Group on Atomic Systems

Riga – Latvia

July 14–17, 2015

Volume Editors

Marcis Auzinsh (Chairman)

Jānis Stonis

Andra Damberga

Alīna Gržibovska

Arnis Voitkāns

Volume number: 39D

ISBN 2-914771-97-5

Published by University of Latvia Press

Managing Editor: Patricia Helfenstein

Contact for the EGAS 47 conference

Mārcis Auziņš

Chair of Experimental Physics

University of Latvia

19 Raina Blvd, Riga, LV-1586, Latvia

marcis.auzins@lu.lv

Copyright and cataloging information

© 2015, European Physical Society.

Reproduction rights reserved.

Europhysics Conference Abstracts are published by the European Physical Society. This volume is published under the copyright of the European Physical Society. We wish to inform the authors that the transfer of the copyright to the EPS should not prevent an author to publish an article in a journal quoting the original first publication or to use the same abstract for another conference. The copyright is just to protect the EPS against using the same material in similar publications. This book is not a formal publication. The summaries of talks contained in it have been submitted by the authors for the convenience of participants in the meeting and of other interested persons. The summaries should not be quoted in the literature, nor may they be reproduced in abstracting journals or similar publications, since they do not necessarily relate to work intended for publication. Data contained in the summaries may be quoted only with the permission of the authors.

This book contains all abstracts accepted as of June 1, 2015. The contributions are identified by

PL for Plenary Lecture

PA for Parallel sessions

IT for Invited Talk

CT for Contributed Talk

P for posters

Local Organizing Committee

Marcis Auzinsh (Chairman), marcis.auzins@lu.lv
Jānis Stonis, janis.stonis@lu.lv
Ruvins Ferbers, ruvins.ferbers@lu.lv
Ilze Klincāre, ilze.klincare@lu.lv
Andra Damberga, andra.damberga@lu.lv

Alīna Gržibovska, aline.grzibovska@lu.lv
Māris Tamanis, maris.tamanis@lu.lv
Florians Gahbauers, florian.gahbauer@lu.lv
Vjačeslavs Kašcejevs, vjaceslavs.kascejevs@lu.lv

EGAS Board Members

EGAS stands for European Group on Atomic Systems, formerly known as European Group on Atomic Spectroscopy (name changed in 2004). EGAS is a section of the AMOPD (Atomic, Molecular and Optical Physics Division) of the EPS (European Physical Society). The board consists of the following 14 members. Check the EGAS website for more information: www.eps-egas.org



PROF. MARCIS AUZINSH
University of Latvia



PROF. HENRI BACHAU
Université de Bordeaux



PROF. PETER BARKER
(SECRETARY)
University College, London



DR. GLEB GRIBAKIN
Queen's University, Belfast



DR. WIM VASSEN
Vrije Universiteit,
Amsterdam



PROF. CHRISTIANE KOCH
University of Kassel



PD DR. JOSE R. CRESPO
LOPEZ-URRUTIA
MPI für Kernphysik,
Heidelberg



DR. LAURENCE PRUVOST
Université de Paris-Sud



PROF. XAVIER URBAIN
Université
Catholique de Louvain



PROF. ANTOINE WEIS
(WEBMASTER)
University of Fribourg



PROF. ROLAND WESTER
(CHAIR)
Universität Innsbruck



PROF. PÄIVI TÖRMÄ
Aalto University



DR. THOMAS UDEM
Max-Planck-Institut für
Quantenoptik



PROF. FRANCESCO
CATALIOTTI
Università degli Studi di
Firenze



DR. ALEXEI
GRUM-GRZHIMAILO
Lomonosov Moscow State
University

Contents

Plenary lectures	13
PL-1 <i>M. Berry</i>	
The singularities of light: intensity, phase, polarization	14
PL-2 <i>R. Celestrino Teixeira, C. Hermann-Avigliano, T. L. Nguyen, T. Cantat-Moltrecht, I. Dotsenko, S. Gleyzes, S. Haroche, M. Brune, and J. M. Raimond</i>	
Microwave Spectroscopy probes	
Dipole Blockade and van der Waals Forces	
in a cold Rydberg Gas	15
PL-3 <i>M. Simon</i>	
Relaxation dynamics of isolated atoms and molecules in the tender x-ray domain (1-12 keV)	16
PL-4 <i>M. S. Safronova</i>	
Search for New Physics with Atoms and Molecules	17
PL-5 <i>Y. Silberberg</i>	
Quantum Walks in Photonic Lattices	18
PL-6 <i>F. Ferlaino</i>	
The Fascination of Lanthanides as Ultracold Quantum Matter	19
PL-7 <i>S. Schlemmer, O. Asvany, S. Brünken, and P. Jusko</i>	
Spectroscopy of Cold Molecular Ions	20
PL-8 <i>D. Budker</i>	
Fundamental symmetries and the Dark Sector	21
PL-9 <i>G. M. Tino</i>	
Precision measurements in gravitational physics with cold atom interferometry	22
PL-10 <i>M. G. Kozlov</i>	
Using atoms and molecules to search for variation of fundamental constants . .	23
Invited talks	25
IT-1 <i>R. Moszynski, W. Skomorowski, B. H. McGuyer, and T. Zelevinsky</i>	
Asymptotic physics with subradiant	
and superradiant states of ultracold molecules	26
IT-2 <i>M. Germann, G. Hegi, K. Najafian, X. Tong, and S. Willitsch</i>	
Observation of forbidden infrared spectra in Coulomb-crystallized molecular ions: Towards precision measurements on single molecules	27
IT-3 <i>G. Clos, M. Enderlein, U. Warring, T. Schaetz, and D. Leibfried</i>	
Decoherence-Assisted Spectroscopy:	
Demonstrated with a Single Mg ⁺ Ion	28
IT-4 <i>B. Bylicka, D. Chruściński, M. Tukiainen, J. Piilo, and S. Maniscalco</i>	
Thermodynamic meaning and power of non-Markovianity	29
IT-5 <i>A. Laliotis, J. C. de Aquino Carvalho, T. Passerat de Silans, P. Chaves de Souza Segundo, I. Maurin, M. Ducloy, and D. Bloch</i>	
Atom in front of a hot surface: Temperature-dependence of the Casimir-Polder interaction and thermal energy transfer	30
Contributed talks	31
CT-1 <i>A. Mooser, C. Smorra, K. Blaum, K. Franke, T. Higuchi, N. Leefer, Y. Matsuda, H. Nagahama, W. Quint, G. Scheider, J. Walz, Y. Yamazaki, and S. Ulmer</i>	
The Magnetic Moments of the Proton and the Antiproton	32

CT-2	<i>D. Bresteau, C. Drag, and C. Blondel</i> Intra-cavity photodetachment microscopy and the electron affinity of germanium	33
CT-3	<i>M. Tajima, N. Kuroda, S. Van Gorp, Y. Nagata, P. Dupré, D. J. Murtagh, B. Radics, H. A. Torii, H. Higaki, B. Horst, Y. Kanai, Y. Matsuda, S. Ulmer, Y. Yamazaki</i> Antihydrogen synthesis with lower energy antiprotons in the ASACUSA double- cusp trap	34
CT-4	<i>M. Zientkiewicz, K. Pachucki</i> High precision calculations for excited states of the hydrogen molecule	35
CT-5	<i>E. Lorek, E. Mårzell, A. Losquin, M. Miranda, A. Harth, C. Guo, R. Svärd, C. Arnold, A. L’Huillier, A. Mikkelsen, and J. Mauritsson</i> Probing ultra-fast nearfield dynamics of individual nano bowtie-antennas	36
CT-6	<i>S. Carlström, J. Preclíková, E. W. Larsen, E. Lorek, S. Bengtsson, C. M. Heyl, D. Paleček, A. L’Huillier, D. Zigmantas, K. J. Schafer, and J. Mauritsson</i> Quantum Path Interferometry using Chirped High-order Harmonic Generation	37
CT-7	<i>M. Génévriez, X. Urbain, A. Cyr, K. M. Dunseath, M. Terao-Dunseath</i> The two-photon detachment of O^-	38
CT-8	<i>Z.-K. Hu, M.-K. Zhou, L.-L. Chen, X.-C. Duan, and Q. Luo</i> Characterizing an ultra-high sensitivity atom interferometry gravimeter	39
CT-9	<i>C. C. Kwong, T. Yang, D. Delande, R. Pierrat, and D. Wilkowski</i> High repetition rate pulse trains emitted by optically thick scattering media	40
CT-10	<i>J. Ulmanis, S. Häfner, R. Pires, E. D. Kuhnle, and M. Weidemüller</i> Heteronuclear Efimov scenario in an ultracold Bose-Fermi mixture of ^{133}Cs and ^6Li	41
CT-11	<i>J. R. Almond, J. S. Bumby, J. Lim, N. J. Fitch, B. E. Sauer, M. R. Tarbutt, and E. A. Hinds</i> Towards a molecular MOT of YbF	42
CT-12	<i>E. Widmann, A. Capon, P. Caradonna, M. Diermaier, B. Kolbinger, S. Lehner, C. Malbrunot, O. Massiczek, C. Sauerzopf, M. C. Simon, M. Wolf, and J. Zmeskal</i> Progress towards in-beam hyperfine spectroscopy of antihydrogen	43
CT-13	<i>J. Pedregosa-Gutierrez, C. Champenois, M. Knoop, L. Schmöger, and J. R. Crespo López-Urrutia</i> Phase transitions of sympathetic cooling of HCl ions	44
CT-14	<i>M. McDonald, B. H. McGuyer, G. Z. Iwata, M. G. Tarallo, A. T. Grier, T. Zelevin- sky, F. Apfelbeck, I. Majewska, W. Skomorowski, and R. Moszynski</i> Experiments with an ultracold molecular lattice clock: subradiance, forbidden transitions, and E1 / M1 / E2 photodissociation	45
CT-15	<i>S. Mannervik, E. Bäckström, D. Hanstorp, O. M. Hole, M. Kaminska, R. F. Nasci- mento, M. Blom, M. Björkhage, A. Källberg, P. Löfgren, P. Reinhed, S. Rosèn, A. Simonsson, R. D. Thomas, H. T. Schmidt, and H. Cederquist</i> Storing keV negative ions for hours: Lifetime measurements in new time domains	46
CT-16	<i>H. Joerg, Z.-K. Hu, H. Bekker, M. A. Bleszenohl, D Hollain, S. Fritzsche, A. Surzhykov, C. Shah, J. R. Crespo López-Urrutia, and S. Tashenov</i> Linear polarization of x-ray transitions due to dielectronic recombination in highly charged ions	47
CT-17	<i>A. Burchianti, G. Valtolina, E. Neri, K. Xhani, A. Trombettoni, A. Smerzi, M. In- guscio, M. Zaccanti, and G. Roati</i> Pushing a Fermi superfluid through a thin optical barrier: from coherent tun- neling to phase slips	48
CT-18	<i>M. S. Cherukattil, C. Lovecchio, M. Alì Khan, F. Caruso, and F. S. Cataliotti</i> Atom-Chip for Quantum Control	49
CT-19	<i>P. K. Molony, P. D. Gregory, A. Kumar, B. Lu, Z. Ji, M. P. Köppinger, C. Ruth Le Sueur, C. L. Blackley, J. M. Hutson, and S. L. Cornish</i> Creation of $^{87}\text{RbCs}$ molecules in the rovibrational ground state	50
CT-20	<i>D. Barredo, H. Labuhn, S. Ravets, T. Lahaye, and A. Browaeys</i> Engineering spin Hamiltonians with 2D arrays of single Rydberg atoms	51
CT-21	<i>P. D. Edmunds, P. F. Barker</i> Trapping ultracold argon atoms	52

CT-22	<i>Y. R. P. Sortais, S. Jennewein, N. Schilder, J.-J. Greffet, A. Browaeys</i> Measurement of the coherent optical response of a cold atomic ensemble in the presence of resonant dipole-dipole interactions	53
CT-23	<i>J. Millen, P. Z. G. Fonseca, T. Mavrogordatos, T. S. Monteiro, and P. F. Barker</i> Cavity cooling a single charged levitated nanosphere	54
CT-24	<i>J. Rodewald, N. Dörre, P. Geyer, U. Sezer, P. Haslinger, and M. Arndt</i> A time domain matter-wave interferometer for testing the mass limits of quantum mechanics	55
CT-25	<i>H. Ulbricht</i> Non-interferometric tests of Macroscopic Quantum Superposition	56
CT-26	<i>B. Fang, I. Dutta, D. Savoie, R. Geiger, C. L. Garrido Alzar, and A. Landragin</i> Continuous Cold-atom Gyroscope with 11 cm ² Sagnac Area at nrad/s Stability	57
CT-27	Cesium atomic magnetometers in experiment searching for a neutron electric dipole moment	58
CT-28	<i>J. Keaveney, M. A. Zentile, D. J. Whiting, E. Bimbard, C. S. Adams, and I. G. Hughes</i> Faraday filtering in atomic vapours: from Hamiltonian to application	59
CT-29	<i>S. Colombo, V. Lebedev, V. Dolgovskiy, Z. D. Grujić, and A. Weis</i> Anharmonic magnetic response of magnetic nanoparticles detected by atomic rf magnetometry	60
CT-30	<i>R. P. M. J. W. Notermans, R. J. Rengelink, W. Vassen</i> Pushing QED to the limit in the helium atom	61
CT-31	<i>L. Schmöger, O. O. Versolato, M. Schwarz, M. Kohnen, A. Windberger, B. Piest, S. Feuchtenbeiner, J. Pedregosa, T. Leopold, P. Micke, A. K. Hansen, T. M. Baumann, M. Drewsen, J. Ulrich, P. O. Schmidt, and J. R. Crespo López-Urrutia</i> Coulomb crystallization of highly charged ions	62
Posters		63
	Cold atoms and quantum gases	63
P-1	<i>C. Andreeva, A. Cinins, A. Ekers, A. Markovski, D. Tretyakov, V. M. Entin, I. Beterov, E. Yakshina, and I. I. Ryabtsev</i> Realization of radio-frequency assisted Förster resonances in an ensemble of a few cold Rb Rydberg atoms	64
P-2	<i>T. Andrijauskas, G. Juzeliūnas, and I. Spielman</i> Optical flux lattice using multi-frequency radiation	65
P-3	<i>B. Décamps, J. Alibert, and A. Gauguet</i> Dual-species BEC source: First step towards matter neutrality test with atom interferometry	66
P-4	<i>G. Dong</i> Hybrid dynamics of an optical field and a Bose-Einstein condensation	67
P-5	<i>R. Faoro, B. Pelle, A. Zuliani, P. Cheinet, E. Arimondo, and P. Pillet</i> Borromean three-body FRET in frozen Rydberg gases	68
P-6	<i>A. Dunning, R. Gregory, J. Bateman, M. Himsworth, and T. Freegarde</i> Interferometric laser cooling of atomic rubidium	69
P-7	<i>L. Del Bino, J. Catani, A. Fioretti, C. Gabbanini, S. Gozzini, M. Inguscio, G. Modugno, and E. Lucioni</i> Progress towards the realization of a quantum degenerate dipolar gas of dysprosium atoms	70
P-8	<i>A. S. Kuraptsev, I. M. Sokolov</i> Coherent light scattering from a disordered ensemble of cold atoms	71
P-9	<i>M. Lepers, O. Dulieu, and J.-F. Wyart</i> Proposal for laser-cooling of rare-earth ions	73

P-10	<u>H. Mas, S. Pandey, V. Bolpasi, K. Poullos, and W. von Klitzing</u> Towards a BEC in a time-averaged adiabatic potential ring waveguide	74
P-11	<u>J. Ruauvel, C. Cabrera-Gutiérrez, M. Jacquy, B. Viaris de Lesegno, and L. Pruvost</u> Dense and cold atomic beam delivered by a 2DMOT repumped and channelled by a Laguerre-Gaussian laser beam	75
P-12	<u>M. Robert-de-Saint-Vincent, E. Maréchal, L. Vernac, O. Gorceix, and B. Laburthe-Tolra</u> Spinor quantum gases with narrow-line control	76
P-13	<u>M. Zeppenfeld, R. Glöckner, A. Prehn, M. Ibrügger, and G. Rempe</u> Rotational State Cooling of Trapped Polyatomic Molecules	77
P-87	<u>W. Yan, S. Bade, M.-A. Buchet, A. Landragin, and C. L. Garrido Alzar</u> Atom chip based guided atom interferometer for rotation sensing	78
Fundamental physics with atoms/molecules		79
P-14	<u>D. K. Efimov, N. N. Bezuglov, and G. Juzeliūnas</u> Description of the evolution of Rydberg systems and interaction of light with multi-level atoms using Floquet technique	80
P-15	<u>A. G. Araujo-Ferreira, T. J. Bonagamba, G. D. de Moraes Neto, M. H. Y. Moussa, and R. Auccaise</u> Generation of Schrödinger cat states in a NMR quadrupolar system	81
P-16	<u>N. A. Belov, Z. Harman</u> Pair creation and annihilation with atoms and channeling nuclei	82
P-17	<u>M. Auzinsh, A. Berzins, R. Ferber, F. Gahbauer, and U. Kalnins</u> Analysis of the spatial dependence of laser-induced fluorescence for alkali metal vapours in an intense laser beam	83
P-18	<u>T. Leopold, J. Rohlén, D. Hanstorp, J. Blahins, A. Apsitis, U. Berzins, and A. Ubelis</u> Designed of a pulsed negative ions source	84
P-19	<u>S. Pustelny, M. Auzinsh, L. Busaite, A. Akulshin, N. Leefer, and D. Budker</u> Nonlinear Magneto-Optical Rotation in Rubidium Vapor Excited to $6^2P_{1/2}$ State	85
P-20	<u>V. Buyadzi, O. Khetselius, A. Svinarenko, and T. Florko</u> Laser-gamma-nuclear spectroscopy of multicharged ions: “Shake-up” and co- operative excitation effects, New data	86
P-21	<u>S. Cohen, A. Dimitriou</u> Electron Spectroscopy of four-photon-ionized strontium in the 715-737 nm wave- length range	87
P-22	<u>P. Kalaitzis, E. Pavlou, A. Marciniak, T. Barillot, F. Lépine, C. Bordas, and S. Cohen</u> Two-photon Stark Spectroscopy and Photoionization Microscopy on the Mg atom	88
P-23	<u>X.-B. Deng, X.-C. Duan, M.-K. Zhou, H.-B. Yao, C.-G. Shao, and Z.-K. Hu</u> Test of the universality of free fall with atoms in different spin Orientations . .	89
P-24	<u>E. A. Dijck, A. Mohanty, N. Valappol, O. Böll, J. O. Grasdijk, A. T. Grier, S. Hoek- stra, K. Jungmann, M. Nuñez Portela, C. J. G. Onderwater, L. Willmann, and H. W. Wilschut</u> High precision spectroscopy of single $^{138}\text{Ba}^+$ ions	90
P-25	<u>E. Lamour, C. Prigent, J.-M. Ramillon, J.-P. Rozet, S. Steydli, M. Trassinelli, and D. Vernhet</u> High-resolution x-ray spectroscopy to probe quantum dynamics in collisions of $\text{Ar}^{17+,18+}$ ions with atoms and solids	91
P-26	<u>I. Fescenko, A. Weis</u> Imaging magnetic fields by fluorescence-detected magnetic resonance in polar- ized atoms	92
P-27	<u>L. Filippin, D. Baye, and M. Godefroid</u> Relativistic two-photon decay rates of hydrogenic atoms with the Lagrange-mesh method	93
P-28	<u>L. Filippin, J. Ekman, S. Fritzsche, M. Godefroid, P. Jönsson</u> Isotope shift parameters in Al I for the $3p - 4s$ and $3p - 3d$ lines	94

P-29	<u>A. Glushkov</u> Atomic and Nuclear quantum optics: Multiphoton and autoionization resonances in a strong DC electric and laser field	95
P-30	<u>J. O. Grasdijk, S. Zimmer, W. Heil, S. Karpuk, K. Tullney, Y. Sobolev, F. Allmendinger, U. Schmidt, K. Jungmann, L. Willmann, H.-J. Krausse, and A. Offenhauser</u> Search for the Permanent Electric Dipole Moment of Xenon.	96
P-31	<u>A. R. Swann, G. F. Gribakin</u> Quadratic-linear B-spline grid for studying Ps-atom interactions in cavities . .	97
P-32	<u>Z. D. Grujić, P. A. Koss, and A. Weis</u> An accurate free spin precession cesium magnetometer	98
P-33	<u>H. Aouchiche, N. Imadouchene, and C. Champion</u> Double ionization of the hydrogen sulfide molecule by electron impact: influence of the target orientation on the fivefold differential cross sections	99
P-34	<u>J. Fiedler, S. Scheel</u> Spectroscopic measurements of free particles by matter-wave interferometry . .	100
P-35	<u>M. R. Kamsap, C. Champenois, J. Pedregosa-Gutierrez, M. Houssin, D. Guyomarc'h, and M. Knoop</u> Fast transport and accumulation of cold ion clouds in a multi-zone RF-trap . .	101
P-36	<u>E. A. Konovalova, M. G. Kozlov</u> Precision calculation of the spectra of Mg-like ions	102
P-37	<u>G. Malcheva, L. Engström, H. Lundberg, H. Nilsson, H. Hartman, K. Blagoev, P. Palmeri, and P. Quinet</u> Radiative Lifetimes and Transition Probabilities in Rh I	103
P-38	<u>L. Engström, H. Lundberg, H. Nilsson, and H. Hartman</u> Lifetimes and Transition Probabilities for High-Lying Levels in Astrophysically Interesting Atoms Using Multi-Photon Excitation	104
P-39	<u>A. Sargsyan, D. Sarkisyan, Y. Pashayan-Leroy, C. Leroy, S. Cartaleva, A. D. Wilson-Gordon, and M. Auzinsh</u> EIT resonance inverted in magnetic field by influence of the alignment effect .	105
P-40	<u>A. Tonoyan, A. Sargsyan, G. Hakhmyan, C. Leroy, Y. Pashayan-Leroy, and D. Sarkisyan</u> Study of atomic transitions of ^{39}K isotope on D_1 line in strong magnetic fields	106
P-41	<u>A. Amiryanyan, A. Sargsyan, A. Tonoyan, Y. Pashayan-Leroy, C. Leroy, and D. Sarkisyan</u> Study of Atomic Transitions of Rb D_2 line in Strong Transverse Magnetic Fields by an Optical Half-Wavelength Cell	107
P-42	<u>E. Mariotti, G. Bianchi, C. Marinelli, A. Vanella, L. Corradi, A. Dainelli, L. Marmugi, L. Ricci, A. Khanbekyan, L. Tomassetti, and R. Calabrese</u> The Radioactive Francium Magneto - Optical Trap in Legnaro: search for new lines in an isotopic series	108
P-43	<u>M. Nakamura, A. Ichimura</u> Double impulse effects during a collision of ions and diatomic molecules	109
P-44	<u>P. Micke, S. Bernitt, J. Harries, L. F. Buchauer, T. M. Bücking, S. Kühn, P. O. Schmidt, and J. R. Crespo López-Urrutia</u> A compact 0.74 T room temperature EBIT	110
P-45	<u>D. Oubaziz, C. Champion, M. A Quinto, and Z. Aitelhadjali</u> H $_2$ O double ionization induced by electron impact	111
P-46	<u>P. Rynkun, G. Gaigalas, P. Jönsson, Ch. Froese Fischer, M. Godefroid</u> Theoretical study of hyperfine structure of ground state in neutral Carbon . .	112
P-47	<u>P. Rynkun, G. Gaigalas, D. Kato, L. Radžiūtė, and P. Jönsson</u> Stark splitting effects for Er^{3+} in Er_2O_3	113
P-48	<u>D. O. Sabulsky, I. J. M. Barr, G. Barontini, Y.-H. Lien, E. A. Hinds</u> Towards a High Sensitivity Atom Accelerometer for Exploring Physics Beyond the Standard Model	114
P-49	<u>S. Bouazza, Ł. M. Sobolewski, J. Kwela</u> Reanalysis and semi-empirical predictions of the hyperfine structure of ^{123}Sb I	115

P-50	<i>V. Patkóš, J. Zamastil, and D. Šimsa</i> Calculation of Lamb shift for states with $j = 1/2$	116
P-51	<i>K. S. Tanaka, M. Aoki, H. Inuma, Y. Ikedo, K. Ishida, M. Iwasaki, K. Ueno, Y. Ueno, T. Okubo, T. Ogitsu, R. Kadono, O. Kamigaito, N. Kawamura, D. Kawall, S. Kanda, K. Kubo, A. Koda, K. M. Kojima, N. Saito, N. Sakamoto, K. Sasaki, K. Shimomura, M. Sugano, M. Tajima, D. Tomono, A. Toyoda, H. A. Torii, E. Torikai, K. Nagamine, K. Nishiyama, P. Strasser, Y. Higashi, T. Higuchi, Y. Fukao, Y. Fujiwara, Y. Matsuda, T. Mibe, Y. Miyake, T. Mizutani, M. Yoshida, and A. Yamamoto</i> Measurement of muonium hyperfine splitting at J-PARC	117
P-52	<i>A. V. Viatkina, M. G. Kozlov</i> Sensitivity of tunneling-rotational transitions in ethylene glycol to the variation of electron-to-proton mass ratio	118
P-53	<i>K. Pachucki, A. Wienczek</i> Nuclear polarizability effects in muonic deuterium	119
P-54	<i>S. Y. Yousif Al-Mulla</i> Spin Polarisation Exchange Scattering from Nickel and Iron	120
P-55	<i>A. Zapara, J. E. van den Berg, S. C. Mathavan, C. Meinema, and S. Hoekstra</i> Deceleration, cooling and trapping of heavy diatomic molecules	121
	High-resolution spectroscopy/Molecular physics	122
P-56	<i>I. Brice, J. Rutkis, I. Fescenko, Ch. Andreeva, and J. Alnis</i> Optical frequency measurement of Rb $5S-5P$ transition with a frequency comb	123
P-58	<i>Ch. Andreeva, D. V. Brazhnikov, V. M. Entin, M. Yu. Basalae, S. M. Ignatovich, I. I. Ryabtsev, A. V. Taichenachev, V. I. Yudin</i> Magneto-optical switch based on high-contrast electromagnetically induced absorption resonance	124
P-59	<i>C. Andreeva, A. Krasteva, S. Cartaleva, A. Sargsyan, D. Sarkisyan, and K. Nasyrov</i> High resolution spectroscopy of Cs atomic layers of nanometric and micrometric thickness	125
P-60	<i>H. Bekker, O. O. Versolato, A. Windberger, R. Schupp, P. O. Schmidt, J. Ullrich, and J. R. Crespo López-Urrutia</i> Identifications of EUV transitions in promethium-like Pt, Ir, Os, and Re	126
P-61	<i>A. Windberger, O. O. Versolato, H. Bekker, P. O. Schmidt, J. Ullrich, and J. R. Crespo López-Urrutia</i> Identifications of optical transitions in Ir ¹⁷⁺ for investigations of variations of fundamental constants	127
P-62	<i>I. Birzniece, O. Nikolayeva, M. Tamanis, and R. Ferber</i> The (2) ¹ Π state in KCs: Fourier-transform spectroscopy and potential construction	128
P-63	<i>G. Cerchiari, E. Jordan, and A. Kellerbauer</i> Towards atomic anion laser cooling	129
P-64	<i>J. Dembczyński, M. Elantkowska, and J. Ruczkowski</i> The effect of the isomeric state ^{229m} Th on the observed hyperfine structure pattern	130
P-65	<i>T. Gantner, X. Wu, S. Chervenkov, M. Zeppenfeld, and G. Rempe</i> Depletion spectroscopy and internal-state thermometry of buffer-gas-cooled polar molecules	131
P-66	<i>A. Glushkov, O. Khetselius, A. Kvasikova, and E. Ponomarenko</i> The Rayleigh and Raman scattering of light on metastable levels of diatomics: An advanced method and new data	132
P-67	<i>PAuthor I. G. Hughes, i.g.hughes@durham.ac.uk, C. S. Adams, E. Bimbard, J. Keaveney, D. J. Whiting, M. A. Zentile, A. Sargsyan, and D. Sarkisyan</i> Absolute absorption and dispersion in dense alkali-metal thermal vapours	133
P-68	<i>J. Lodewyck, J.-L. Robyr, S. Bilicki, E. Bookjans, and R. Le Targat</i> Strontium optical lattice clocks	134

P-69	<i>K. Alps, A. Kruzins, O. Nikolayeva, M. Tamanis, R. Ferber, A. V. Stolyarov, and E. A. Pazyuk</i> Study of $(3)^1\Pi$ and $(5)^1\Sigma^+$ states of RbCs based on $(3)^1\Pi \rightarrow (A - b)$ and $(5)^1\Sigma^+ \rightarrow (A - b)$ Fourier transform spectra analysis	135
P-70	<i>A. Kruzins, K. Alps, O. Docenko, I. Klincare, M. Tamanis, R. Ferber, E. A. Pazyuk, A. V. Stolyarov</i> Fourier transform spectroscopy and deperturbation analysis of the spin-orbit coupled $A^1\Sigma^+$ and $b^3\Pi$ states in RbCs	136
P-71	<i>A. Papoyan, A. Sargsyan, G. Hakhumyan, and D. Sarkisyan</i> Alkali atoms in a strong transverse magnetic field: “guiding” transitions foretell behavior of all transitions of D ₁ line	137
P-72	<i>A. Papoyan, S. Shmavonyan, A. Khanbekyan, A. Gogyan, and M. Movsisyan</i> Selective reflection from dense Rb ₂ molecular vapor	138
P-73	<i>F. Gebert, Y. Wan, F. Wolf, J. C. Heip, J. Berengut, C. Shi, and P. O. Schmidt</i> Precision isotope shift measurements of calcium ions using photon recoil spectroscopy	139
P-74	<i>K. Alps, A. Kruzins, M. Tamanis, R. Ferber, E. A. Pazyuk, and A. V. Stolyarov</i> Energies and radiative properties of the $A^1\Sigma^+ - b^3\Pi$ complex in KRb: towards optimal ground-state transfer ultracold molecules	140
P-75	<i>P. Kowalczyk, J. Szczepkowski, W. Jastrzebski, E. A. Pazyuk, and A. V. Stolyarov</i> Direct deperturbation analysis of the $A^1\Sigma^+ \sim b^3\Pi$ complex in LiCs based on polarization labelling spectroscopy and <i>ab initio</i> calculation	141
P-76	<i>K. Alps, A. Kruzins, M. Tamanis, R. Ferber, A. V. Stolyarov, and E. A. Pazyuk</i> High resolution study and deperturbation analysis of the $A^1\Sigma^+ - b^3\Pi$ complex in KRb	142
P-77	<i>Z. Uddin, I. A. Siddiqui, R. U. Rehamn, M. Jahangir, and L. Windholz</i> Progress in the classification of spectral lines of Praseodymium	143
P-78	<i>M. Zawada, P. Morzyński, M. Bober, A. Cygan, S. Wójtewicz, K. Bielska, P. Mastowski, D. Lisak, and R. Ciuryło</i> Optical lattice atomic clocks as a reference for spectroscopy	144
P-79	<i>F. Zeeshan, J. Hoszowska, L. Loperetti, and J.-Cl. Dousse</i> In-house XAS measurements using a von Hamos curved crystal spectrometer and an X-ray tube	145
	Mesoscopic quantum systems	146
P-80	<i>J. Klocans, E. Potanina, G. Barinova, and V. Kashcheyevs</i> Single-electron manipulation with resonant impurity states in silicon nanoelectronic circuits	147
	Photophysics of atoms and ions and AMO and FEL physics at large facilities	148
P-81	<i>M. Génévriez, X. Urbain</i> The photodetachment cross section of H ⁻ : an animated-crossed-beam measurement	149
P-82	<i>A. N. Grum-Grzhimailo, E. V. Gryzlova, E. I. Staroselskaya, J. Venzke, and K. Bartschat</i> Interference effects in one-photon and two-photon ionization by femtosecond VUV pulses due to an intermediate state	150
P-83	<i>A. Pelevkin, K. Miculis, A. Ubelis, N. S. Titova, and A. M. Starik</i> Photodissociation of oxygen molecules upon the absorption in Shumann-Runge bands in various environments: modeling study	151
P-84	<i>C. Shah, P. Amaro, R. Steinbrügge, C. Beilmann, S. Bernitt, S. Fritzsche, A. Surzhykov, J. R. Crespo López-Urrutia, S. Tashenov</i> Complete measurements of anisotropic x-ray emission following recombination of highly charged ions	152
	Quantum optics/information including cold ions	153

P-85	<i>V. Buyadzhi, A. Glushkov, G. Prepelitsa, and V. Ternovsky</i> Nonlinear optics and dynamics of atoms, molecules in an electromagnetic field and laser systems with elements of a chaos	154
P-86	<i>H. R. Hamedí, G. Juzeliūnas</i> Transient switching of the Kerr nonlinearity and effect of Doppler broadening in a five-level Quantum system	155
P-88	<i>R. A. Nyman, J. Marelic</i> BEC of photons in a dye-filled microcavity: inhomogeneities, coherence and interactions	156
Ultrafast processes	157
P-89	<i>Chr. Papadopoulou, S. Kaziannis, and C. Kosmidis</i> Investigation of the H- (D-) loss from toluene's isotopologues in the fs timescale	158
Applications of AMO Physics: Astrophysics, sensors, plasma physics,	159
P-57	<i>J. Alnis, Z. Gavare, A. Abola, V. Fyodorov, and E. Bogans</i> Investigation of Hg resonance 184.9 nm line in a capillary low-pressure discharge	160
P-90	<i>P. Eberle, A. Dörfler, R. Krishnamurthy, S. Willitsch, H. da Silva Jr., M. Raoult, and O. Dulieu</i> Next-Generation Ion-Atom Hybrid Traps with Increased Control over Collision Energies	161
P-91	<i>A. Berzins, S. Lourette, J. Smits, K. Erglis, A. Jarmola, F. Gahbauer, M. Auzinsh, D. Budker, A. Cebers, and R. Ferber</i> Imaging the magnetic field distributions of chains of magnetic particles using nitrogen-vacancy centres in diamonds	162
P-92	<i>S. Bouazza, J. Ruczkowski, M. Elantkowska, and J. Dembczyński</i> Hyperfine Structure, Lifetimes and Oscillator Strengths of V II	163
P-93	<i>Y.-Y. Xu, X.-C. Duan, M.-K. Zhou, J.-F. Cui, H.-B. Yao, X. Xiong, and Z.-K. Hu</i> Development of a Transportable Atom Gravimeter in HUST	164
P-94	<i>X. Zhang, T. Mazzoni, R. Del Aguila, L. Salvi, N. Poli, and G. M. Tino</i> Large-momentum-transfer Bragg interferometer with Strontium atoms	165
Other	166
P-95	<i>L. Bernard Carlsson, C. Prigent, S. Cervera, A. Lévy, E. Lamour, S. Macé, J.-P. Rozet, S. Steydli, M. Trassinelli, and D. Vernhet</i> X-ray spectroscopy as a tool to enlighten the growth of Van der Waals nanoparticles in a supersonic jet	167
P-96	<i>P. Palmeri, P. Quinet, and D. Batani</i> Vanadium Fine-Structure K-shell Electron Impact Ionization Cross Sections for Fast-Electron Diagnostic in Laser-Solid Experiments	168
P-97	<i>S. Bouazza, P. Quinet, and P. Palmeri</i> Semi-empirical studies of atomic transition probabilities, oscillator strengths and radiative lifetimes in Hf II	169

List of Authors

Plenary lectures

The singularities of light: intensity, phase, polarization

M. Berry¹

¹*H H Wills Physics Laboratory, University of Bristol, UK*

Presenting Author: asymptotico@bristol.ac.uk

Geometry dominates modern optics, in which we understand light through its singularities. These are different at different levels of description. The coarsest level is geometrical optics, where the singularities are caustics: focal lines and surfaces: the envelopes of ray families. These singularities of bright light are classified by the mathematics of catastrophe theory. Wave optics smooths these singularities and decorates them with rich and ubiquitous interference patterns. Wave optics also introduces phase, which has its own singularities. These are optical vortices, a.k.a nodes or wavefront dislocations. Geometrically these singularities of dark light are lines in space, or points in the plane. They occur in all types of quantum or classical waves. Incorporating the vector nature of light leads to polarization singularities, also geometrical, describing lines where the polarization is purely circular or linear. As well as representing physics at each level, these optical and wave geometries illustrate the idea of asymptotically emergent phenomena. The levels form a hierarchy, leading to predictions of new phenomena at the quantum level.

Microwave Spectroscopy probes Dipole Blockade and van der Waals Forces in a cold Rydberg Gas

R. Celestrino Teixeira¹, C. Hermann-Avigliano¹, T. L. Nguyen¹, T. Cantat-Moltrecht¹, I. Dotsenko¹,
S. Gleyzes¹, S. Haroche¹, M. Brune¹, and J. M. Raimond¹

¹*Laboratoire Kastler Brossel, Collège de France, CNRS, ENS-PSL Research University, UPMC-Sorbonne
Universités*

Presenting Author: jmr@lkb.ens.fr

Rydberg atoms undergo strong, long-range dipole-dipole interactions [1]. A dense, cold cloud of Rydberg atoms is a complex many-body system, and could be used as a quantum simulator of less controllable solid-states systems [2].

We study dipole-dipole interactions in a cold ⁸⁷Rb atomic sample magnetically trapped on a superconducting atom chip, evaporatively cooled close to the BEC transition [3]. Rydberg states laser-excited in this sample are prone to large perturbations due to stray electric fields. The patch field produced by unavoidable Rubidium adsorption on the chip is particularly annoying. We solved this problem by coating the chip with a thick metallic Rubidium layer. In a dilute sample, we observed coherence times in the millisecond range for the 60S to 61S microwave two-photon transition, a quite encouraging result for the on-chip coherent manipulation of Rydberg atoms [4].

In a dense sample, microwave spectroscopy performed on the two-photon 60S to 57S transition directly measures the interaction energy distribution of a single Rydberg atom with its neighbors and, hence, provides information on spatial correlations between Rydberg atoms [5]. We studied the energy distribution as a function of the detuning of the excitation laser. At resonance, we excite atoms at large mutual distances, compatible with dipole blockade. For a blue laser detuning, we preferentially excite atoms at short mutual distances, so that the interaction energy compensates for laser detuning.

The measured interaction energy spectrum varies with time, revealing directly the expansion of the Rydberg cloud due to the strong repulsive dipole-dipole interaction. We observed that the “frozen gas approximation” is valid only for very short times, in the μ s range. The cloud ‘explosion’ at high densities proceeds in a hydrodynamic regime where many-body interactions play an essential role. These results open promising perspectives for quantum simulation with Rydberg atom samples.

References

- [1] M. Saffman, T.G. Walker and K. Molmer, *Rev. Mod. Phys.* **82**, 2313 (2010)
- [2] H. Weimer, M. Muller, I. Lesanovsky, P. Zoller and H.P. Buchler, *Nat. Phys.* **6**, 382 (2010)
- [3] C. Roux *et al.*, *EPL*, **81** 56004 (2008)
- [4] C. Hermann-Avigliano *et al.* *Phys. Rev. A* **90**, 040502 (2014)
- [5] R. Celestrino Teixeira *et al.* Submitted, ArXiv 1502.04179

Relaxation dynamics of isolated atoms and molecules in the tender x-ray domain (1-12 keV)

M. Simon¹

¹*LCPMR, CNRS and University Pierre and Marie CURIE, Paris, FRANCE*

Presenting Author: marc.simon@upmc.fr

Understanding of the processes resulting from interaction between light and matter is of interest in many diverse fields such as photochemistry, astrophysics, as well as in biology and medicine. The lifetime of electronic states created by the absorption of a photon by an atom or a molecule determines the time scale within which these processes will occur, and the resulting reactions. When tender X-rays are absorbed, deep electron shells are excited. The significant time scale then becomes of the order of a few femtoseconds. Photoionization of deep atomic core shell is followed by a number of relaxation processes. The primary hole is unstable and the atom will relax mainly through the emission of Auger electrons: an electron from a shallower shell fills the hole and another electron is emitted carrying the excess energy. The atom is then ionized again by Auger decay. A cascade can develop when a series of electrons "tumble" to fill the core holes created subsequently in different electron shells and several Auger electrons are emitted one after the other. Thus, Auger relaxation is a dynamical process that leads to the formation of multiply charged ionic species and involves many intermediate electronic states.

I will describe two original experimental setup we use at the French synchrotron source SOLEIL : CELIMENE has been designed to provide the full momentum vectors of coincident particles emitted after deep core-level photoexcitation [1]. We have also developed a Photoemission setup, permanent endstation of SOLEIL, unique for gases [2].

Photoexcitation of deep inner shells produce instable species in the femtosecond or subfemtosecond time range. This provides useful internal clock to measure chemical bonds elongation dynamics [3]. Cascade Auger effect occur in the electronic relaxation process providing opportunities to study Post Collision Interaction close to the ionization threshold [4]. Multiply charged ions created after the cascade Auger effect were measured in coincidence with the photoelectron allowing to deduce the delocalization dynamics of the initial deep inner shell in the CS₂ molecule [5]. Several keV above the ionization threshold, momentum conservation induces a strong recoil in the ion recently observed through Auger Doppler [6]. I will show how High resolution spectroscopy of Double Core Hole states have been characterized [7].

References

- [1] C. Bomme *et al.* Rev. Sci. Instrum. **84** 103104 (2013)
- [2] D. Céolin *et al.* J. Electron Spectrosc. Relat. Phenom. **190** 188 (2013)
- [3] M. Simon *et al.* Phys. Rev. A **73** 020706 (2006)
- [4] R. Guillemin *et al.* Phys. Rev. Lett. **109** 013001 (2012)
- [5] R. Guillemin *et al.* Nature Communications **6** 6166 (2015)
- [6] M. Simon *et al.* Nature Communications **5** 4069 (2014)
- [7] R. Püttner *et al.* Phys. Rev. Lett. **114** 093001 (2015)

Search for New Physics with Atoms and Molecules

M. S. Safronova^{1,2}

¹*Department of Physics and Astronomy, University of Delaware, Newark, Delaware 19716, USA*

²*Joint Quantum Institute, NIST and the University of Maryland, College Park, Maryland 20899, USA*

Presenting Author: msafrono@udel.edu

Recent advances in both experimental and theoretical atomic, molecular, and optical physics provide remarkable new opportunities for precision measurements and tests of fundamental physics, including searches for permanent electric-dipole moments, parity violation studies, searches for variation of fundamental constants, gravity studies, tests of local Lorentz invariance, search for dark matter and many others. I will give a brief introduction to this subject and review the role of theory. The main part of the talk will focus on the search for the variation of the fine-structure constant α [1] and tests of local Lorentz invariance [2], including recent highly-charged ion proposals.

References

[1] *Highly-charged ions for atomic clocks, quantum information, and search for α -variation*, M. S. Safronova, V. A. Dzuba, V. V. Flambaum, U. I. Safronova, S. G. Porsev, and M. G. Kozlov, *Phys. Rev. Lett.*, **113**, 030801 (2014).

[2] *A Michelson-Morley Test of Lorentz Symmetry for Electrons*, T. Pruttivarasin, M. Ramm, S. G. Porsev, I. I. Tupitsyn, M. Safronova, M. A. Hohensee, and H. Haffner, *Nature* **517**, 592 (2015).

Quantum Walks in Photonic Lattices

Y. Silberberg¹

¹*Department of Physics of Complex Systems, Weizmann Institute of Science, Rehovot, Israel*

Presenting Author: yaron.silberberg@weizmann.ac.il

Photonic lattices in the form of arrays of optical waveguides with nearest-neighbour evanescent coupling offer a rich playground for the study of linear and nonlinear effect in periodic media. Such lattices have been used by my group and others for more than a decade to study some of the most basic phenomena of wave propagation in periodic and quasi-periodic structures, from Bloch Oscillations to Anderson Localization. While most work with such lattices have studied wave propagation using coherent laser light, we have shown that they could also serve as an excellent decoherence-free platform for the study of quantum dynamics, and in particular of quantum walks [1]. Random quantum walk is the process describing the motion of a quantum particle that hops randomly, yet coherently, from site to site on a lattice. We have extended this concept to more complex random walks of several particles [2-4], and have shown that such walks by indistinguishable particles lead to new and surprising effects on the quantum correlations of the copropagating walkers in periodic lattices. Even more surprises are found when the quantum walkers move in a disordered lattice where the particles are also constrained via Anderson localization [5-7]. I will present recent experiments on such systems, and review the effects of interactions on such correlations [8].

References

- [1] H. Perets *et al.* Phys. Rev. Lett. **100** 170506 (2008)
- [2] Y. Bromberg, Y. Lahini, R. Morandotti and Y. Silberberg, Phys. Rev. Lett. **102**, 253904 (2009)
- [3] Y. Bromberg, Y. Lahini, Y. Silberberg, Phys. Rev. Lett. **105** 263604 (2010)
- [4] A. Peruzzo *et al.* Science **329** 1500-1503 (2010)
- [5] Y. Lahini *et al.* Phys. Rev. Lett. **100** 013906 (2008)
- [6] M. Segev, Y. Silberberg and D.N. Christodoulides Nature Photonics **7** 197 (2013)
- [7] Y. Lahini, Y. Bromberg, D.N. Christodoulides and Y. Silberberg, Phys. Rev. Lett. **105**, 163905 (2010).
- [8] Y. Lahini *et al.* Phys. Rev. A **86** 011603 (2012)

The Fascination of Lanthanides as Ultracold Quantum Matter

F. Ferlaino¹

¹*Institut für Experimentalphysik, University of Innsbruck and Institut für Quantenoptik und Quanteninformation (IQOQI), Austria*

Presenting Author: Francesca.Ferlaino@uibk.ac.at

Ultracold atomic quantum gases have exceptional properties and offer an ideal test-bed to elucidate intriguing phenomena of modern quantum physics. The great appeal of such systems stems from the possibility to control almost on demand the interaction between the particles. This interaction is commonly isotropic and short-ranged. However, recent studies have demonstrated the power of a novel class of exotic atomic elements belonging to the lanthanides family for quantum-matter physics. Lanthanides, such as Er (erbium) that is here discussed, have more complex and rich interaction than the commonly-used alkali atoms, opening new research scenarios for scattering and many-body quantum physics.

Because of their large magnetic moment, the fundamental interaction between the atoms has a non-isotropic nature and a long-range character. In addition, in their ground-state the atoms experience a highly non isotropic orbital distribution of electrons around the atom's nucleus. This orbital anisotropy is reflected in the appearance of anisotropic van der Waal contributions to the molecular potentials. Due to these characteristics, we observe a number of novel fascinating effects from the distortion of the Fermi surface in a gas of fermions near zero temperature, to the appearance of a correlated net of Feshbach resonances in the atomic scattering.

Spectroscopy of Cold Molecular Ions

S. Schlemmer¹, O. Asvany¹, S. Brünken¹, and P. Jusko¹

¹*I. Physikalisches Institut, Universität zu Köln, Zùlpicher Strasse 77, 50937 Köln, Germany*

Presenting Author: schlemmer@ph1.uni-koeln.de

Ions play an important role in many interesting environments like planetary atmospheres or the interstellar medium. These molecules are the messengers of the physical (pressure, number density) and chemical conditions. Therefore their spectra and chemical reactivity have to be known in the laboratory to interpret the data from remote sensing observations. Ion trapping is used in our laboratory to investigate both aspects of molecular physics. Over many years the method of laser induced reactions (LIR) has been used to study the spectra and state specific processes of molecular ions at low temperatures. The main advantages of this technique are: mass selection of the primary ion, low temperature trapping, and most importantly an unprecedented sensitivity as only a few hundred ions per wavelength step are needed to, e.g., record a spectrum. Moreover, the method only needs a single photon compared to other, more popular trap based spectroscopy methods like infrared multiple photon dissociation (IRMPD).

Recently our group pushed the limits of ro-vibrational spectroscopy of CH_2D^+ and CD_2H^+ [1] to predict rotational spectra in the THz regime helping to identify this molecule in astrophysical observations. Employing a frequency comb in combination with cw-OPOs, transition frequencies of ro-vibrational lines of CH_5^+ have determined with sub-MHz resolution [2]. This can be considered a breakthrough since it paves the road to pinpoint combination differences (CDs) of complex spectra where thousands of lines lead to an enormous number of CDs [3]. Within the last year pure rotational transitions of several molecular ions have been detected by using the state-dependent association rate of these ions with He at 4 K. This is another significant advancement since this approach allows to record THz spectra of virtually any ion. Very recently such laboratory spectra led to the identification of $1\text{-C}_3\text{H}^+$ in space [4]. Also IR-THz two photon double resonance spectroscopy has been used to record the $J=1-0$ rotational transition of OH^- [5].

References

- [1] S. Gärtner, J. Krieg, A. Klemann, O. Asvany, S. Brünken, S. Schlemmer, *J. Phys. Chem. A*, 117 (2013) 9975–9984.
- [2] O. Asvany, J. Krieg, and S. Schlemmer, *Review of Scientific Instruments*, 83 (2012), 076102.
- [3] O. Asvany, K.M.T. Yamada, S. Brünken, A. Potapov, S. Schlemmer, *Science* 347 (2015) 1346-1349.
- [4] S. Brünken, L. Kluge, A. Stoffels, O. Asvany, and S. Schlemmer, *Astrophysical Journal* 783 (2014) L4.
- [5] P. Jusko, O. Asvany, A.-C. Wallerstein, S. Brünken, S. Schlemmer, *Phys.Rev.Lett.* 112 (2014) 253005.

Fundamental symmetries and the Dark Sector

D. Budker¹

¹*Helmholtz-Institute Mainz and University of California, Berkeley*

Presenting Author: dbudker@gmail.com

“Fundamental symmetry” refers to invariance of the laws of Nature, including the values of fundamental constants, with respect to a continuous or discrete transformation such as translation in space or time, rotation, spatial (P), time (T), or charge (C) reversal, combinations of these, or permutation of identical quantum particles. All discrete symmetries except for the combined CPT and the permutation symmetry are experimentally known to be violated by the weak interactions; intense searches are conducted for possible small violations of the still-standing discrete as well as the continuous symmetries, which may result from exotic beyond-the-standard-model interactions. In this talk, I will describe some of the recent fundamental-symmetry tests involving our research group (for up-to-date bibliography see <http://budker.berkeley.edu/PubList.html>), including measuring the effect of the gravitation-field gradient on the value of the fine-structure “constant,” and searching for transient and oscillating effects on atomic magnetometers and clocks. The apparent time-dependent symmetry violations may, in fact, be manifestations of feeble interactions with the particles and fields that are possible constituents of dark matter and dark energy, the Dark Sector.

Precision measurements in gravitational physics with cold atom interferometry

G. M. Tino¹

¹*Dipartimento di Fisica e Astronomia and LENS - Università di Firenze, INFN - Sezione di Firenze, Via Sansone 1, 50019 Sesto Fiorentino, Italy*

Presenting Author: guglielmo.tino@fi.infn.it

I will describe experiments we are conducting for precision tests of gravitational physics using cold atom interferometry. In particular, I will report on the measurement of the Newtonian gravitational constant [1] and of the gravity-field curvature [2] with a Rb Raman interferometer, and on experiments based on Bloch oscillations of Sr atoms in optical lattices for gravity measurements at small spatial scales [3] and for testing the Einstein equivalence principle [4]. Future prospects for experiments in space will be also discussed [5].

References

- [1] G. Rosi, F. Sorrentino, L. Cacciapuoti, M. Prevedelli, G. M. Tino, Precision Measurement of the Newtonian Gravitational Constant Using Cold Atoms, *Nature* 510, 518 (2014).
- [2] G. Rosi, L. Cacciapuoti, F. Sorrentino, M. Menchetti, M. Prevedelli, G. M. Tino, Measurement of the gravity-field curvature by atom interferometry, *Phys. Rev. Lett.* 114, 013001 (2015).
- [3] F. Sorrentino, A. Alberti, G. Ferrari, V. V. Ivanov, N. Poli, M. Schioppo, G. M. Tino, Quantum sensor for atom-surface interactions below $10\mu\text{m}$, *Phys. Rev. A* 79, 013409 (2009).
- [4] M.G. Tarallo, T. Mazzoni, N. Poli, D.V. Sutyurin, X. Zhang, G. M. Tino, Test of Einstein Equivalence Principle for 0-Spin and Half-Integer-Spin Atoms: Search for Spin-Gravity Coupling Effects, *Phys. Rev. Lett.* 113, 023005 (2014).
- [5] G. M. Tino et al., Precision Gravity Tests with Atom Interferometry in Space, *Nuclear Physics B (Proc. Suppl.)* 243-244, 203 (2013).

Using atoms and molecules to search for variation of fundamental constants

M. G. Kozlov^{1,2}

¹*Petersburg Nuclear Physics Institute, Gatchina, Russia*

²*St. Petersburg Electrotechnical University "LETI", St. Petersburg, Russia*

Presenting Author: mgk@mfl309.spb.edu

Frequencies of atomic and molecular transitions depend on the values of the fine structure constant $\alpha = \frac{e^2}{\hbar c}$ and electron to proton mass ratio $\mu = \frac{m_e}{m_p}$. High precision spectroscopy for narrow optical transitions in atoms and molecules put very stringent limits on the time variation of α and μ on the time scale of few years. Astrophysical high redshift observations constrain space-time variations on the cosmological scale on the order of 10 billion years.

In the talk I will discuss several examples of the transitions with high sensitivity to the fundamental constants in molecules and in highly charged ions. In particular, I will focus on the transitions between quasi degenerate levels. Quasi degeneracy can be caused either by some approximate symmetry, or by the accidental cancellation between different contributions to the energy of the atomic system. The latter case is particularly important for the laboratory experiments, where the absolute sensitivity to the variation of the fundamental constants is as important as the relative sensitivity. For the astrophysical observations, where the lines are Doppler broadened, the relative sensitivity plays the main role [1].

Molecular physics gives us many examples of the quasi degeneracy of both types, which leads to the high relative sensitivity of the molecular microwave transitions to the variation of the fundamental constants. Such transitions are particularly interesting to the astrophysics. Recently it was pointed out that one can observe very narrow optical transitions in the highly charged ions [2]. These transitions appear when there is level crossing between different atomic shells in the isoelectronic sequences of ions. On the energy scale typical to ions such crossings can be considered as an accidental degeneracy. Corresponding optical transitions can be used as very sensitive probes to the variation of the fine structure constant α in the laboratory tests [2,3].

References

- [1] M. G. Kozlov & S. A. Levshakov *Annalen der Physik* **525**, 452-471 (2013)
- [2] J. C. Berengut, V. A. Dzuba, and V. V. Flambaum, *Phys. Rev. Lett.* **105**, 120801 (2010)
- [3] M. S. Safronova *et al.* *Phys. Rev. Lett.* **113**, 030801 (2014)

Invited talks

Asymptotic physics with subradiant and superradiant states of ultracold molecules

R. Moszynski¹, W. Skomorowski^{1,2}, B. H. McGuyer³, and T. Zelevinsky³

¹Department of Chemistry, University of Warsaw, Poland

²Institute of Physics, University of Kassel, Germany

³Department of Physics, Columbia University, New York, USA

Presenting Author: robert.moszynski@tiger.chem.uw.edu.pl

We present a combined theoretical and experimental study of weakly bound rovibrational levels of ultracold strontium molecules near the atomic intercombination line. Some physical properties of these levels, such as the lifetimes or Zeeman shifts, are fully determined by the internal symmetries of the wave functions. For instance, the symmetry of the electronic wave function specifies if the excited state has a superradiant or subradiant character.

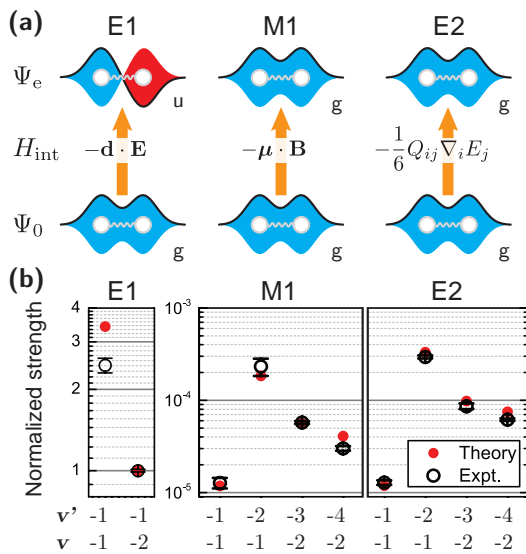


Figure 1: Optical transitions to superradiant and subradiant molecular states of Sr_2

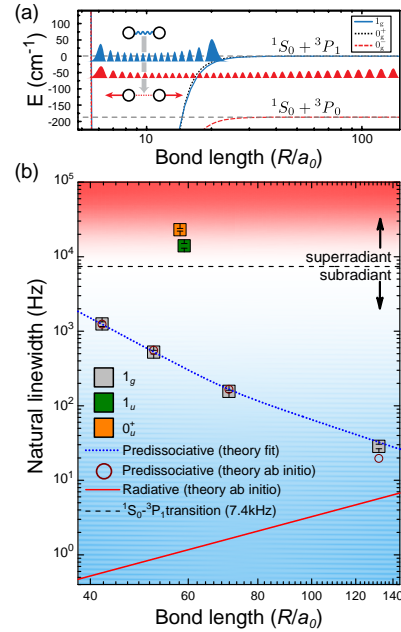


Figure 2: Natural linewidths of weakly bound subradiant and superradiant molecular states of Sr_2

We precisely characterize [1] the subradiant states of the Sr_2 molecule, and show how their properties are strongly affected by the nonadiabatic and relativistic effects. In particular, we show that the observed finite lifetimes of the subradiant states are limited by the gyroscopic predissociation due to the nonadiabatic Coriolis coupling in the short range of the interatomic potential. We quantitatively describe and compare strongly forbidden magnetic-dipole and electric-quadrupole transitions to subradiant excited states proving their unusual asymptotic behavior and relativistic nature.

We also demonstrate how the nonadiabatic mixing between the excited interaction potentials leads to anomalously large linear, quadratic, and higher Zeeman shifts of weakly bound Sr_2 molecules [2,3]. All these phenomena are illustrated with the results from high-precision measurements and state-of-the-art *ab initio* calculations.

References

- [1] B. H. McGuyer *et al.* Nature Physics **11** 32 (2015)
- [2] B. H. McGuyer *et al.* Phys. Rev. Lett. **111** 243003 (2013)
- [3] B. H. McGuyer *et al.* arXiv:1503.05946

Observation of forbidden infrared spectra in Coulomb-crystallized molecular ions: Towards precision measurements on single molecules

M. Germann¹, G. Hegi¹, K. Najafian¹, X. Tong¹, and S. Willitsch¹

¹*Department of Chemistry, University of Basel, Switzerland*

Presenting Author: stefan.willitsch@unibas.ch

The recent progress in the preparation of neutral molecules and ions at temperatures close to the absolute zero point has paved the way for a range of new research directions in atomic, molecular and chemical physics. Ensembles of cold, spatially localized ions in traps, often referred to as Coulomb crystals, are particularly attractive systems in this context in which it is possible to observe, manipulate and control single isolated particles under precisely controlled conditions [1].

The long storage times (exceeding tens of minutes) of Coulomb-crystallized ions in the minimally perturbed environment of an ion trap enable to perform highly sensitive spectroscopic experiments and study molecular spectra which have not been accessible before. Here, we present recent results on the - to our knowledge first - observation of the electric-dipole forbidden infrared spectrum of a molecular ion. Specifically, we studied hyperfine components of rotational lines in the infrared fundamental excitation of N_2^+ in a Coulomb crystal [2]. These extremely weak and therefore narrow transitions, the line strength of which is about ten orders of magnitude smaller than the one of typical dipole-allowed infrared lines, form an ideal basis for precision-spectroscopic measurements. Applications include the development of precise clocks and tests of fundamental concepts such as a possible time variation of fundamental physical constants [3,4]. In the talk, we will discuss new developments in the study of forbidden spectra of molecular ions and present an outlook towards realizing precision-spectroscopic measurements on single isolated molecules [5].

References

- [1] S. Willitsch, *Int. Rev. Phys. Chem.* **31**, 175 (2012)
- [2] M. Germann, X. Tong, S. Willitsch, *Nature Phys.* **10**, 820 (2014)
- [3] S. Schiller, D. Bakalov, and V. I. Korobov, *Phys. Rev. Lett.* **113**, 023004 (2014)
- [4] M. Kajita et al., *Phys. Rev. A* **89**, 032509 (2014)
- [5] J. Mur-Petit et al., *Phys. Rev. A* **85**, 022308 (2012)

Decoherence-Assisted Spectroscopy: Demonstrated with a Single Mg^+ Ion

G. Clos¹, M. Enderlein¹, U. Warring¹, T. Schaetz¹, and D. Leibfried²

¹*Albert-Ludwigs-University Freiburg, Hermann-Herder-Strasse 3, 79104 Freiburg, Germany*

²*National Institute of Standards and Technology, 325 Broadway, Boulder, Colorado 80305, USA*

Presenting Author: tobias.schaetz@physik.uni-freiburg.de

We describe a spectroscopy method that takes advantage of decoherence, typically thought of as detrimental when controlling quantum systems. The occurrence of a single excitation event is detected by enhancing its impact via a complete loss of coherence of a superposition of two ground states [1]. Thereby, transitions of a single isolated atom nearly at rest are recorded efficiently with high signal-to-noise ratios. The Spectra display symmetric line shapes without stray-light background from spectroscopy probes. We demonstrated this method on a ^{25}Mg ion to measure one-, two-, and three-photon transition frequencies from the 3S ground state to the 3P, 3D, and 4P excited states, respectively. In combination with an additional logic ion [2], and incorporating the motional degrees of freedom, our method may also be applicable to species without cooling and detection transitions as well as molecular ions.

Please note that also other techniques based on the detection of momentum kicks altering the occupation of motional states from few absorbed photons have been developed recently [3-4].

References

- [1] G. Clos *et al.* Phys. Rev. Lett. **112** 113003 (2014)
- [2] D.J. Wineland Rev. Mod. Phys. **85**, 1103 (2013)
- [3] Y. Wan *et al.* Nat. Commun. **5** 4096 (2014)
- [4] C. Hempel *et al.* Nat. Phot. **7** 630 (2013)

Thermodynamic meaning and power of non-Markovianity

B. Bylicka¹, D. Chruściński², M. Tukiainen³, J. Piilo³, and S. Maniscalco³

¹*ICFO-Institut de Ciències Fotoniques, Mediterranean Technology Park, 08860 Castelldefels (Barcelona), Spain*

²*Institute of Physics, Faculty of Physics, Astronomy and Informatics, Nicolaus Copernicus University, Grudziądzka 5/7, 87-100 Toruń, Poland*

³*Turku Centre for Quantum Physics, Department of Physics and Astronomy, University of Turku, FI-20014, Turun Yliopisto, Finland*

Presenting Author: smanis@utu.fi

The connection between thermodynamics and information theory, expressed by Landauer's principle, is a milestone of the physics of the last century. According to this principle, the erasure of information stored in a system requires an amount of work proportional to the entropy of the system. The natural framework to discuss thermodynamics at the quantum level is the theory of open quantum systems. A number of recent results have shown that memory effects arising from strong system-environment correlations may lead to information back-flow, hence prolonging the life of quantum properties. Open systems exhibiting such behaviour are known as non-Markovian. The relation between non-Markovianity and quantum thermodynamics has been until now largely unexplored. Here we establish this missing link by means of Landauer's principle. We show that memory effects control the amount of work that one can extract from an open quantum system. Hence, the work extraction can be optimised via reservoir engineering techniques.

Atom in front of a hot surface: Temperature-dependence of the Casimir-Polder interaction and thermal energy transfer

A. Laliotis¹, J. C. de Aquino Carvalho¹, T. Passerat de Silans^{1,2}, P. Chaves de Souza Segundo^{1,3},
I. Maurin¹, M. Ducloy¹, and D. Bloch¹

¹LPL, CNRS-UMR 7538, Université Paris13 - Sorbonne Paris Cité, 93430 Villetaneuse, France

²also at Universidade Federal de Paraíba, João Pessoa, Brazil

³now at Universidade Federal de Campina Grande, Cuité, Brazil

Presenting Author: daniel.bloch@univ-paris13.fr

The temperature dependence of the Casimir-Polder (CP) atom-surface interaction addresses fundamental issues for understanding vacuum and thermal fluctuations. Recently, we have shown that the CP interaction can be strongly modified by the temperature effects [1]. In our regime of short distances ($\sim 100\text{nm}$, i.e. electrostatic limit), the atom becomes a probe, with a high-frequency selectivity, of the near-field thermal emission, which strongly differs from the long-distance (material-independent) blackbody emission. The observed increase of the interaction with temperature (fig. 1), by up to 50%, relies on the coupling between atomic virtual transitions — located in the *thermal* infrared range — and thermally excited surface-polariton modes. The experiments were performed on $Cs(7D_{3/2})$, through a selective reflection spectroscopy technique on a vapour at the interface of a hot superpolished sapphire window. The measurements rely on an elaborate fitting of the data to a catalogue of universal lineshapes.

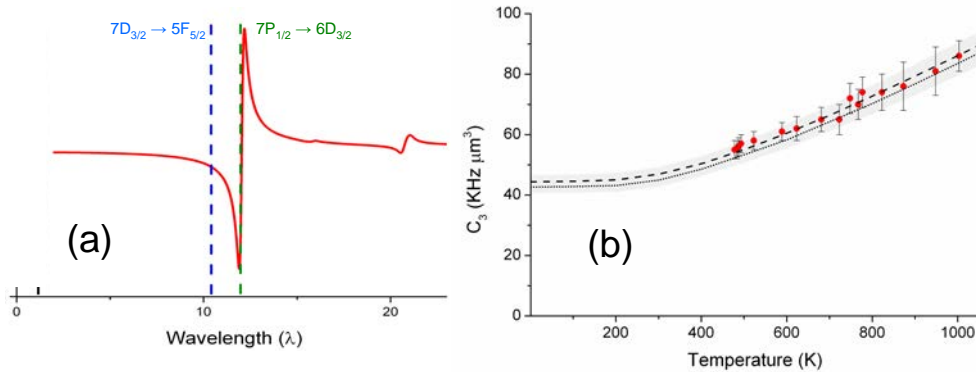


Figure 1: (a) the sapphire surface resonance around $12\mu\text{m}$, and (b) the temperature dependence of the CP interaction for $Cs(7D_{3/2})$ (see [1]), mostly related to the $10.8\mu\text{m}$ coupling [see (a)].

We are now extending these experiments to $Cs(7P_{1/2})$ and $Cs(7P_{3/2})$, at the same interface (superpolished sapphire). For $Cs(7P_{1/2})$, the dominant coupling (to $6D_{3/2}$) at $12.15\mu\text{m}$ falls in a strong coincidence with the sapphire surface resonance (fig.1a), yielding the reverse effect of the resonant repulsion previously observed on $Cs(6D_{3/2})$ at a sapphire interface [2]. Conversely, the couplings from $Cs(7P_{3/2})$, at $14 - 15\mu\text{m}$, are far away from this sapphire resonance, and major differences are predicted for the temperature dependence. At stake is the possibility of an original and precise way to probe surface resonances, predicted to soften and shift with temperature, which are commonly extrapolated from broadband data on the entire spectrum (e.g. through Kramers-Kronig relation). The thermal emission of sapphire may also induce a transfer $Cs(7P_{1/2}) \rightarrow 6D_{3/2}$, involving a real transition where the thermal energy is selectively absorbed by the neighbouring atom. A refined analysis of the spectrum on the 459nm line may be able to provide an evidence of the corresponding temperature-modification of the atomic lifetime of $Cs(7P_{1/2})$.

One of us (J.C.A.C.) thanks the “Ciências sem fronteiras” programme. The France-Brazil cooperation is supported by CAPES-COFECUB programme Ph 740-12.

References

- [1] A. Laliotis et al., Nature Comm. **5**, 5634 (2014) doi:10.1038/ncomms5364
- [2] H. Failache et al., Phys. Rev. Lett., **83**, 5467 (1999)

Contributed talks

The Magnetic Moments of the Proton and the Antiproton

A. Mooser¹, C. Smorra^{1,2}, K. Blaum³, K. Franke^{1,3}, T. Higuchi^{1,4}, N. Leefer⁵, Y. Matsuda⁴,
H. Nagahama^{1,4}, W. Quint⁶, G. Scheider⁷, J. Walz^{5,7}, Y. Yamazaki⁸, and S. Ulmer¹

¹*RIKEN, Ulmer Initiative Research Unit, Japan*

²*CERN, Switzerland*

³*Max-Planck-Institut für Kernphysik, Germany*

⁴*University of Tokyo, Japan*

⁵*Helmholtz-Institut Mainz, Germany*

⁶*GSI - Helmholtzzentrum für Schwerionenforschung GmbH, Germany*

⁷*Johannes Gutenberg-Universität Mainz, Germany*

⁸*RIKEN, Atomic Physics Laboratory, Japan*

Presenting Author: andreas.mooser@cern.ch

One of the fundamental properties of the proton/antiproton is the spin magnetic moment $\mu_p/\mu_{\bar{p}}$. In case of the proton the most precise value of μ_p was based on spectroscopy of atomic hydrogen conducted in 1972. Significant theoretical bound-state corrections had to be applied to indirectly determine μ_p with a relative precision of 9 ppb [1]. Very recently, we improved this value by a factor of 2.5 by directly measuring μ_p using a single proton in a Penning trap [2]. In case of the antiproton $\mu_{\bar{p}}$ is known with a relative precision at the ppm level [3]. By applying our methods to $\mu_{\bar{p}}$, we aim at a thousandfold improvement in precision of its value. To this end, we were setting up the BASE (Baryon Antibaryon Symmetry Experiment) experiment at the antiproton decelerator of CERN [4], to eventually provide a stringent test of CPT-invariance with baryons.

In a Penning trap the measurement of $\mu_p/\mu_{\bar{p}}$ is based on the determination of two frequencies of a single proton/antiproton, the Larmor and the cyclotron frequency. Based on a statistical detection of spin transitions we measured the Larmor frequency of a single proton for the first time [5], which resulted in a direct determination of μ_p with a fractional precision at the ppm level [6]. The precision was improved significantly by using a double Penning-trap technique. This required the detection of single spin flips, which was achieved with an improved apparatus and by using Bayesian data analysis [7]. Our developments ultimately culminated in the most precise and first direct high-precision measurement of μ_p with a fractional accuracy of 3.3 ppb.

For BASE a significantly improved setup using a state-of-the-art trapping system has been developed. We successfully commissioned our four-Penning trap system with antiprotons provided by the antiproton decelerator of CERN. Within our first experiments we were able to demonstrate cyclotron frequency measurements with fractional precisions at the level of 70 ppt. The achieved precision will enable us to perform the aimed antiproton magnetic moment measurement. Moreover, an improvement in precision of the proton-to-antiproton charge-to-mass ratio is in reach. A detailed status update will be presented.

References

- [1] S. G. Karshenboim, V. G. Ivanov *Phys. Lett. B* **566**, 27 (2003)
- [2] A. Mooser *et al.* *Nature* **509**, 59 (2014)
- [3] J. DiSciaccia *et al.* *Phys. Ref. Lett.* **110**, 130801 (2013)
- [4] C. Smorra *et al.* *Hyperfine Interact.* **228**, 31 (2014)
- [5] S. Ulmer *et al.* *Phys. Ref. Lett.* **106**, 253001 (2011)
- [6] C. C. Rodegheri *et al.* *New J. Phys.* **14**, 063011 (2012)
- [7] A. Mooser *et al.* *Phys. Ref. Lett.* **110**, 140405 (2013)

Intra-cavity photodetachment microscopy and the electron affinity of germanium

D. Bresteau¹, C. Drag¹, and C. Blondel¹

¹Laboratoire Aimé-Cotton, Centre national de la recherche scientifique, université Paris-sud, école normale supérieure de Cachan, bâtiment 505, F-91405 Orsay cedex, France

Presenting Author: david.bresteau@u-psud.fr

Photodetachment microscopy is performed inside an optical cavity, on an ion beam and with an optical mode narrow enough not to blur out the output electron interferogram. This setting is used for an updated measurement of the electron affinity of germanium. Amplification of the photodetachment probability obtained in an optical cavity also opens the way to photodetachment microscopy with a p electron wave, even though photodetachment cross-sections are reduced considerably in this case, when compared to s-wave detachment, by the centrifugal barrier.

A linear optical cavity is set across a beam of Ge⁻ ions, itself produced by a cesium sputtering ion source. The optical cavity is injected with a single mode ring Ti:Sa laser, the wavenumber of which can be set either above the highest ³P₂ fine-structure excitation threshold, or just above the ³P₁, intermediate fine-structure threshold of the ³P ground-term of Ge I. The freed photoelectron is accelerated towards an imaging detector by a uniform electric field of about 350 Vm⁻¹. When the initial kinetic energy is of the order of 50 m⁻¹, an electron interferogram can be observed, which semi-classically corresponds to the existence of a pair of trajectories bound to every detection point.

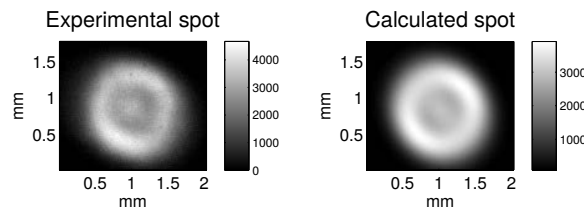


Figure 1: Intracavity-produced electron interferogram. In this example, photodetachment of Ge⁻ at wavenumber $\lambda^{-1} = 1135\,258.9(1)\text{ m}^{-1}$, within an electric field of 357.6 Vm^{-1} , produces an electron interferogram of apparent energy $\epsilon = 44.2(15)\text{ m}^{-1}$. Persistence of a ring pattern, with fringes not much more than $100\text{ }\mu\text{m}$ wide, shows that the ion beam diameter has been reduced to smaller values.

Fitting these interferograms with the expected form of the uniform acceleration Green function, one gets a measure of the electron's initial kinetic energy. The precision of the method can be three orders of magnitude larger than the precision of classical electron spectrometry. Provided that the two photoelectron energies produced by the two opposite wave vectors contained in the optical cavity are not too different, i.e. provided that the illumination angle remains close to 90° , subtraction of the mean photoelectron energy from the photon energy directly provides a high accuracy measurement of the electron affinity.

A Doppler-free measurement of the photodetachment threshold can thus be produced, in an optical cavity, even more directly than with the usual double spot photodetachment microscopy method [1], at the only expense of a slight reduction of the contrast in the interferograms. The obtained value of the electron affinity of germanium is $994\,220.6(10)\text{ m}^{-1}$ or $1.232\,6764(12)\text{ eV}$, one order of magnitude more precise and a little smaller than the last measured value $994\,249(12)\text{ m}^{-1}$ or $1.232\,712(15)\text{ eV}$ [2].

References

- [1] C. Blondel *et al.* Eur. Phys. J. D **33**, 335 (2005)
- [2] M. Scheer *et al.* Phys. Rev. A **58** 2844 (1998)

Antihydrogen synthesis with lower energy antiprotons in the ASACUSA double-cusp trap

M. Tajima^{1,2}, N. Kuroda¹, S. Van Gorp², Y. Nagata^{2,3}, P. Dupré², D. J. Murtagh², B. Radics²,
H. A. Torii¹, H. Higaki⁴, B. Horst⁵, Y. Kanai², Y. Matsuda¹, S. Ulmer⁶, and Y. Yamazaki²

¹*Institute of Physics, Graduate School of Arts and Sciences, University of Tokyo, Tokyo 153-8902, Japan*

²*Atomic Physics Research Unit, RIKEN, Saitama 351-0198, Japan*

³*Department of Applied Physics, Tokyo University of Agriculture and Technology, Koganei, Tokyo 184-8588, Japan*

⁴*Graduate School of Advanced Sciences of Matter, Hiroshima University, Hiroshima 739-8530, Japan*

⁵*CERN, Geneva 23, Switzerland*

⁶*Ulmer Initiative Research Unit, RIKEN, Saitama 351-0198, Japan*

Presenting Author: tajima@radphys4.c.u-tokyo.ac.jp

We, the ASACUSA collaboration, have developed a source of antihydrogen atoms at the CERN Antiproton Decelerator in order to test CPT symmetry through in-flight ground-state hyperfine spectroscopy. The production of antihydrogen beams was already demonstrated in [1].

During a long shutdown of the CERN accelerators, we upgraded the trap system with a double-cusp magnetic field. It improved the focusing power for the antiatomic beam and achieved a low leak field at the position of the spectrometer line next to the double-cusp trap, which is required for the planned high-precision spectroscopy.

Antihydrogen atoms were synthesized by injecting a slow antiproton cloud from an antiproton accumulator into a positron plasma confined in the double-cusp trap.

Since the production rate strongly depends on the temperature of the positron plasma, it is mandatory to inject a cold antiproton cloud at slightly above the potential energy of the plasma in order to suppress unnecessary heat up. We attempted to prepare a cold antiproton cloud in the accumulator by improving the manipulation. And then, we transported it while keeping the energy spread as small as possible by a modified magnetic transportation scheme at low kinetic energies. In 2014, we are succeeded in transporting antiprotons with a lower energy of 50 eV compared to 150 eV in 2012 and confirmed antihydrogen synthesis in the double-cusp trap. The current status will be discussed.

References

[1] N. Kuroda *et al.* Nat. Commun. **5** 3089 (2014)

High precision calculations for excited states of the hydrogen molecule

M. Zientkiewicz¹, K. Pachucki¹

¹Faculty of Physics, University of Warsaw

Presenting Author: magz@fuw.edu.pl

We performed high-precision nonrelativistic calculations for 12 excited states of the hydrogen molecule. The explicitly correlated exponential wave functions were used, which, unlike popular Gauss-type functions, do have correct asymptotic behavior in large and small interparticle distances, which is crucial for further calculations of relativistic and QED corrections. Following the Born–Oppenheimer approach, nuclei positions were treated as a fixed parameter $R = r_{AB}$ and varied from $0.1a_0$ to $20a_0$. For R up to about $9a_0$, the James–Coolidge basis set was used:

$$\phi_{n_0\dots n_4} = e^{-\alpha(r_{1A}+r_{1B})} e^{-\beta(r_{2A}+r_{2B})} r_{12}^{n_0} (r_{1A} - r_{1B})^{n_1} (r_{2A} - r_{2B})^{n_2} (r_{1A} + r_{1B})^{n_3} (r_{2A} + r_{2B})^{n_4}$$

where 1, 2 – electrons, A, B – nuclei. In this case, all necessary integrals have been derived in close analytical form [1]. However, this basis set does not reproduce the dissociation limit correctly. Thus, for large R values, the more general Kołos–Wolniewicz basis set was used:

$$\begin{aligned} \phi_{n_0\dots n_4} = & e^{-y(r_{1A}-r_{1B})-x(r_{2A}-r_{2B})-u(r_{1A}+r_{1B})-w(r_{2A}+r_{2B})} \\ & \times r_{12}^{n_0} (r_{1A} - r_{1B})^{n_1} (r_{2A} - r_{2B})^{n_2} (r_{1A} + r_{1B})^{n_3} (r_{2A} + r_{2B})^{n_4} r^{-n_0-n_1-n_2-n_3-n_4-3} \end{aligned}$$

In this case, the integrals were calculated by Taylor expansion in R , which we found numerically stable and efficient.

Our results have relative accuracy varying from about 10^{-10} to about 10^{-16} , which exceeds the best previous results of this kind [2,3] by several orders of magnitude. This opens a window for high-precision theoretical predictions for excited states of molecular hydrogen.

References

- [1] K. Pachucki Phys. Rev. A **80**, 032520 (2009)
- [2] G. Staszewska, L. Wolniewicz J. Mol. Spectr. **198.2**, 416–420 (1999)
- [3] G. Staszewska, L. Wolniewicz J. Mol. Spectr. **212.2**, 208–212 (2002)

Probing ultra-fast nearfield dynamics of individual nano bowtie-antennas

E. Lorek¹, E. Mårzell¹, A. Losquin¹, M. Miranda¹, A. Harth¹, C. Guo¹, R. Svård¹, C. Arnold¹,
A. L'Huillier¹, A. Mikkelsen¹, and J. Mauritsson¹

¹Department of Physics, Lund University, Lund

Presenting Author: eleonora.lorek@fysik.lth.se

By illuminating nano antennas with light, and excite collective electron oscillations known as plasmons, light can be focused down to below the diffraction limit and be greatly enhanced. For many applications of such antennas the near-field and its temporal aspects are relevant. The optical techniques capable of characterizing the ultrafast optical far-field response from micro- and nanostructures in time ([1],[2]) face the diffraction limit.

Photoemission electron microscopy (PEEM) combined with fs laser pulses and optical interferometry has, however, been demonstrated as a powerful tool in probing laser induced near-field dynamics with nanometer spatial resolution [3]. We apply the technique, using 6 fs, 800 nm central wavelength pulses from a Ti:Sapph oscillator, to nano bowtie-antennas of gold. Varying the size of the antennas during the fabrication process (Figures 1 a, b) allows for tuning their response to the excitation field (Figure 1 c). Changes in their ultrafast response are recorded with the PEEM, laser and interferometer as differences in the resulting near-field autocorrelation traces (Figure 1.d) from the different antenna sizes. Combined with an accurate characterization of the incoming pulses, the results are compared to Finite difference time domain numerical simulations.

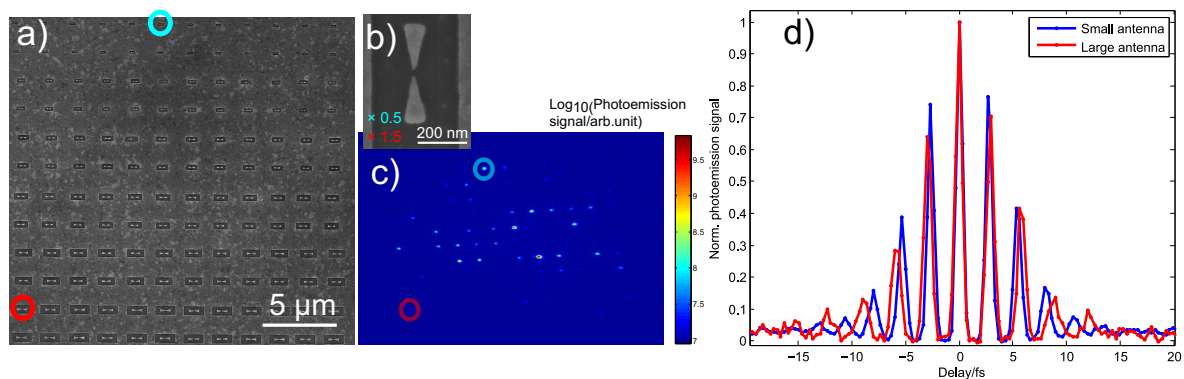


Figure 1: a) A Scanning electron microscopy image of an array of bowtie antennas that vary in size. One small (blue) and one large (red) bowtie are marked in the image. b) The dimensions of the bowties. The small bowtie has the dimensions in the image scaled by a factor of 0.5 and the large one has the dimensions scaled by 1.5. c) A laser PEEM image showing the photoemission spots resulting from field enhancement at the gap of the antennas. d) The photoemission signals as a function of pulse delay (the near-field autocorrelation traces) for the two antennas selected.

References

- [1] A. Andersson *et al.* Nano Lett. **10** 2519 (2010)
- [2] N. Accanto *et al.* Nano Lett. **14** 4078 (2014)
- [3] A. Kubo *et al.* Nano Lett. **5** 1123 (2005)

Quantum Path Interferometry using Chirped High-order Harmonic Generation

S. Carlström¹, J. Preclíková^{1,2}, E. W. Larsen¹, E. Lorek¹, S. Bengtsson¹, C. M. Heyl¹, D. Paleček^{3,4}, A. L'Huillier¹, D. Zigmantas³, K. J. Schafer⁵, and J. Mauritsson¹

¹Department of Physics, Lund University, PO Box 118, SE-22100 Lund, Sweden

²Institute of Technology and Physics, University of Bergen, Allégatan 55, 5007 Bergen, Norway

³Department of Chemical Physics, Lund University, PO Box 124, SE-22100 Lund, Sweden

⁴Department of Chemical Physics and Optics, Charles University in Prague, Ke Karlovu 3, 121 16 Praha 2, Czech Republic

⁵Department of Physics and Astronomy, Louisiana State University, Baton Rouge, LA 70803, USA

Presenting Author: stefanos.carlstrom@fysik.lth.se

High-order harmonic generation (HHG) is a process usually described by a three-step model in which (i) an atom is ionized in a strong field which (ii) may accelerate the electron and force it back to its parent ion where (iii) it might recombine [1]. The electrons follow two major classes of trajectories in step (ii), termed the short and long trajectories, depending on the excursion time of the electron.

These three steps have been helpful to understand the basic principles of HHG, but the finer details are not captured in this crude model. The emission of the radiation is strongly dependent on the quantum paths of the electrons and each harmonic will have an intrinsic chirp, depending on which trajectory (short/long) that it originates from [2]. By chirping the driving field, the intrinsic chirp can be enhanced or cancelled leading to spectral broadening or narrowing, respectively. Since the emitted radiation from the short and the long trajectories overlap spectrally and spatially in the far-field, we can observe the interference between them [3] and control it by varying the chirp of the driving field. This is an analogue of an interferometer in that we can control the chirp of the individual “arms”, akin to how one controls the path length in a conventional interferometer.

Experimental data is compared to time-dependent Schrödinger equation calculations and a simple interference model based on Gaussian beams. The different interferences observed hint at the possibility of reconstructing the temporal structure of the full attosecond pulse train.

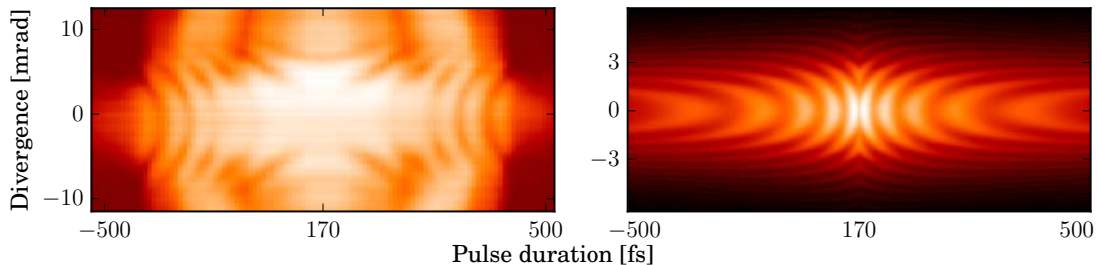


Figure 1: Spatial lineouts of the 17th harmonic of 1030 nm, for different pulse durations. A negative sign of the duration corresponds to negative chirp (red edge first, blue edge last) and vice versa. To the left, experimental data are shown, while to the right, the results from the simple Gaussian model are shown.

References

- [1] P. B. Corkum, Phys. Rev. Lett., **71**(13), 1994–1997, (1993)
- [2] K. Varjú *et al.*, J. Mod. Optic., **52**(2–3), 379–394 (2005)
- [3] A. Zaïr *et al.*, Phys. Rev. Lett., **100**(14) (2008)

The two-photon detachment of O^-

M. Génévriez¹, X. Urbain¹, A. Cyr², K. M. Dunseath², and M. Terao-Dunseath²

¹*Institute of Condensed Matter and Nanosciences, Université catholique de Louvain, Louvain-la-Neuve B-1348, Belgium*

²*Institut de Physique de Rennes, UMR 6251 CNRS-Université de Rennes 1, Campus de Beaulieu, F-35042 Rennes cedex, France*

Presenting Author: matthieu.genevriez@uclouvain.be

The two-photon detachment of the $O^-(1s^2 2s^2 2p^5 \ ^2P^o)$ state has not been widely studied, and the agreement between the few results available is not particularly good. The only existing experiment gives a generalized cross section of $4.2 \times 10^{-50} \text{ cm}^4 \text{ s}$ at a wavelength of 1064 nm [1]. An early calculation based on perturbation theory and a model potential [2] however yields, after interpolation, a value of $1.8 \times 10^{-49} \text{ cm}^4 \text{ s}$, more than four times larger. The results obtained using an adiabatic theory [3] are almost an order of magnitude larger than the experimental value. Clearly there is room for improvement. Here we report new experimental and theoretical results.

The two-photon detachment cross section has been measured with a 12 ns seeded Nd:YAG laser. The effects of the interaction volume were disentangled by repeatedly sweeping the laser beam across the ion beam [4]. The deconvolution of the detachment signal with the ion current density and its inverse Abel transformation were performed with Gaussian basis functions, and provided the instantaneous detachment probability under the assumption of a cylindrically symmetric laser beam. The absolute cross section is then expressed in terms of easily measurable quantities such as the pulse energy and the ion beam current.

Calculations were performed using the *R*-matrix Floquet (RMF) method. Wave functions for the three $1s^2 2s^2 2p^4$ states of the residual Oxygen atom, together with three pseudo-states, were built from Slater-type orbitals chosen to optimize the polarizability of the ground state [5]. The binding energy of O^- is -0.053800 Hartree, compared to the experimental value of -0.053695 Hartree. As the laser field breaks the spherical symmetry of space, the generalized cross sections for $O^- (|M_L| = 0, 1)$ are computed separately and subsequently averaged.

The results, in excellent mutual agreement, are presented in Fig. 1, together with previous experimental and theoretical data [1, 2].

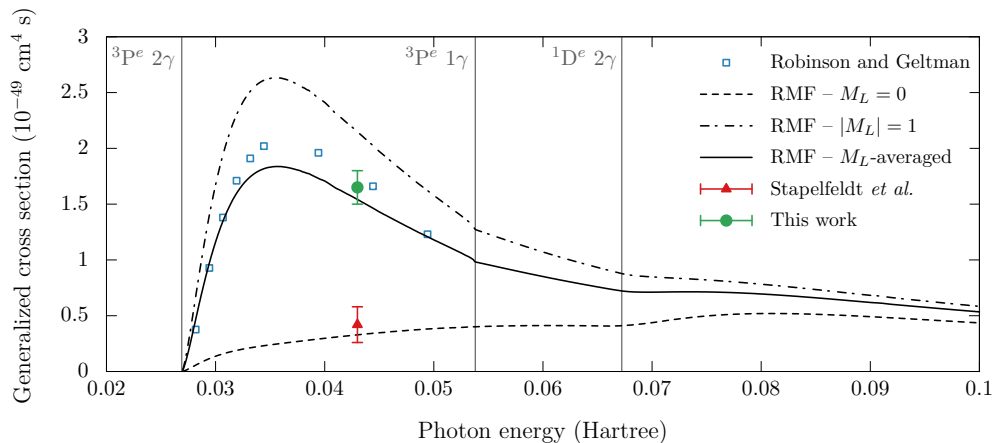


Figure 1: Generalized cross sections. The vertical lines indicate the position of thresholds.

References

- [1] H. Stapelfeldt, C. Brink, H. K. Haugen *J. Phys. B: Atom. Mol. Opt. Phys.* **24**, L437 (1991)
- [2] E. J. Robinson, S. Geltman *Phys. Rev. A* **153** 4 (1967)
- [3] G. F. Gribakin, M. Y. Kuchiev *J. Phys. B: Atom. Mol. Opt. Phys.* **30**, L657 (1997)
- [4] M. Génévriez, X. Urbain *Phys. Rev. A* **91**, 033403 (2015)
- [5] A. Cyr, *PhD thesis*, Université de Rennes 1, unpublished

Characterizing an ultra-high sensitivity atom interferometry gravimeter

Z.-K. Hu¹, M.-K. Zhou¹, L.-L. Chen¹, X.-C. Duan¹, and Q. Luo¹

¹*MOE Key Laboratory of Fundamental Physical Quantities Measurement, School of physics, Huazhong university of Science and technology, Wuhan 430074, China*

Presenting Author: zkhu@hust.edu.cn

Precisely measuring gravity acceleration g is of great interest for both fundamental research and practical applications. Instruments used to measure the absolute value of g have been highly developed during the last decades. In the recent development of gravimetry, cold-atom interferometry gravimeters play a crucial role for their high sensitivity and advantage of performing long time measurements. For high-precision gravity measurements and gravitational experiments, a cold-atom interferometry gravimeter with the aimed resolution of sub-micro Gal is being built in our cave laboratory. An atomic fountain based absolute gravimeter with a sensitivity of $4.2 \mu\text{Gal}/\sqrt{\text{Hz}}$ is demonstrated after dramatically suppression of the vibration noise. The main noise sources are analyzed, and a sensitivity calibration experiment is performed. The accuracy of this sub-micro Gal atom gravimeter depends on the analyzing of systematic errors. The systematic errors induced by some physical effects, such as the alignment of the Raman laser, the light shift, the gravity gradient and so on, have been measured with modulation experiments.

References

- [1] Min-Kang Zhou, Zhong-Kun Hu, Xiao-Chun Duan, Bu-Liang Sun, Le-Le Chen, Qiao-Zhen Zhang, and Jun Luo, Performance of a cold-atom gravimeter with an active vibration isolator, *Physical Review A*. **86**, 043630 (2012)
- [2] Zhong-Kun Hu, Bu-Liang Sun, Xiao-Chun Duan, Min-Kang Zhou, Le-Le Chen, Su Zhan, Qiao-Zhen Zhang, and Jun Luo, Demonstration of an ultrahigh-sensitivity atom-interferometry absolute gravimeter, *Physical Review A*. **88**, 043610 (2013)
- [3] Min-Kang Zhou, Zhong-Kun Hu, Xiao-Chun Duan, Bu-liang Sun, Jin-Bo Zhao and Jun Luo, Precisely mapping the magnetic field gradient in vacuum with an atom interferometer, *Physical Review A*. **82**, 061602R, (2010)
- [4] Zhong-Kun Hu, Xiao-Chun Duan, Min-Kang Zhou, Bu-liang Sun, Jin-Bo Zhao and Jun Luo, Simultaneous differential measurement of a magnetic-field gradient by atom interferometry double fountains, *Physical Review A*. **84**, 013620, (2011)

High repetition rate pulse trains emitted by optically thick scattering media

C. C. Kwong¹, T. Yang², D. Delande³, R. Pierrat⁴, and D. Wilkowski^{1,2,5}

¹*School of Physics and Mathematical Science, Nanyang Technological University, 637371 Singapore.*

²*Centre for Quantum Technologies, National University of Singapore, 117543 Singapore.*

³*Laboratoire Kastler Brossel, UPMC, CNRS, ENS, Collège de France, 4 Place Jussieu, 75005, Paris, France.*

⁴*ESPCI ParisTech, PSL Research University, CNRS, Institut Langevin, 1 rue Jussieu, 75005, Paris, France*

⁵*MajuLab, CNRS-University of Nice-NUS-NTU International Joint Research Unit UMI 3654, Singapore.*

Presenting Author: kwon0009@e.ntu.edu.sg

The coherent transmission through a scattering medium results from the interference between the incident field and the field scattered in the forward direction. In previous studies, it was shown that a high intensity flash, the so-called superflash, can be emitted in the forward direction just after an abrupt switch-off of a near resonant incident probe [1-2]. Similar flashes can also be generated by abruptly changing the phase of the incident field. Since it is a cooperative effect, the duration of the flash, in an optically thick medium, can be much shorter than the lifetime of a single atom excited state. More precisely, the flash decay time depends inversely on the optical thickness at resonance and zero temperature. When a phase change of π is applied periodically, a train of flashes will be emitted cooperatively with a repetition time that can be much shorter than the single atom excited state lifetime.

Recently, we experimentally demonstrated this phenomenon, using the narrow intercombination line of strontium [3]. An example of the pulse train generated in our experiment is shown in Fig. 1. Surprisingly, it is possible to suppress single atom fluorescence and transfer almost all the power in the incident probe to the pulse train. Remarkably, this is achievable while having a high intensity contrast in the pulse.

In this talk, we will review the underlying mechanism of the (super)flash effect with a particular emphasis on its temporal properties. Then, we will describe the experiment to observe the pulse trains. We will discuss the performance and potential applications of this pulse generating method.

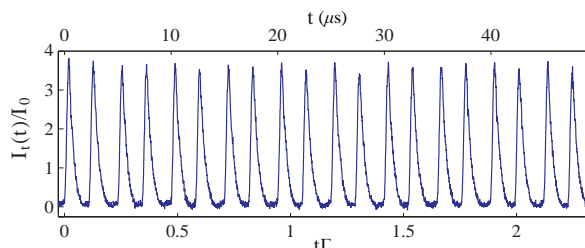


Figure 1: An example of a pulse train generated in our experiment. The repetition time of this pulse train is $0.12\Gamma^{-1}$, which is shorter than the lifetime of the transition, showing that cooperative effect are at play.

References

- [1] M Chalony *et al.*, Phys. Rev. A **84**, 011401(R) (2011).
- [2] C. C. Kwong *et al.*, Phys. Rev. Lett. **113**, 223601 (2014).
- [3] C. C. Kwong *et al.*, arXiv:1504.05077 [physics.atom-ph] (2015).

Heteronuclear Efimov scenario in an ultracold Bose-Fermi mixture of ^{133}Cs and ^6Li

J. Ulmanis¹, S. Häfner¹, R. Pires¹, E. D. Kuhnle¹, and M. Weidemüller^{1,2}

¹Physics Institute, Heidelberg University, Im Neuenheimer Feld 226, 69120 Heidelberg, Germany

²Hefei National Laboratory for Physical Sciences at the Microscale and Department of Modern Physics and CAS Center for Excellence and Synergetic Innovation Center in Quantum Information and Quantum Physics, University of Science and Technology of China, Hefei, Anhui 230026, China

Presenting Author: ulmanis@physi.uni-heidelberg.de

The Efimov scenario, where pairwise resonantly interacting particles form an infinite series of bound three-body states with universal scale invariance, has been a prominent topic in fundamental quantum physics for a long time. Presently the study of it mostly relies on the use of Feshbach resonances that allows one to precisely tune the interparticle interaction strength and probe these weakly bound trimers. An ultracold mixture of Cs and Li constitute a prototypical heteronuclear system with large mass imbalance, for which the scaling constant is drastically reduced. This is advantageous for the investigation of excited Efimov states under common experimental conditions.

Here we present the first observation of three consecutive Efimov resonances through measurements of three-body loss coefficients near a broad Feshbach resonance [1] (Fig. 1, left). The previous analysis of Feshbach resonances [2] is extended with radiofrequency association of LiCs Feshbach molecules [3] to precisely map the applied magnetic field onto the scattering length (Fig. 1, right). We measure dimer binding energies close to Feshbach resonances and extract Li-Cs scattering properties from them. The new parametrization allows us to quantitatively test few-body theories in the LiCsCs system. The refined positions and scaling factors of the Efimov resonances demonstrate both, universal behavior *and* non-universal deviations from the zero-range limit.

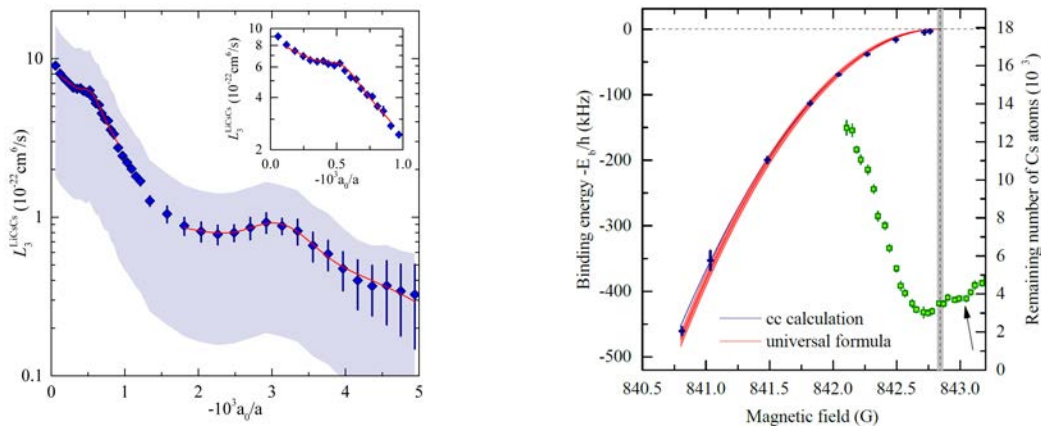


Figure 1: Left: LiCsCs three-body loss coefficient and fits (red lines) to the Efimov resonance positions. The inset shows a zoom in to the region of the first excited Efimov resonance. Right: Measured binding energies (blue crosses), molecular state energies from the coupled-channels model (blue line), and the universal binding energy $E_b = \hbar^2/(2\mu a^2)$ (red line) of LiCs Feshbach molecules near 843 G. The remaining Cs atom number (green squares) [1] indicates the second excited Efimov resonance. The vertical dashed line displays the determined Feshbach resonance pole position and its uncertainty.

References

- [1] R. Pires, J. Ulmanis, S. Häfner, E. D. Kuhnle and M. Weidemüller, Phys. Rev. Lett **112**, 250404 (2014)
- [2] R. Pires, J. Ulmanis, M. Repp, E. D. Kuhnle, M. Weidemüller, T. Tiecke, B. Ruzic, C. Greene, J. Bohn and E. Tiemann, Phys. Rev. A **90**, 012710 (2014)
- [3] J. Ulmanis, S. Häfner, R. Pires, E. D. Kuhnle, M. Weidemüller, E. Tiemann, New J. Phys. **17**, 055009 (2015)

Towards a molecular MOT of YbF

J. R. Almond¹, J. S. Bumby¹, J. Lim¹, N. J. Fitch¹, B. E. Sauer¹, M. R. Tarbutt¹, and E. A. Hinds¹

¹The Centre for Cold Matter, Blackett Laboratory, Imperial College London, UK

Presenting Author: j.almond13@imperial.ac.uk

The magneto-optical trap has been a powerful tool for producing ultracold atoms for a huge variety of applications. Magneto-optical trapping of molecules is new and is important for many applications including precision measurement, quantum simulation, quantum information processing and ultracold chemistry. Recently, such a molecular MOT has been demonstrated [1].

The molecular species, ytterbium fluoride (YbF) has been used to measure the electron's electric dipole moment (eEDM) [2]. Laser cooling of YbF is feasible by addressing the set of transitions illustrated in Fig. 2 [3]. We are building an experiment where YbF molecules will be captured and cooled to low temperatures in a MOT, and then launched into a fountain [4], as illustrated in Fig. 1. This fountain apparatus will greatly lengthen the transit time of the molecules through the eEDM experiment, which will allow us to make a new eEDM measurement with increased precision over the best previous measurement [5].

We will present our scheme for the YbF MOT, our work towards building the laser system and molecular source, and first results towards laser cooling of this molecule.

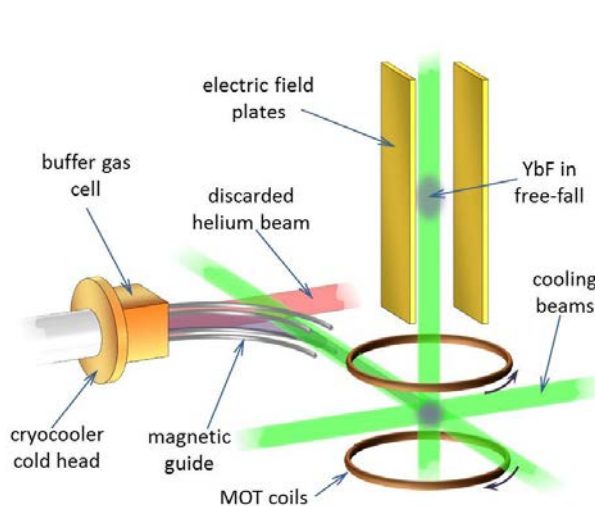


Figure 1: Schematic of the experimental design. YbF molecules are produced in a thermal beam from a cryogenic buffer gas source; the molecules are cooled by collisions with helium at 4 K. The YbF is deflected out of the beam and is brought to rest in a MOT. Trapped molecules are then launched upward to form a fountain in which the eEDM is measured.

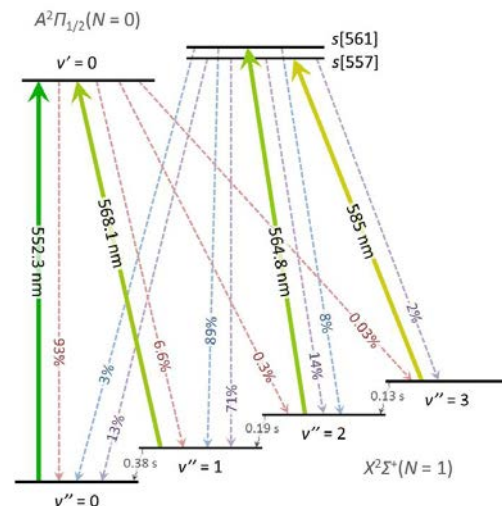


Figure 2: The molecular transitions we use for laser cooling and the required wavelengths of the cooling lasers. v'' and v' are the vibrational quantum numbers of the ground and excited states respectively. Franck-Condon factors are given as percentages. The linewidth of the $v' = 0$ state is 5.7 MHz.

References

- [1] J. Barry *et al.*, Nature **512** 286 (2014)
- [2] J. Hudson *et al.*, Nature **473** 493 (2011)
- [3] I. Smallman *et al.*, J. Mol. Spectrosc. **300**, 3 (2014)
- [4] M. Tarbutt *et al.*, New J. Phys. **15** 05034 (2013)
- [5] The ACME Collaboration, Science **343** 269 (2014)

Progress towards in-beam hyperfine spectroscopy of antihydrogen

E. Widmann¹, A. Capon¹, P. Caradonna¹, M. Diermaier¹, B. Kolbinger¹, S. Lehner¹, C. Malbrunot¹, O. Massiczek¹, C. Sauerzopf¹, M. C. Simon¹, M. Wolf¹, and J. Zmeskal¹

¹*Stefan Meyer Institute for subatomic Physics, Vienna, Austria*

Presenting Author: eberhard.widmann@oeaw.ac.at

Antihydrogen is the simplest atom consisting purely of antimatter. Its matter counterpart, hydrogen, is one of the best studied atomic systems in physics. Thus comparing the spectra of hydrogen and antihydrogen offers some of the most sensitive tests of matter-antimatter symmetry. The ASACUSA collaboration is pursuing an experiment to measure the ground-state hyperfine splitting of antihydrogen in a polarized beam [1,2], a quantity which was measured in hydrogen in a beam to a relative precision of 4×10^{-8} [3] and in a maser to better than 10^{-12} [4,5].

After recently reporting the first observation of a beam of antihydrogen atoms 2.7 m downstream of the formation region in a field-free environment [6], the atomic resonance beam apparatus to perform a hyperfine measurement was completed. During the shutdown of CERN, a source of cold polarized hydrogen atoms was built and experiments were performed to characterize the apparatus with a hydrogen beam of similar properties as compared to the expected antihydrogen beam. Hyperfine structure spectra of hydrogen showing encouraging results for the achievable precision for a measurement with antihydrogen will be reported.

References

- [1] E. Widmann *et al.*, in *The Hydrogen Atom: Precision Physics of Simple Atomic Systems* (ed. S. Kahrshenboim) pp. 528–542 (Lecture Notes in Physics vol. 570), Springer (2001)
- [2] E. Widmann *et al.*, *Hyperfine Interact.* **215** 1 (2013)
- [3] A. G. Prodel and P. Kusch, *Physical Review* **88** 184 (1952)
- [4] H. Hellwig *et al.*, *IEEE Trans. Instr. Meas.* **IM 19** 200 (1970)
- [5] L. Essen *et al.*, *Nature* **229** 110 (1971)
- [6] N. Kuroda *et al.*, *Nature Communications* **5** 3089 (2014)

Phase transitions of sympathetic cooling of HCI ions

J. Pedregosa-Gutierrez¹, C. Champenois¹, M. Knoop¹, L. Schmöger^{2,3}, and J. R. Crespo López-Urrutia²

¹*Aix Marseille Université, CNRS, PIIM UMR 7345, 13397, Marseille, France*

²*Max-Planck-Institut für Kernphysik, D-69116, Heidelberg, Germany*

³*Physikalisch-Technische Bundesanstalt, Bundesallee 100, 38116 Braunschweig, Germany*

Presenting Author: jofre.pedregosa@univ-amu.fr

An ion cloud confined in a linear RF-quadrupole trap is an example of a non-neutral plasma, a plasma consisting of particles with a single sign of charge. When laser-cooled, the trapped ions form ordered structures, called Coulomb crystals [1]. The morphology of these crystals depends on the ratio of the axial and radial motional frequencies associated to the effective harmonic potentials that form the RF linear trap. Particles of different charge-to-mass ratio, e/m can be trapped and allow to create multi-species crystals. Coulomb crystals are ideal candidates for the study of structural transitions, of particular interest is the second order phase transition associated to the morphological change from one chain to a zig-zag [2].

At this 47th EGAS conference, we will present a numerical study, performed using molecular dynamics simulations, concerning the phase transition of Highly Charged Ions (HCI) sympathetically cooled by laser-cooled simple atomic ions in a multispecies crystal. Due to the different charge-to-mass ratio, the HCI are located in the centre of the crystal. The screening introduced by the surrounding ions is expected to modify the behaviour of the chain to zig-zag transitions. While the present study is purely numerical, recent experimental work has demonstrated first evidence for the feasibility of such systems [3].

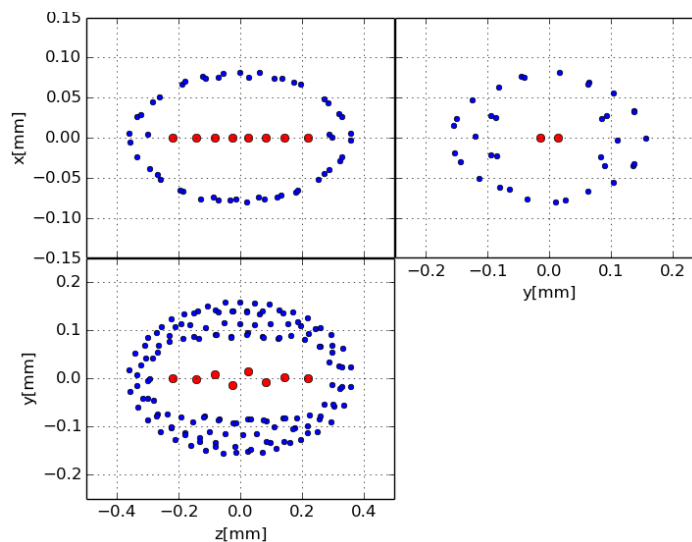


Figure 1: Sympathetically cooled Ar^{13+} (5 ions) by laser cooled Be^+ (256 ions). The HCI are in a zig-zag structure while the Be ions form a 3D crystal around.

References

- [1] P. Rowe, *et al.*, Phys. Rev. Letters **82**, 2071 (1999).
- [2] G. Morigi and S. Fishman, Phys. Rev. E **70**, 066141 (2004).
- [1] L. Schmöger, *et al.*, Science **347**, 1233 (2015).

Experiments with an ultracold molecular lattice clock: subradiance, forbidden transitions, and E1 / M1 / E2 photodissociation

M. McDonald¹, B. H. McGuyer¹, G. Z. Iwata¹, M. G. Tarallo¹, A. T. Grier¹, T. Zelevinsky¹, F. Apfelbeck², I. Majewska³, W. Skomorowski^{3,4}, and R. Moszynski³

¹*Department of Physics, Columbia University, 538 West 120th Street, New York, NY 10027-5255*

²*Faculty of Physics, Ludwig Maximilian University of Munich, Schellingstrasse 4, D-80799 Munich, Germany*

³*Quantum Chemistry Laboratory, Department of Chemistry, University of Warsaw, Pasteura 1, 02-093 Warsaw, Poland*

⁴*Present address: Institute of Physics, University of Kassel, Heinrich-Plett-Strasse 40, 34132 Kassel, Germany*

Presenting Author: mpm2153@columbia.edu

When a molecule is subjected to laser light tuned above a dissociation threshold, the molecule can break apart into fragments whose angular distribution depends critically on the character of the particular channel by which dissociation occurs. When the initial state is well-defined, the angular distributions of the photofragments at various frequencies above threshold can be fitted to determine the shapes of the final molecular potentials involved as well as the relative strengths of the contributing pathways.

We measure the photofragment distributions of photodissociated state-selected ⁸⁸Sr₂ molecules via absorption imaging, with an imaging beam parallel to the probe axis. The molecules are produced via photoassociation from ⁸⁸Sr atoms cooled to a few μ K, trapped in a 1D optical lattice, and probed along the lattice axis. The resulting images show rings of atoms whose angular distributions encode the strength and character of the participating dissociation pathways. We present measurements of one- and two-photon photodissociation of either E1 or M1 / E2 character. The measurements of M1 / E2 photodissociation are achieved by coherently populating a subradiant excited state for which E1 photodissociation to the ground state is forbidden, and can therefore only occur due to higher order processes.

In addition to photodissociation experiments, we present recent work toward the realization of a molecular clock, including: magnetic field-enabled control of highly forbidden ($\Delta J = 2,3$) transitions between weakly bound rovibrational levels¹; production and precision characterization of long-lived “subradiant” states, so-called because quantum mechanical symmetries forbid E1 decay to the ground state²; and a new method for characterizing the temperature of a cloud of particles confined to a roughly harmonic trap by examining the lineshape produced by “carrier transitions”, i.e. those transitions which preserve motional quantum number between initial and final state³.

References

- [1] B. H. McGuyer *et al.* arXiv:1503.05946v1 (2015)
- [2] B. H. McGuyer *et al.* Nature Physics **11** 32–36 (2015)
- [3] M. McDonald *et al.* Physical Review Letters **114** 023001 (2015)

Storing keV negative ions for hours: Lifetime measurements in new time domains

S. Mannervik¹, E. Bäckström¹, D. Hanstorp², O. M. Hole¹, M. Kaminska^{1,3}, R. F. Nascimento¹, M. Blom¹, M. Björkhage¹, A. Källberg¹, P. Löfgren¹, P. Reinhed¹, S. Rosèn¹, A. Simonsson¹, R. D. Thomas¹, H. T. Schmidt¹, and H. Cederquist¹

¹Department of Physics, Stockholm University, AlbaNova University Center, SE-106 91 Stockholm, Sweden

²Department of Physics, University of Gothenburg, SE-412 96 Göteborg, Sweden

³Institute of Physics, Jan Kochanowski University, 25-369 Kielce, Poland

Presenting Author: mannervik@fysik.su.se

We have measured the radiative lifetime of the ${}^2P_{1/2}^o$ level in S^- using the cryogenic electrostatic ion-storage ring DESIREE (Double ElectroStatic Ion Ring ExpEriment) [1–3]. The ${}^2P_{1/2}^o$ fine structure level is metastable and decays to the ${}^2P_{3/2}^o$ ground state through a slow magnetic dipole (M1) transition. We utilized a laser probing technique photo-detaching small fractions of the ions in a stored beam by a series of laser pulses. By using two different laser wavelengths we monitored the neutral yield due to detachment of ions in the metastable state only and due to detachment of ions in both the ground- and metastable states. The inverse of the longer (1/e)-lifetime when both states were detached was taken as a measure of the residual-gas density. We repeated these steps at slightly elevated ring temperatures of 15–17 K, which gave higher residual-gas densities than at 13 K. In Fig. (1) we show the decay rates for different residual-gas densities. The intercept with the vertical axis in Fig. (2) gives the inherent spontaneous lifetime of the ${}^2P_{1/2}^o$ level ($\tau=503\pm 43$ s) [3]. This is by far the longest lifetime ever measured for a negatively charged ion. The difference from the theoretical prediction 437 s is 1.3σ showing that the multi-configuration Dirac-Fock method applied in [4] may be appropriate to describe the features of excited fine-structure levels in atomic anions at this level of precision. The present results demonstrate the power of the new method and opens up for a broad survey of lifetimes of excited states in atomic ions in the time range from some tens of milliseconds to tens of minutes.

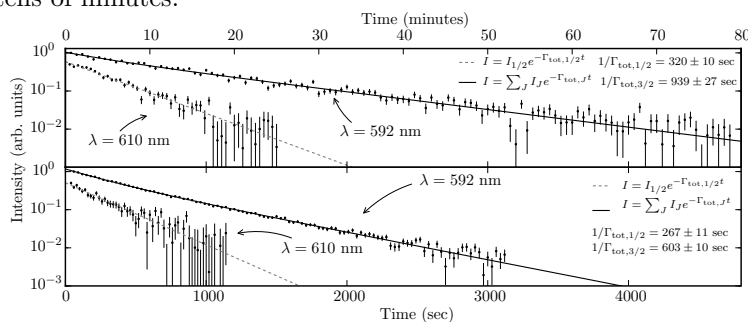


Figure 1: Laser-probing measurements of only metastable (points for $\lambda = 610$ nm) and both metastable and ground-state-level populations (points for $\lambda = 592$ nm) as functions of time at 13 K (top) and at 15 K (bottom) (from ref. [3]).

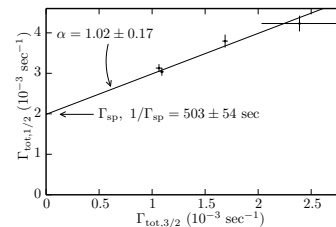


Figure 2: Measured decay rate of the ${}^2P_{1/2}^o$ level (ordinate) plotted with measured decay rate of the ${}^2P_{3/2}^o$ level (abscissa) (from ref. [3]).

References

- [1] R. D. Thomas *et al.* Rev. Sci. Instrum. **82** 065112-1–18 (2011)
- [2] H. T. Schmidt *et al.* Rev. Sci. Instrum. **84** 055115-1–6 (2013)
- [3] E. Bäckström *et al.* Phys. Rev. Lett. **114** 143003-1–5 (2015)
doi:10.1103/PhysRevLett.114.143003
- [4] P. Andersson *et al.* Phys. Rev. A **73** 032705-1–8 (2006)

Linear polarization of x-ray transitions due to dielectronic recombination in highly charged ions

H. Joerg¹, Z.-K. Hu¹, H. Bekker², M. A. Blessenohl², D. Hollain², S. Fritzsche^{3,4}, A. Surzhykov⁴, C. Shah¹, J. R. Crespo López-Urrutia², and S. Tashenov¹

¹Department of Physics, University of Heidelberg, Heidelberg

²Max-Planck Institute for Nuclear Physics, Heidelberg

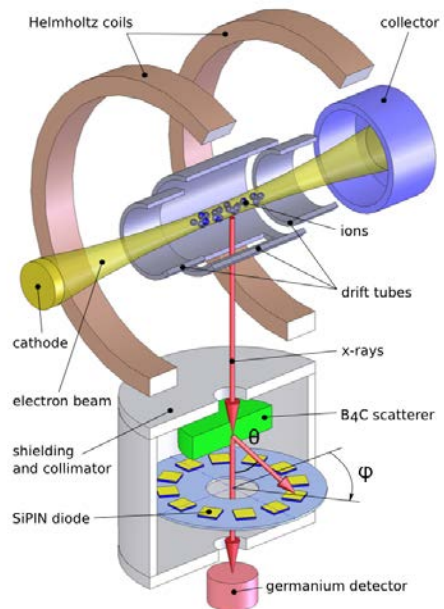
³Theoretisch-Physikalisches Institut, Friedrich-Schiller-University Jena, Jena

⁴Helmholtz-Institut Jena, Jena

Presenting Author: hjoerg@physi.uni-heidelberg.de

We report the first measurement of linear polarization of x rays emitted in the process of dielectronic recombination (DR) into highly charged xenon ions. We observed that the polarization of x rays, following the dielectronic capture exciting the state $[1s2s^22p_{1/2}]_1$, is highly sensitive to the Breit interaction. The experimental results for this transition rule out by 5σ calculations not taking the Breit interaction into account. The latter accounts for retardation and magnetic contributions to the Coulomb repulsion between electrons. The ions in the He- though O-like charge states were produced in an electron beam ion trap (EBIT). The electron-ion collision energy was tuned into the KLL DR resonance, where an electron recombines into the L- shell and an electron from the ion is excited from the K- to the L-shell. The polarization of x rays which were emitted perpendicular to the electron beam propagation direction was analyzed using Compton polarimetry. For this the x rays were Compton scattered in a block of boron carbide. The scattered x rays were detected by an array of SiPIN diodes which sampled the azimuthal angular scattering distribution. The Klein-Nishina formula was fitted to the measured distribution having the degree of linear polarization as a free parameter. The degree of polarization was extracted with the typical accuracy of below 10%, ranging between -43% to 53%. This first measurement of the degree of polarization of DR transitions opens possibilities for polarization diagnostics of hot plasmas. Such diagnostics will be sensitive to the directionality of the electron-ion collisions and thus revealing the plasma anisotropies.

Figure 1: Scheme of the experiment: x rays emitted by the xenon ions, that are produced and trapped in the EBIT, are scattered by a block of boron carbide. The azimuthal distribution of the scattered x rays is measured by an array of SiPIN diodes. A germanium detector registered unscattered x rays.



References

- [1] H. Joerg *et al.* Phys. Rev. A. **91** 042705 (2015)

Pushing a Fermi superfluid through a thin optical barrier: from coherent tunneling to phase slips

A. Burchianti^{1,2}, G. Valtolina^{1,2,3}, E. Neri^{1,2}, K. Khani^{1,2}, A. Trombettoni⁴, A. Smerzi⁵, M. Inguscio⁶, M. Zaccanti^{1,2}, and G. Roati^{1,2}

¹INO-CNR, via Nello Carrara 1, I-50019 Sesto Fiorentino, Italy

²LENS and Università di Firenze, via Nello Carrara 1, I-50019 Sesto Fiorentino, Italy

³Scuola Normale Superiore, Piazza dei Cavalieri 7, I-56126 Pisa, Italy

⁴SISSA and INFN, Sezione di Trieste, via Beirut 2/4, I-34151 Trieste, Italy

⁵QSTAR, INO-CNR and LENS, Largo Fermi 2, I-50125 Firenze, Italy

⁶INRIM, Strada delle Cacce 91, I-10135 Torino, Italy

Presenting Author: burchianti@lens.unifi.it

We study, across the whole BEC-BCS crossover, the dynamics of a Fermi superfluid flowing in the presence of a thin barrier ($d \sim 5k_F^{-1}$). For this purpose, we produce a two-component ${}^6\text{Li}$ quantum gas [1] in a double-well potential created by superimposing a repulsive optical barrier of micrometric thickness on the harmonic optical trap. The dynamics is started by establishing an initial difference in the number of particles between the two wells. We explore different regimes, from a BEC of composite molecules to a BCS superfluid, by magnetically controlling the two-spin interaction by means of a Fano-Feshbach resonance. By tuning the barrier height and the starting imbalance, we observe either Josephson tunneling or dissipation via phase slips. In the former case, occurring for small amplitude oscillations as the barrier height reaches or exceeds the chemical potential, we find that the superfluid current exhibits a maximum at the unitarity, as a consequence of the interplay between phonon excitations and pair-breaking [2–4]. The phase slip mechanism is instead observed for larger starting imbalances and is associated to the superfluid flow dissipation caused by the formation of topological defects [5]. In our geometry, we observe vortex rings detaching from the barrier and penetrating the cloud; since the vortices take energy from the flow, the superfluid current drops. This process is analog to the one observed in superfluid ${}^4\text{He}$ forced through a constriction [6]. We found that also the critical velocity for vortex nucleation is maximum on the crossover further confirming the superfluidity robustness for resonant atomic interactions [7].

References

- [1] A. Burchianti *et al.* Phys. Rev. A **90**, 043408 (2014)
- [2] R. Combescot, M.Yu. Kagan, S. Stringari Phys. Rev. A **74**, 042717 (2006)
- [3] A. Spuntarelli, P. Pieri, G.C. Strinati Phys. Rev. Lett. **99**, 040401 (2007)
- [4] P. Zou, F. Dalfovo J. Low Temp. Phys. **177**, 240–256 (2014)
- [5] F. Piazza, Lee A. Collins, A. Smerzi New J. Phys. **13**, 043008 (2011)
- [6] E. Hoskinson *et al.* Nat. Phys. **2**, 23–26 (2006)
- [7] D. E. Miller *et al.* Phys. Rev. Lett. **99**, 070402 (2007)

Atom-Chip for Quantum Control

M. S. Cherukattil¹, C. Lovecchio¹, M. Ali Khan¹, F. Caruso^{1,2}, and F. S. Cataliotti^{1,2}

¹*LENS and Università di Firenze, via Nello Carrara 1, I-50019 Sesto Fiorentino, Italy*

²*QSTAR, Largo Enrico Fermi 2, 50125 Firenze, Italia*

Presenting Author: shahid@lens.unifi.it

We implemented a versatile set-up where bi-chromatic radiation in a Raman configuration can be shined onto a Bose-Einstein condensate produced in an Atom-Chip. The Atom-Chip is also equipped with RF sources for coherent transfer of atoms between internal states in order to realize an atom interferometer capable of fully characterizing the atomic state. We demonstrated a completely new scheme for the tomographic reconstruction of atomic states that combines the inherent stability of the atom chip setup with the flexibility of optimization schemes. This scheme allowed confirming of the superb control on parameters allowed by the experimental set-up and put it to use on improved control algorithms to realise arbitrary superposition states. With our Atom-Chip, we were also able to demonstrate, for the first time, Quantum Zeno dynamics.

References

[1] C. Lovecchio, S. Cherukattil, B. Cilenti, I. Herrera, F. S. Cataliotti, S. Montenegro, T. Calarco, F. Caruso arXiv:1504.01963 [quant-ph] 8 Apr 2015

Creation of $^{87}\text{RbCs}$ molecules in the rovibrational ground state

P. K. Molony¹, P. D. Gregory¹, A. Kumar¹, B. Lu¹, Z. Ji¹, M. P. Köppinger¹, C. Ruth Le Sueur²,
C. L. Blackley², J. M. Hutson², and S. L. Cornish¹

¹Joint Quantum Centre (JQC) Durham/Newcastle, Department of Physics, Durham University, South Road,
Durham DH1 3LE, United Kingdom

²Joint Quantum Centre (JQC) Durham/Newcastle, Department of Chemistry, Durham University, South
Road, Durham, DH1 3LE, United Kingdom

Presenting Author: p.k.molony@dur.ac.uk

Ultracold and quantum degenerate mixtures of two or more atomic species open up many new research avenues, including the formation of ultracold heteronuclear ground-state molecules possessing a permanent electric dipole moment [1]. The anisotropic, long range dipole-dipole interactions between such molecules offer many potential applications, including novel schemes for quantum information processing [2] and simulation [3]. Heteronuclear ground-state molecules have been created in KRb [4] and, very recently, in RbCs [5]. Here we present our recent results including, the complete Feshbach spectroscopy of an ultracold $^{85}\text{Rb-Cs}$ mixture [6] and the formation of ultracold Cs_2 and $^{87}\text{RbCs}$ Feshbach molecules [7,8]. Finally we show a simple design for a tuneable, narrow-linewidth, two-colour laser system [9] and demonstrate transfer of the $^{87}\text{RbCs}$ Feshbach molecules into the rovibrational ground state via Stimulated Raman Adiabatic Passage (STIRAP) [10].

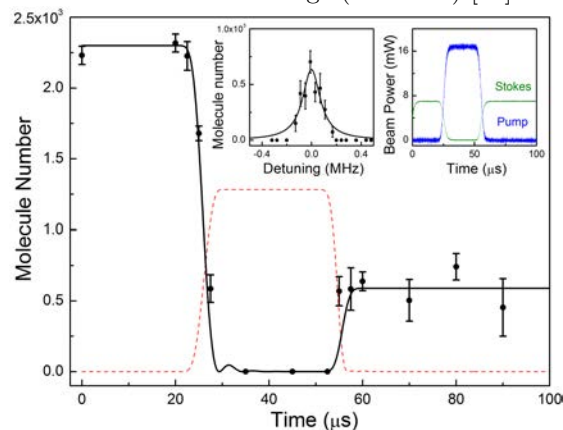


Figure 1: STIRAP transfer between the Feshbach and rovibrational ground states. Plotted is the number of molecules remaining in the Feshbach state when both STIRAP lasers are switched off at various points during the routine. From this, we measure a one-way efficiency of 50%. A model is shown based on the measured Rabi frequencies (not including laser noise), with the Feshbach- and ground-state populations shown in black solid and red dashed lines respectively. Left inset: The same STIRAP sequence as a function of Stokes detuning. Right inset: The pump and Stokes beam powers during the STIRAP pulse sequence.

References

- [1] L.D. Carr et al., *New J. Phys.* **11**(5), 055049 (2009)
- [2] D. DeMille, *Phys. Rev. Lett.* **88**, 067901 (2002)
- [3] A. Micheli et al., *Nat. Phys.* **2**, **341** (2006)
- [4] K.-K. Ni et al., *Science* **322**, 5899 (2008)
- [5] T. Takekoshi et al., *Phys. Rev. Lett.* **113**, 205301 (2014)
- [6] H-W. Cho et al., *Phys. Rev. A* **87**, 010703(R) (2013)
- [7] M.P. Köppinger et al. *New J. Phys.* **16** 115016 (2014)
- [8] M.P. Köppinger et al. *Phys. Rev. A* **89**, 033604 (2014)
- [9] P.D. Gregory et al. *New J. Phys.* **17**, 055006 (2015)
- [10] P.K. Molony et al., *Phys. Rev. Lett.* **113**, 255301 (2014)

Engineering spin Hamiltonians with 2D arrays of single Rydberg atoms

D. Barredo¹, H. Labuhn¹, S. Ravets¹, T. Lahaye¹, and A. Browaeys¹

¹Laboratoire Charles Fabry, Institut d'Optique, CNRS, Univ Paris Sud, 2 avenue Augustin Fresnel, 91127 Palaiseau cedex, France

Presenting Author: daniel.barredo@institutoptique.fr

Cold Rydberg atoms are a promising scalable platform for the quantum simulation of spin models that describe a large variety of quantum many-body phenomena in condensed matter physics.

We will present the latest results of our experiment, where we exploit van der Waals [1] and dipole-dipole interactions [2,3] between single Rydberg atoms in fully configurable 2D arrays to engineer different type of spin Hamiltonians. As proof-of-principle experiments we study the coherent dynamics of spin excitations in systems of three Rydberg atoms. We show that their dynamics are accurately described by parameter-free theoretical models and we analyze the role of the small remaining experimental imperfections [1,3]. In larger arrays of a few tens of spins (Fig. 1), either fully ordered or disordered, we measure the coherent evolution of the particles interacting under an Ising-type Hamiltonian after a quantum quench.

Our results open exciting possibilities in quantum magnetism to study, for example, the role of disorder and the emergence of geometry-induced frustration in such systems.

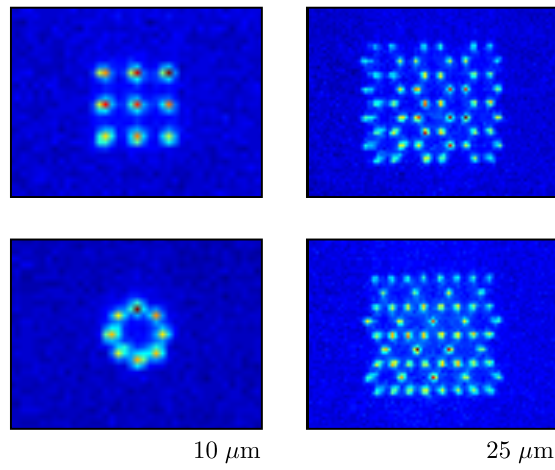


Figure 1: Fluorescence images of single atoms trapped in microtrap arrays with different geometries [4].

References

- [1] D. Barredo *et al.* Phys. Rev. Lett. **112**, 183002 (2014)
- [2] S. Ravets *et al.* Nat. Phys. **10**, 914 (2014)
- [3] D. Barredo *et al.* Phys. Rev. Lett. **114**, 113002 (2015)
- [4] F. Nogrette *et al.* Phys. Rev. X **4**, 021034 (2014)

Trapping ultracold argon atoms

P. D. Edmunds¹, P. F. Barker¹

¹*Department of Physics and Astronomy, University College London, Gower Street, London WC1E 6BT, United Kingdom*

Presenting Author: p.edmunds@ucl.ac.uk

Thermalising collisions between molecules and laser cooled atoms are a promising general method for dissipative cooling, but typical laser cooled species are reactive and cannot generally be utilised [1]. Trapped noble gas atoms in their ground state appear to be ideal candidates for the sympathetic cooling as they are chemically inert and can be laser cooled to μK temperatures in an excited metastable state.

We describe the dipole trapping of both metastable and ground state argon atoms for sympathetic cooling. Metastable argon atoms are first Doppler-cooled down to $\sim 80 \mu\text{K}$ in a magneto-optical trap (MOT) and are loaded into a dipole trap formed within the focus of an optical build-up cavity. The optical cavity's well depth could be rapidly modulated [2]: allowing efficient loading of the trap, characterisation of trapped atom temperature, and reduction of intensity noise. Collisional properties of the trapped metastable atoms were studied within the cavity and the Penning and associative losses from the trap calculated.

Ground state noble gas atoms were also trapped for the first time by optically quenching metastable atoms to the ground state and then trapping the atoms in the cavity field (shown in figure 1) [3]. Although the ground state atoms could not be directly probed, we detected them by observing the additional collisional loss from co-trapped metastable argon atoms. This trap loss was used to determine an ultra-cold elastic cross section between the ground and metastable states and was shown to lead to type of sympathetic evaporation of the metastable atoms. Using a parametric loss spectroscopy we also determined the polarisability of metastable argon at the trapping wavelength of 1064 nm.

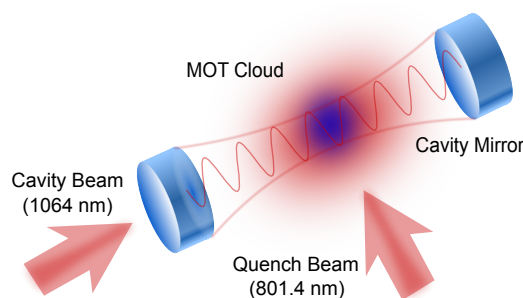


Figure 1: Schematic of the optical cavity. Metastable argon is first cooled in a MOT, and then quenched down to the ground state. Both species can be trapped in the lattice formed within the optical build-up cavity.

References

- [1] M. Lara *et al.*, Physical Review Letters **97**, 183201 (2006)
- [2] P. D. Edmunds, P. F. Barker, Review of Scientific Instruments **84**, 083101 (2013)
- [3] P. D. Edmunds, P. F. Barker, Physical Review Letters **113**, 183001 (2014)

Measurement of the coherent optical response of a cold atomic ensemble in the presence of resonant dipole-dipole interactions

Y. R. P. Sortais¹, S. Jennewein¹, N. Schilder¹, J.-J. Greffet¹, and A. Browaeys¹

¹Laboratoire Charles Fabry, Institut d'Optique, CNRS, Univ. Paris Sud, 2 avenue Augustin Fresnel, 91127 Palaiseau cedex, France

Presenting Author: yvan.sortais@institutoptique.fr

When light scatters on an ensemble of randomly positioned particles, the scattered field has a coherent component, corresponding to its average over many realizations of the random distribution of particles, and an incoherent component, corresponding to the fluctuations of the field around the configuration-averaged field. When the inter-particle distance becomes small in comparison to the wavelength of light, resonant dipole-dipole interactions play an increasing role and modify the way the light is scattered. Using a microscopic and dense atomic cloud, we have for instance recently demonstrated that the incoherent response is no longer proportional to the number of atoms in the presence of interactions, but is rather strongly suppressed. This can be interpreted using a microscopic approach and solving for the time-evolution of the atomic dipoles driven by the external light field as well as the fields scattered by the neighboring dipoles [1].

The near-resonance coherent optical response of cold atomic gases is also modified by dipole-dipole interactions and has been at the focus of recent investigations by several groups, both experimentally [2,3] and theoretically [4,5]. Partly to test the textbook theory of the local-field correction used to describe the coherent optical response of dense atomic media : this theory explains the recently measured cooperative Lamb-shift in hot vapour cells [6] but is predicted to break down when inhomogeneous broadening is absent [5]. Also, one may expect that a dense atomic medium would imprint a large phase shift on the coherently scattered field, a feature of great interest in the context of cold-atom based quantum technologies. Recent experiments performed with single ions, atoms, and molecules have demonstrated in a quite impressive way that single particles can imprint a phase of a few degrees on a laser beam [7,8,9], thus making the observation of a large phase shift induced by a many-body system much wanted.

Here I will present the first observation of a large phase shift (~ 1 rad) imprinted on a laser beam by a dense atomic cloud. This phase shift results from the interference of the incident laser field and the field that is coherently scattered in the direction of propagation of the laser. We measure this phase shift by directly recording the transmission signal on a photodiode in counting mode. In contrast with previous experiments performed with dense atomic media, this large phase shift is associated to a moderate extinction in our case, even at resonance. As in the incoherent case, the saturation of the extinction is a signature of the collective behaviour of the atomic cloud, which has a transverse size smaller than the wavelength of light. Also, the large phase shift is associated to a large group delay (up to -10 ns), which we measure independently by measuring the time resolved coherent response of the atomic cloud to a pulse of light. This corresponds to a very low and negative group velocity (-300 m/s).

References

- [1] J. Pellegrino *et al*, Phys. Rev. Lett. **113**, 133602 (2014).
- [2] C.C. Kwong *et al*, Phys. Rev. Lett. **113**, 223601 (2014).
- [3] K. Kemp *et al*, arXiv:1410.2497 [physics.atom-ph].
- [4] J. Javanainen, J Ruostekoski, Y. Li and S.-M. Yoo *et al*, Phys. Rev. Lett. **112**, 113603 (2014).
- [5] J. Javanainen and, J Ruostekoski, arXiv:1409.4598 [physics.atom-ph].
- [6] J. Keaveney *et al*, Phys. Rev. Lett. **108**, 173601 (2012).
- [7] S.A. Aljunid *et al*, Phys. Rev. Lett. **103**, 153601 (2009).
- [8] M. Pototschnig *et al*, Phys. Rev. Lett. **107**, 063001 (2011).
- [9] A. Jechow *et al*, Phys. Rev. Lett. **110**, 113605 (2013).

Cavity cooling a single charged levitated nanosphere

J. Millen¹, P. Z. G. Fonseca², T. Mavrogordatos², T. S. Monteiro², and P. F. Barker²

¹*Faculty of Physics, University of Vienna, Boltzmannngasse 5, A-1090 Wien, Austria*

²*Department of Physics and Astronomy, University College London, Gower Street, London WC1E 6BT, United Kingdom*

Presenting Author: ucappzu@ucl.ac.uk

The cooling of the centre-of-mass motion of a levitated macroscopic particle is seen as an important step towards the creation of long-lived macroscopic quantum states and the study of quantum mechanics and nonclassicality at large mass scales [1]. Levitation in vacuum minimizes coupling to the environment, while the lack of clamping leads to extremely high mechanical quality factors of the oscillating particle [2]. The ability to rapidly turn off the levitation coupled with cooling, offers the prospect of interferometry in the absence of any perturbations other than gravity [3]. However, like cold atoms trapped in vacuum, levitated nanoparticles are sensitive to parametric noise and internal heating via even a small absorption of the levitating light field [4]. To date this has limited the lower pressure at which particles can be stably trapped and cavity cooled. We overcome this problem by levitating a naturally charged silica nanosphere in a hybrid electro-optical trap by combining a Paul trap with an optical dipole trap formed from a single mode optical cavity (figure 1). We show that the hybrid nature of the trap introduces an unexpected synergy where the Paul trap plays an important role in the cavity cooling dynamics by introducing a cyclic displacement of the equilibrium point of the mechanical oscillations in the optical field [5]. This eliminates the need for a second, dedicated cooling optical mode of the cavity [6] and importantly allows us to cool the trapped particle in vacuum to mK temperatures.

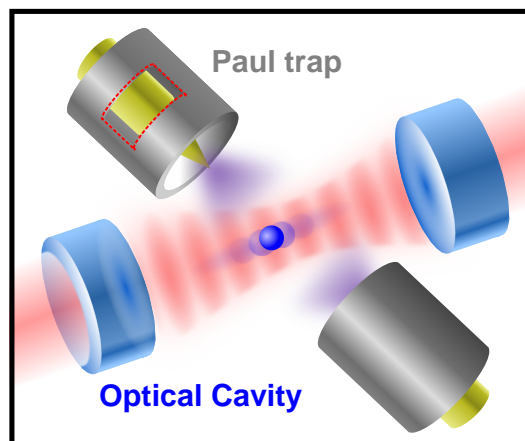


Figure 1: A schematic diagram of the hybrid trap consisting of a Paul trap and standing wave optical cavity potential.

References

- [1] P. F. Barker, M. N. Shneider, *Phys. Rev. A*, **81**, 023826 (2010)
- [2] D. E. Chang, *et al.* *Proc. Natl Acad. Sci. USA*, **107**, 1005 (2010)
- [3] O. Romero-Isart, *et al.* *Phys. Rev. Lett.* **107**, 020405 (2011)
- [4] J. Millen, *et al.* *Nature Nano.*, **9**, 425 (2014)
- [5] J. Millen, *et al.* *Phys. Rev. Lett.* **114**, 123602 (2015)
- [6] G. A. T.Pender, *et al.* *Phys. Rev. A* **85**, 021802 (2012).

A time domain matter-wave interferometer for testing the mass limits of quantum mechanics

J. Rodewald¹, N. Dörre¹, P. Geyer¹, U. Sezer¹, P. Haslinger¹, and M. Arndt¹

¹*Faculty of Physics, University of Vienna, Vienna Center for Quantum Science and Technology (VCQ), Vienna, Austria*

Presenting Author: jonas.rodewald@univie.ac.at

We demonstrate a matter-wave interferometer in the time domain (OTIMA) as a powerful tool for testing the validity of quantum theory for increasingly heavy and large particles [1,2]. The interferometer operates in the near-field regime and utilizes three pulsed standing laser wave gratings. These imprint, on the one hand, a periodic phase pattern on to the traversing matter waves and, on the other hand, the photo depletion probability is modulated periodically with the distance from the reflecting mirror. Depending on the particle's ionization or fragmentation cross section and optical polarizability such gratings thus act as absorptive masks and phase gratings with an exceptionally small grating period of less than 80nm [3,4]. The pulsed scheme of the experiment facilitates interference measurements in the time domain which offers high count rate, visibility and measuring precision [5]. Since the action of optical gratings is non-dispersive the experiment is well suited for interference experiments on an increasingly large mass scale in the quest for novel decoherence effects and objective collapse mechanisms such as continuous spontaneous localization [2]. Experiments with various organic clusters and monomers have demonstrated the functionality of the interferometer and serve as a motivation for investigating the wave-particle character of particles with masses up to 10^5 amu and beyond.

References

- [1]P. Haslinger *et al.* Nat. Phys. **9**, 144 (2013)
- [2]S. Nimmrichter *et al.* Phys. Rev. A **83**, 43621 (2011)
- [3]N. Dörre *et al.* Phys. Rev. Lett. **113**, 233001 (2014)
- [4]N. Dörre *et al.* J. Opt. Soc. Am. B **32**, 114 (2014)
- [5]S. Nimmrichter *et al.* New J. Phys. **13**, 75002 (2011)

Non-interferometric tests of Macroscopic Quantum Superposition

H. Ulbricht¹

¹*Physics and Astronomy, University of Southampton, SO17 1BJ, Southampton, UK*

Presenting Author: hendrik.ulbricht@soton.ac.uk

Recent progress in technological developments allow to explore the quantum properties of very complex systems, bringing the question of whether also macroscopic systems share such features, within experimental reach. It seems feasible to generate for instance quantum superposition states of particles of mass of one million amu (atomic mass unit) [1]. The interest in such experiments is increased by the fact that, on the theory side, many suggest that the quantum superposition principle is not exact, departures from it being the larger, the more macroscopic the system [2].

We will report on new proposals to experimentally test the superposition principle with non-interferometric methods. Testing the superposition principle intrinsically also means to test suggested extensions of quantum theory, so-called collapse models. Such collapse models predict a heating effect, which results in a random motion of any isolated particle in space. The heating can be monitored using optomechanical systems even in the classical regime, if competing sources of heat can be reduced sufficiently. We will emphasise levitated optomechanical systems and discuss the possibility to test the heating effect by detecting the motion of the particle in space [4] as well as in the frequency domain where heating is manifested as spectral broadening [5].

We will show quantitative calculations for experiments in both regimes and compare to the state-of-the-art. We will also report on the status of our experiments on optical levitation and parametric feedback cooling of the 3d motion of dielectric nanoparticles at high vacuum conditions of 10^{-6} mbar.

References

- [1] Bateman, J., S. Nimmrichter, K. Hornberger, and H. Ulbricht, *Near-field interferometry of a free-falling nanoparticle from a point-like source*, Nat. Com. 5, 4788 (2014).
- [2] Bassi, A., K. Lochan, S. Satin, T.P. Singh, and H. Ulbricht, *Models of Wave-function Collapse, Underlying Theories, and Experimental Tests*, Rev. Mod. Phys. **85**, 471 - 527 (2013).
- [3] Bahrami, M., A. Bassi, and H. Ulbricht, *Testing the quantum superposition principle in the frequency domain*, Phys. Rev. **A 89**, 032127 (2014),
- [4] Bera, S., B. Motwani, T.P. Singh, and H. Ulbricht, *A proposal for the experimental detection of CSL induced random walk*, Sci. Rep. 5, 7664 (2015).
- [5] Bahrami, M., M. Paternostro, A. Bassi, and H. Ulbricht, *Non-interferometric Test of Collapse Models in Optomechanical Systems*, Phys. Rev. Lett. 112, 210404 (2014).

Continuous Cold-atom Gyroscope with 11 cm² Sagnac Area at nrad/s Stability

B. Fang¹, I. Dutta¹, D. Savoie¹, R. Geiger¹, C. L. Garrido Alzar¹, and A. Landragin¹

¹*SYRTE, Observatoire de Paris, PSL Research University, CNRS, Sorbonne Universités, UPMC Univ. Paris 06, LNE, 61 avenue de l'Observatoire, 75014 Paris, France*

Presenting Author: bess.fang@obspm.fr

We report the latest results from our gyroscope based on interferometry with cold atoms. We launch laser-cooled Cesium atoms in a fountain configuration and interrogate them in a Mach-Zehnder like geometry using stimulated Raman transitions. According to the Sagnac effect, the sensitivity to rotation is proportional to the physical area enclosed by the two arms of the interferometer. We demonstrate an unprecedented interferometric area of 11 cm², which is 30 times larger than ever reported [1]. Using classical accelerometers, we are able to reject vibration noise by a factor 20 and obtain a state-of-the-art sensitivity of 1.2×10^{-7} rad/s/ $\sqrt{\text{Hz}}$ at short term. We achieve a 2 nrad/s sensitivity after about few hours of integration [1,2]. We also demonstrate the possibility to operate our gyroscope without deadtime [3], which represents a big progress for continuous inertial sensing and more generally for applications requiring high bandwidth atom interferometry such as gravitational wave detection.

References

- [1] I. Dutta *et al.*, to be published.
- [2] B. Barrett *et al.*, C. R. Physique **15**, 875–883 (2014).
- [3] M. Meunier *et al.*, Phys. Rev. A **90**, 063633 (2014).

Cesium atomic magnetometers in experiment searching for a neutron electric dipole moment

M. Kasprzak¹, the nEDM collaboration²

¹*Institute for Nuclear and Radiation Physics, KU Leuven, Leuven, Belgium*

²<http://nedm.web.psi.ch/>

Presenting Author: malgorzata.kasprzak@fys.kuleuven.be

The existence of a non-zero neutron electric dipole moment (nEDM) violates both parity (P) and time reversal (T) invariance and, through the conservation of the combined symmetry CPT, also violates CP symmetry (C being the charge conjugation operator). The violation of CP symmetry is one of the possible explanations why there is almost no antimatter in the Universe. The CP violation mechanism is implemented in the Standard Model of particle physics, however it is not sufficient to explain the matter - antimatter asymmetry. The theories beyond the Standard Model, such as Supersymmetry, contain additional sources of CP violation and predict the nEDM in the range $10^{-27} - 10^{-29} e \cdot cm$ [1], considerably larger than the value predicted by the Standard Model ($10^{-31} e \cdot cm$ [1]).

In the nEDM experiment at the Paul Scherrer Institute in Switzerland, the Ramsey technique of (time-)separated oscillatory fields [2] is applied to the polarized neutrons exposed to magnetic B and electric E fields oriented either parallel(+) or anti-parallel (-). Any non-zero difference in the neutron precession frequency ν_L between the two field configurations will indicate the presence of a nEDM (d_n):

$$\frac{h}{4E}(\nu_L^+ - \nu_L^-) = d_n + \mu_n \frac{B^+ - B^-}{2E}, \quad (1)$$

where μ_n is the magnetic moment of a neutron. The spatial and temporal magnetic field distribution has to be precisely known in order to sufficiently suppress any systematic effects associated with field changes. The array of sixteen Cesium magnetometers located around the neutron precession chamber is measuring the stability of the magnetic field in time and its spatial distribution (Fig. 1). The principle of magnetic field measurements is based on the optical detection of the Larmor precession frequency of the polarized Cs atoms. The Cs atoms, confined in a paraffin coated glass cell of 30 mm diameter [3], are spin polarized by the resonant laser light by means of optical pumping. A weak oscillating magnetic field (rf field) resonantly drives the spin precession at the Larmor frequency. The magnetic field measurements are done in the fast(ms) high sensitivity phase-stabilized mode [4]. In this contribution the current status of the nEDM experiment will be discussed, with a focus on the Cs magnetometry aspects.

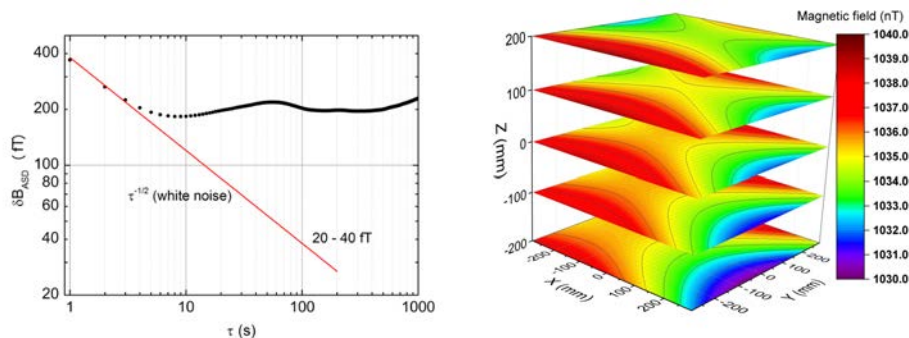


Figure 1: Left: Allan standard deviation versus averaging time measured for Cs magnetometer. Right: Magnetic field map derived by multipole moment fit [5] to all Cs data.

References

- [1] S. K. Lamoreaux and R. Golub “Neutron EDM experiments”. In B. L. Roberts, W. J. Marciano “Lepton Dipole Moments”, World Scientific Publishing (2010).
- [2] N. F. Ramsey, Phys. Rev. **78**, 695 (1950)
- [3] N. Castagna *et al.* Appl. Phys. B. **96** 763–772 (2009)
- [4] S. Groeger *et al.* Eur. Phys. J. D **38** 239–247 (2006)
- [5] S. Afach *et al.* Phys. Lett. B **739**, 128–132 (2014)

Faraday filtering in atomic vapours: from Hamiltonian to application

J. Keaveney¹, M. A. Zentile¹, D. J. Whiting¹, E. Bimbard¹, C. S. Adams¹, and I. G. Hughes¹

¹*Joint Quantum Centre Durham-Newcastle, Department of Physics, Durham University, Durham, UK*
Presenting Author: james.keaveney@durham.ac.uk

The interaction between atoms and light is of essential importance in many areas of physics, and a quantitative understanding of this interaction is therefore beneficial for a variety of reasons, both from the point of view of fundamental physics and for designing applications. We have developed a detailed numerical model [1] of the electric susceptibility (*ElecSus*) for alkali-metal vapours that calculates transition strengths and frequencies, and accounts for applied magnetic field, Doppler broadening and several other experimental effects.

ElecSus can be used as a tool to fit experimental data [2] or predict novel effects, and has already found use in designing an atomic optical isolator [3]. Here we explore one particular application of *ElecSus*; Faraday filtering (often called FADOF filters). A Faraday filter is a high-contrast, ultra-narrow bandpass filter that utilises the birefringent and dichroic properties of atomic media in an applied magnetic field. The filter's transmission profile is strongly dependent on the magnetic field strength and the atomic number density. *ElecSus* has been used to optimise the performance of such filters, and we see excellent agreement between the theoretical prediction and experimental data [4].

Finally, we explore a further application of Faraday filtering in the context of laser design. Frequency selection is achieved by placing an atomic Faraday filter inside the external cavity of a diode laser system. By carefully engineering the optimal conditions for Faraday filter performance, it is possible to realise a single-mode, single-frequency laser which operates only at the cooling/repump transition frequencies. We envisage that such a system can become a turn-key, maintenance-free laser system for laser cooling experiments.

References

- [1] M. A. Zentile *et al.*, *ElecSus*: A program to calculate the electric susceptibility of an atomic ensemble, *Comp. Phys. Commun.* **189**, 162-174 (2015).
- [2] M. A. Zentile *et al.*, The hyperfine Paschen-Back Faraday effect, *J. Phys. B* **47**, 075005 (2014)
- [3] L. Weller *et al.*, Optical isolator using an atomic vapor in the hyperfine Paschen-Back regime, *Opt. Lett.* **37**, 3405 (2012).
- [4] M. A. Zentile *et al.*, Atomic Faraday filter with equivalent noise bandwidth less than 1 GHz, *Opt. Lett.* **40**, 2000 (2015).

Anharmonic magnetic response of magnetic nanoparticles detected by atomic rf magnetometry

S. Colombo¹, V. Lebedev¹, V. Dolgovskiy¹, Z. D. Grujić¹, and A. Weis¹

¹Department of Physics, University of Fribourg, Fribourg, Switzerland

Presenting Author: simone.colombo@unifr.ch

Harmonically-excited magnetic nanoparticles (MNP) produce an anharmonic magnetic field $B_{MNP}(t)$, consisting of fundamental (ω_{exc}) and higher ($n\omega_{exc}$) harmonics of the excitation field. We explore the recording of these harmonics with a laser-pumped atomic rf magnetometer (ARFM), operated in two different modes, and report on sensitivity, bandwidth, and constraints thereof.

In the first mode, the ARFM is operated as an M_x -magnetometer [1] based on the optical detection of magnetic resonance in a spin-polarized atomic Cs vapor in a paraffin-coated glass cell. The Cs vapor is exposed to a DC magnetic field B_0 which splits the Zeeman sublevels by $\hbar\omega_L$ (Larmor frequency) and to an rf-magnetic field which leads to a spin-depolarization when the rf frequency matches ω_L . A circularly-polarized laser beam resonant with the Cs $D_1(4 \rightarrow 3)$ hyperfine transition pumps the atoms into non-absorbing dark states. The rf-induced depolarization increases the absorption of the Cs vapor, thereby changing the light transmission in a resonant manner. In this operation mode we tune B_0 such that its Larmor frequency matches one of the harmonics $n\omega_{exc}$ of the $B_{MNP}(t)$ oscillation. The amplitude of the corresponding resonance is a direct measure of the respective harmonic's amplitude. However, the magnetometer readout at higher harmonics is perturbed by multiphoton rf-transitions induced by the excitation field. The corresponding signals cannot be distinguished from the MNP signals proper. We have studied this multiphoton depolarization by supplying a purely harmonic rf-field. The detected multiphoton amplitudes A_n (Fig. 1, left) increase with a $A_n \propto B_{\omega_{exc}}^n$ power law of the driving field amplitude [2,3], and the corresponding cross-sections (Fig. 1, center) obey the anticipated $\sigma_n \propto \omega_L^{-(n-1)}$ law.

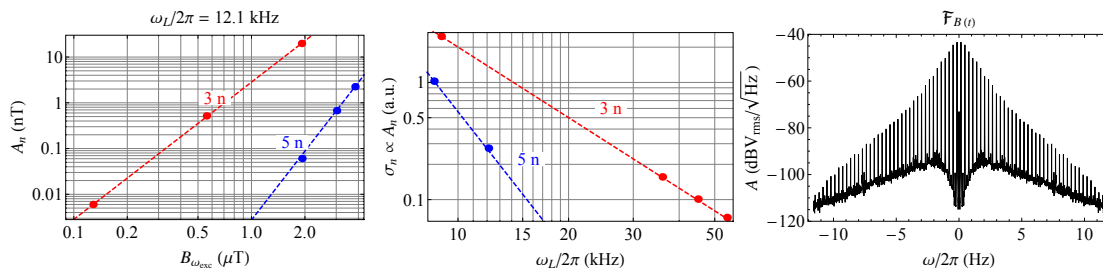


Figure 1: Left and central graphs show the $A_n \propto B_{\omega_{exc}}^n$ and $\sigma_n \propto \omega_L^{-(n-1)}$ dependencies of the multiphoton process, respectively. The right graph shows the Fourier spectrum of a 157 Hz square-wave modulated $B(t)$ field measured by a self-oscillating magnetometer.

In order to avoid the multi-photon perturbations we deployed the ARFM in its self-oscillating mode of operation [4]. We orient the magnetometer such that $\vec{B}_{MNP}(t)$ has a large projection onto \vec{B}_0 , which leads to a frequency modulation of the Larmor frequency. This translates into a transmitted light intensity spectrum given by $\omega_L \pm n\omega_{exc}$. The bandwidth of self-oscillating magnetometers is known to be limited only by the photodetection bandwidth. As anticipated, this mode of operation allows an unperturbed detection of large number of harmonics as evidenced by our recording of a square wave-modulated magnetic field (157 Hz) with a bandwidth exceeding 10 kHz.

References

- [1] G. Bison *et al.* J. Opt. Soc. Am. B **22** 77-87 (2005)
- [2] T. Yabuzaki, N. Tsukada, T. Ogawa J. Phys. Soc. Japan **32.4** 1069-1077 (1972)
- [3] V. S. Korol, A. N. Kozlov Sov. Phys. JETP **29.4** 591-594 (1969)
- [4] A. L. Bloom Appl. Opt. **1** 61-68 (1962)

Pushing QED to the limit in the helium atom

R. P. M. J. W. Notermans¹, R. J. Rengelink¹, and W. Vassen¹

¹*LaserLaB, Department of Physics and Astronomy, VU University, Amsterdam*

Presenting Author: r.p.m.j.w.notermans@vu.nl

QED theory remains one of the most well-tested theories in physics to date. Both theorists and experimentalists keep pushing the limits to which QED continues to accurately predict the electron anomalous magnetic moment, the fine-structure constant α , and electronic energy levels in atoms and ions. At the LaserLaB in Amsterdam we test QED by measuring (doubly) forbidden transitions in helium. We are able to observe such weak transitions because we perform spectroscopy in ultracold quantum degenerate metastable helium ($T \approx 1 \mu\text{K}$) confined in an optical dipole trap. Apart from the significantly reduced Doppler broadening in this system, the ultracold trapped gas can also be very well characterized. This is essential for controlling the systematic effects typically limiting the error budget in high-precision spectroscopy.

We have recently determined the ionization energy of the 2^1P_1 state of ^4He to 6.7×10^{-10} relative accuracy by directly measuring the forbidden $2^3S_1 \rightarrow 2^1P_1$ transition at 887 nm [1]. This determination agrees with results obtained by a different group [2] but disagrees by over 3σ with the most accurate QED calculations to date [3]. As the QED calculations agree with all other low-lying electronic states in helium, these results indicate that there might be a particular issue with the 2^1P_1 state. In addition to the determined ionization energy, the measured lineshape of the transition provides the most accurate determination of the lifetime of the 2^1P_1 state to date, which is in excellent agreement with theory and other experiments.

Pushing towards even higher accuracy, measurements exceeding the accuracy of QED theory allow extraction of the nuclear charge radius from the QED calculations. This has recently been used in hydrogen and muonic hydrogen spectroscopy, where an over 7σ discrepancy was found in the determined charge radius of the proton. This discrepancy is also known as the *proton radius puzzle* [4]. Apart from ongoing work to perform similar measurements in muonic helium ions [5], our group has previously measured the doubly forbidden $2^3S \rightarrow 2^1S$ transition at 1557 nm (natural linewidth $2\pi \times 8$ Hz) to a few kHz precision in both ^3He and ^4He . The results were combined with QED calculations to determine the ^3He - ^4He nuclear charge radius difference with 1.1% accuracy [6]. A similar recent determination based on the measurement of the $2^3S \rightarrow 2^3P$ transition shows a disagreement of 4σ with our result [7].

We are currently working on a new measurement of the $2^3S \rightarrow 2^1S$ transition with sub-kHz precision as this can shed more light on the 4σ discrepancy. Furthermore this will provide a more accurate nuclear charge radius difference for comparison with the muonic helium ion measurements of which the first results are expected soon. We have made several improvements on the previous experiment. First the previously measured linewidth of the transition (~ 100 kHz) is reduced by improving the stability of the spectroscopy laser. Second the Zeeman shift is measured with better precision than before or even eliminated using atoms in the $M_J = 0$ state. Third we implement a magic wavelength optical dipole trap operating at 319.8 nm to significantly reduce the ac Stark shift [8], and we are currently able to produce the required UV light at a CW power of 2 Watts which is more than sufficient for our purposes.

References

- [1] R.P.M.J.W. Notermans, W. Vassen PRL **112**, 253002 (2014)
- [2] P.-L. Luo *et al.* PRL **111**, 012002 (2013); **111**, 179901(E) (2013); PRA **88**, 054501 (2013)
- [3] V.A. Yerokhin, K. Pachucki PRA **81**, 022507 (2010)
- [4] J.C. Bernauer, R. Pohl Scientific American **310** (2), 32–39 (2014)
- [5] A. Antognini *et al.* Can. J. Phys. **89**, 47–57 (2011)
- [6] R. van Rooij *et al.* Science **333**, 196–198 (2011)
- [7] P. Cancio Pastor *et al.* PRL **108**, 143001 (2012)
- [8] R.P.M.J.W. Notermans, R.J. Rengelink, W. Vassen PRA **90**, 052508 (2014)

Coulomb crystallization of highly charged ions

L. Schmöger^{1,2}, O. O. Versolato^{1,2}, M. Schwarz^{1,2}, M. Kohlen², A. Windberger¹, B. Piest¹,
S. Feuchtenbeiner¹, J. Pedregosa³, T. Leopold², P. Micke^{1,2}, A. K. Hansen⁴, T. M. Baumann⁵,
M. Drewsen⁴, J. Ullrich², P. O. Schmidt^{2,6}, and J. R. Crespo López-Urrutia¹

¹*Max-Planck-Institut für Kernphysik, Heidelberg, Germany*

²*Physikalisch-Technische Bundesanstalt, Braunschweig, Germany*

³*Physique des Interactions Ioniques et Moléculaires, Aix-Marseille Université, Marseille, France*

⁴*Department of Physics and Astronomy, Aarhus University, Aarhus, Denmark*

⁵*NSCL, Michigan State University, East Lansing, Michigan, USA*

⁶*Institut für Quantenoptik, Leibniz Universität Hannover, Hannover, Germany*

Presenting Author: lisa.schmoeger@mpi-hd.mpg.de

In highly charged ions (HCIs), the electronic wavefunction is much reduced in size. Subsequent advantages for precision spectroscopy are: higher sensitivity to electron-nucleus interactions and QED terms in general, and an extremely suppressed sensitivity to external field perturbations. Further, electric dipole forbidden optical transitions found near level crossings in HCIs are extremely sensitive to possible drifts in the fine structure constant α [1]. Thus, cold, strongly localized HCIs are of particular interest for bound-state QED studies (g-factor measurements), metrology (development of novel optical clocks) and the search for α variation. We report on Coulomb crystallization of highly-charged $^{40}\text{Ar}^{13+}$ ions through sympathetic cooling with co-trapped, laser-cooled $^9\text{Be}^+$ ions to final translational temperatures of about 200 mK or less [2]. The Ar^{13+} ions are produced in, and extracted from an electron beam ion trap (EBIT). They are decelerated and precooled by means of two serrated interlaced pulsed drift tubes before they are injected into the cryogenic Paul trap CryPTEch [3]. Subsequently, they are forced to interact multiple times with a Coulomb crystal of laser-cooled Be^+ ions, thereby losing enough energy to end up implanted as dark structures of spherical shape in the bright fluorescing Be^+ crystal. The combination of an EBIT with a linear Paul trap operating at ~ 7 K facilitates not only the formation of mixed-species 3D Coulomb crystals, but also of 1D Coulomb crystals down to a single HCI cooled by a single Be^+ ion (Fig.1). This is a necessary step for future quantum logic spectroscopy at a potential 10^{-19} level accuracy. Our preparation technique of cold Ar^{13+} is readily applicable to a broad range of other highly charged elements and is thus a significant step forward for precision spectroscopy of HCIs.

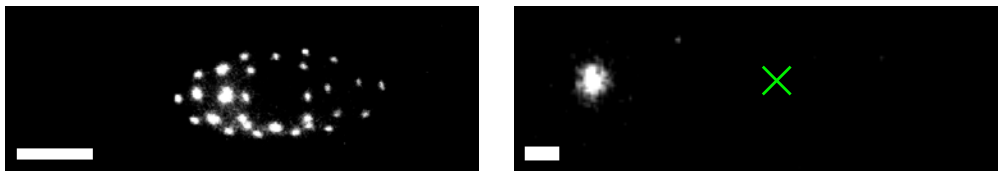


Figure 1: *Left: A single Ar^{13+} ion sympathetically cooled by several Be^+ ions. White scale bar denotes 100 μm . Right: A single Ar^{13+} ion (position marked by cross) sympathetically cooled by a single laser-cooled Be^+ ion. White scale bar denotes 20 μm .*

References

- [1] J. C. Berengut et al., Phys. Rev. Lett. **106**, 210802 (2011)
- [2] L. Schmöger et al., Science **347**, 1233-1236 (2015)
- [3] M. Schwarz. et al., Rev. Sci. Instr. **83**, 083115 (2012)

Posters

Cold atoms and quantum gases

Realization of radio-frequency assisted Förster resonances in an ensemble of a few cold Rb Rydberg atoms

C. Andreeva¹, A. Cinins², A. Ekers³, A. Markovski⁴, D. Tretyakov⁵, V. M. Entin⁵, I. Beterov^{5,6},
E. Yakshina^{5,6}, and I. I. Ryabtsev^{5,6}

¹*Institute of Electronics, Bulgarian Academy of Sciences, Sofia*

²*Institute of Atomic Physics and Spectroscopy, Latvian University, Riga*

³*King Abdullah University of Science and Technology, Saudi Arabia*

⁴*Faculty of Automatics, Technical University of Sofia, Bulgaria*

⁵*Institute of Semiconductor Physics, Russian Academy of Sciences, Novosibirsk*

⁶*Novosibirsk State University, Russia*

Presenting Author: christina_andreeva@yahoo.com

We present the realization of radio-frequency-assisted Förster resonances in cold Rb Rydberg atoms in a magneto-optical trap [1]. Förster resonances occur due to dipole-dipole interaction between Rydberg atoms when the atoms are laser-excited to a level that lies midway between two other levels of opposite parity. In the standard experiments, the resonant condition is realized by tuning the levels by means of weak electric field.

In our experiments we excite cold Rb atoms to the initial 37P state. At dc electric field of 1.79 V/cm there is a single Förster resonance $37P+37P \rightarrow 37S+38S$ and Rydberg atoms in the final state 37S are detected by means of selective field ionization technique. If we admix a radio-frequency electric field to the dc field, it can induce additional Förster resonances. The rf photons compensate for the energy defect of the Förster resonance and induce additional resonances, which correspond to the induced absorption or emission of rf photons. If the rf amplitude is large enough, it can even induce multiphoton transitions of high orders.

Not all levels can be used to realize Förster resonances by tuning dc electric field. An example of such „inaccessible” Förster resonance is the $39P+39P \rightarrow 39S+40S$, for which the dc field alone increases the energy detuning. However, our experience with the Förster resonance for the 37P state suggests that the rf-field can induce transitions between collective states, so the Förster resonance occurs irrespective of the possibility to tune it by the dc field alone. The dc field, however, should be applied to increase its efficiency. We have obtained a Förster resonance at $39P+39P \rightarrow 39S+40S$ with rf-field at multiple frequencies. The position of the rf-assisted Förster resonance depends on the rf-frequency, while its width and height depend on the number of atoms N .

These resonances correspond to single- and multiphoton rf-transitions between many-body collective states of a Rydberg quasi-molecule or to intersections of the Floquet sidebands of Rydberg levels appearing in the rf-field. We have shown that they can be induced both for the "accessible" Förster resonances, which are tuned by the dc field, and for those which cannot be tuned and are "inaccessible". The van der Waals interaction of almost arbitrary high Rydberg states can thus be efficiently transformed to resonant dipole-dipole interaction using the rf-field with frequencies below 1 GHz. This strongly enhances the interaction strength and distance and can give rise to much stronger dipole blockade effect, which is used in numerous applications of Rydberg atoms.

This work was supported by RFBR (Grant Nos. 13-02-00283 and 14-02-00680), the Russian Academy of Sciences, and the Russian Quantum Center.

References

- [1] D.B. Tretyakov *et al.* Phys. Rev. A **90** 041403(R) (2014)

Optical flux lattice using multi-frequency radiation

T. Andrijauskas¹, G. Juzeliūnas¹, and I. Spielman^{2,3}

¹*Institute of Theoretical Physics and Astronomy, Vilnius university, A. Goštauto 12, Vilnius LT-01108, Lithuania*

²*Joint Quantum Institute, University of Maryland, College Park, Maryland 20742-4111, 20742, USA*

³*National Institute of Standards and Technology, Gaithersburg, Maryland 20899, USA*

Presenting Author: tomas.andrijauskas@tfai.vu.lt

Ultracold atomic gases are systems exhibiting various condensed matter phenomena. The ultracold atoms are neutral, so under usual circumstance they do not exhibit important magnetic phenomena, like the quantum Hall effect. Possible ways to create artificial magnetic field for ultracold atoms include rotation of an atomic cloud, laser-assisted tunnelling, shaking of optical lattices [1]. Yet it is difficult to reach considerable magnetic fluxes required for achieving the fractional Hall effect.

Here we theoretically analyse another way of creating a non-staggered magnetic flux for ultra-cold atoms by using a periodic sequence of short laser pulses providing a multi-frequency perturbation. In particular, we consider a possibility to create a square flux lattice for ultra-cold atom characterized by two internal states. The energies of the two internal states have opposite gradients in one spatial direction. Hamiltonian of such system reads,

$$H_0 = \frac{\mathbf{p}^2}{2m}I + bx\sigma_z,$$

where b is coefficient of linear dependence of the spatial gradient and σ_z is the z -th Pauli matrix. The driving consists of periodic in time pulses that couple the internal states and propagate in a direction perpendicular to the energy gradient. Such pulses can be created using multi-frequency radiation:

$$V(t) = \hbar\Omega|1\rangle\langle 2| \left(e^{-iky} \sum_n e^{-i2n\gamma t} + e^{iky} \sum_n e^{-i(2n+1)\gamma t} \right) + \text{H. c.}$$

Here Ω is the coupling strength in frequency units, γ is the comb frequency and k is the wave-number. The time-dependent perturbation effectively creates a square optical lattice, described by the periodic coupling $V_{\text{eff}} = \boldsymbol{\sigma} \cdot \mathbf{B}$, where \mathbf{B} is a real three dimensional vector field and $\boldsymbol{\sigma}$ is a vector of Pauli matrices. We show that this effective optical lattice produces a non-staggered magnetic flux [2], described by a geometric vector potential, which contains Aharonov-Bohm type singularities. Finally we explore topological properties of such a lattice.

References

- [1] J. Dalibard *et al.* Rev. Mod. Phys. **83** 1523–1543 (2011)
- [2] G. Juzeliūnas, I. Spielman New J. Phys, **14**, 123022 (2012)

Dual-species BEC source: First step towards matter neutrality test with atom interferometry

B. Décamps¹, J. Alibert¹, and A. Gauguet¹

¹LCAR UMR5589, Université Paul Sabatier, Toulouse

Presenting Author: decamps@univ.ups-tlse.fr

We are building a new atom interferometer[1] using Bose-Einstein Condensate for applications in precision measurements. A first objective of the project is to create an atom interferometer based on a new type of BEC source compatible with transportable applications. This source combines on a chip[2], the magnetic trapping with microscopic wires and an optical dipole trap. It will also be possible to condense the two isotopes of rubidium. Besides these technological developments, we plan to apply this new atom interferometer to test the neutrality of atoms with a new method[3,4]. Since the electrical neutrality of atoms is directly connected to elementary charges (electron and quark), this measurement is of a great significance in fundamental theory of particles. The target sensitivity of this experiment might improve the current laboratory limits by 3 orders of magnitude[5]. In this poster, I will present the technological choices implemented on this new experiment(Fig. 1).

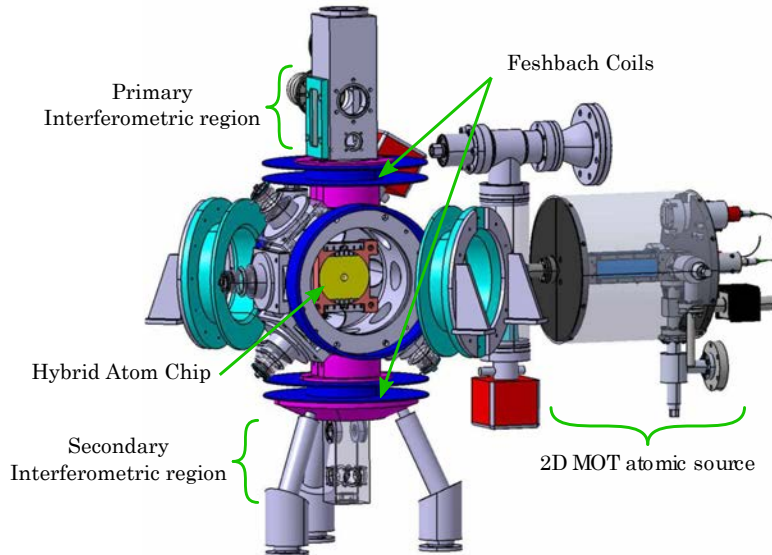


Figure 1: *Experimental setup featuring the dual species atomic source (2D MOT), the Hybrid Atom chip allowing for fast evaporative cooling, the Feshbach Coils necessary for tuning the interactions in the Rubidium 85 condensate and the interferometer regions where multi $\hbar k$ Bragg pulses will allow for large spatial separations and long (~ 15 ms) interaction times.*

References

- [1] G.M. Tino, M.A. Kasevich, *Atom Interferometry* (IOS Press, 2014)
- [2] J. Reichel and V. Vuletic, *Atom Chips* (Wiley, 2011)
- [3] J. Vigué et al., *Lecture note in Physics*, vol. **570**, p. 554-563 (2001).
- [4] M. Kasevich et al., *Phys. Rev. Lett.*, **100**, 120407 (2008).
- [5] C. S. Unnikrishnan et al., *Metrologia*, **41**, S125 (2004)

Hybrid dynamics of an optical field and a Bose-Einstein condensation

G. Dong¹

¹*State Key Laboratory of Precision Spectroscopy, East China Normal University, Shanghai, China*

Presenting Author: gj.dong@qq.com

Optical fields have played a critical role in manipulating ultracold atomic or molecular gases for precision measurement and quantum emulation. However, in most of these researches, the local field effect (or the feedback effect) of ultracold gases on the optical field propagation has been ignored. However, our recent research [1,2,3] shows that including the feedback effect, the optical field propagation and matter wave dynamics cannot be separated, i.e., we enter a regime that hybrid dynamics of the optical field and the matter wave is dominant. Using our theory, we have successfully explained asymmetric matter wave diffraction observed by Li et al. [4], and predicted polaritonic solitons in a soft optical lattice. Most recently, we further have proposed magnetic local field effect [3] which deals with the hybrid dynamics of a spinor gas and a microwave field, and predicted the generation of monopole-like subwavelength microwave soliton and matter wave soliton which could be useful for realizing atomic laser. Our theory of hybrid optical wave and matter wave could be further extended to study precision measurement, to study polariton in far-off resonant regime and to study the subwavelength phenomena.

References

- [1] Jiang Zhu, Guangjiong Dong, Mikhail N. Shneider, and Weiping Zhang, *Phys. Rev. Lett.* **106**, 210403 (2011)
- [2] Guangjiong Dong, Jiang Zhu, Weiping Zhang, and Boris A. Malomed, *Phys. Rev. Lett.* **110**, 250401 (2013)
- [3] Jieli Qin, Guangjiong Dong, Boris A. Malomed, <http://arxiv.org/abs/1503.03101>
- [4] K. Li et al., *Phys. Rev. Lett.* **101**, 250401 (2008)

Borromean three-body FRET in frozen Rydberg gases

R. Faoro^{1,2}, B. Pelle¹, A. Zuliani¹, P. Cheinet¹, E. Arimondo^{2,3}, and P. Pillet¹

¹Laboratoire Aimé Cotton, CNRS, Univ. Paris-Sud, ENS Cachan, Bât. 505, 91405 Orsay, France

²Università di Pisa, Largo Pontecorvo 3, I-56127 Pisa, Italy

³INO-CNR, Via G. Moruzzi 1, 56124 Pisa, Italy

Presenting Author: riccardo.faoro@u-psud.fr

Cold Rydberg atoms are a promising tool for studying few-body and many-body interaction because of their strong and long-range dipole-dipole interactions. Applying an external electric field, it is possible to induce a huge dipole moment and then tune dipole-dipole interactions. A well known example are Förster resonances [1] that consists in a transfer of energy between two different two-atoms states analogous to FRET in biology [2].

We have observed 3-body Stark-tuned resonances in a cold Cs Rydberg gas for different principle quantum number n . The two processes that we have studied can be described by the following equations:

$$3 \times np \leftrightarrow (n+1)s + ns + np' \quad (1)$$

$$3 \times np' \leftrightarrow (n+1)s + ns + np \quad (2)$$

where np and np' differ respectively for $m_J = 1/2$ and $m_J = 3/2$. These new three-body FRET resonances are a general process that can be observed for all kind of atoms that present a two-body FRET resonance and with a total angular momentum $J > 1/2$.

They are by themselves the first observation of a Borromean interaction in Rydberg atoms [3]. Moreover a possible generalization to many-body Brunian interaction [4] could open the way to a new investigation on the transition from few to many body physics.

Three-body FRET resonances could find several application in quantum optics and quantum computing: they can be used to design a three-body Fredkin gate or for the realization of a 3-body entangled state. They could also provide an effective Quantum Non Demolition measure of entanglement between 2 atoms measuring the 3rd.

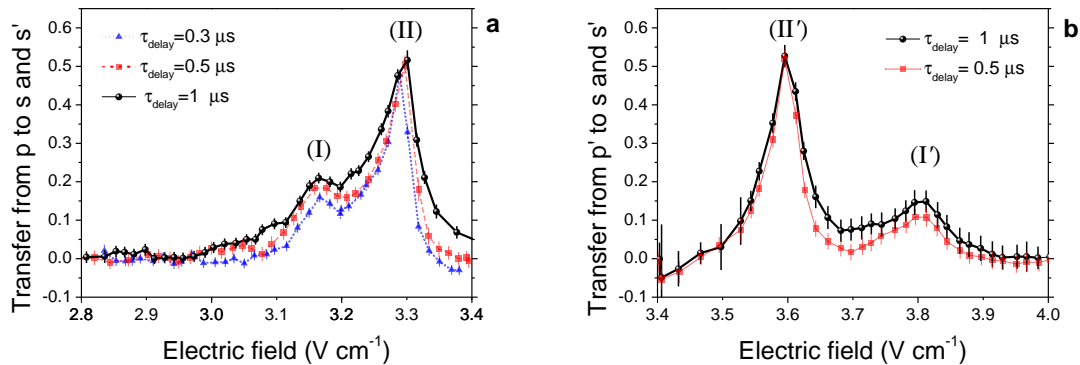


Figure 1: Averaged transfer ratio from the initial np state (a) or np' state (b) to $ns + ns'$ states for $n = 35$ at different τ_{delay} versus the electric field. The peaks labelled with (I) and (I') correspond to 3-body resonances described respectively by eq. (1) and eq. (2). The other two peaks (II) and (II') correspond to the well known to 2-body process respectively for np and np' .

References

- [1] K.A.Safinya *et al.* Phys. Rev. Lett. **47** 405-408 (1981)
- [2] E.A. Jares-Erijman and T. Jovin Nat. Biotech. **21**, 1387-1395 (2003)
- [3] M.Kiffer, M. Li, D. Jaksch Phys. Rev. Lett. **111** 233003 (2013)
- [4] M. T. Yamashita, D. V. Federov, A.S. Jensen Phys. Rev. A **81** 063607 (2013)

Interferometric laser cooling of atomic rubidium

A. Dunning¹, R. Gregory², J. Bateman², M. Himsworth², and T. Freearge²

¹*UCLA Department of Physics & Astronomy, 475 Portola Plaza, Los Angeles, CA 90095, U.S.A.*

²*School of Physics & Astronomy, University of Southampton, Highfield, Southampton, SO17 1BJ, U.K.*

Presenting Author: tim.freearge@soton.ac.uk

We report the 1-D cooling of ⁸⁵Rb atoms using a velocity-dependent optical force based upon Ramsey matter-wave interferometry. The velocity-dependent interferometer phase, which stems from the change in kinetic energy when a photon is absorbed, is that which in a differential configuration is the basis for a range of atom interferometric accelerometers and gyroscopes [1, 2]. Here, as proposed by Weitz and Hänsch [3], it provides a cooling effect within the atomic sample. In this first demonstration, we omit the intervening compensation pulses of the original proposal.

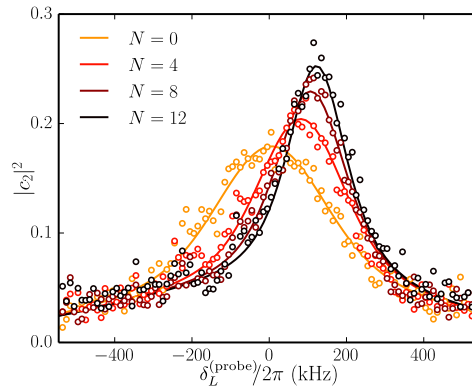


Figure 1: Raman velocimetry measurements after N interferometric cooling cycles. Each point is the average of 16 fluorescence measurements at probe detuning $\delta_L^{(probe)}$, and the lines for $N = 0, 4, 8$ and 12 cycles are numerical simulations for temperatures of $21 \mu\text{K}$, $10 \mu\text{K}$, $4.8 \mu\text{K}$ and $3.2 \mu\text{K}$ respectively. The same $250 \mu\text{K}$ background is present in each case.

Using stimulated Raman transitions between ground hyperfine states, detuned by ~ 10 GHz from the 780 nm single-photon resonance, each cooling cycle comprises a pair of $\pi/2$ ‘beamsplitter’ pulses separated by around 600 ns. The velocity distribution is then probed by weak Raman pulses of longer duration, whose Raman detuning $\delta_L^{(probe)}$ is scanned across the Doppler-sensitive hyperfine resonance. As shown in Figure 1, 12 cycles of the interferometer sequence cool a freely-moving atom cloud, initially prepared in a conventional magneto-optical trap, from $21 \mu\text{K}$ to $3 \mu\text{K}$ [4]. The accompanying shifts of the velocity distributions in this first configuration could be eliminated by switching the directions of the counter-propagating Raman beams after each cycle.

This pulsed analogue of continuous-wave Doppler cooling is effective at temperatures down to the recoil limit; with augmentation pulses to increase the interferometer area [3, 5, 6] and using composite pulse error-correction [7], it should cool more quickly than conventional methods, and suit species that lack a closed radiative transition. By interleaving the beamsplitter and augmentation pulses, more complex manipulations are conceivable, resembling the operations of a momentum-state quantum computer [8].

References

- [1] M. Kasevich, S. Chu, Phys. Rev. Lett. **67**, 181 (1991)
- [2] T. L. Gustavson, P. Bouyer, M. A. Kasevich, Phys. Rev. Lett. **78**, 2046 (1997)
- [3] M. Weitz, T. W. Hänsch, Europhys. Lett. **49**, 302 (2000)
- [4] A. Dunning *et al.*, <http://arxiv.org/abs/1408.6877>, submitted for publication (2014)
- [5] J. S. Bakis *et al.*, Phys. Rev. A **53**, 285 (1996)
- [6] T. Freearge, G. Daniell, D. Segal, Phys. Rev. A **73**, 033409 (2006)
- [7] A. Dunning *et al.*, Phys. Rev. A **90**, 033608 (2014)
- [8] T. Freearge, D. Segal, Phys. Rev. Lett. **91**, 037904 (2003)

Progress towards the realization of a quantum degenerate dipolar gas of dysprosium atoms

L. Del Bino^{1,2}, J. Catani^{1,2}, A. Fioretti³, C. Gabbanini³, S. Gozzini³, M. Inguscio^{2,4}, G. Modugno^{1,2}, and E. Lucioni^{1,2}

¹*Istituto Nazionale di Ottica (INO) del CNR, UOS Sesto Fiorentino, 50019 Sesto Fiorentino, Italy*

²*LENS and Dip. di Fisica e Astronomia, Università di Firenze, 50019 Sesto Fiorentino, Italy*

³*Istituto Nazionale di Ottica (INO) del CNR, UOS Pisa, via Moruzzi 1, 56124, Pisa, Italy*

⁴*INRIM, 10135 Torino, Italy*

Presenting Author: carlo.gabbanini@ino.it

Long-range interactions, such as Coulomb interaction between electrons and dipolar interaction between magnetic spins, govern the behavior of many physical systems. A controlled experimental environment to study quantum effects of long-range interactions is therefore of general interest. Quantum gases with strong magnetic dipolar interactions offer the possibility to study paradigm systems that can lead to better understand some physical mechanisms of real matter and possibly to engineer new materials. Moreover, the ability to hold them in the ordered environment provided by an optical lattice opens the way to studies of strongly-correlated systems in different dimensionalities.

We plan to realize a quantum gas of dysprosium atoms to perform quantum simulations of strongly-correlated dipolar systems. Contrary to alkali atoms, usually employed in cold atoms experiments, dysprosium has the largest magnetic dipole moment, 10 Bohr magnetons, among all elements. For this reason, besides interacting via van der Waals interaction, which has substantially a contact nature, Dy atoms also interact via dipole-dipole magnetic interaction, which is both long-range and anisotropic. The combination of these two ingredients leads to the appearance of peculiar quantum phenomena so far only barely explored [1]. Moreover, Dy isotopes, with both fermionic and bosonic nature, can be brought to quantum degeneracy [2,3], allowing statistics-dependent studies.

The actual state of the experiment at INO will be described. An effusive beam of dysprosium atoms has been slowed by a laser beam on the stronger blue resonance at 421 nm in a Zeeman slower. The weaker resonance line at 626 nm will be used to implement a magneto-optical trap. Using laser cooling on that narrow line transition, the trapped Dy atoms will be at a temperature low enough to be efficiently loaded into a dipole trap and successively evaporated to degeneracy.

References

- [1] C. Trefzger, C. Menotti, B. Capogrosso-Sansone, and M. Lewenstein, *J. Phys. B: At. Mol. Opt. Phys.* **44**, 193001 (2011)
- [2] Mingwu Lu, Nathaniel Q. Burdick, Seo Ho Youn, and Benjamin L. Lev, *Phys. Rev. Lett.* **107**, 190401 (2011)
- [3] Mingwu Lu, Nathaniel Q. Burdick, and Benjamin L. Lev, *Phys. Rev. Lett.* **108**, 215301 (2012)

Coherent light scattering from a disordered ensemble of cold atoms

A. S. Kuraptsev⁵, I. M. Sokolov^{1,2}

⁵*Institute of Physics, Nanotechnology and Telecommunications, Saint-Petersburg State Polytechnical University, Saint-Petersburg, Russia*

¹*Institute for Analytical Instrumentation, Saint-Petersburg, Russia*

Presenting Author: aleksej-kurapcev@yandex.ru

Improvements in techniques for cooling atoms in atomic traps [1] make their use very promising for practical applications in various areas of fundamental science and technology such as metrology, the development of frequency standards, and quantum information problems [2-3]. The vast majority of these applications presuppose usage of optical detection methods which are based on analysis of radiation scattered from an atomic ensemble. Among these methods ones based on measurements of coherent reflection have a range of advantages.

Coherent light reflection from an ensemble of cold atoms is possible only if the atomic density is sufficiently big so that $n\lambda^3 \sim 1$ (n is the atomic density and λ is the resonant wavelength). In this case atoms can not be considered as independent scatterers of electromagnetic waves. Interatomic dipole-dipole interaction significantly influences on the optical characteristics of a medium.

For theoretical description of light scattering from dense and cold atomic ensemble we use the consequent quantum microscopic approach [4] in which the amplitude of scattered light is calculated as sum of individual contributions from all the atoms. This approach is based on solution of non-stationary Schrodinger equation for the wave function ψ of the joint system consisting of atoms and electromagnetic field. The Hamiltonian of the system H can be presented as the sum of the Hamiltonians H_0 of the free atoms and the free field, and the operator V of their interaction. We use dipole approximation and seek the wave function ψ as an expansion in a set of eigenstates of H_0 .

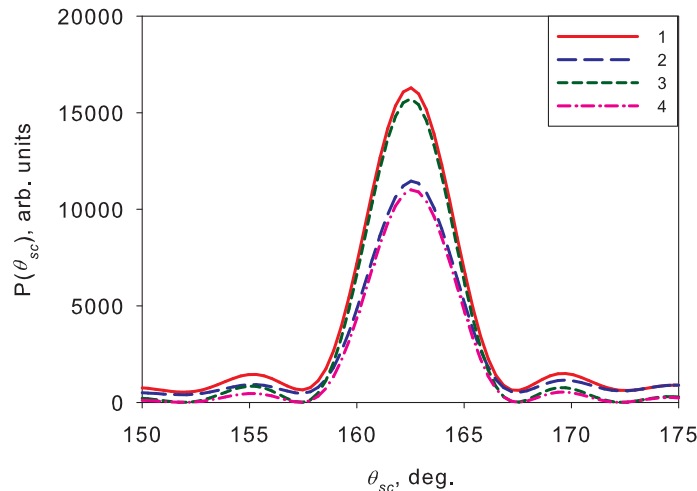


Figure 1: Angle distribution of the scattered light power $P(\theta_{sc})$. 1, 3 s- polarization; 2, 4 p- polarization; 1, 2 total; 3, 4 coherent component

Probe radiation is assumed to be weak coherent plane wave so that we can approximate its state as a superposition of vacuum and a small admixture of one-photon state. It allows us to restrict the total number of states of the joint system taken into account by the set of states with no more than one photon, see [4] for detail. This set consists of a infinite number of states but we can pick out the finite system of equations for the one-fold atomic excited states. Other states can be calculated via one-fold atomic excited states. Thus, we obtain the wave function ψ which allows us to calculate any characteristics of the scattered light and atomic ensemble.

The approach employed here allows us to consider atomic ensembles with different shapes and with arbitrary atomic spatial distributions. In the present work we focus our attention on the coherent reflection. For this purpose we consider model plane layer with uniform distribution of atomic density. We analyze main regularities of the reflection, particularly angular distribution of reflected light, the ratio between coherent and incoherent components of scattered light, the depth of subsurface layer responsible for the coherent reflection, and the reflectivity for different angles of incidence and

polarizations. Our analysis reveals a discrepancy between microscopic calculations and the Fresnel equations. In our opinion, it can be explained by the fact that for resonant light the mean free path of photon is comparable with the average interatomic distance. As example of our calculation in Fig. 1 we show angular distribution of light reflected from a plane surface of ensemble. Probe light is exactly resonant to the transition of a free atom, the angle of incidence $\theta_0 = 17.5^\circ$. The maximum of all the curves in Fig. 1 corresponds to the classical reflection angle as predicted by classical theory.

References

- [1] H. G. Metcalf, P. van der Straten *Laser Cooling and Trapping* (Springer, New York, 1999)
- [2] B. J. Bloom *et al.* *Nature* **506** 71–75 (2014)
- [3] D. Bouwmeester *et al.* *The Physics of Quantum Information* (Springer-Verlag, Berlin, 2001)
- [4] I. M. Sokolov, D. V. Kupriyanov, M. D. Havey *J. Exp. Theor. Phys.* **112** 246 (2011)

Proposal for laser-cooling of rare-earth ions

M. Lepers¹, O. Dulieu¹, and J.-F. Wyart^{1,2}

¹Laboratoire Aimé Cotton, CNRS/Univ. Paris-Sud/ENS-Cachan, 91405 Orsay, France

²LERMA, Observatoire de Paris-Meudon, Univ. Pierre et Marie Curie, 92195 Meudon, France

Presenting Author: maxence.lepers@u-psud.fr

Ultracold gases of rare-earth neutral atoms are nowadays very promising in the context of dipolar scattering, many-body physics or metrology. In spite of their complex electronic structure, laser-cooling of rare-earth atoms turns out to be remarkably simple. In the pioneering experiment on erbium [1], McClelland and coworkers observed a strong cascade mechanism toward the ground state, which even made repumping unnecessary. That work inspired various studies which led *e.g.* to the Bose-Einstein condensation of dysprosium [2] and erbium [3].

Laser-cooling of trapped ions, which is today routinely achieved [4], has allowed for setting up extremely accurate clocks, and for observing chemical reactions in the ultracold regime [5]. However ion laser-cooling is limited to species with a closed electronic core and a single valence electron.

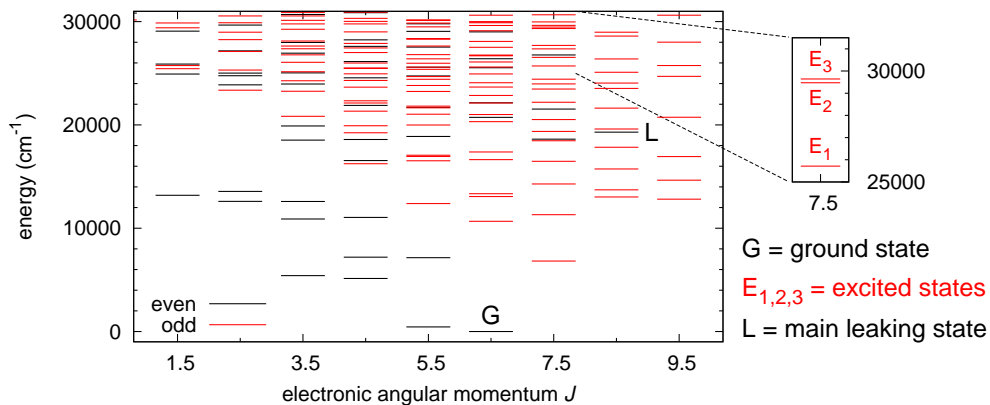


Figure 1: Energy diagram of Er^+ . The inset shows the three odd-parity excited states E_1 , E_2 and E_3 with $J = 15/2$ which are the most suitable for laser-cooling.

In this work we address the feasibility of laser-cooling of open- $4f$ -shell rare-earth ions, taking the example of Er^+ , whose spectrum was interpreted in great details [6]. To that end, using a semi-empirical approach based on the Cowan codes [7], we compute transition dipole moments between the ground state “G” and excited states suitable for cooling (“ $E_{1,2,3}$ ”), but also with all states which represent possible leaks from the cooling cycle (see “L” on Fig. 1). By solving rate equations based on our computed Einstein coefficients, we demonstrate that laser-cooling of Er^+ does require repumping, and we identify a possible repumping scheme from the atomic state “L”. We also observe a cascade dynamics, within a fraction of second, to the ground and first-excited states. This dynamics is found insensitive to the inclusion of electric-quadrupole and magnetic-dipole transitions in our model. Our results suggest that laser-cooling of Er^+ is feasible, with two repumping lasers, and within a time scale which is compatible with the stability of ion traps.

References

- [1] J.J. McClelland, and J.P. Hannsen, Phys. Rev. Lett. **96**, 143005 (2006)
- [2] M. Lu, N.Q. Burdick, S.H. Youn, and B.L. Lev, Phys. Rev. Lett. **107**, 190401 (2011)
- [3] K. Aikawa, A. Frisch, M. Mark, S. Baier, A. Ritzler, R. Grimm, and F. Ferlaino, Phys. Rev. Lett. **108**, 210401 (2012)
- [4] D. Wineland, Rev. Mod. Phys. **85**, 1103 (2013)
- [5] F.H.J Hall, M. Aymar, N. Bouloufa-Maafa, O. Dulieu, and S. Willitsch, Phys. Rev. Lett. **107**, 243202 (2011)
- [6] J.-F. Wyart, and J.E. Lawler, Phys. Scr. **79**, 045301 (2009)
- [7] M. Lepers, J.-F. Wyart, and O. Dulieu, Phys. Rev. A **89**, 022505 (2014)

Towards a BEC in a time-averaged adiabatic potential ring waveguide

H. Mas¹, S. Pandey¹, V. Bolpasi¹, K. Poullos¹, and W. von Klitzing¹

¹*Institute of Electronic Structure and Laser, Foundation for Research and Technology-Hellas, P.O. Box
1527, 71110 Heraklion, Greece*

Presenting Author: hector.mas@iesl.forth.gr

Guided matter-wave experiments have become a testbed for fundamental quantum physics while at the same time pushing the limits of interferometry through development of new quantum sensors for precision measurements. For instance, confinement and coherent control of a Bose-Einstein condensate (BEC) in a ring-shaped potential would pave the way to what will probably be the most sensitive Sagnac-type interferometer to date.

A favorable route towards this goal are time-averaged adiabatic potentials (TAAP) [1], which allow flexible and smooth shaping of the potential, including a ring, and promise coherent manipulation of BEC.

Here we introduce a simple scheme for loading a sample of cold atoms onto the ring and present preliminary results on the RF dressing required for the TAAP.

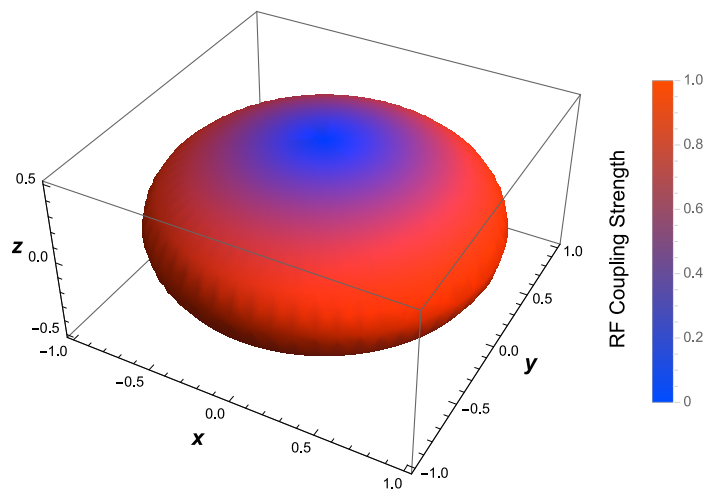


Figure 1: Exact calculation of the normalized coupling strength of a linear RF dressing field in the vertical direction of a quadrupole trap.

References

- [1] I. Lesanovsky, W. von Klitzing Phys. Rev. Lett. **99**, 083001 (2007)

Dense and cold atomic beam delivered by a 2DMOT repumped and channelled by a Laguerre-Gaussian laser beam

J. Ruaudel¹, C. Cabrera-Gutiérrez¹, M. Jacquy¹, B. Viaris de Lesegno¹, and L. Pruvost¹

¹Laboratoire Aimé Cotton, CNRS, ENS Cachan, Univ Paris Sud, bat 505, 91405 Orsay, France

Presenting Author: laurence.pruvost@u-psud.fr

Nowadays, 2DMOTs are atomic sources currently used for trap loading, 3DMOTs for example. Indeed, they deliver slow and cold atom beams: typically for rubidium, the transverse temperature is 0.4 mK and the longitudinal velocity in the 10-50 m/s range. Nevertheless, the divergence of the output beam being about 40 mrad leads to a rapid decrease of the atomic density as the beam propagates. It is the reason why the 3DMOTs are installed close to the 2DMOT exit and require cooling-laser beams with a large diameter and a large power. The divergence can be reduced with an additional far-blue-detuned Laguerre-Gaussian (LG) mode set on the 2DMOT axis, which operates as a 2D-dipole trap on exiting atoms [1].

In the present version the LG mode, frequency-locked to the ^{87}Rb $5s_{1/2}$ $F=1 \rightarrow 5p_{3/2}$ $F'=2$ transition, is set along the main axis of a vapor-cell 2D-magneto-optical trap (2DMOT) and, realizes both functions, namely repumping atoms inside the 2DMOT and channelling atoms exiting the cell. It avoids any other repumping light. The output atomic beam properties (flux, density) depend on the LG power (enough to repump and to channel) and order (large enough for minimize atom losses due to residual heating), as shown in the figure. We show that with about 50-100 mW the density gain exceeds 100. As preliminary result we will present a LG2DMOT-loaded 3DMOT realized with millimeter-sized cooling laser beams.

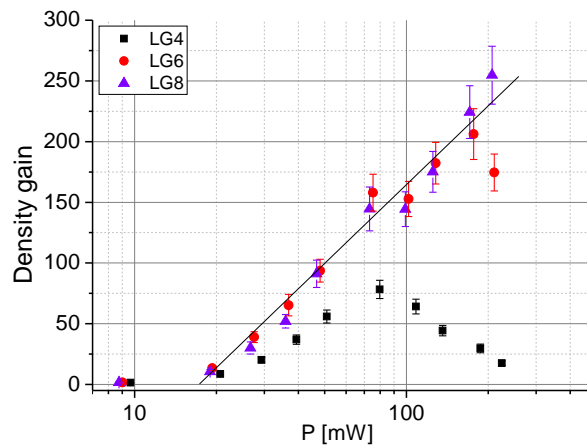


Figure 1: Density gain of the LG2DMOT observed at 300 mm, versus the LG power, for orders equal to 4, 6 and 8.

References

- [1] V. Carrat, C. Cabrera-Gutiérrez, M. Jacquy, J. R. W. Tabosa, B. Viaris de Lesegno, and L. Pruvost, *Opt. Lett.* **39**, 719-722, (2014).
- [2] C. Cabrera-Gutiérrez, PhD Thesis, université Paris-Sud, Orsay, (2014).

Spinor quantum gases with narrow-line control

M. Robert-de-Saint-Vincent¹, E. Maréchal¹, L. Vernac¹, O. Gorceix¹, and B. Laburthe-Tolra¹

¹*Université Paris 13, Sorbonne Paris Cité, Laboratoire de Physique des Lasers, Villetaneuse*

Presenting Author: martin.rdsv@univ-paris13.fr

Degenerate atomic gases provide a new realization of magnetic systems, which permit to revisit questions encountered in condensed matter, while providing access to a new range of physical situations. Alkali-earth species combine the attractive properties of large-spin fermionic isotopes, and of narrow spectroscopic lines commonly used in the context of metrology. Our project aims at taking full advantage of the spectroscopic properties of Strontium 87 to study the many-body physics of a 10-component spinor fermionic gas in lattice geometry [1]. The 7 kHz wide $^1S_0 \rightarrow ^3P_1$ transition will be used for site- and spin-selective state transfer and detection. The mHz wide "clock" transition $^1S_0 \rightarrow ^3P_0$ offers prospects for the optical control of interactions and for the preparation of metastable magnetic impurities [2]. The optical frequency reference from the optical clocks at Observatoire de Paris, disseminated to Laboratoire de Physique des Lasers through a fiberized link [3], will permit to assess the frequency stability of the laser sources involved in narrow-line control of this many-body system.

References

- [1] A. Gorshkov *et al.* Nature Physics **6**, 289-295 (2010)
- [2] M. Foss-Feig, M. Hermele, and A. M. Rey, Physical Review A **81**, 051603(R) (2010)
- [3] F. Kéfélian *et al.* Optics Letters **34**, 1575-1575 (2009)

Rotational State Cooling of Trapped Polyatomic Molecules

M. Zeppenfeld¹, R. Glöckner¹, A. Prehn¹, M. Ibrügger¹, and G. Rempe¹

¹MPI für Quantenoptik, Garching, Germany

Presenting Author: martin.zeppenfeld@mpq.mpg.de

Due to their rich internal structure and long-range dipole-dipole interactions, polar molecules cooled to cold and ultracold temperatures promise fascinating applications ranging from cold chemistry to quantum information processing. In addition to cooling of the motional degrees of freedom, a key prerequisite for such applications is to gain and maintain control over the internal molecular states.

In this contribution, we present rotational state cooling of methyl fluoride (CH₃F) molecules. By exploiting a vibrational spontaneous decay, molecules in 16 *M*-sublevels of four rotational states are optically pumped into a single *M*-sublevel. Combined with motional Sisyphus cooling [1,2], this results in a cold (30 mK) ensemble of trapped CH₃F molecules with more than 70% of all molecules populating a single rotational state. We expect our method to be applicable to a wide variety of molecule species, thus opening a route for quantum controlled experiments with polyatomic molecules.

References

- [1] M. Zeppenfeld *et al.* Phys. Rev. A **80** 041401 (2009)
- [2] M. Zeppenfeld *et al.* Nature **491** 570–573 (2012)

Atom chip based guided atom interferometer for rotation sensing

W. Yan¹, S. Bade¹, M.-A. Buchet¹, A. Landragin¹, and C. L. Garrido Alzar¹

¹SYRTE, Observatoire de Paris, PSL Research University, CNRS, Sorbonne Universités, UPMC Univ. Paris 06, LNE, 61, avenue de l'Observatoire, 75014 Paris, France

Presenting Author: carlos.garrido@obspm.fr

In this work, the physical aspects as well as the experimental progress towards the realization of a rotation sensor using cold atoms magnetically guided on an atom chip are presented. The design and derivation of the magnetic guiding potential, the expected sensitivity, and the study of a highly efficient matter-wave beam splitter are in detail analyzed. This device is designed taking into account the stringent requirements of inertial navigation. Besides the usual constraints imposed on the physical dimensions and power consumption for the aforementioned application, we also investigate here the on-chip incorporation of keys elements needed in the realization of a cold atom interferometer. In particular, we discuss different strategies to overcome the fundamental limitations of guided [1] and free falling atom interferometer inertial sensors [2]: wire roughness induced decoherence, cloud fragmentation, interrogation time and quantum projection noise.

The working principle of this inertial sensor is based on a magnetic polarized cloud of cold ⁸⁷Rb atoms coherently split by a $\pi/2$ pulse that creates a superposition of two opposite wave-packet propagation modes. Both wave-packets will be constrained to propagate along a circular guide of a few millimeters diameter. At the output of the guide, the application of a second $\pi/2$ pulse produces an interference signal sensitive to rotation via the Sagnac effect, measured as an atom number imbalance. In Fig. 1 we show the expected sensitivity of the designed device for an interrogation time of 1s and different launching velocities. For a typical launching velocity obtained via a Bragg process ($v/v_{\text{recoil}} = 2$), the required guide radius is $500\mu\text{m}$ and the reached sensitivity, when using $\sim 10^6$, is $3 \times 10^{-8} \text{ rad}\cdot\text{s}^{-1}/\sqrt{\text{Hz}}$ or equivalently $6 \times 10^{-3} \text{ deg/hr}/\sqrt{\text{Hz}}$. Such a sensitivity is already close to the navigation grade bias stability requirement for a gyroscope which is on the order of 10^{-4} deg/hr .

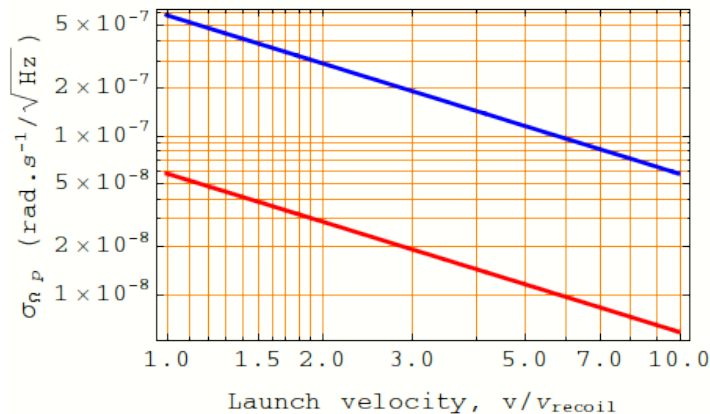


Figure 1: Expected sensitivity at the projection noise limit for 10^4 (blue) and 10^6 (red) atoms.

References

- [1] J.-B. Trebbia, C. L. Garrido Alzar, R. Cornelussen, C. I. Westbrook, and I. Bouchoule. Phys. Rev. Lett. **98**, 263201 (2007)
- [2] B. Canuel, F. Leduc, D. Holleville, A. Gauguet, J. Fils, A. Viridis, A. Clairon, N. Dimarcq, Ch. J. Borde, and A. Landragin. Phys. Rev. Lett. **97**, 010402 (2006)

Fundamental physics with atoms/molecules

Description of the evolution of Rydberg systems and interaction of light with multi-level atoms using Floquet technique

D. K. Efimov¹, N. N. Bezuglov¹, and G. Juzeliūnas²

¹*St. Petersburg State University, St.Petersburg, Russia*

²*Institute of Theoretical Physics and Astronomy, Vilnius University, Lithuania*

Presenting Author: dmitry.efimov@de29866.spb.edu

The Floquet theory treats the first order linear differential equations systems having time-dependent periodic coefficients. The Floquet' main theorem outlines a canonical form for special fundamental solutions of a specific linear system. It is a temporal analogue of the Bloch's theorem which describes solutions features for spatially periodic systems. The Floquet theorem indicates a canonical way to construct solutions for the evolution of a particle in time-periodic potentials induced, for instance, with monochromatic external electrical fields.

The essence of the Floquet technique is as follows. We extend the phase space for classical problems, or the Hilbert space in the quantum case by introducing the new "phase" variable θ . Rewritten in the new extended spaces, the Hamiltonian equation, or Schroedinger's equation, becomes time-independent, resulting in essential simplification of its solutions.

We consider two examples in the field of atomic physics, where the application of the technique turns out to be constructive. The first one deals with the classical treatment of a hydrogen Rydberg atom evolution under the influence of a monochromatic microwave field with the frequency ω [1]. The electron's motion under the Floquet representation is described in $(2 \cdot 3 + 2)$ -dimensional space with two additional canonical "action-angle" types variables I, θ . The Floquet Hamiltonian imposes a trivial solution $\theta = \omega t$ for the angular variable. Correspondingly, there is one more non-trivial Hamiltonian equation for I . Such a trick allows one to provide analysis of the time-dependent problem with the use of methods which are valid only in steady-state cases.

The second example considers interaction of multilevel atoms with a set of n laser fields having different frequencies. Here a standard application of the RWA is impossible, so one needs to use a smarter technique [2]. We have constructed a new Hilbert space with extra n dimensions. The modified Schroedinger's equation in the new extended space becomes time-independent, a fact that allows one to use conventional approximations valid only for time-independent problems.

References

- [1] D. K. Efimov, N. N. Bezuglov, A. N. Klyucharev, Yu. N. Gnegin, K. Miculis, A. Ekers, *Opt. and Spectr.* 117-1, 8 (2014)
- [2] S. Guerin and H. R. Jauslin, *Adv. Chem. Phys.* 125, 147 (2003)

Generation of Schrödinger cat states in a NMR quadrupolar system

A. G. Araujo-Ferreira¹, T. J. Bonagamba¹, G. D. de Moraes Neto¹, M. H. Y. Moussa¹, and R. Auccaise²

¹ Instituto de Física de São Carlos, Universidade de São Paulo, Caixa Postal 369, 13560-970 São Carlos, São Paulo, Brazil

² Departamento de Física, Universidade Estadual de Ponta Grossa, Av. Carlos Cavalcanti, 4748, 84030-900 Ponta Grossa, Paraná, Brazil

Presenting Author: raestrada@uepg.br

One of the most intriguing theoretical concepts between classical and quantum mechanics is the Schrödinger cat state [1,2], which plays a distinguished role in quantum computation as a resource for universal computation and a good control for quantum systems. Therefore, a challenging task is the development of efficient strategies for achieving an experimental implementation of a Cat state. On this behalf, experimental demonstrations of the efficiency of quantum protocols using trapped ions [3], and also a pair of photons [4], allowed the recognition of their quantum advantages. Thus, the effort of extending those systems for more qubits became a major issue for many experimentalists. Later, this kind of state was implemented using six-atoms in a cavity at ultra cold temperatures [5], also, in the light scenario, in which up to several dozens of photons were used [6,7], and also in superconducting devices with the number equivalence of five photons [8].

The main strategy in those implementations was exploring the atom-field interaction [6,7] (except in [8]), but that is not the only possible strategy. In the context of atomic physics there is a theoretical proposal which explores the atom-atom interaction [9]. This strategy was developed using the total angular momentum description $\hat{\mathbf{J}} = (\hat{J}_x, \hat{J}_y, \hat{J}_z)$, the SU(2) algebra and the appropriate coupling strength between particles of a two mode Bose-Einstein Condensate. From the point of view of algebraic structures, the spin angular momentum description, $\hat{\mathbf{I}} = (\hat{I}_x, \hat{I}_y, \hat{I}_z)$, belongs and obeys the SU(2) algebra, and this special characteristic allows us to transfer the knowledge developed for a many body system into a spin system [10]. In this work, we will show how a nuclear spin system, $I = 7/2$, achieves an analogous behaviour of a few ultra-cold atoms particles, $N = 7$, in a trap to generate a Schrödinger cat state.

References

- [1] V. Bužek and P. L. Knight, *Quantum interference, superposition states of light, and nonclassical effects*, Progress in Optics XXXIV (ed. E. Wolf) 1–158 (Elsevier, Netherland - 1995).
- [2] G. S. Agarwal, *Quantum Optics* (Cambridge, USA - 2013).
- [3] C. Monroe *et al.*, A Schrödinger cat superposition state of an atom, *Science* **272**, 1131–1136 (1996).
- [4] D. Bouwmeester *et al.*, Experimental quantum teleportation, *Nature* **390**, 575–579 (1997).
- [5] D. Leibfried *et al.*, Creation of a six-atom Schrödinger cat state, *Nature* **438**, 639–642 (2005).
- [6] S. Deléglise *et al.*, Reconstruction of non-classical cavity field states with snapshots of their decoherence, *Nature* **455**, 510–514 (2008).
- [7] B. Vlastakis *et al.*, Deterministically encoding quantum information using 100-photon Schrödinger cat states, *Science* **342**, 607–610 (2013).
- [8] M. Hofheinz *et al.*, Synthesizing arbitrary quantum states in a superconducting resonator, *Nature Letters* **459**, 546–549 (2009).
- [9] G. S. Agarwal *et al.*, Atomic Schrödinger cat states, *Physical Review A* **56**, 2249–2254 (1997).
- [10] R. Auccaise *et al.*, Spin Squeezing in a Quadrupolar Nuclei NMR System, *Physical Review Letters* **114**, 043604 (2015).

Pair creation and annihilation with atoms and channeling nuclei

N. A. Belov¹, Z. Harman¹

¹Max Planck Institute for Nuclear Physics, Saupfercheckweg 1, 69126 Heidelberg, Germany

Presenting Author: belov@mpi-hd.mpg.de

We theoretically investigate different processes connected with pair production and annihilation in atoms and highly charged ions. These fundamental features include nuclear excitation by resonant positron annihilation (NERPA) and the electron-positron pair creation in heavy ion channeling.

In the annihilation of a positron with a bound atomic electron, the virtual photon created may excite the atomic nucleus. We put forward this effect as a spectroscopic tool for an energy-selective excitation of nuclear transitions [1]. This scheme can efficiently populate nuclear levels of arbitrary multiplicities in the MeV regime, including giant resonances and monopole transitions. NERPA constitutes a way to excite nuclei which is alternative to photo- and Coulomb excitation. It has an attractive combination of advantages of both methods: the resonant character of the excitation and a significant cross section regardless of the multipolarity. Furthermore, in certain cases, it has higher cross sections than the conventionally used Coulomb excitation and it can even occur with high probability when the latter is energetically forbidden. The resonant character of nuclear excitation by positron annihilation opens a way to investigate the structure of broad nuclear resonances. For instance, it allows to efficiently excite certain energy regions of a Giant Resonance (GR) in heavy nuclei. For certain GR, our predicted NERPA resonance strengths are 8 orders of magnitude higher than the largest NERPA resonance strengths investigated so far.

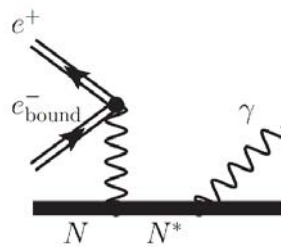


Figure 1: Lowest-order Feynman diagram for NERPA followed by γ -emission.

The time-reversed process, i.e. bound-free electron-positron pair production is a channel of monochromatic positron creation in nucleus-nucleus collisions. We suggest an alternative way to investigate this phenomenon by channeling of accelerated ions through a crystal. This scheme increases the pair production rate coherently and thus enhances the investigation of nuclear pair conversion [2]. It also allows to depopulate nuclei in metastable states, and convert the nuclear energy stored to electron-positron pairs. Pair creation by channeling ions can be also regarded as an extension of resonant coherent excitation of highly charged ions to higher frequencies and higher ion velocities, which has been investigated at the GSI before [3]. This novel channel of pair creation can be examined at the upcoming FAIR facility (see e.g. [3] and references therein) in the near future.

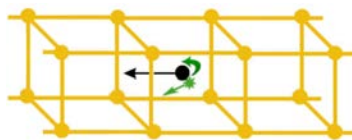


Figure 2: Schematic view of electron-positron pair creation in heavy ion channeling.

References

- [1] N. A. Belov, Z. Harman, Phys. Lett. B **741**, 61 (2015)
- [2] N. A. Belov, Z. Harman, submitted (2014); arXiv:1411.5711
- [3] Y. Nakano *et al.* Phys. Rev. A **87** 060501 (2013)

Analysis of the spatial dependence of laser-induced fluorescence for alkali metal vapours in an intense laser beam

M. Auzinsh¹, A. Berzins¹, R. Ferber¹, F. Gahbauer¹, and U. Kalnins¹

¹Laser Centre, University of Latvia, Rīga

Presenting Author: andris.berzins@lu.lv

Magneto-optical resonances in alkali vapours have been studied for a long time [1], but a long-standing problem has been the difficulty in describing the resonance shapes in detail when high laser powers are used. In this study we tried a new approach to solving this problem theoretically, and the theoretical calculations were confirmed by experimental results.

The study consisted of two parts: - first, we described magneto-optical signals in alkali vapour obtained with a single laser. For this part we used an advanced theoretical model, which was an improved version of a model that had worked well for low laser powers [2] and had been used already to describe magneto-optical effects gas cells that were only a few hundred nanometers thick [3]. In this case, the shapes of magneto-optical resonances were determined by collisions with the cell walls and not by the fly-trough relaxation, which is one of the most important factors that influence resonance shape in ordinary cells. The additional feature that was added to the model described in [2] was dividing the Gaussian profile of the laser beam into multiple regions and performing calculations for each of them, taking into account the actual intensity in that region. Stationary solutions were obtained for each region, but the regions were coupled by the exchange of atoms between them. Measurements were done on the ⁸⁷Rb D₁ line.

For the second part, we described the population distribution and spatial intensity distribution by scanning a spatially narrow, weak probe laser through a spatially broad, intense pump laser. In this way, we could measure directly processes that took place at different parts of a Gaussian laser beam at larger laser power densities. In Fig. 1 one can see 3D plots of the experimentally measured fluorescence intensity (a) and the results of theoretical calculations (b) for the Cs D₁ line. The intensity profiles agree qualitatively.

We gratefully acknowledge support from Latvian National Research Programme (VPP) project IMIS².

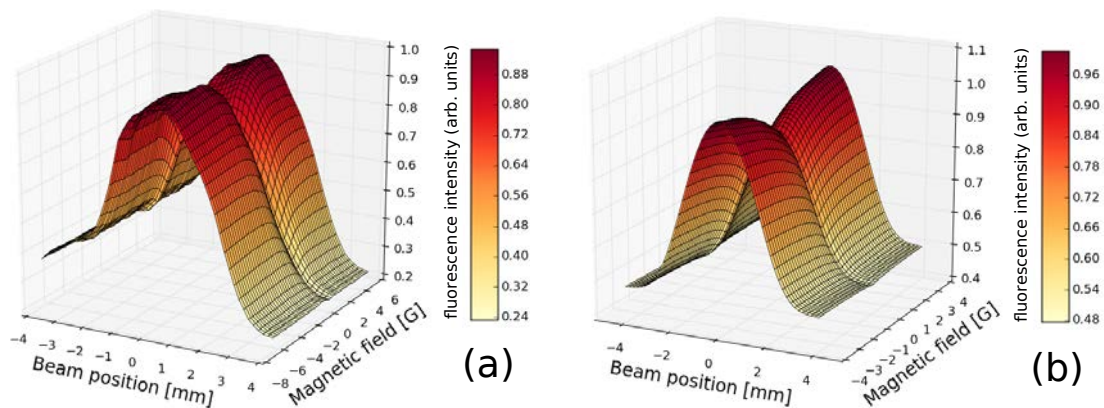


Figure 1: 3D plots of magneto-optical resonances: experimental measurements (a) and theoretical calculation (b) for Cs D₁ line transition $F_g=3$ to $F_e=4$ for the probe beam and $F_g=4$ to $F_e=4$ for the pump beam

References

- [1] M. Auzinsh, D. Budker, and S. M. Rochester, *Optically Polarized Atoms* (Oxford University Press, Great Clarendon Street, 2010), ISBN 978-0-19-956512-2
- [2] M. Auzinsh, R. Ferber, F. Gahbauer, A. Jarmola, and L. Kalvans, Phys. Rev. A **78**, 013417 (2008)
- [3] M. Auzinsh, A. Berzins, R. Ferber, F. Gahbauer, L. Kalvans, A. Mozers, and A. Spiss, Physical Review A **87**, 033412 (2013)

Designed of a pulsed negative ions source

T. Leopold^{1,2}, J. Rohlén¹, D. Hanstorp¹, J. Blahins³, A. Apsitis³, U. Berzins³, and A. Ubelis³

¹*Department of Physics, University of Gothenburg, SE*

²*Institut für Physik, Johannes Gutenberg-Universität Mainz, DE*

³*Institute of Atomic Physics and Spectroscopy, Association FOTONIKA-LV, University of Latvia, LV*

Presenting Author: Janis_59@inbox.lv

The Middleton sputter source is the most versatile source for production of beams of atomic negative ions [1]. In this source Cs+ ions are created and accelerated towards a cathode holding a sample containing the element to be produced. Atoms and small molecules are sputtered from the sample with a substantial fraction being in the negative charge states. Cathodes of refractory metals last for many hours producing stable negative ion beams. Non-conducting elements or metals with low melting points are more difficult to produce. The lifetime of some cathodes are only a few hours, and the reproducibility of the cathodes are low. This hampers experimental investigations of such elements. However, in many experiments the negative ions are investigated with pulsed laser where only a small fraction of the duty cycle is used. We have therefore investigated the possibility to pulse the ion source in order to extend the lifetime of the cathode.

We have designed a system where we are able to pulse the ions source in order synchronize it with a 10 Hz, 6 ns Nd:YAG laser. This was achieved by pulsing the high voltage between the ionizer, where the Cs+ are produced, and the cathode. We choose to produce 500 μ s long ion pulses.

Figure 1 (red rectangles) shows the number of neutral atoms produce from the beam of negative ions. We observe an increased in the ion production over the first 150 μ s, where after the production is essentially constant. A laser pulse was intersecting the ion beam at $t = 170 \mu$ s. The resulting photodetachment signal is shown as the blue rectangle. This data clearly shows that we can produce a pulsed ion beam which can be synchronized with the laser pulse.

As a final test, two identical aluminum cathodes were operated for 24 hours. One was continuously operated whereas the other was run in pulsed mode with a 1% duty cycle. A deep hole was created in the cathode run in the continuous mode, whereas the cathode operated in the pulsed mode looked essentially unused. This was confirmed by their measured mass losses of $\Delta m_1 = (9.0 \pm 0.2) \text{ mg}$, $\Delta m_2 = (0.2 \pm 0.2) \text{ mg}$, respectively. This means that a single cathode operated in pulsed mode will last for many hundreds of hours of operation.

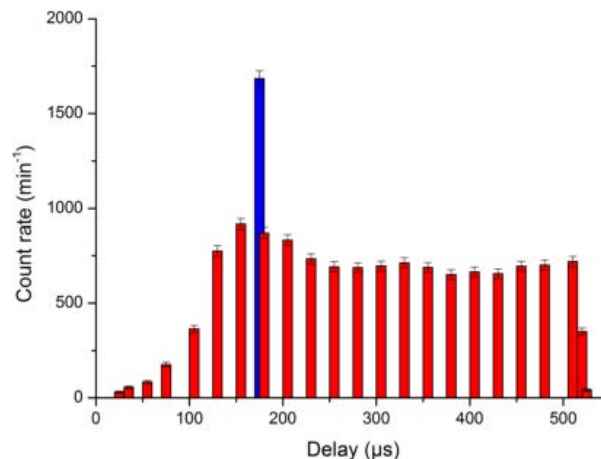


Figure 1: Collisional detached negative ions (red), and photodetached negative ions (blue).

References

- [1] A negative ion cookbook <http://www.pelletron.com/cookbook.pdf>

Nonlinear Magneto-Optical Rotation in Rubidium Vapor Excited to $6^2P_{1/2}$ State

S. Pustelny^{1,5}, M. Auzinsh², L. Busaite², A. Akulshin³, N. Leefer⁴, and D. Budker^{4,5}

¹*Institute of Physics, Jagiellonian University, Reymonta 4, 31-007, Kraków, Poland*

²*Laser Centre, University of Latvia, 19 Rainis Boulevard, Rīga, Latvia, LV-1586*

³*Swinburne University of Technology, PO Box 218, Hawthorn Victoria, Australia 3122*

⁴*Helmholtz-Institut Mainz, Johannes Gutenberg Universität Mainz, 55128 Mainz, Germany*

⁵*Department of Physics, University of California, Berkeley, CA 94720-7300, USA*

Presenting Author: laima.busaite@lu.lv

Most commonly nonlinear magneto-optical rotation (NMOR) has been extensively studied at strong D_1 or D_2 lines. In such systems, a good agreement between theoretical predictions and experimental observations has been demonstrated [1]. The wide range of successful applications of the method results in a demand for its extension to different optical transitions.

We present research of NMOR under different physical conditions, i.e., we explore the effect in rubidium atoms excited to higher-energy states (the $6^2P_{1/2}$ state). This results in more complex repopulation of the ground-state levels. In addition to the direct repopulation of the ground state hyperfine levels, these levels may be repopulated via several intermediate states ($6^2S_{1/2}$, $4^2D_{3/2}$, $5^2P_{1/2}$ and $5^2P_{3/2}$) (Fig. 1)

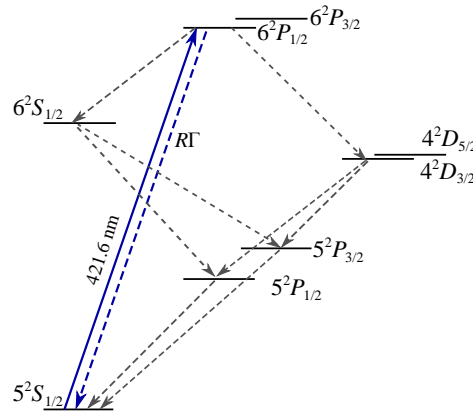


Figure 1: Relevant energy levels and transitions of Rb atom excited by resonant radiation at 421.6 nm.

A specific goal of this research is a comparison of the experimental results of the, so-called, blue NMOR, where excitation and probing at the $5^2S_{1/2} \rightarrow 6^2P_{1/2}$ absorption line is performed using 421 nm light, with the results of theoretical calculations performed based on the model developed in Ref. [2]. In the theoretical model, NMOR is described as a three-stage process, consisting of pumping, evolution and probing of quantum states of atoms, constituting a medium interacting with light.

It is verified that the real (complex but closed) system can be adequately described with a single relaxation parameter responsible for ground-state repopulation as it was assumed in the model.

The authors would like to thank Simon Rochester for his role in the development of the theoretical model of NMOR. LB and MA acknowledge support from ERAF project Nr. 2010/0242/2DP/2.1.1.1.0/10/APIA/VIAA/036, NATO Science for Peace and Security Programme project SfP983932, and the Latvian Council of Science project 119/2012. SP acknowledges support from the Polish Ministry of Science and Higher Education within the grant Iwentus Plus.

References

- [1] D. Budker *et al.* Reviews of Modern Physics **74** 1153 (2002)
- [2] M. Auzinsh, D. Budker, and S. M. Rochester, Phys. Rev. A **80**, 1 (2009)

Laser-gamma-nuclear spectroscopy of multicharged ions: “Shake-up” and co-operative excitation effects, New data

V. Buyadzhi¹, O. Khetselius¹, A. Svinarenko¹, and T. Florko¹

¹*Odessa State University - OSENU, Odessa*

Presenting Author: vbuyad@mail.ru

We study the class of problems which have been arisen and connected with modelling the cooperative laser-electron-nuclear phenomena such as the electron shell shake-up and NEET or NEEC (nuclear excitation by electron transition or capture) effects in heavy neutral atomic/nuclear systems [1-3]. Though the shake-up effects in the neutral atoms (molecules) are quite weak (because of the weak coupling of the electron and nuclear degrees of freedom), the possibilities of their realization significantly differ in a case of the multicharged ions and neutral atoms correspondingly.

We develop an advanced relativistic approach to calculation of the probabilities of the different co-operative laser electron-gamma-nuclear processes in the multicharged ions (characteristics of the electron satellites in gamma-spectra of nuclei of the multicharged ions and the resonant NEET (NEEC) effects in heavy nuclei of multicharged ion). The theory is based on the relativistic energy approach (S-matrix formalism of Gell-Mann and Low) and relativistic many-body perturbation theory [3,4]. Within the energy approach, decay and excitation probability (of the electron shell shake-up process or etc) is linked with the imaginary part of energy of the excited state for the “electron shell-nucleus-photon” system. For radiative decays it is manifested as effect of retarding in interaction and self-action and calculated within QED perturbation theory formalism. We present new data about intensities of the electron satellites in gamma-spectra of nuclei in the neutral (low lying transitions) and the F-like, Ne-like multicharged ions for isotopes ^{133}Cs , ^{169}Tm , ^{173}Yb , which show existence of an new effect of the giant increasing (up 3-4 orders) electron satellites intensities (electron shell shake-up probabilities) under transition from the neutral atoms to the corresponding multicharged ions. We present the similar relativistic energy approach to the NEET (NEEC) process in the heavy multicharged ions and present new quantitative estimates of the corresponding NEET probabilities in the nuclei of ^{193}Ir , ^{235}U of the corresponding multicharged ions. The presented data demonstrate an effect of changing the corresponding NEET probabilities under transition from the neutral atomic/nuclear systems to the corresponding multicharged ions.

References

- [1] M Morita *Progr.Theor.Phys.* **49**, 1574–1592 (1973); L.N. Ivanov, V. S. Letokhov *JETP*. **93**, 396–408 (1987); A. V. Glushkov, L.N. Ivanov *Phys. Lett.* **A170**, 33–37 (1992); A. Glushkov, L. Ivanov, V. Letokhov *Preprint ISAN N-AS4* (Moscow-Troitsk, ISAN, 1992), 12p.
- [2] I. Ahmad *et al.* *Phys. Rev.* **C61**, 051304 (2000); S. Kishimoto *et al.* *Phys. Rev.* **C74**, 031301 (2006); A. Palffy *et al.* *Phys. Rev.* **A73**, 012145 (2006); E Tkalya *Phys.Rev.A.* **75**, 022509 (2007)
- [3] A. Glushkov O. Khetselius, S. Malinovskaya *Frontiers in Quantum Systems in Chemistry and Physics Ser.: Progress in Theoretical Chemistry and Physics, Eds. S. Wilson et al* (Springer, Berlin, 2008) **18**, 523-545; *Europ. Phys. Journ.* **T160**, 195–208 (2009)
- [4] O. Khetselius *Int. J. Quant. Chem.* **109**, 3330-3336 (2009); *Phys. Scripta.* **T135**, 014023 (2009); *J. of Phys: C Ser.* **397**, 012012 (2012)

Electron Spectroscopy of four-photon-ionized strontium in the 715-737 nm wavelength range

S. Cohen¹, A. Dimitriou¹

¹Atomic and Molecular Physics Laboratory, Physics Department, University of Ioannina, 45110 Ioannina, Greece

Presenting Author: scohen@uoi.gr

We report on electron energy analysis experiments aiming to elucidate the single and double ionization pathways when ground state strontium atoms interact with dye laser pulses of ≈ 5 ns duration and $\approx 4 \times 10^{11}$ W/cm² maximum intensity. Within the examined 715–737 nm wavelength range there are the $4d5p\ ^1P_1$ and $(4d5p+5s5f)\ ^1F_3$ three-photon resonant, four-photon ionized bound states and the four-photon excited $5p^2\ ^1S_0$ highly correlated autoionizing state, located just above the first ionization threshold. The recorded electron spectra (Fig.1) probe the accumulation of population in the excited $4d_j$ and $5p_j$ Sr^+ states. This observation signifies the absorption of at least two photons above the first ionization threshold. However, the $4d_j$ state is found to be much more heavily populated than the $5p_j$ one. This finding identifies the dominant pathway to double-ionization within the same laser pulse, as stemming from multiphoton ionization out of the $4d_{3/2,5/2}$ levels of Sr^+ . Hence, this question, which remained open in earlier work performed using the same excitation and ionization scheme but based solely on the detection of ion and ionic-fluorescence yields [1] is here clarified. Finally, the recording of photoelectron angular distributions from four- as well as higher-photon ionization for selected laser wavelengths, revealed the dominant contributing partial waves at each ionization step. These latter results are compared to those obtained by relevant earlier studies on magnesium atom [2,3].

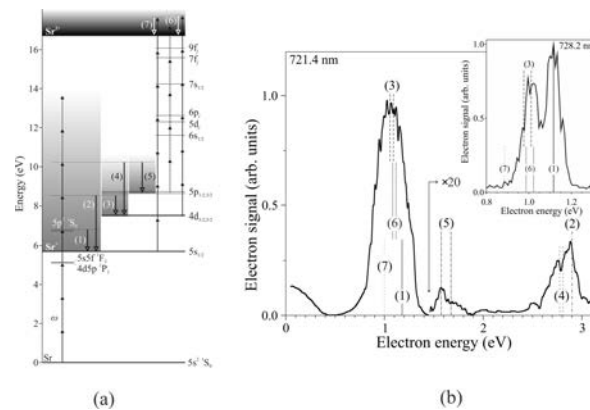


Figure 1: (a) Energy level diagram and single/double ionization pathways. (b) Electron spectra recorded at selected wavelengths. The main graph refers to the $5s5f\ ^1F_3$ resonance and it was obtained with a resolution of $\Delta E \sim 0.3$ eV. The inset shows the corresponding electron spectrum at the $4d5p\ ^1P_1$ resonance ($\Delta E \sim 0.06$ eV). Various single and double ionization channels are numbered in (a) and (b).

Acknowledgement

This research has been co-financed by the European Union (European Social Fund — ESF) and Greek national funds through the Operational Program "Education and Lifelong Learning" of the National Strategic Reference Framework (NSRF) — Research Funding Program: THALES (ISEPUMA). Investing in knowledge society through the European Social Fund.

References

- [1] I. Liontos *et al.* J. Phys. B: At. Mol. Opt. Phys **41**, 045601 (2008)
- [2] A. Dimitriou *et al.* J. Phys. B: At. Mol. Opt. Phys **44**, 135001 (2011)
- [3] A. Dimitriou *et al.* J. Phys. B: At. Mol. Opt. Phys **45**, 205003 (2012)

Two-photon Stark Spectroscopy and Photoionization Microscopy on the Mg atom

P. Kalaitzis¹, E. Pavlou¹, A. Marciniak², T. Barillot², F. Lépine², C. Bordas², and S. Cohen¹

¹Atomic and Molecular Physics Laboratory, Physics Department, University of Ioannina, 45110 Ioannina, Greece

²Institut Lumière Matière, Université Lyon 1, CNRS, UMR 5306, 10 rue Ada Byron 69622 Villeurbanne Cedex, France

Presenting Author: scohen@uoi.gr

Photoionization microscopy (PM) allows the visualization of the atomic wave function at a macroscopic scale. PM refers to photoionization of an atom in the presence of a uniform static electric field and the subsequent magnified imaging of the liberated slow (\sim meV) electrons on an MCP/phosphor-screen detector. PM was initially tested in the heavy ($Z=54$) Xe atoms but the recorded images revealed solely the continuous part of the electronic wave-function [1]. Recently, the wave-functions of quasi-bound Stark states in the light Li [2], H [3] and He [4] atoms ($Z=3,1$ and 2 , respectively) were recorded and verified 30-year-old theoretical predictions [5]. Here we present two-photon Stark spectra (Figs. 1(a) and 1(b-i)) of the magnesium atom ($Z=12$) near the saddle point energy and the corresponding, preliminary, PM images (Fig. 1(c)). Stark spectra constitute a necessary first step towards the identification of Stark resonances, as well as the accurate determination of the classical saddle point energy ($E_{sp}=-2F^{1/2}$ atomic units, where F is the electric field strength). As it may be seen in Figs. 1(b-i) and 1(b-ii), the rise of the Mg^+ signal occurs slightly before the E_{sp} value determined by a fit to the outer (so-called indirect [6]) radii of the recorded PM images. The radii-based E_{sp} determination leads to the knowledge of the field strength within 1%. These findings are to be presented in detail in the conference.

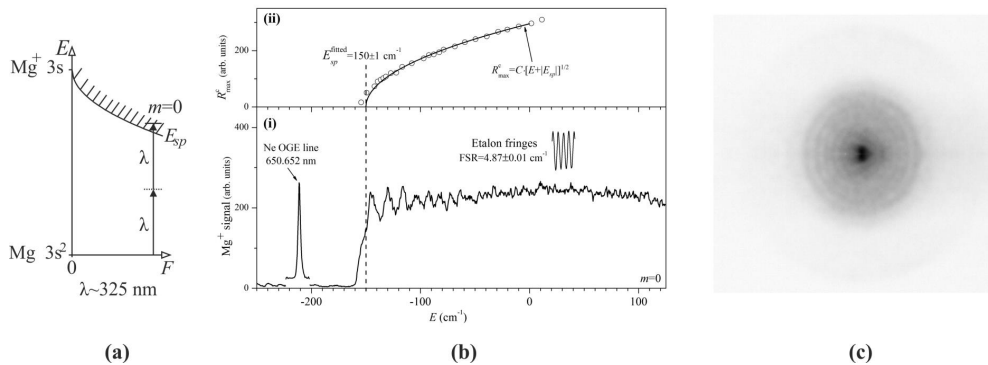


Figure 1: (a) Excitation scheme. (b-i) Stark spectrum ($F \approx 600$ V/cm) near the saddle point E_{sp} including the zero field ionization threshold ($E=0$). Laser polarization parallel to the electric field. A Ne optogalvanic line and etalon fringes provide wavelength calibration. (b-ii) Outer radii obtained from the recorded PM images (circles) and the fitted classical curve (line). (c) PM image showing the direct and the, hardly visible, indirect contributions ($F \approx 430$ V/cm and $E/|E_{sp}| \approx -0.2$).

Acknowledgement

The authors gratefully acknowledge financial support from Joseph and Ester Gani Foundation.

References

- [1] C. Nicole *et al.*, Phys. Rev. Lett. **88**, 133001 (2002)
- [2] S. Cohen *et al.*, Phys. Rev. Lett. **110**, 183001 (2013)
- [3] A.S. Stodolna *et al.* Phys. Rev. Lett. **110**, 213001 (2013)
- [4] A.S. Stodolna *et al.* Phys. Rev. Lett. **113**, 103002 (2014)
- [5] V. D. Kondratovich, V. N. Ostrovsky, J. Phys. B **23**, 3785 (1990)
- [6] C. Bordas, Phys. Rev. A **58**, 400 (1998)

Test of the universality of free fall with atoms in different spin Orientations

X.-B. Deng¹, X.-C. Duan¹, M.-K. Zhou¹, H.-B. Yao¹, C.-G. Shao¹, and Z.-K. Hu¹

¹MOE Key Laboratory of Fundamental Physical Quantities Measurement, School of physics, Huazhong university of Science and technology, Wuhan 430074, China

Presenting Author: xiaobingdeng@hust.edu.cn

We present our recent work on test of the universality of free fall (UFF) with atoms in different spin orientations (Figure 1), namely, the ^{87}Rb atoms in $m_F = +1$ and $m_F = -1$. A Mach-Zehnder-type atom interferometer is exploited to sequentially measure the free fall accelerations of the atoms in the two sublevels. The spin-orientation related Eötvös parameter η_s is obtained by comparing the measured gravity accelerations, correspondingly, and the preliminary result is $\eta_s = (-0.2 \pm 1.5) \times 10^{-5}$. Since the atoms in $m_F = +1$ and $m_F = -1$ are highly sensitive to magnetic field inhomogeneity, which mainly limits the precision of our UFF test, three steps are taken to alleviate the influence of the magnetic field inhomogeneity. Firstly, a relative homogeneous magnetic field space is selected for the interfering to take place, and an anti-Helmholtz coil is added to compensate the magnetic field gradient in vertical direction, ulteriorly. Secondly, the direction of the effective Raman laser wave number \mathbf{k}_{eff} is reversed to make a differential measurement for each m_F . The influence which is independent of \mathbf{k}_{eff} can be canceled. However, with the Raman lasers configured in $+k_{\text{eff}}$ versus $-k_{\text{eff}}$, the directions of the recoil velocities are opposite. This induces a tiny difference between the atoms' trajectories, and consequently causes a residual influence in the differential measurement result. The third step is to correct this residuum using the common mode result for the two interfering configurations of \mathbf{k}_{eff} .

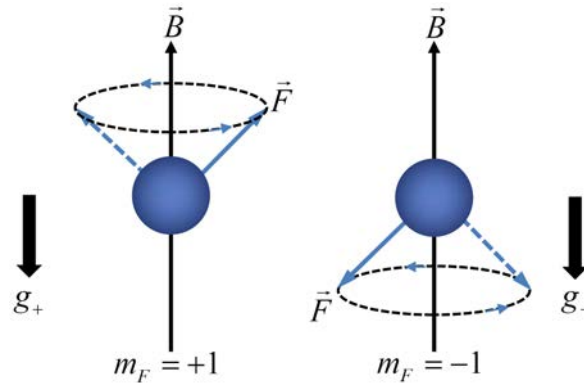


Figure 1: Schematic of the spin orientations for ^{87}Rb atoms in $m_F = +1$ and $m_F = -1$.

References

[1] Xiao-Chun Duan, Min-Kang Zhou, Xiao-Bing Deng, Hui-Bin Yao, Cheng-Gang Shao, Jun Luo, and Zhong-Kun Hu, arXiv: 1503.00433v1.

High precision spectroscopy of single $^{138}\text{Ba}^+$ ions

E. A. Dijck¹, A. Mohanty¹, N. Valappol¹, O. Böll¹, J. O. Grasdijk¹, A. T. Grier¹, S. Hoekstra¹, K. Jungmann¹, M. Nuñez Portela¹, C. J. G. Onderwater¹, L. Willmann¹, and H. W. Wilschut¹

¹Van Swinderen Institute, University of Groningen, The Netherlands

Presenting Author: e.a.dijck@rug.nl

We investigate single trapped, laser cooled Ba^+ and Ra^+ ions as ideal candidates for high precision measurements of the weak mixing angle in atomic systems; furthermore, the same experimental setup can be employed to build an atomic clock with a fractional frequency uncertainty of 10^{-18} [1]. For these applications of high precision spectroscopy a good understanding of the optical line shapes involved is indispensable.

We have studied the transition frequencies between low-lying energy levels in a single trapped $^{138}\text{Ba}^+$ ion using laser spectroscopy [2]. The levels of this alkaline earth ion form a Λ -type system, where two lasers are used for laser cooling and probing. A frequency comb that is referenced to a GPS-disciplined Rb clock is used to control the laser frequencies. By extracting the one-photon and two-photon components of the line shape using an eight-level optical Bloch model (see Fig. 1), we achieved order 100 kHz accuracy for the frequencies of the transitions between the $6s\ ^2S_{1/2}$, $6p\ ^2P_{1/2}$ and $5d\ ^2D_{3/2}$ levels. This forms an improvement in the absolute accuracy of more than two orders of magnitude.

In addition, the lifetime of the metastable levels of these ions provides a probe of the atomic structure and can also be used as a sensitive diagnostic for perturbations to the ion. We have used quantum jump spectroscopy of a single trapped Ba^+ ion to measure the lifetime of its $5d\ ^2D_{5/2}$ level [3].

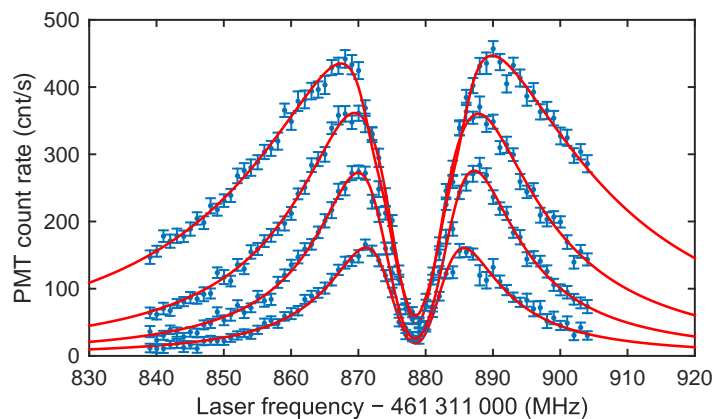


Figure 1: Spectra of the $5d\ ^2D_{3/2} - 6p\ ^2P_{1/2}$ transition in a single $^{138}\text{Ba}^+$ ion recorded for different laser light intensities [2]. The dip in the spectra is caused by a two-photon effect when both lasers driving the ion transitions are on resonance. The solid lines correspond to the results of fitting the optical Bloch model to the data. The widths of the spectra display power broadening.

References

- [1] M. Nuñez Portela *et al.*, Appl. Phys. B **114**, 173 (2014)
- [2] E. A. Dijck *et al.* (2015), arXiv:1504.01285 [physics.atom-ph]
- [3] A. Mohanty *et al.*, Hyperfine Interact. (2015), doi:10.1007/s10751-015-1161-9

High-resolution x-ray spectroscopy to probe quantum dynamics in collisions of $\text{Ar}^{17+,18+}$ ions with atoms and solids

E. Lamour¹, C. Prigent¹, J.-M. Ramillon², J.-P. Rozet¹, S. Steydli¹, M. Trassinelli¹, and D. Vernhet¹

¹Sorbonne Universités, UPMC, Institut des NanoSciences de Paris (INSP), CNRS-UMR 7588, F-75005 Paris, France

²CIMAP, CEA-CNRS-ENSICAEN, BP 5133, 14070, Caen France

Presenting Author: dominique.vernhet@insp.jussieu.fr

High-resolution x-ray spectroscopy has proved to be a very powerful tool to investigate quantum dynamics in highly charged ions (HCI) collisions with matter of whatever nature, dilute or condensed. In particular, the population of projectile HCIs' excited states (in their quantum component nl_jm_j) can be accurately determined and also tracked, for instance, during their transport in dense medium. Those studies gave rise to many results over the past two-decades enabling the identification of the different processes involved and highlighting specific effects that occur in dense targets compared to dilute media. Of course, the situation very much depends upon the collision system and the projectile velocity that define the collision regime. Here, we specifically put into perspective the results obtained in the so-called low and high energy collision regimes, investigating either ion-atom or ion-solid collisions [1].

Comparative studies of Ar^{q+} np excited state populations are presented when Ar^{17+} or Ar^{18+} collide either with gaseous targets of N_2 , Ar , and CH_4 or with carbon solid foils at different projectile energies, 13.6 MeV/u [2] or 7 keV/u [3]. As an example, Figure 1 exhibits high-resolution x-ray spectra obtained with gaseous targets in the high (left) and low (right) collision regimes that reveal very different interaction dynamics in the population of excited states by the single electron capture process. It clearly illustrates the well-known $1/n^3$ law at high velocity, and the preferential population in high n levels ($n \approx 8 - 9$ here) at low velocity. In solid, same high resolution spectra have been recorded. At high velocity, beside evidence for collective response of the target electrons produced by the wake field induced by HCI passing through solid-bulk, damping due to (intra- and inter-shell) excitation and ionization processes can be quantified. In the low velocity regime, spectra are characteristic of the multistep collisions that lead to production of more dressed ions.

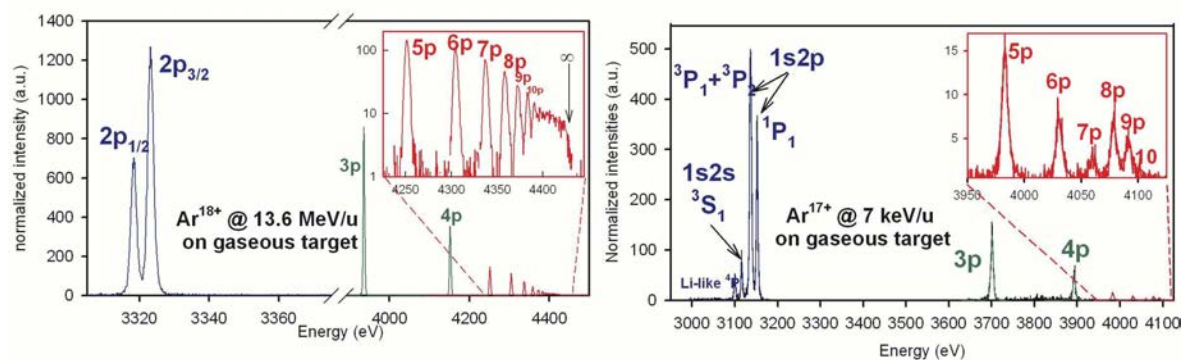


Figure 1: High-resolution x-ray spectra obtained at high collision velocity (left) and at low velocity (right) with highly charged argon ions on N_2 or Ar gaseous targets

References

- [1] E. Lamour *et al.* accepted in J. Phys. B special issue
- [2] M. Seliger *et al.* Phys. Rev. A **75** (2007) 032714
- [3] M. Trassinelli *et al.*, J.Phys. Conf. Ser. **388** (2012) 082009

Imaging magnetic fields by fluorescence-detected magnetic resonance in polarized atoms

I. Fescenko^{1,2}, A. Weis¹

¹Physics Department, University of Fribourg, Switzerland

²Institute of Atomic Physics and Spectroscopy, University of Latvia, Riga, Latvia

Presenting Author: iliafes@gmail.com

Spin polarization created in an alkali vapor by optical pumping represents—in general—a so-called dark state, characterized by strongly reduced fluorescence emission. The polarization, stabilized by a static magnetic field \vec{B}_0 , can be destroyed by a transverse magnetic field oscillating at $\omega_L \propto B_0$, thus leading to an increased fluorescence. We have developed a magnetic field imaging system based on these properties [1]. A thin sheet of laser light tuned to the $D_1(4 - 3)$ transition prepares a 2D-layer of spin-oriented atoms in a cubic Cs vapor cell containing Ar/Ne buffer gas (left graph). When exposed to an inhomogeneous magnetic field, a frequency comb of weak oscillating magnetic fields depolarizes the medium at specific spatial positions. The CCD recording of the fluorescence emitted by the Cs layer shows the depolarized regions as bright lines that represent iso- B_0 lines. The middle and right graphs of the figure show an experimental recording of field lines from a quadrupole coil, and the corresponding algebraic modeling. The spatial and magnetometric resolution obtained in a magnetically unshielded environment are 1 mm and 2 nT, respectively. We currently implement the method in a magnetic shield, anticipating a strongly increased performance.

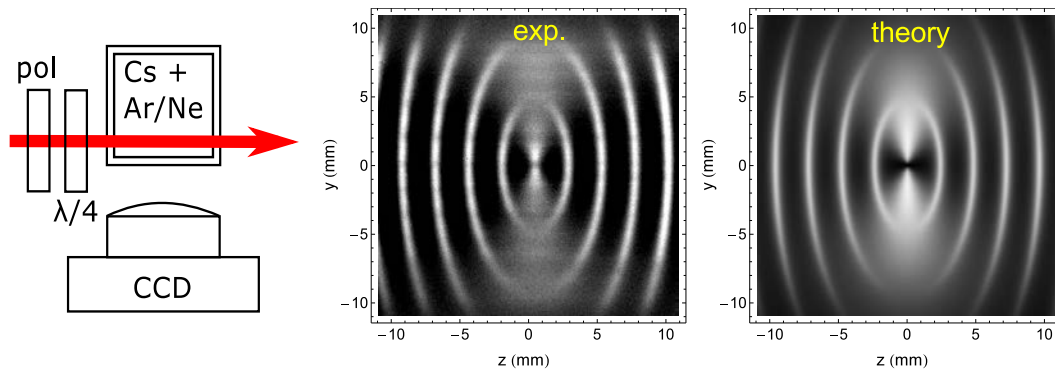


Figure 1: Left: Principle of the experiment. Experimental recording (middle) and anticipated lines of constant $|\vec{B}_0|$ (right) produced by a quadrupole (anti-Hemholtz) coil. The elliptical lines (from inside to outside) represent field values B_0 of 19, 37.5, 56, 74.5, 93 μT .

References

- [1] I. Fescenko and A. Weis, J. Phys. D: Appl. Phys, **47**, 235001 (2014).

Relativistic two-photon decay rates of hydrogenic atoms with the Lagrange-mesh method

L. Filippin¹, D. Baye², and M. Godefroid¹

¹*Chimie Quantique et Photophysique, Université Libre de Bruxelles, Brussels, Belgium*

²*Physique Quantique, and Physique Nucléaire Théorique et Physique Mathématique, Université Libre de Bruxelles, Brussels, Belgium*

Presenting Author: Livio.Filippin@ulb.ac.be

The simultaneous emission of two electric dipole photons is the dominant decay mechanism to the ground state for the $2s_{1/2}$ state of hydrogen [1]. This transition is one of the most widely studied atomic transitions in which selection rules forbid the emission of one electric dipole photon [2]. The calculation of this second-order process involves an infinite number of intermediate states. However, excellent results can be obtained with a finite number of pseudostates [1, 2, 3]. This calculation is simplified by the Lagrange-mesh method.

The Lagrange-mesh method is an approximate variational calculation using a special basis of N functions, called Lagrange functions, related to a set of N mesh points and the Gauss quadrature associated with this mesh [4]. It combines the high accuracy of a variational approximation and the simplicity of a calculation on a mesh [5, 6]. The variational equations take the form of mesh equations with a diagonal representation of the potential only depending on values of this potential at the mesh points [4, 6].

For the exactly solvable Coulomb-Dirac problem describing hydrogenic atoms, numerically exact energies and wave functions, i.e. exact up to rounding errors, are obtained for any state and for any nuclear charge with very small numbers of mesh points [7]. Tests with the Yukawa potential also provide very accurate results. The approximate wave functions provide multipole polarizabilities that are also extremely precise [8].

In this work, we calculate accurate numerical two-photon decay rates from the Dirac equation with the Lagrange-mesh method. We use the obtained energies and wave functions from Ref. [7] to study the $2s_{1/2} - 1s_{1/2}$ transition in the hydrogenic and Yukawa cases. A test of the general requirement of gauge invariance for the relativistic results is successfully performed, which emphasizes the high accuracy of the numerical method for both types of potentials.

For a Coulomb potential, the results obtained for $Z = 1$ to 92 with the Lagrange-mesh method are in excellent agreement with a benchmark calculation involving Bernstein polynomial (B-polynomial) finite-basis sets [3]. For Yukawa potentials, we study the influence of the screening length on the $2s_{1/2}$ two-photon decay rate of a hydrogen atom embedded in a Debye plasma.

References

- [1] S. P. Goldman and G. W. F. Drake, *Phys. Rev. A* **24**, 183 (1981)
- [2] J. P. Santos, F. Parente, and P. Indelicato, *Eur. Phys. J. D* **3**, 43 (1998)
- [3] P. Amaro *et al.*, *J. Phys. A* **44**, 245302 (2011)
- [4] D. Baye and P.-H. Heenen, *J. Phys. A* **19**, 2041 (1986)
- [5] D. Baye, M. Hesse, and M. Vincke, *Phys. Rev. E* **65**, 026701 (2002)
- [6] D. Baye, *Physics Reports* **565**, 1-107 (2015)
- [7] D. Baye, L. Filippin, and M. Godefroid, *Phys. Rev. E* **89**, 043305 (2014)
- [8] L. Filippin, D. Baye, and M. Godefroid, *Phys. Rev. A* **90**, 052520 (2014)

Isotope shift parameters in Al I for the $3p - 4s$ and $3p - 3d$ lines

L. Filippin¹, J. Ekman², S. Fritzsche³, M. Godefroid¹, and P. Jönsson²

¹*Chimie Quantique et Photophysique, Université Libre de Bruxelles, Brussels, Belgium*

²*Materials Science and Applied Mathematics, Malmö University, Malmö, Sweden*

³*Helmholtz-Institut Jena, and Theoretisch-Physikalisches Institut, Friedrich-Schiller-Universität Jena, Jena, Germany*

Presenting Author: Livio.Filippin@ulb.ac.be

When the effects of the finite mass and the spatial charge distribution of the nucleus are taken into account in a Hamiltonian describing an atomic system, the isotopes of an element have different electronic energy levels [1]. The isotope shift (IS), which consists of the field shift and the mass shift, plays a key role in extracting nuclear properties of an isotope such as its nuclear mean-square charge radius $\langle r^2 \rangle$ [2]. For a given atomic transition k with frequency ν_k , it is assumed that the *electronic response* of the atom to variations of the nuclear mass and charge distribution can be described by only two parameters : the mass-shift parameter M_k and the field-shift parameter F_k , respectively [2].

Five transitions are of interest for laser spectroscopy experiments of neutral aluminium (Al I) radioactive isotopes in order to determine their nuclear properties : $3s^2 3p \ ^2P_{3/2} \rightarrow 3s^2 4s \ ^2S_{1/2}$ (396.26 nm), $3s^2 3p \ ^2P_{1/2}^o \rightarrow 3s^2 4s \ ^2S_{1/2}$ (394.51 nm), $3s^2 3p \ ^2P_{1/2}^o \rightarrow 3s^2 3d \ ^2D_{3/2}$ (308.30 nm), $3s^2 3p \ ^2P_{3/2}^o \rightarrow 3s^2 3d \ ^2D_{3/2}$ (309.37 nm) and $3s^2 3p \ ^2P_{3/2}^o \rightarrow 3s^2 3d \ ^2D_{5/2}$ (309.36 nm).

We perform *ab initio* calculations of IS parameters using the multi-configuration Dirac-Hartree-Fock (MCDHF) method implemented in the RIS3/GRASP2K [1,3] and RATIP packages [4]. Two strategies are adopted. A first one consists in extracting the relevant parameters from the calculated line shifts for given triads of isotopes. A second one is based on the estimation of the expectation values of the one- and two-body recoil Hamiltonian for a given isotope, including the Shabaev relativistic corrections [5], combined with the calculation of the theoretical total electron densities at the origin. The results of the two approaches are compared. In both of them, different correlation models are explored in a systematic way to determine a reliable computational strategy and estimate theoretical error bars.

References

- [1] C. Nazé *et al.*, Comput. Phys. Commun. **184**, 2187 (2013)
- [2] B. Cheal, T. E. Cocolios and S. Fritzsche, Phys. Rev. A **86**, 042501 (2012)
- [3] P. Jönsson *et al.*, Comput. Phys. Commun. **184**, 2197 (2013)
- [4] S. Fritzsche, Comput. Phys. Commun. **183**, 1525 (2012)
- [5] V. M. Shabaev, Theor. Math. Phys. **63**, 588 (1985); Sov. J. Nucl. Phys. **47**, 69 (1988)

Atomic and Nuclear quantum optics: Multiphoton and autoionization resonances in a strong DC electric and laser field

A. Glushkov¹

¹Odessa State University - OSENU, Odessa

Presenting Author: dirac13@mail.ru

We present an advanced combined relativistic operator perturbation theory (PT) and energy approach [1,2] and apply it to studying interaction dynamics of the finite Fermi systems (heavy atoms, nuclei, molecules) with an intense external (DC electric and laser) field. The approach allows uniform, consistent treating the strong field and quasistationary and collisional problems. It is based on the Gell-Mann and Low adiabatic formalism and method of the relativistic Green's function for the Dirac equation with complex energy. The essence of the operator PT is the inclusion of the well-known method of "distorted waves approximation" in the frame of the formally exact PT. Results of the calculation for the multi-photon resonance and ionization profile in *Na, Cs, Ba* atoms are listed. We have studied the cases of single-, multi-mode, coherent, stochastic laser pulse shape. An account for stochastic fluctuations in a field effect is of a great importance.

New data on the DC, AC strong field Stark resonances, multi-photon and autoionization resonances, ionization profiles for a few heavy atoms (*Eu, Tm, Gd, U*) are presented. It has been firstly studied earlier discovered a giant broadening effect of the autoionization resonance width in a sufficiently weak electric (laser) field for uranium. It is declared that probably this effect is universal for optics and spectroscopy of lanthanides and actinides and even superheavy elements.

The direct interaction of super intense laser fields in the optical frequency domain with nuclei is studied within the operator PT and the relativistic mean-field (plus Dirac-Woods-Saxon) model [2]. The ac-Stark shifts of the same order as in typical quantum optical systems relative to the respective transition frequencies are feasible with state-of-the-art or near-future laser field intensities. A nuclear dynamic (AC) Stark shift of low-lying nuclear states due to off-resonant excitation by laser field (10^{25} - 10^{35} W/cm^2) is studied and is described within the operator PT and the relativistic mean-field (RMF) model for the nucleus [2]. We present the results of AC Stark shifts of single proton states in the nuclei ^{16}O , ^{168}Er and compared these data with known results by Keitel et al [3]. New data are also listed for the ^{57}Fe and ^{171}Yb nuclei. Shifts of several keV are reached at intensities of roughly 10^{34} W/cm^2 for ^{16}O , ^{57}Fe and 10^{32} W/cm^2 for heavier nuclei. It is firstly presented a consistent relativistic theory of multi-photon resonances in nuclei and first estimates of energies and widths for such resonances are presented for ^{57}Fe and ^{171}Yb nuclei.

References

- [1] A. Glushkov *et al.* Eur. Phys. J. **T160**, 196-208 (2008); Phys.Scripta. **T135**, 014022 (2009)
- [2] A. V. Glushkov *et al.*, *Adv. in Theory of Quantum Systems in Chem. and Phys., Ser.: Progress in Theor.Phys. and Chem., Eds. P.Hoggan, E.Brandas et al* (Springer, Berlin, 2011) **22**, 51-70; J.Phys.: C Ser. **397**, 012011 (2012)
- [3] V. Gol'dansky and V. Letokhov JETP. **78** 213-218 (1974); T. Burvenich, J. Evers, C.Keitel Phys.Rev. **C74**, 044601 (2007)

Search for the Permanent Electric Dipole Moment of Xenon.

J. O. Grasdijk^{3,1}, S. Zimmer¹, W. Heil¹, S. Karpuk¹, K. Tullney¹, Y. Sobolev¹, F. Allmendinger²,
U. Schmidt², K. Jungmann³, L. Willmann³, H.-J. Krausse⁴, and A. Offenhauser⁴

¹*Institut für Physik, Universität Mainz*

²*Universität Heidelberg*

³*van Swinderen Institute, University of Groningen*

⁴*Forschungszentrum Jülich*

Presenting Author: j.o.grasdijk@rug.nl

A permanent electric dipole moment (EDM) implies breakdown of P (parity) and T (time reversal) symmetries. Provided CPT holds, this implies CP violation. Observation of an EDM at present and near future achievable experimental sensitivity would provide unambiguous evidence for physics beyond the Standard Model. This could give a hint towards understanding the observed matter-antimatter asymmetry in the universe. Experimental searches for atomic and particle EDMs have ruled out more speculative models than other individual experimental approaches. We aim to improve the current experimental limit on an EDM in ^{129}Xe ($|d_{\text{Xe}}| < 3 \times 10^{-27}$ ecm [1]) by some 4 orders of magnitude.

A sensitive experimental approach is a spin clock, in our case co-located spin polarized ^3He and ^{129}Xe . SQUID detectors are used to monitor the free spin precession. With a co-magnetometer the spin precession can be exploited as an ultra-sensitive probe for nonmagnetic spin interactions [2]. A possible Xenon EDM results in a contribution to the spin precession frequency of $\Delta\nu \propto d_{\text{Xe}} \cdot E$. The magnetic dipole interaction drops out due to the use of ^3He as a co-magnetometer [3,4].

The achievable spin coherence times and measurement sensitivity will provide for obtaining $|d_{\text{Xe}}| < 10^{-29}$ ecm in one day.

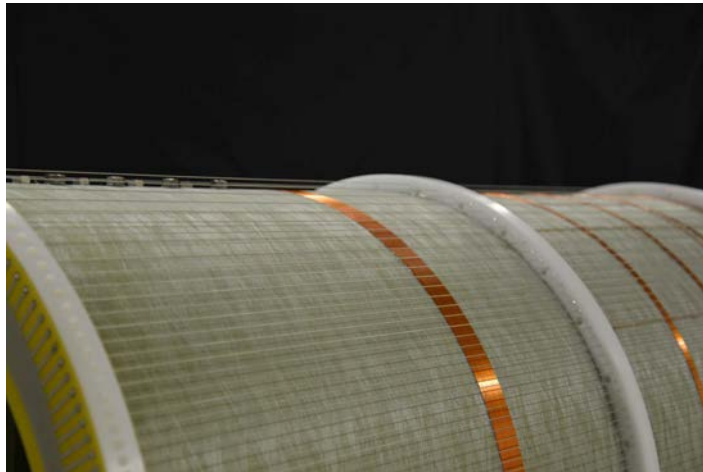


Figure 1: A sensitive ^{129}Xe EDM search requires a magnetic field coil configuration to produce a field of high homogeneity.

References

- [1] M. Rosenberry, T. Chupp. Phys. Rev. Lett. **86**, 22-25 (2001)
- [2] F. Allmendinger et al. Phys. Rev. Lett. **112**, 110801 (2014)
- [3] C. Gemmel et al. Eur. Phys. J. D **47**, 303 (2010)
- [4] C. Gemmel et al. Phys. Rev. D **82**, 111901(R) (2010)

Quadratic-linear B -spline grid for studying Ps-atom interactions in cavities

A. R. Swann¹, G. F. Gribakin¹

¹*School of Mathematics & Physics, Queen's University Belfast, Belfast BT7 1NN, United Kingdom*

Presenting Author: g.gribakin@qub.ac.uk

The B -spline basis set was first introduced in 1946 [1] but has become ubiquitous in atomic physics since the 1990s [2, 3]. B -spline functions are square-integrable piecewise polynomials defined in a restricted domain (the *cavity*) over a set of non-decreasing points r_j (the *knot sequence*). The appropriate choice of knot sequence depends on the problem at hand. An exponential sequence, viz.,

$$r_j = r_0[\exp(\sigma j) - 1], \quad (1)$$

where r_0 and σ are constants, works well for describing electronic states of atoms and calculation of many-body-theory diagrams [2, 4]. However, it is ill-suited for describing continuum states of an electron (or positron) accurately.

We plan to use many-body theory to study Ps-atom interactions by calculating Ps states in the spherical cavity with the atom at the centre. This requires an accurate description of both the atomic bound states and the Ps continuum states. We also need to know the effect of the cavity wall on Ps, i.e., its effective radius. Though for us the cavity is a computational tool, for experimentalists it is a physical tool or even the object of study, e.g., where pore sizes are derived from Ps lifetime spectroscopy (see, e.g., [5, 6]).

It is known that an equispaced (linear) knot sequence can be used to describe states of free Ps in the cavity accurately [7]. Examining the atomic potential suggests that inside the atom an economical quadratic grid should be appropriate [3]. Thus, we propose the following grid for studying Ps-atom interactions:

$$r_j = Aj^2/(B + j), \quad (2)$$

where A and B are constants. For $j < B$, the dominant nature of the sequence is quadratic, while for $j > B$ it is linear. The value of B is chosen so that the change of the dominant nature occurs at ~ 1 a.u. We refer to this knot sequence as the *quadratic-linear* grid.

In the present work we used a set 40 B -splines of order 6. Table 1 compares the energies of the ground-state orbitals of Ar using the exponential and quadratic-linear grids. The agreement is excellent: at least 6 significant figures. Table 2 likewise compares several energies of free Ps in the cavity. The agreement is at the level of 0.2% or better.

The next stage will be to use the quadratic-linear grid to build states of Ps in the field of the atom, treating it as a static potential source. Then we will proceed to describe the system using accurate many-body techniques.

Orbital	Exponential	Quadratic-linear
1s	-118.6103533	-118.6103516
2s	-12.3221526	-12.3221540
2p	-9.5714664	-9.5714662
3s	-1.2773533	-1.2773531
3p	-0.5910179	-0.5910175

Table 1: Energies (in a.u.) of Ar orbitals using exponential and quadratic-linear grids.

$nl(N, L)$	Linear	Quadratic-linear
1s(1, 0)	-0.216100	-0.216121
1s(2, 0)	-0.120167	-0.120246
2s(1, 0)	0.0239796	0.0239507
1s(3, 0)	0.0309400	0.0308777
2p(1, 1)	0.0768631	0.0768559

Table 2: Energies of Ps in a cavity of radius 10 a.u. Internal state: nl , external state: (N, L) .

References

- [1] I. J. Schoenberg, Quart. Appl. Math. **4**, 45 (1946).
- [2] J. Sapirstein and W. R. Johnson, J. Phys. B **29**, 5213 (1996).
- [3] H. Bachau *et al.*, Rep. Prog. Phys. **64**, 1815 (2001).
- [4] G. F. Gribakin and J. Ludlow, Phys. Rev. A **70**, 032720 (2004).
- [5] D. W. Gidley *et al.*, Phys. Rev. B **60**, R5157 (1999).
- [6] D. B. Cassidy *et al.*, Phys. Rev. Lett. **106**, 023401 (2011).
- [7] R. Brown, Q. Prigent, A. R. Swann and G. F. Gribakin (unpublished).

An accurate free spin precession cesium magnetometer

Z. D. Grujić¹, P. A. Koss², and A. Weis¹

¹*Department of Physics, University of Fribourg, Switzerland*

²*Instituut voor Kern- en Stralingsfysica, Katholieke Universiteit Leuven, B-3001 Leuven, Belgium*

Presenting Author: zoran.grujic@unifr.ch

An ongoing search [1] for a permanent neutron electric dipole moment (nEDM) at the Paul Scherrer Institute (Switzerland) calls for an utmost control of the applied $\approx 1 \mu\text{T}$ magnetic field B_0 . The nEDM experiment consists in searching for a change of the spin precession frequency of ultracold neutrons (UCN) induced by a static electric field applied either parallel or anti-parallel to the magnetic field. The precession frequency is measured using Ramsey's method of (time-)separated $\pi/2$ -pulses with a free spin precession time of ~ 100 s. Within the multinational nEDM collaboration our team is responsible for monitoring spatial and temporal variations of the magnetic field and its gradient around the UCN precession chamber mounted inside of a 5 layer μ -metal shield. For this we currently operate an array of 16 Cs magnetometers mounted both above the high-voltage electrode and below the ground electrode used to apply the electric field to the neutrons. Although extremely sensitive ($\approx 10 \text{ fT/Hz}^{1/2}$), the M_x -mode of operation of our magnetometers has an accuracy in the upper pT range due to unavoidable phase setting errors in the deployed phase-feedback method of the M_x method. While a high magnetometric sensitivity is key to achieving a high nEDM sensitivity, high accuracy is a *sine qua non* prerequisite for inferring gradient values from the readings of distinct sensors.

In view of improving the accuracy of Cs magnetometry we have investigated the free-spin-precession (FSP) in antirelaxation-coated [2] vapor cells using an all-optical mode of operation. Atomic spin orientation is produced by a circularly-polarized amplitude-modulated pump beam with $\vec{k} \perp \vec{B}_0$ that is resonant with $4 \rightarrow 3$ transition of the Cs D_1 line. After 20 ms of pumping with a large light intensity, the FSP is recorded with a lower intensity probe beam for 80 ms, the pump-probe process being repeated periodically. The recorded FSP data is bandpass filtered and the Larmor frequency is extracted by fitting a decaying sine wave to the filtered data. The sine wave's oscillation frequency (Larmor frequency) ω_L is a measure of the magnetic field's modulus according to $B_0 = \omega_L / \gamma_F$, where $\gamma_{F=3}$ is the gyromagnetic ratio of the Cs $F=4$ ground state that is known with an accuracy of 10^{-7} . We have experimentally optimized all parameters of the pump and read-out process and estimated a sensitivity below $100 \text{ fT}/\sqrt{\text{Hz}}$ in the (light) shotnoise limit. In small fields the accuracy should be on par with the sensitivity. The quadratic Zeeman effect (QZE) resulting from the Breit-Rabi interaction was expected to affect the accuracy at the level of a few pT in a $1 \mu\text{T}$ field when the readout laser beam is not perpendicular to \vec{B}_0 . We have measured the anticipated systematic shift $\delta B = \beta_{\text{QZE}} B_0^2$ due to the QZE, by comparing the FSP frequencies of two readout lasers, one perpendicular to and a second propagating at an angle of 52° with respect to \vec{B}_0 . To our surprise we found that the experimental difference frequencies are rather described by $\delta B = b_{\text{offset}} + \beta_{\text{QZE}} B_0^2$. While β_{QZE} agrees well with model calculations, the offset field $b_{\text{offset}} \approx 50 \text{ pT}$, derived from the $B_0 \rightarrow 0$ limit of $(\omega_L^{90^\circ} - \omega_L^{52^\circ}) / \gamma_F$ poses a serious problem. Experimental and theoretical efforts towards a better understanding of this 'offset problem' are in progress.

This work was supported by the grant 200020_140421/1 of the Swiss National Science Foundation.

References

- [1] I. Altarev *et al.* Nucl. Instr. Meth. A, **611**(23):133 – 136, 2009.
- [2] Z. D. Grujić, P. A. Koss, G. Bison, and A. Weis, accepted in Eur. Phys. J. D (2015) <http://dx.doi.org/10.1140/epjd/e2015-50875-3>

Double ionization of the hydrogen sulfide molecule by electron impact: influence of the target orientation on the fivefold differential cross sections

H. Aouchiche¹, N. Imadouchene¹, and C. Champion²

¹*Laboratoire de Mécanique Structure et Energétique, Université Mouloud Mammeri, B.P. 17, Tizi Ouzou 15000, Algérie*

²*Centre d'Etudes Nucléaires de Bordeaux Gradignan (CENBG), CNRS/IN2P3, Université de Bordeaux, B.P. 120, 33175 Gradignan, France*

Presenting Author: nora.imady@gmail.com

A fivefold differential cross sections (5 DCSs) for electron-impact double ionization of hydrogen sulfide molecule are calculated for high incident energy (1 keV) and for three particular target orientations. The theoretical procedure is based on the first Born approximation (FBA) model using a partial wave functions development [1, 2, 3]. In this approach, the incident (scattered) electron is described by a plane wave, while a Coulomb wave function is used for modeling the two ejected electrons. Furthermore, we identify clearly the signature of the usual mechanisms involved in the ($e, 3e$) reaction, namely, the shake-off and the two-step 1.

References

- [1] C. Champion, D. Oubaziz, H. Aouchiche, Yu. V. Popov, C. Dal Cappello, Phys. Rev. A **81**, 032704–1–032704–11 (2010)
- [2] D. Oubaziz, H. Aouchiche, C. Champion, Phys. Rev. A **83**, 012708–1–012708–10 (2011)
- [3] D. Oubaziz, C. Champion, H. Aouchiche, Phys. Rev. A **88**, 042709–1–042709–11 (2013)

Spectroscopic measurements of free particles by matter-wave interferometry

J. Fiedler¹, S. Scheel¹

¹*Institute of Physics, University of Rostock, Rostock, Germany*

Presenting Author: johannes.fiedler@uni-rostock.de

Matter-wave interference experiments with large particles have provided a wealth of insight into the particle-wave duality that is at the heart of our physical understanding. Experiments with material gratings [1,2,3] showed that the matter wave collects an additional phase shift caused by the Casimir–Polder interaction between the particles and the grating surface [2,4]. Casimir–Polder forces are a subclass of dispersion forces that are caused by the ground-state fluctuation of the electromagnetic field, and whose strength is determined by the polarisability of the particles [5].

We present an experimental setup which uses the far-field interference of matter waves and which has the surprising feature that a reconstruction of the Casimir–Polder potential can be done very easily. With the knowledge of the used geometry that includes all scattering properties — geometric shape and dielectric response — we present an algorithm for the determination of the polarisability of the particle. The advantage of this setup is a spectroscopic measurement of the polarisability of the particle in free space that covers the entire electromagnetic spectrum in one measurement.

References

- [1] M. Arndt *et al.*, *Nature* **401**, 680 (1999).
- [2] T. Juffmann *et al.*, *Nature Nanotechnology* **7**, 297 (2012).
- [3] M. Sclafani *et al.*, *New Journal of Physics* **15**, 083004 (2013).
- [4] S.Y. Buhmann *et al.*, *Phys. Rev. A* **85**, 042513 (2012).
- [5] S. Scheel and S.Y. Buhmann, *Acta Physica Slovaca* **58**, 675 (2008).

Fast transport and accumulation of cold ion clouds in a multi-zone RF-trap

M. R. Kamsap¹, C. Champenois¹, J. Pedregosa-Gutierrez¹, M. Houssin¹, D. Guyomarc'h¹, and M. Knoop¹

¹*Physique des Interactions Ioniques et Moléculaires: UMR 7345, Aix-Marseille Université, CNRS, Centre de Saint Jérôme, 13397 Marseille cedex 20, France*

Presenting Author: marius.kamsap@univ-amu.fr

Transporting charged particles between multiple traps has become an important feature in quantum information, high-precision spectroscopy, cold chemistry or frequency metrology experiments. In this work, we study experimentally the transport and accumulation of a large ion sample in a multi-zone trap. Our trapping device is composed of two quadrupole (first and second zone) and an octupole (third zone) linear trap mounted inline.

Our transport protocol consists in the variation of the potential barrier between two trap zones following a hyperbolic tangent gate [1]. The result shows that, for some well identified transport parameters, the transport efficiency from the first to the second zone (distance 23 mm) is independent of the ion number as long as this number is larger than 2000 ions and can reach 90% in such case. For clouds smaller than 2000 the efficiency is higher and can reach 100% in 100 μ s [2] (see figure 1).

The number of leaving ions depends strongly on the duration of the transport protocol, alternating between 0 and 100% several times before these oscillations are damped. This oscillation of the fraction of leaving ions is not symmetric. Under certain experimental conditions, ions are transported from the first to the second part, but do not return from the second zone for the same set parameters. This asymmetry can be used to accumulate ions in the second trap [3]. This technique allows to create very large ion clouds in the trap by accumulation. As the transport efficiency to the octupole is low, we use the described accumulation process to create a large ion sample in octupole trap.

In the ideal case, the cold ion cloud in a linear octupole trap organizes in a hollow structure, formed of concentric tubes. However, in our octupole trap we observe some local harmonic potential wells where the ions samples organize themselves into very prolate strings or zigzag structures and to ellipse structures for large samples. This feature can be due to a defect in the geometry of the RF-electrodes. We exploit this observed structures to verify the theoretical laws for string, zigzag or ellipse structures.

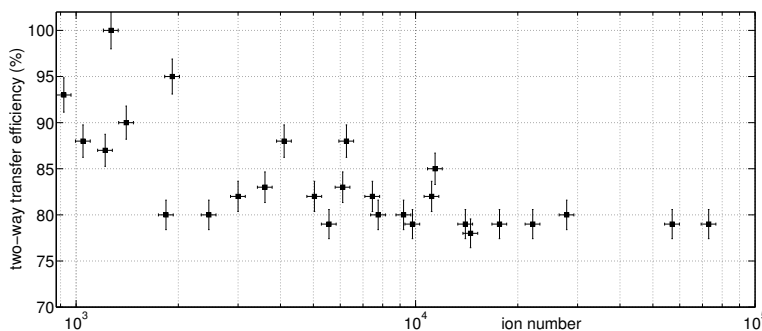


Figure 1: Ratio of the number of ions after shuttling back and forth from trapping zone 2 with two identical transport protocols, versus the initial number of ions

References

- [1] J. Pedregosa-Gutierrez, C. Champenois, M. R. Kamsap and M. Knoop; Ion transport in macroscopic RF linear traps International Journal of Mass Spectrometry; doi:10.1016/j.ijms.2015.03.008 (2015).
- [2] M.R. Kamsap, J. Pedregosa-Gutierrez, C. Champenois, D. Guyomarc'h, M. Houssin, and M. Knoop ; Fast and efficient transport of large ion clouds; Submitted (2015).
- [3] M.R. Kamsap, C. Champenois, J. Pedregosa-Gutierrez, M. Houssin and M. Knoop ; Fast accumulation of ion in dual trap; submitted (2015).

Precision calculation of the spectra of Mg-like ions

E. A. Konovalova¹, M. G. Kozlov^{1, 2}

¹Neutron Research Department, Petersburg Nuclear Physics Institute, Gatchina, Russia

²Department of Physics, St. Petersburg Electrotechnical University "LETI", St. Petersburg, Russia

Presenting Author: lenaakonovalova@gmail.com

Many calculations performed within the method which combines the configuration-interaction (CI) with the many-body perturbation theory showed its advantage in comparison with other methods. In this work the low-lying states of Mg-like ions (Mg I, Al II, Si III, P IV, S V, Cl VI) are calculated within the CI method, the CI plus many-body perturbation theory (CI+MBPT) method, and the CI plus all-order (CI+AO) method [1, 2]. The effect of the Breit corrections and QED-corrections are considered. These corrections grow with the nuclear charge Z and improve agreement with experimental data [3] for the most heavy ions, QED corrections being more important than Breit corrections.

The accuracy of each of these methods grows with the Z , while the difference between the results of CI+MBPT and CI+AO methods decreases. The final precision of our calculation is about 0.1%.

In the Table 1 the energies of some low-lying states are presented.

Element	State	Energies (cm ⁻¹)				
		Exper.	CI	CI+MBPT	CI+AO	Breit and QED contribution
Mg I	¹ S ₀	182939	179554	182685	182875	14
	³ P ₀	21850	20919	21792	21851	7
	³ P ₁	21871	20939	21814	21872	7
	³ P ₂	21911	20980	21857	21916	7
	¹ P ₁	35051	34471	35030	35052	7
Cl VI	¹ S ₀	1702996	1695325	1702847	1703001	187
	³ P ₀	98062	97047	98064	98115	91
	³ P ₁	98621	97624	98647	98701	91
	³ P ₂	99782	98813	99854	99916	91
	¹ P ₁	148947	150326	149154	149102	94

Table 1: Examples of some calculated energies for atom Mg I and ion Cl VI.

References

- [1] M. G. Kozlov Int. J. Quant. Chem. **100**, 336–342 (2004)
- [2] M. S. Safronova, M. G. Kozlov, W. R. Johnson, and D. Jiang Phys. Rev. A **80** 012516 (2009)
- [3] <http://www.physics.nist.gov>

Radiative Lifetimes and Transition Probabilities in Rh I

G. Malcheva¹, L. Engström², H. Lundberg², H. Nilsson³, H. Hartman^{3,4}, K. Blagoev¹, P. Palmeri⁵, and P. Quinet^{5,6}

¹*Institute of Solid State Physics, Bulgarian Academy of Sciences, 72 Tzarigradsko Chaussee, BG-1784 Sofia, Bulgaria*

²*Department of Physics, Lund University, Box 118, 221 00 Lund, Sweden*

³*Lund Observatory, Lund University, Box 43, 22100 Lund, Sweden*

⁴*Applied Mathematics and Material Science, Malmö University, 20506 Malmö, Sweden*

⁵*Astrophysique et Spectroscopie, Université de Mons, B-7000 Mons, Belgium*

⁶*IPNAS, Université de Liège, B-4000 Liège, Belgium*

Presenting Author: lars.engstrom@fysik.lth.se

Rhodium is one of the refractory elements observed in the solar photosphere and in meteorites [1]. To determine abundances the intrinsic transition probability (A -value) or oscillator strength (f -value) must be known for the observed lines. Radiative lifetimes of 17 high-lying excited states in Rh I are measured using the Time-Resolved, Laser-Induced Fluorescence (TR-LIF) method. Out of these lifetimes, 13 are new and the remaining four confirm previous TR-LIF measurements [2,3]. Furthermore, we report the first theoretical investigation of Rh I, where the radiative decay properties of all experimentally known levels below 47000 cm⁻¹ are calculated using a pseudo-relativistic Hartree-Fock method including core polarization effects. The theoretical calculations are found to be in very good agreement with the experimental results. A large set of new transition probabilities is presented for lines of astrophysical interest in the spectral range 2200 – 10000 Å.

This work has received funding from LASERLAB-EUROPE (grant agreement no. 284464, EC's Seventh Framework Programme), the Swedish Research Council through the Linnaeus grant to the Lund Laser Centre and a project grant 621-2011-4206, and the Knut and Alice Wallenberg Foundation. P.P. and P.Q. are respectively Research Associate and Research Director of the Belgian National Fund for Scientific Research F.R.S.-FNRS from which financial support is gratefully acknowledged.

References

- [1] A. G. W. Cameron, *Essays in Nuclear Astrophysics*, ed. by C. A. Barnes, D. D. Clayton and D. N. Schramm (Cambridge University Press, p. 23, 1981)
- [2] M. Kwiatkowski *et al.* *Astron. Astrophys.* **112** 337 (1982)
- [3] S. Salih, D. W. Duquette, and J. E. Lawler *Phys. Rev. A* **27**, 1193 (1983)

Lifetimes and Transition Probabilities for High-Lying Levels in Astrophysically Interesting Atoms Using Multi-Photon Excitation

L. Engström¹, H. Lundberg¹, H. Nilsson², and H. Hartman^{2,3}

¹*Department of Physics, Lund University, Box 118, 221 00 Lund, Sweden*

²*Lund Observatory, Lund University, Box 43, 22100 Lund, Sweden*

³*Applied Mathematics and Material Science, Malmö University, 20506 Malmö, Sweden*

Presenting Author: lars.engstrom@fysik.lth.se

In spectroscopy of stellar atmospheres the atomic transitions most often appear as absorption lines. To use these lines for quantitative analysis of the population distribution and abundance determinations, reliable transition probabilities or f -values must be available. A standard technique for this purpose is to combine measurements of the lifetime of the upper level with experimentally determined branching fractions from an intensity calibrated source. Since experimental studies are naturally limited in the number of levels that can be investigated, it is very fruitful to use the experimental data to benchmark detailed and comprehensive theoretical calculations.

We will discuss the recent progress at the Lund Laser Centre, aiming to extend previous studies to more highly excited levels and also to levels with the same parity as the ground configurations. The lifetime measurements are performed using the Time-Resolved Laser-Induced Fluorescence (TR-LIF) technique, and the key element to reach the new levels is by either two-photon excitation (from a single laser) or by two step excitations (from two different lasers). Recent results using two-photon excitations in Cr II and Fe II can be found in [1,2]. Current projects involving two-step excitations (Ti II, Ni II, Mn II and Co II) are performed in collaboration with K. Blogaev at the Bulgarian Academy of Sciences and P. Palmeri and P. Quinet in the theory group at the Université de Mons in Belgium.

References

- [1] L. Engström *et al.* *Astron. Astrophys.* **570** (2014) DOI:10.1051/0004-6361/201424762
- [2] H. Hartman *et al.* Submitted to *Astron. Astrophys.* 2015

EIT resonance inverted in magnetic field by influence of the alignment effect

A. Sargsyan¹, D. Sarkisyan¹, Y. Pashayan-Leroy², C. Leroy², S. Cartaleva³, A. D. Wilson-Gordon⁴, and M. Auzinsh⁵

¹Institute for Physical Research, NAS of Armenia - Ashtarak-2, 0203, Armenia

²Laboratoire Interdisciplinaire Carnot de Bourgogne, UMR CNRS 6303, Université de Bourgogne, France

³Institute of Electronics, Bulgarian Academy of Sciences, Sofia, Bulgaria

⁴Department of Chemistry, Bar-Ilan University, Ramat Gan 52900, Israel

⁵Department of Physics, University of Latvia, 19 Rainis Blvd., Riga LV-1586, Latvia

Presenting Author: yevgenya.pashayan-leroy@u-bourgogne.fr

The electromagnetically induced transparency (EIT) effect still attracts great interest, partly through the development of chip-scale atomic clocks, such as micro-fabricated atomic clocks. Here we present for the first time (to our knowledge) the influence of alignment on the EIT resonances.

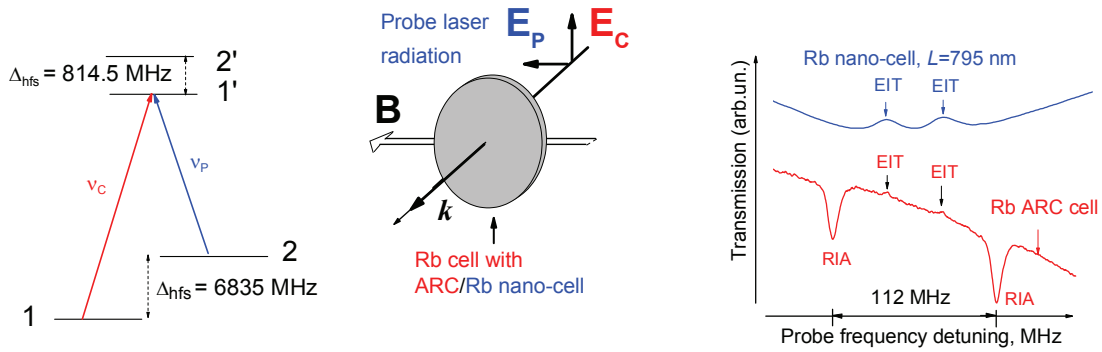


Figure 1: a) Λ -system of the ^{87}Rb D_1 line, powers P_c and P_p are 14 and 0.5 mW, respectively; b) the configuration of \mathbf{B} , \mathbf{k} , \mathbf{E}_p and \mathbf{E}_c ($B = 27$ G); c) the upper and lower spectra show EIT-resonances for NC and ARC, respectively.

In Fig. 1a the system of the ^{87}Rb , D_1 line is shown. The coupling laser frequency is in resonance with the $1 \rightarrow 1'$ transition, while the probe laser frequency is scanned through the $2 \rightarrow 1'$ transition. Two cells filled with Rb are used: an 8 mm-long cell having anti-relaxation coating (ARC) and a nano-cell (NC) with thickness $L = \lambda = 795$ nm. An external magnetic \mathbf{B} -field is directed along the probe \mathbf{E}_p field, while \mathbf{E}_c is perpendicular to the \mathbf{B} -field (see Fig. 1b). Due to the Zeeman optical pumping (ZOP) effect the whole population of level $F_g = 2$ is concentrated in the sublevels $m_F = \pm 2$, i.e. alignment occurs [1]. In this case the population $N(F_g = 2, m_F = 2) > N(F_g = 1, m_F = 0, \pm 1)$ and a strong absorption of the probe radiation ν_p occurs via a two-photon Raman-type process. ZOP efficiency is proportional to Ω_p/R , where Ω_p is the probe Rabi-frequency and R is the relaxation time ($\gamma_R < 1$ kHz for the ARC cell, and $\gamma_R > 1$ MHz for the NC). In Fig. 1c), the upper and lower spectra show EIT-resonances for the cases of NC and ARC, respectively. We see that in the upper spectrum the EIT-resonances show a reduction in the absorption (ZOP is absent due to the large value of γ_R), while the resonances in the lower spectrum show an increase in absorption, that is why we call them resonances inverted by alignment (RIA). A theoretical model explaining RIA formation is developed. The results of other configurations of \mathbf{B} , \mathbf{k} , \mathbf{E}_p and \mathbf{E}_c are presented.

The research was conducted in the scope of the International Associated Laboratory IRMAS (CNRS-France & SCS-Armenia), and was partially supported by a M-C Intern. Research Staff Exchange Scheme Fellowship within the 7th Europ. Comm. Framework Prog. "Coherent optics sensors for medical applications-COSMA" (grant No PIRSES-GA-2012-295264).

References

[1] M. Auzinsh, D. Budker, S. Rochester, *Optically Polarized Atoms, Understanding light-atom interactions* (Oxford: Oxford University Press) ISBN 978-0-19-956512-2 (2010).

Study of atomic transitions of ^{39}K isotope on D_1 line in strong magnetic fields

A. Tonoyan^{1,2}, A. Sargsyan¹, G. Hakhumyan¹, C. Leroy², Y. Pashayan-Leroy², and D. Sarkisyan¹

¹Institute For Physical Research, National Academy of Sciences of Armenia, 0203 Ashtarak, Armenia

²Laboratoire Interdisciplinaire Carnot de Bourgogne, UMR CNRS 6303, Université de Bourgogne, 21078 Dijon, France

Presenting Author: claude.leroy@u-bourgogne.fr & yevgenya.pashayan-leroy@u-bourgogne.fr

The magnetic field required to decouple the electronic total angular momentum J and the nuclear magnetic momentum I is given by $B \gg B_0 = A_{hfs}/\mu_B$, where A_{hfs} is the ground-state hyperfine coupling coefficient and μ_B is the Bohr magneton. For such strong magnetic fields when I and J are decoupled (Hyperfine Paschen Back (HPB) regime) the eigenstates of the Hamiltonian are described in the uncoupled basis of J and I projections ($m_J; m_I$).

Among all the alkali metals, ^{39}K atom has the smallest value of the ground state hyperfine coupling coefficient: $A_{hfs}(^{39}\text{K}) = 231\hbar$ MHz. Consequently, the magnetic field required to decouple total electronic angular momentum J and nuclear spin momentum I (HPB regime) is $B \gg B_0(^{39}\text{K}) = 160$ G. Note that $B_0(^{85}\text{Rb}) \simeq 0.7$ kG and $B_0(^{87}\text{Rb}) \simeq 2.4$ kG. Thus, $B_0(^{39}\text{K})$ value is more than 4 times smaller than that for ^{85}Rb and 15 times smaller than that for ^{87}Rb . This means that complete HPB regime for ^{39}K can be observed for much smaller external magnetic fields [1]. It is demonstrated that the use of recently developed setup based on nano-cell filled with K metal ($L = 770$ nm) allows us to study behavior of atomic transition of ^{39}K atoms D_1 line in a wide range of magnetic fields.

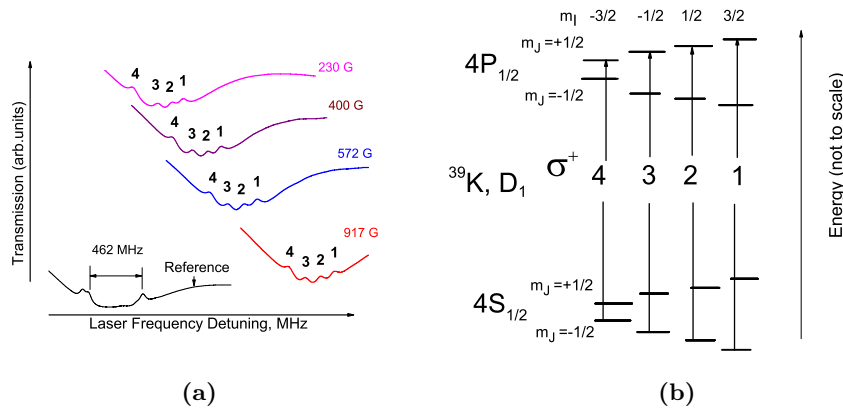


Figure 1: (a) Transmission spectrum of ^{39}K vapor contained in the nano-cell with $L = 770$ nm for $B = 230, 400, 572$ and 917 G and σ^+ excitation. (b) The diagram of the hyperfine structure of the D_1 line of the ^{39}K HPB regime, the selection rules are $\Delta m_J = 1, \Delta m_I = 0$.

It is experimentally demonstrated that from 12 Zeeman transitions allowed at low B -field only 4 transitions remain in absorption spectra at $B > 200$ G (Fig. 1a). A complete HPB regime for relatively low magnetic fields $B \simeq 1.6$ kG has been observed. The theoretical model very well describes the experiment.

The research was conducted in the scope of the International Associated Laboratory IRMAS (CNRS-France & SCS-Armenia).

References

- [1] A. Sargsyan, A. Tonoyan, G. Hakhumyan, etc., <http://www.arxiv.org/abs/1502.07564v1>

Study of Atomic Transitions of Rb D_2 line in Strong Transverse Magnetic Fields by an Optical Half-Wavelength Cell

A. Amiryan^{1,2}, A. Sargsyan¹, A. Tonoyan^{1,2}, Y. Pashayan-Leroy², C. Leroy², and D. Sarkisyan²

¹*Institute for Physical Research, NAS of Armenia - Ashtarak-2, 0203, Armenia*

²*Laboratoire Interdisciplinaire Carnot de Bourgogne, UMR CNRS 6303, Université de Bourgogne - Dijon, France*

Presenting Author: claude.leroy@u-bourgogne.fr

It is demonstrated that the use of the $\lambda/2$ method allows one to effectively investigate individual atomic transitions of the D_2 line of Rb in strong transverse magnetic fields (with laser radiation of π -polarization) up to 7 kG. The method is based on strong narrowing of the absorption spectrum (which provides sub-Doppler resolution) of a rubidium filled thin cell with the thickness L equal to the half-wavelength ($L = \lambda/2$) of the laser radiation ($\lambda = 780$ nm) resonant with the D_2 line. In particular, the $\lambda/2$ method has allowed us to resolve completely 12 and 8 atomic transitions of the ^{85}Rb and ^{87}Rb , correspondingly. These 20 atomic transitions are contained within two groups of ten atomic transitions each (see Fig.1). We have determined their frequency positions, fixed (within each group) frequency slopes, the probability characteristics of the transitions, and other important characteristics of the hyperfine structure of Rb in the hyperfine Paschen–Back regime (HPB), which means that when a strong magnetic field is applied there is a decoupling of the total electronic angular momentum \mathbf{J} and nuclear momentum \mathbf{I} [1]. The theoretical model very well describes the experiment.

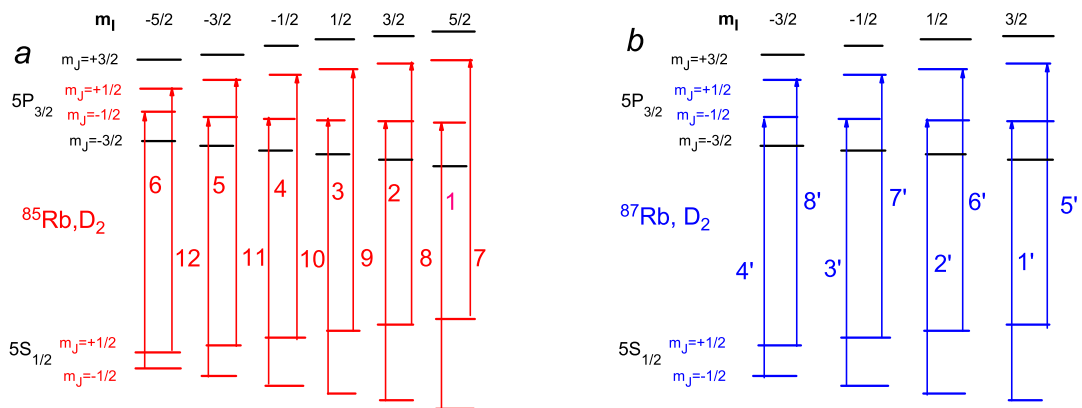


Figure 1: Diagram of the hyperfine structure of the D_2 line of the ^{85}Rb (a) and ^{87}Rb (b) in the HPB regime. The selection rules are $\Delta m_J = 0$, $\Delta m_I = 0$. There are 12 and 8 transitions of the ^{85}Rb and the ^{87}Rb , correspondingly.

The research was conducted in the scope of the International Associated Laboratory IRMAS (CNRS-France & SCS-Armenia).

References

- [1] A. Sargsyan *et al.* Optics Lett. **37** 1379 (2012)

The Radioactive Francium Magneto - Optical Trap in Legnaro: search for new lines in an isotopic series

E. Mariotti¹, G. Bianchi¹, C. Marinelli¹, A. Vanella¹, L. Corradi², A. Dainelli², L. Marmugi^{1,3}, L. Ricci⁴, A. Khanbekyan^{1,5}, L. Tomassetti⁵, and R. Calabrese⁵

¹CNISM - DSFTA, University of Siena

²INFN - LNL

³Department of Physics and Astronomy, University College of London

⁴Department of Physics, University of Trento

⁵INFN - Department of Physics, University of Ferrara

Presenting Author: mariotti@unisi.it

There are Four facilities where an experiment on Francium either has being performed or is in preparation. At ISOLDE (CERN) the magnetic dipole moments and changes in mean-square charge radii of the neutron-rich ^{218m,219,229,231}Fr isotopes were measured with the newly-installed Collinear Resonance Ionization Spectroscopy (CRIS) beam line [1]. At RCNP/CYRIC in Sendai, Japan, an experiment will search for Permanent Electric Dipole Moments of Francium Atom [2]. At TRIUMPH, Canada, a collaboration has successfully trapped ²⁰⁷Fr, ²⁰⁹Fr and ²²¹Fr, as a preparation of studies of the weak interaction through measurements of atomic parity non-conservation [3].

At Legnaro National Laboratories of INFN, we have recently introduced a simple detection method devoted to the measurement of hyperfine splittings of a series of Francium isotopes, again in the framework of possible Atomic Parity Violation developments [4]. At the moment, we studied the $7P_{3/2} \rightarrow 7D_{3/2,5/2}$ transitions for both ^{209,210}Fr [5]. We will apply the same scheme, using different laser sources, to magnetic dipole and electric quadrupole lines, in order to get useful information of the nucleus structures and to progressively go towards the weakest intensities, interesting for APV. At the same time we have successfully used Light Induced Atom Desorption in order to optimize the trapping efficiency [6].

References

- [1] K.M. Lynch *et al.*, Phys Rev X **4**, 011055 (2014) Eur. Phys. J. D **61**, 171–180 (2011)
- [2] T. Inoue *et al.* Hyperfine Interactions **231** 157–162 (2015)
- [3] L.Orozco, Nuclear Physicis News, **23** 17–20 (2013)
- [4] L.Moi *et al.*, Meas.Sci.Technol. **24** 015201 (2013)
- [5] S.Agustsson *et al.*, LNL Annual Report **240** 22–23 (2014)
- [6] V.Coppolaro *et al.*, J.Chem.Phys. **141** 134201 (2014); E.Mariotti *et al.*, in preparation

Double impulse effects during a collision of ions and diatomic molecules

M. Nakamura¹, A. Ichimura²

¹College of Science and Technology, Nihon University, Funabashi

²Institute of Space and Astronautical Science, JAXA, Sagamihara

Presenting Author: mooming@phys.ge.cst.nihon-u.ac.jp

In large angle scattering of ions (atoms) from diatomic molecules at hyperthermal incident energies (1-100 eV), short range repulsive forces play dominant roles in the energy transfer from translational to internal degrees of freedom. In such a collision, the hard-potential model [1-2] or the hard-shell model [3] well describes the mechanism of the energy and angular momentum transfer. These models assume that an impulse is exerted at a point on the hard-shell, which is given by the equipotential surface at the collision energy. If the incident energy is almost exhausted by the first impulse, the 'second impulse' would be possible to occur during a single collision event [4]. In fact, Tanuma *et al.* [5] reported a structure which cannot be explained by these models in the energy-loss spectrum of $\text{Na}^+ - \text{N}_2$. They presented a possibility of the 'double impulse' effect through an analysis based on the classical trajectory calculation.

In the present work, we investigate the double impulse effect within the framework of the hard-shell model. We calculate systematically trajectories of ions scattered by molecules with varying projectile mass and shell anisotropy at an incident energy of 1 a.u. The shape of the shell is assumed to be a sum of monopole and quadrupole deformations as $r_s(\gamma) = r_0(1 + \beta_2 P_2(\cos \gamma))$. In Figure 1, we draw trajectories of K^+ scattered by N_2 as an example. We take a fixed-in-space molecule before the first impulse and switch the frame rotating with the molecular axis after the impulse. As shown in the right panel of the figure, we see that a trajectory hits the shell again after the first impulse when the anisotropy of the hard-shell is larger ($\beta_2 = 0.4$). Such an event is not observed in the left panel where the anisotropy is smaller ($\beta_2 = 0.3$). The double impulse effect is observed in the collision where the ion is heavier than the molecule and the anisotropy of the interaction potential is strong.

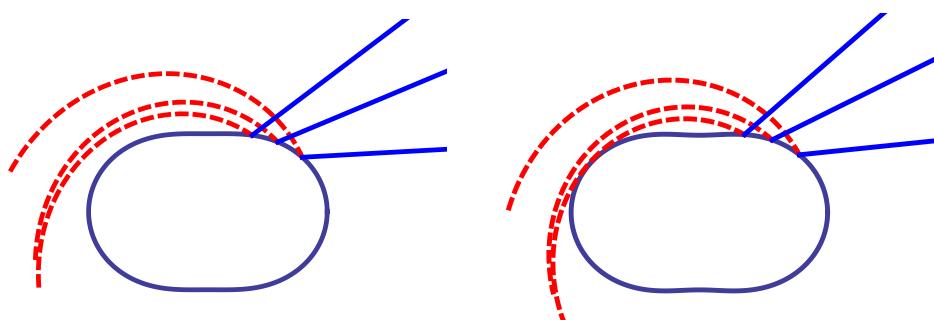


Figure 1: Trajectories of K^+ scattered from N_2 by the hard-shell model. Solid lines and dashed curves indicate the incident and the scattered orbits, respectively, in a molecular frame. In the left (right) panel, β_2 , the anisotropy of the hard-shell is 0.3 (0.4).

References

- [1] A. Ichimura and M. Nakamura, Phys. Rev. A **69**, 022716 (2004)
- [2] M. Nakamura and A. Ichimura, Phys. Rev. A **71**, 062701 (2005)
- [3] D. Beck *et al.* Z. Phys. A **293** 107 (1979)
- [4] D. Beck *et al.* Chem. Phys. **126** 12 (1988)
- [5] H. Tanuma *et al.* Phys. Rev. A **38** 5053 (1988)

A compact 0.74 T room temperature EBIT

P. Micke^{1,2}, S. Bernitt^{1,3}, J. Harries⁴, L. F. Buchauer¹, T. M. Bücking¹, S. Kühn¹, P. O. Schmidt^{2,5}, and J. R. Crespo López-Urrutia¹

¹Max-Planck-Institut für Kernphysik, Heidelberg, Germany

²Physikalisch-Technische Bundesanstalt, Braunschweig, Germany

³Friedrich-Schiller-Universität Jena, Germany

⁴SPRING-8, Hyogo, Japan

⁵Leibniz Universität Hannover, Germany

Presenting Author: peter.micke@quantummetrology.de

Research on moderately and highly charged ions (HCIs) is of great interest not only for atomic physics but also fundamental studies. Electron beam ion traps (EBITs) have proven to be versatile and indispensable tools for the production and study of such ions.

In an EBIT, an electron beam is compressed by a strong, inhomogeneous magnetic field to breed the ions efficiently. Usually the field is generated by superconducting magnet coils. To ease operation we introduce a novel magnetic design based on permanent magnets for a 0.74 tesla EBIT. It allows operation at room temperature, resulting in a low-cost and low-maintenance apparatus. An open trap design offers access to the trap center with a large solid angle.

Our EBIT is intended to serve as a reliable source for HCIs. Additionally a new off-axis gun is under construction, which will enable the trap to be used for energy calibration at synchrotron and free-electron laser light sources by means of spectroscopy on HCIs. The photon beam can pass through the EBIT and is available for beamline users.

Currently, first experiments with a prototype are carried out regarding trapping and extraction of HCIs.

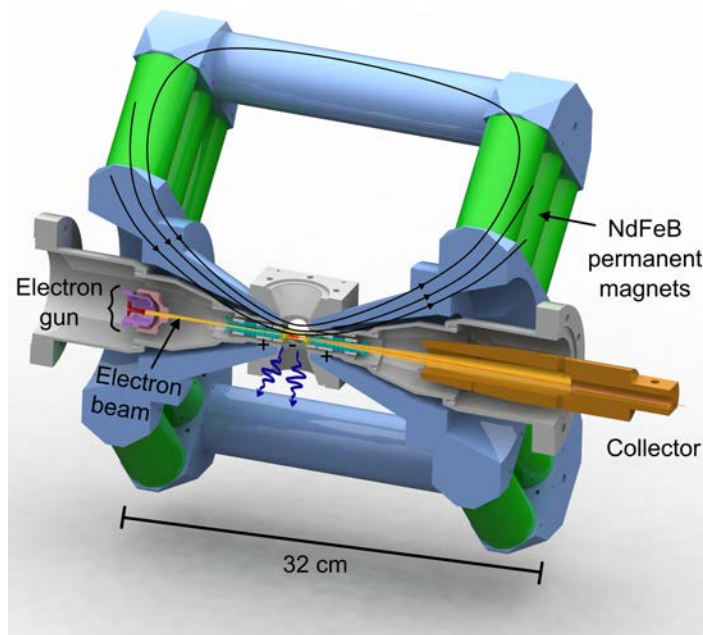


Figure 1: A cross section of the EBIT showing vacuum chamber, magnetic system, and electrode configuration. The design gives a measured magnetic field of 0.74 T at the trap center. Four ports for optical access with an opening angle of 60° are available.

H2O double ionization induced by electron impact

D. Oubaziz¹, C. Champion², M. A Quinto², and Z. Aitelhadjali³

¹*Laboratoire de Mécanique, Structures et Energétique, Université Mouloud Mammeri de Tizi-Ouzou, BP 17, Tizi-Ouzou 15000, Algérie*

²*Centre d'Etudes Nucléaires de Bordeaux Gradignan, Université de Bordeaux, CNRS/IN2P3, BP 120, 33175, Gradignan, France*

³*Laboratoire de Sciences Nucléaires et Interaction rayonnement- Matière, Faculté de Physique, USTHB, Alger 16000, Algérie*

Presenting Author: doubagha@yahoo.com

Double ionization of water molecules remains, still today, rarely investigated on both the experimental and the theoretical side. In this context, the present work reports on a quantum mechanical approach providing a quantitative description of the electron-induced double ionization process on isolated water molecules for impact energies ranging from the target ionization threshold up to about 10 keV. The cross section calculations are here performed within the first Born approximation framework in which the initial state of the system includes a molecular ground-state wave function expressed as a single-center linear combination of atomic orbitals [1] while the final state of the system is characterized by two independent Coulomb wave functions used for describing the two ejected electrons coupled by a Gamov factor used for modeling the electron-electron repulsion. In comparison with the rare available experiments [2], the double vs single ionization cross section ratio shows an overall good agreement. Besides, in absence of measurement of absolute total cross sections in water vapor, the current theoretical predictions are compared with isoelectronic neon data. A very good agreement is observed over the whole incident energy range investigated. Finally, we report an average energy transfer of the double ionization process and clearly demonstrate the absolute necessity of considering the double ionization process in particular in a radiobiological context.

References

[1] R. Moccia, *J. Chem. Phys.* **40**, 2186–2192 (1964)

[2] F. Frémont, C. Leclercq, A. Hajaji, A. Naja, P. Lemennais, S. Boulbain, V. Broquin, and J.-Y. Chesnel, *Phys. Rev. A* **72**, 042702–042707 (2005)

Theoretical study of hyperfine structure of ground state in neutral Carbon

P. Rynkun¹, G. Gaigalas¹, P. Jönsson², Ch. Froese Fischer³, and M. Godefroid⁴

¹*Institute of Theoretical Physics and Astronomy, Vilnius University, Vilnius, Lithuania*

²*Group for Materials Science and Applied Mathematics, Malmö University, Malmö, Sweden*

³*National Institute of Standards and Technology, Gaithersburg, USA*

⁴*Chimie Quantique et Photophysique, Université Libre de Bruxelles, Brussels, Belgium*

Presenting Author: pavel.rynkun@fai.vu.lt

In this work, hyperfine constants are reported for $1s^2 2s^2 2p^2 \ ^3P_{1,2}$ states of C I using multiconfiguration Hartree-Fock (MCHF) [1] and a (deconstrained) partitioned correlation function interaction ((D)PCFI) [2–3] method. Systematic calculations were performed with the principal quantum number $n = 4 \dots 8$ and with orbital quantum numbers up to $l = l_{max}$. Configuration state functions (CSFs) were constructed by allowing single- (S) and double- (D) substitutions from a multireference (MR) set. Present calculations were performed with a MR set consisting of CSFs belonging to 11 configurations.

The PCFI [2–3] method was applied using three PCFs: 1) the first one, $\Lambda_{1s-1s1s}$, targets SD excitations from the core (1s) orbital; 2) a second one, Λ_{1s-nl} , targets S excitations from the 1s core shell and S excitation from the valence (nl) orbital; 3) a third one, Λ_{nl-nl} , targets SD excitations from the valence (nl) orbitals (where $n = 2, 3$ and $l = s, p, d$). The wave-function for $1s^2 2s^2 2p^2 \ ^3P$ would be

$$|\Psi(1s^2 2s^2 2p^2 \ ^3P)\rangle = |\Psi^{MR}(\ ^3P)\rangle + \alpha_{CC} |\Lambda_{1s-1s1s}\rangle + \alpha_{CV} |\Lambda_{1s-nl}\rangle + \alpha_{VV} |\Lambda_{nl-nl}\rangle. \quad (1)$$

Also performed were calculations where the $\Lambda_{1s-1s1s}$ PCF was split into two subspaces ($\Lambda_{1s-1s1s} \rightarrow \Lambda_{1s} + \Lambda_{1s1s}$). The Λ_{1s} PCF focusing on the S excitations is dedicated to capture core-polarization (CP) effects. The many-electron wave-function is then written as the MR function corrected by four different PCFs.

From Table 1 it is seen that splitting of $\Lambda_{1s-1s1s}$ PCF in the two groups improves the hyperfine structure results. The results are in better agreement with the experiment. Results are compared with previous theoretical data and with experimental results. Calculations are in progress, additional schemes of calculations (choosing different MR set, etc.) are tested to improve the results.

Method	n	$A (J=1)$			$A (J=2)$			Reference
		6	7	8	6	7	8	
MCHF		3.017	2.461	2.339	147.831	147.842	148.365	this work
DPCFI		-1.861	7.415		145.984	152.384		this work
CP-PCFI		3.559	4.229	4.083	148.444	148.958	148.900	this work
CP-DPCFI		1.962	3.917	2.665	147.608	149.440	148.079	this work
Unrestricted HF				13.7			160.6	[4]
MCHF				2.36			147.9	[5]
SD-MR-CI				2.28			148.1	[6]
MCHF				3.225			148.747	[7]
CI(CIV3)				7.63			152.0	[8]
Experiment				2.838(17)			149.055(10)	[9]
Experiment							149.0(3)	[10]

Table 1: Comparison of the magnetic dipole constants (in MHz) for the $1s^2 2s^2 2p^2 \ ^3P_{1,2}$ states in C I.

References

- [1] Ch. Froese Fischer, T. Brage, and P. Jönsson, *Computational Atomic Structure: An MCHF Approach* (Bristol: Institute of Physics Publishing, 1997)
- [2] S. Verdebout *et al.* J. Phys. B: At. Mol. Phys. **43** 074017 (2010)
- [3] S. Verdebout *et al.* J. Phys. B: At. Mol. Phys. **46** 085003 (2013)
- [4] P. J. Hay, W. A. Goddard Chem. Phys. Lett. **9** 356 (1971)
- [5] P. Jönsson, Ch. Froese Fischer Phys. Rev A **48** 4113 (1993)
- [6] P. Jönsson, Ch. Froese Fischer, M. R. Godefroid J. Phys. B: At. Mol. Phys. **29** 2393 (1996)
- [7] T. Carette and M. R. Godefroid Phys. Rev A **83** 062505 (2011)
- [8] R. Glass, A. Hibbert J. Phys. B **11** 2257 (1978)
- [9] G. Wolber *et al.* Z. Phys. **236** 337 (1970)
- [10] H. Klein *et al.* ApJ. **494** L125 (1998)

Stark splitting effects for Er^{3+} in Er_2O_3

P. Rynkun¹, G. Gaigalas^{1,2}, D. Kato^{2,3}, L. Radziūtė¹, and P. Jönsson⁴

¹*Institute of Theoretical Physics and Astronomy, Vilnius University, Vilnius, Lithuania*

²*National Institute for Fusion Science, Oroshi-cho, Toki, Japan*

³*Department Fusion Science, SOKENDAI (The Graduate University for Advanced Studies), Oroshi-cho, Toki, Japan*

⁴*Group for Materials Science and Applied Mathematics, Malmö University, Malmö, Sweden*

Presenting Author: pavel.rynkun@tfai.vu.lt

In the present work a fully *ab-initio* method was used to calculate Stark splitting effects of Er^{3+} in Er_2O_3 . Crystal field effects were included by treating external ions as point charges at fixed positions. Charges and positions of the external ions are parameters (which depend on the compound) in the calculations. The coordinates of the external ions were obtained by molecular statics calculations based on density functional theories performed with the VASP code [1, 2]. Using first order perturbation theory, splitting of the degenerate atomic energy levels in the crystal electric field (Stark effect) can be calculated. To perform such calculations the GRASP2K [3] relativistic atomic structure program was extended to include programs for calculating the crystal field operator matrix elements and diagonalizing the full atomic Hamiltonian matrix [4].

Stark splitting of the ground state $4f^{11} {}^4I_{15/2}^o$ and the excited state $4f^{11} {}^4F_{9/2}^o$ of Er^{3+} in the Er_2O_3 crystal were computed from relativistic configuration interaction wave functions including Breit and QED effects. Different strategies to include electron correlation effects were tested. Also the effects of different number of neighbor ions (6 ions or 2 159 ions) and the influence of J -mixing were evaluated. The results are summarized in Table 1. It is clear that number of neighbor ions has a big impact and changes results dramatically. J -mixing influence to the Stark splitting is small. To calculate the transitions of Stark levels between states of Er^{3+} different strategies to include crystal field should be used.

MR S		DHF SD		DHF+5d		DHF+5d + 5f + 5g		Exp.
6 ions	2 159 ions	6 ions	2 159 ions	6 ions	2 159 ions	6 ions	2 159 ions	[5]
Stark levels of ground state $[\text{Xe}]4f^{11} {}^4I_{15/2}^o$								
0	0	0	0	0	0	0	0	0
31.27	28.33	30.01	26.01	31.44	28.28	34.94	31.66	38
84.18	73.71	79.65	69.28	84.38	73.59	93.95	81.37	75
145.14	117.88	134.66	108.10	145.53	117.89	163.87	132.49	88
214.52	158.34	189.92	143.22	215.99	159.30	248.19	177.06	159
330.37	166.00	290.98	153.56	331.76	166.60	381.11	191.40	265
498.38	308.03	448.09	285.23	499.91	308.16	567.84	344.24	490
578.06	325.09	513.81	299.64	580.46	325.80	664.05	365.82	505
Stark levels of excited state $[\text{Xe}]4f^{11} {}^4F_{9/2}^o$								
0	0	0	0	0	0	0	0	0
271.00	141.24	219.22	118.56	243.16	129.78	265.95	142.09	74
445.70	206.41	356.06	169.19	397.88	186.22	435.26	203.66	149
532.38	229.42	416.64	184.94	468.70	205.10	511.73	224.24	218
689.10	322.47	551.42	265.25	616.67	293.88	674.52	322.12	306

Table 1: Comparison of computed energy (Stark) levels (in cm^{-1}) of Er^{3+} in Er_2O_3 without J -mixing induced by the crystal field. MR S: configuration state functions (CSFs) generated by single excitations from all core shells in to 5d shell. DHF SD: CSFs generated by single double (SD) excitations from all shells in to 4f shell. DHF+5d: CSFs generated by selected SD excitations from all shells in to 4f and 5d shells. DHF+5d + 5f + 5g: CSFs generated by selected SD excitations from all shells in to 4f, 5d, 5f, and 5g shells.

References

- [1] G. Kresse and J. Futhmüller Phys. Rev. B **54**, 11169 (1996)
- [2] G. Kresse, and D. Joubert Phys. Rev. B **59**, 1758 (1999)
- [3] P. Jönsson *et al.* Comput. Phys. Commun. **184**, 2197 (2013)
- [4] G. Gaigalas *et al.* NIFS-DATA-115, (2014)
- [5] J. B. Gruber *et al.* J. Appl. Phys. **108**, 023109 (2010)

Towards a High Sensitivity Atom Accelerometer for Exploring Physics Beyond the Standard Model

D. O. Sabulsky¹, I. J. M. Barr¹, G. Barontini¹, Y.-H. Lien¹, and E. A. Hinds¹

¹Centre for Cold Matter, Blackett Laboratory, Imperial College London, Prince Consort Road, London SW7 2AZ, United Kingdom

Presenting Author: d.sabulsky@imperial.ac.uk

Theories of dark energy usually invoke a screening mechanism to explain why their scalar fields do not produce observable long range fifth forces; a primary example of this mechanism is the so-called chameleon field. However, it is now known, from [1,2], that individual atoms are not massive enough and large enough to screen the chameleon field inside a large vacuum chamber under UHV. We present the design for an atom interferometer experiment that will place strong new constraints on the chameleon and other similar scalar fields [1].

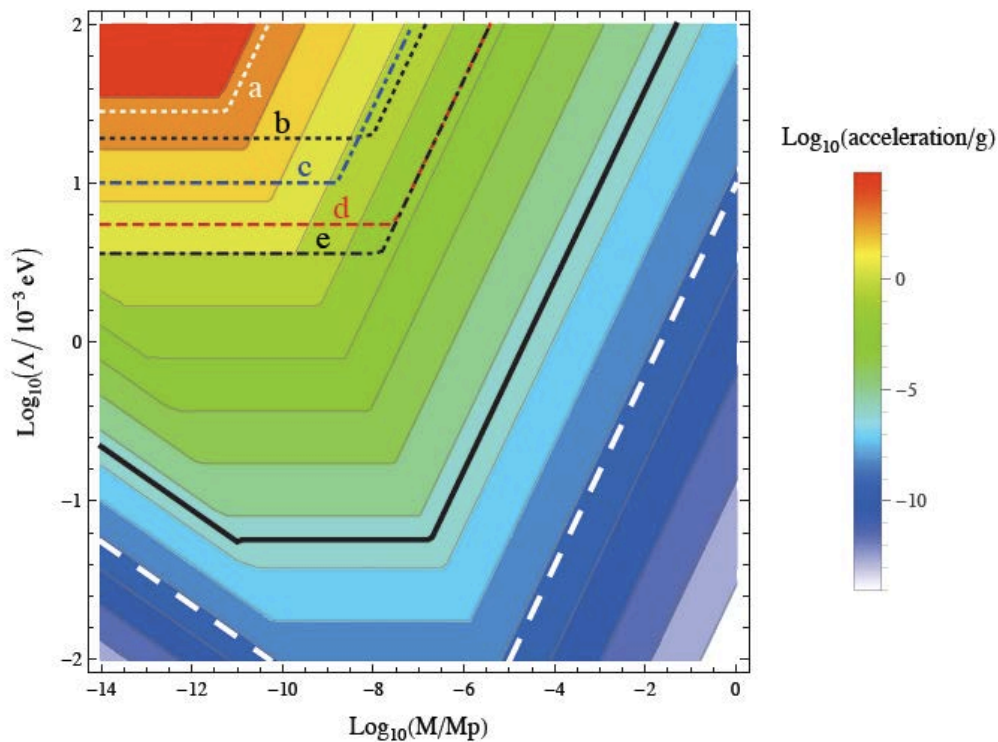


Figure 1: Contour plot showing acceleration of rubidium atoms, normalized to the acceleration of free fall on earth g , due to the chameleon force outside a sphere of radius $R_A = 1$ cm and screening factor $\lambda_A = \frac{3M_A \phi_b g}{\rho_A R_A^2}$. The $L - M$ area above the heavy solid line will be excluded by a first atom interferometer experiment measuring $10^6 g$. With modest attention to systematic errors, this can move down to the heavy dashed line. For $\Lambda \geq 10$ meV, atom interferometry could sense chameleon physics up to the Planck mass MP . We calculate that measurements on atoms and neutrons near surfaces, (a)-(e), already exclude the top-left corner, as indicated by the light-weight lines.

References

- [1] C. Burrage, E. J. Copeland and E. A. Hinds. arXiv: 1408.1409
- [2] P. Hamilton *et al.* arXiv: 1502.03888

Reanalysis and semi-empirical predictions of the hyperfine structure of $^{123}\text{Sb I}$

S. Bouazza¹, Ł. M. Sobolewski², and J. Kwela²

¹LISM, EA 4695, Université de Reims-Champagne, UFR SEN, BP 1039, F-51687 Reims Cedex 2, France

²Institute of Experimental Physics, University of Gdansk, ul. Wita Stwosza 57, 80-952 Gdansk, Poland

Presenting Author: safa.bouazza@univ-reims.fr

The hyperfine and Zeeman structures of 14 lines of $^{123}\text{Sb I}$ covering the UV-NIR spectral range have been examined. The Zeeman effect studies were performed for transverse direction of observation and separated $\pi(\Delta M = 0)$ and $\sigma(\Delta M = \pm 1)$ components of lines. The complete set of fine structure parameters of the two level parities are determined, discarding some levels, previously mentioned in literature [1]. Furthermore we give those missing up to 70000 cm^{-1} . New Landé-factors and hyperfine structure (hfs) constants of 12 odd- and 6 even- parity levels of ^{123}SbI were measured and the single-electron hfs parameters, treated as free in the least squares fit to these measured hfs constant values were extracted. We give the 3 main deduced values: $a_{6s}^{10}(5p^26s) = 49.09\text{ mK}$, $a_{5p}^{01}(5p^26s) = 29.63\text{ mK}$, $a_{5p}^{01}(5p^3) = 27.63\text{ mK}$ Finally a complete list of the predicted hfs constant A of all studied system levels was generated.

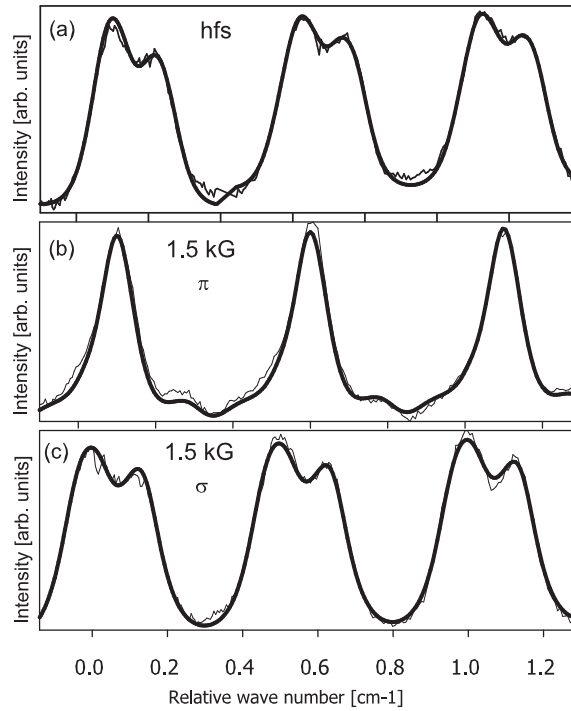


Figure 1: The recorded hyperfine structure of the 792.5 nm line of $^{123}\text{Sb I}$ (a) and Zeeman patterns π -view (b) and σ -view (c) at 1.50 kG magnetic field. The thin line represents the experimental trace and the thick line shows the computer-generated contour.

References

- [1] Hassini F, Ben Ahmed Z., Robaux O., Verges J. and Wyart J.F. (1988) JOSA B5, 2060

Calculation of Lamb shift for states with $j = 1/2$

V. Patkóš¹, J. Zamastil¹, and D. Šimsa¹

¹*Department of Chemical Physics and Optics, Faculty of Mathematics and Physics, Charles University, Prague*

Presenting Author: simsadan@gmail.com

The Lamb shift in the light hydrogen-like atom yields one of the most stringent test of quantum electrodynamics. It is customary to write the Lamb shift of general S -state in the form

$$\Delta E_n = \frac{n^3 \Delta E_n - \Delta E_1}{n^3} + \frac{\Delta E_1}{n^3}, \quad (1)$$

where n is the principal quantum number of the state under consideration. The first and the second terms on the right-hand side are referred to as the state-dependent and the state-independent parts, respectively. The state-dependent part of the S -states is nearly completely given by the self-energy effect in one-loop approximation which is usually expressed in the form

$$\Delta E_n = \frac{\alpha}{\pi} \frac{(Z\alpha)^4}{n^3} F(n, l_j, Z\alpha), \quad (2)$$

where l and j are the orbital and total angular quantum numbers of the state under consideration, Z is the charge of the nucleus in units of elementary charge e , $\alpha = e^2/(4\pi)$ is the fine structure constant.

It was suggested in [1,2] to calculate the dimensionless function F by means of relativistic generalization of multipole expansion (RME)

$$F = \sum_{v=1}^{\infty} F_v, \quad (3)$$

where F_v are the "relativistic multipoles" (for formulas see Eq. (73) of [2]).

Here, we report the evaluation of the state-dependent part of the S -states and $P_{1/2}$ states by means of RME. We obtain the results for $Z = 1 - 50$ and $n = 2 - 10$.

The results for low Z are the most accurate results given so far in the literature. In the case of hydrogen the uncertainty is significantly less than 1 Hz. Some of the results are presented in the following table.

Term	State	$Z = 1$	$Z = 2$	$Z = 3$	$Z = 4$
Lead	$2s - 1s$	0.229991606931	0.230390709933	0.230936267290	0.231594004269
	F_3	0.000039870858	0.000154033610	0.000336061748	0.000581009986
	F_4	6.241492×10^{-8}	4.634566×10^{-7}	1.469760×10^{-6}	3.298274×10^{-6}
Total		0.2300315402(3)	0.230545207(2)	0.231273799(6)	0.23217831(1)
Lead	$3s - 1s$	0.288771400893	0.289100037681	0.289541947085	0.290067435815
	F_3	0.000048953133	0.000189443771	0.000413949977	0.000716666402
	F_4	7.723537×10^{-8}	5.752828×10^{-7}	1.829313×10^{-6}	4.115199×10^{-6}
Total		0.2888204313(3)	0.289290057(2)	0.289957726(8)	0.29078822(2)
Lead	$4s - 1s$	0.312542251722	0.312795865525	0.313129873756	0.313519935279
	F_3	0.000052358450	0.000202772029	0.000443363221	0.000768038994
	F_4	8.348329×10^{-8}	6.226729×10^{-7}	1.982136×10^{-6}	4.463102×10^{-6}
Total		0.3125946937(3)	0.312999260(3)	0.313575219(8)	0.31429244(2)

Table 1: Contribution of individual multipoles to the normalized difference of S -states for $n = 2 - 4$. Lead stands for first two multipoles, $F_1 + F_2$.

References

- [1] J. Zamastil, V. Patkóš, Phys. Rev. A **86**, 042514 (2012).
 [2] J. Zamastil, V. Patkóš, Phys. Rev. A **88**, 032501 (2013).

Measurement of muonium hyperfine splitting at J-PARC

K. S. Tanaka^{1,3}, M. Aoki⁴, H. Iinuma², Y. Ikedo², K. Ishida³, M. Iwasaki³, K. Ueno², Y. Ueno¹, T. Okubo², T. Ogitsu², R. Kadono², O. Kamigaito³, N. Kawamura², D. Kawall⁸, S. Kanda^{2,6}, K. Kubo⁷, A. Koda², K. M. Kojima², N. Saito², N. Sakamoto³, K. Sasaki², K. Shimomura², M. Sugano², M. Tajima¹, D. Tomono⁹, A. Toyoda², H. A. Torii¹, E. Torikai⁵, K. Nagamine², K. Nishiyama², P. Strasser², Y. Higashi¹, T. Higuchi¹, Y. Fukao², Y. Fujiwara⁶, Y. Matsuda¹, T. Mibe², Y. Miyake², T. Mizutani¹, M. Yoshida², and A. Yamamoto²

¹Graduate School of Arts and Sciences, University of Tokyo; 3-8-1 Komaba, Meguro-ku, Tokyo 153-8902, Japan

²KEK; 1-1 Oho, Tsukuba, Ibaraki 305-0801, Japan

³RIKEN; 2-1 Hirosawa, Wako, Saitama 351-0198, Japan

⁴Osaka University; Toyonaka, Osaka 560-0043, Japan

⁵University of Yamanashi; Kofu, Yamanashi 400-8511, Japan

⁶Graduate School of Science, University of Tokyo; 7-3-1 Hongo, Bunkyo-ku, Tokyo 113-0033, Japan

⁷International Christian University (ICU); Mitaka, Tokyo 181-8585, Japan

⁸University of Massachusetts Amherst, USA

⁹Graduate School of Science, Kyoto University; Sakyo-ku, Kyoto 606-8501, Japan

Presenting Author: tanaka@kaduo.jp

We are planning a measurement of the ground state hyperfine structure of muonium at J-PARC/MLF. Muonium is a hydrogen-like bound state only consist of leptons, and its HFS is a good probe for testing QED theory. Fundamental constants of muon such as mass and magnetic moment have been so far determined by the muonium HFS experiment at LAMPF[1]. The high intensity beam (H-line)[2] soon to be available at J-PARC allows one order of magnitude more accurate determination of those constants, which also plays an important role in the new measurement of anomalous magnet moment of muons. Muonium atoms are formed by electron capture reaction with Krypton gas and their spin are flipped by microwave magnetic field (Figure. 1). Furthermore, we are planning a measurement of its HFS at zero-field as a trial of the setup end of this year. In this contribution, we present the progress of preparations for this measurement.

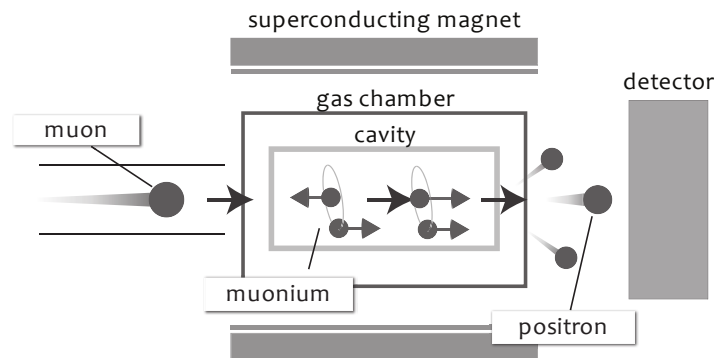


Figure 1: Setup of this experiment

References

- [1] W. Liu et al., Phys. Rev. Lett., 82,711 (1999)
- [2] N. Kawamura et al., JPS Conf. Proc. 2, 010112 (2014)

Sensitivity of tunneling–rotational transitions in ethylene glycol to the variation of electron-to-proton mass ratio

A. V. Viatkina^{1,2}, M. G. Kozlov²

¹*Department of Physics, St. Petersburg State University, Russia*

²*Petersburg Nuclear Physics Institute, Gatchina, Russia*

Presenting Author: anna.viatkine@gmail.com

The parameters of the Standard model considered unchanging over time and space are usually called fundamental constants. But since their exact values cannot be calculated within the Standard model, it is natural to question their invariability. Molecular spectra can be used to study variation of electron-to-proton mass ratio μ .

Ethylene glycol $\text{OH}-\text{CH}_2-\text{CH}_2-\text{OH}$ in its ground conformation $g'Ga$ has tunneling transition with the frequency about 7 GHz. This leads to a rather complicated tunneling-rotational spectrum. Because tunneling and rotational energies have different dependence on μ , some transitions can be highly sensitive to the possible μ variation.

Let ω be a present-day experimentally observed transition frequency and ω' a frequency shifted due to possible time (and space) change of μ . This shift $\Delta\omega = \omega - \omega'$ is linked to the change $\Delta\mu$ through dimensionless sensitivity coefficient Q_μ :

$$\frac{\Delta\omega}{\omega} = Q_\mu \frac{\Delta\mu}{\mu} \quad (1)$$

We used relatively simple 14 parameter effective Hamiltonian and known experimental spectrum from [1] to calculate Q_μ 's of the tunneling-rotational transitions below 60 GHz, since low-frequency lines are more likely to be highly sensitive to the μ shift. We found out that Q_μ 's lie in the range from -17 to +18. The big difference $Q_\mu^{(max)} - Q_\mu^{(min)} \approx 34$ increases sensitivity of the future experiments or observations to μ variation and allows effective control over systematic effects.

Ethylene glycol has been detected in the interstellar medium [2] and in the comet C/1995 O1 (Hale-Bopp) [3]. Observation of the spectrum from extragalactic sources can give us new information about the time-drift of μ . Spectral lines from cold molecular clouds in the Milky Way can be very narrow allowing for high precision spectroscopy. This may be used to study possible dependence of μ on the local matter density, which is predicted by models with chameleon scalar fields.

Results of our work were published in [4].

References

- [1] D. Christen, L. H. Coudert *et al.* *J. of Mol. Spect.* **172** 57–77 (1995)
- [2] J. M. Hollis, F. J. Lovas *et al.* *Astrophys. J.* **571** L59 (2002)
- [3] J. Crovisier, D. Bockelée-Morvan *et al.* *Astron. Astrophys.* **418** L35-L38 (2004)
- [4] A. V. Viatkina, M. G. Kozlov, *J. of Mol. Spect.* **300** 94–98 (2014)

Nuclear polarizability effects in muonic deuterium

K. Pachucki¹, [A. Wienczek](#)¹

¹*Faculty of Physics, University of Warsaw, Poland*

Presenting Author: albert.wienczek@fuw.edu.pl

The nuclear charge radius can be determined from spectroscopic measurements in muonic atoms, provided the atomic structure is well known and the influence of nuclear excitation on atomic levels is properly accounted for. The latter is problematic due to the difficulty in solving quantum chromodynamics in low energy scale. We perform calculations in perturbative approach by the expansion in ratio of the nuclear excitation energy over the muon mass. We pay special attention on the nuclear mass dependence and separation of the so-called pure recoil corrections. We aimed to calculate the nuclear effects as accurately as possible, in order to extract precise nuclear charge radii from the muonic atom spectroscopy. Numerical results for muonic deuterium is obtained by using the AV18 potential with the help of a discrete variable representation method for solving the Schrodinger equation. The obtained result for the 2P-2S transition of 1.717(20) meV serves for determination of the nuclear charge radius from the spectroscopic measurement in muonic deuterium.

References

- [1] K. Pachucki, A. Wienczek Phys. Rev. A **91**, 040503(R)

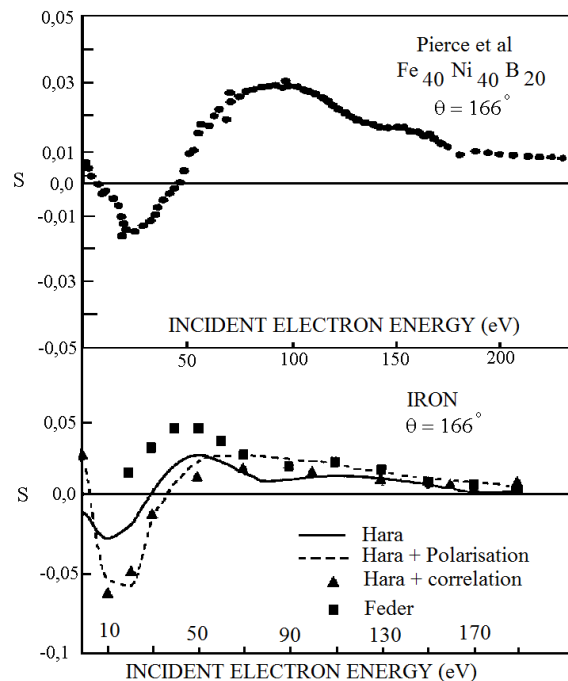
Spin Polarisation Exchange Scattering from Nickel and Iron

S. Y. Yousif Al-Mulla¹

¹ College of Engineering, University of Borås, S-50190 Borås, Sweden

Presenting Author: samir.al-mulla@hb.se

It is well known that the structure information through the use of Spin Polarised Low Energy Electron Diffraction (SPLEED) is highly sensitive to the interaction potential between the primary electrons and the electrons of the target, especially to the exchange interaction. Since the electrons in SPLEED penetrate the surface only a few lattice spacing, it is extremely sensitive to the spin structure of a magnetic surface. The early study of Feder [1] on Fe(110) provides a strong indication in this direction. The main objective of this work is to use the insights of our recent work [2,3] to study the spin polarisation of the exchange-correlation potential. The differential cross sections for electron scattering from atoms with net spin, namely nickel and iron, have been calculated together with studying the energy/wave vector dependence of the exchange scattering from surfaces of nickel and iron in glasses by calculating differential cross sections and the spin asymmetry using Dirac equation. Comparison of predictions with observed spin dependent scattering intensities in amorphous magnetic alloys will give insight into surface magnetisation in these systems[4].



References

- [1] R. Feder, Solid State Comm. 31,821 (1979).
- [2] S. Y. Yousif Al-Mulla, J. Phys. B:At. Mol. Opt. Phys. 37, 305 (2004).
- [3] S. Y. Yousif Al-Mulla, Eur. Phys.J.D 42,11 (2007).
- [4] D. T. Pierce et al, Phys. Rev.26, 2566(1982).

Deceleration, cooling and trapping of heavy diatomic molecules

A. Zapara¹, J. E. van den Berg¹, S. C. Mathavan¹, C. Meinema¹, and S. Hoekstra¹

¹ Van Swinderen Institute, University of Groningen, The Netherlands

Presenting Author: a.zapara@rug.nl

In the recent few decades there is a great interest in cooling and controlling of neutral molecules, motivated by a wide range of possible applications. We are developing methods of deceleration, cooling and trapping of certain diatomic molecules that are suitable for study of physics beyond the Standard Model. Traditional Stark decelerator is inefficient for slowing down of heavy diatomic molecules due to overfocusing. Therefore, we are building an inherently stable 4.5m long travelling-wave decelerator [1] to decelerate strontium monofluoride molecules and bring them to a complete standstill. SrF is a sensitive probe for search of parity violation and that is the motivation for our work.

Following the deceleration, we plan to laser cool molecules and transfer them to a deep optical dipole trap. Laser cooling of SrF is possible due to highly diagonal Franck-Condon factors and a short radiative lifetime, and optical trapping can be implemented in an optical cavity. A sample of ultracold trapped molecules provides a large increase of the interaction time and is an ideal starting point for high precision spectroscopy. We report the latest results [2] and the current status of our experiment (Fig. 1).

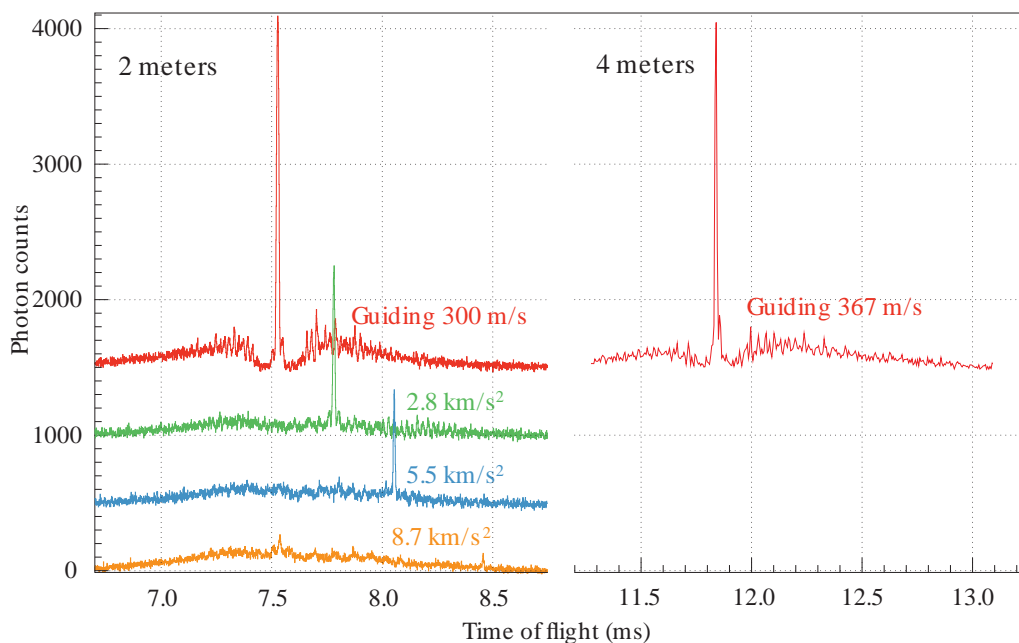


Figure 1: Time-of-flight measurements of guiding and deceleration of SrF molecules for different decelerator lengths. On the left side guiding and deceleration results with 2m decelerator. On the right side guiding result with 4m decelerator. Deceleration with 4m decelerator is in progress.

References

- [1] J.E. van den Berg *et al.* Eur. Phys. J. D **66** 235 (2012)
- [2] J.E. van den Berg *et al.* J. Mol. Spec. **300** 22–25 (2014)

High-resolution spectroscopy/Molecular physics

Optical frequency measurement of Rb 5S-5P transition with a frequency comb

I. Brice¹, J. Rutkis¹, I. Fescenko¹, Ch. Andreeva¹, and J. Alnis¹

¹*Institute of Atomic Physics and Spectroscopy, University of Latvia, Riga, Latvia*

Presenting Author: Janis.Alnis@lu.lv

Femtosecond optical frequency comb technology [1] allows to count optical frequencies against radiofrequency clock. We used an erbium-fiber-based fs comb made by *Menlo Systems* to measure frequency of optical transitions in rubidium atomic vapor against a commercial rubidium clock. The Rb clock was continuously calibrated against GPS satellite time allowing to achieve 11 digits of precision in absolute frequency determination.

We have set up an external cavity diode laser at 780 nm that excites D_2 line in Rb vapor and recorded saturation spectroscopy peaks from ^{85}Rb and ^{87}Rb isotopic hyperfine transitions. The Rb optical cell was placed inside a magnetic shield to minimize Zeeman shift. Diode laser was scanned across the Rb spectrum and its absolute optical frequency was measured precisely from a beatnote with the optical frequency comb. For extraction of hyperfine transition frequencies it is important to use multiple peak fit. Peak positions agree within 1 MHz with the literature [2].

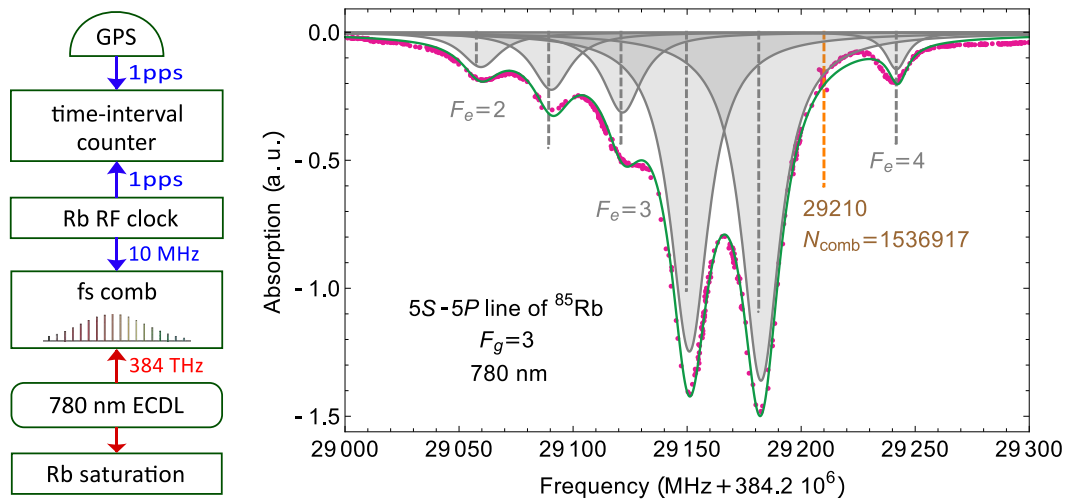


Figure 1: Left: Experimental scheme. Right: Precision measurement of absolute frequencies of Rb saturation peaks using optical frequency comb. Multiple peaks fitting using Lorentz functions is shown.

References

- [1] T.W. Hänsch et al, Phil. Trans. Roy. Soc. London A **363**, 2155 (2005).
- [2] D. Steck, Rubidium Numbers, 2010.

Magneto-optical switch based on high-contrast electromagnetically induced absorption resonance

Ch. Andreeva¹, D. V. Brazhnikov^{2,3}, V. M. Entin⁴, M. Yu. Basalaev^{2,3,5}, S. M. Ignatovich²,
I. I. Ryabtsev^{3,4}, A. V. Taichenachev^{2,3}, and V. I. Yudin^{2,3,5}

¹*Institute of Electronics, Sofia, Bulgaria*

²*Institute of Laser Physics, Novosibirsk, Russia*

³*Novosibirsk State University, Novosibirsk, Russia*

⁴*Institute of Semiconductor Physics, Novosibirsk, Russia*

⁵*Novosibirsk State Technical University, Novosibirsk, Russia*

Presenting Author: christina_andreeva@yahoo.com

The phenomenon of coherent population trapping (CPT), since its discovery in 1976 [1, 2], has found many interesting applications in atom physics. Electromagnetically induced transparency (EIT) is the spectroscopic manifestation of CPT. The width of the EIT resonance can be much less than the natural linewidth, therefore such resonances are often called subnatural-width ones. The narrow transparency window in the absorption signal, resulting from EIT, is also accompanied by very steep refractive-index dispersion of the medium. These brilliant properties of EIT make it attractive for applying in laser physics and laser spectroscopy, optical communications and quantum metrology (miniature atomic clocks and magnetometers).

In 1997 subnatural-width resonance with opposite sign was obtained – electromagnetically induced absorption (EIA) [3]. First that resonance was observed under a bichromatic laser field, composed of two co-directional mutually coherent waves with opposite circular polarizations. Then the effect was also studied with a single-frequency laser wave accompanied by a scanned dc magnetic field applied along the wave vector (magneto-optical or, so-called, Hanle configuration) [4]. Since its discovery, the scope of EIA applications happened to be rather small in comparison with the EIT resonances due to some serious difficulties. Indeed, many methods suggested for observing EIA signals could not provide narrow (< 1 kHz) and simultaneously high-contrast (> 20 -30 %) subnatural-width resonances.

In papers [5, 6] we have proposed the “unconventional” scheme for observing EIA signals in Hanle configuration. It implies using two counterpropagating light waves with the same frequency and orthogonal linear polarizations (“probe” and “pump” beams). Here we further develop that method for using as a simple magneto-optical switch for laser radiation. The key requirements of the modified method consist in 1) using an open (non-cyclic) dipole transition, 2) a vapour cell filled with alkali work atoms and buffer gas or a cell with anti-relaxation coating of the walls, 3) high concentration of work atoms (e.g. $F=1 \rightarrow F'=1$ transition in D_1 line of ^{87}Rb with vapour density $\sim 5 \times 10^{11} \text{ cm}^{-3}$). These conditions can provide the best contrast (close to 100 %) and narrow width (< 1 kHz) of the resonance. The switch works as follows. Absorption of the probe beam is monitored as a function of the dc magnetic field B , applied along the wave vectors. As the conditions are satisfied, the probe-beam transmittance almost equals zero (< 0.5 %) in the vicinity of $B=0$. Otherwise, when $B \neq 0$, the probe transmittance is very close to 100 %. At that, the magnetic field B can be as low as just several mG for effective control of the probe transmittance. This implies a device that can be low-power and compact, high-sensitive and easy to control.

The new scheme for observing magneto-optical EIA signals can be applied also in laser physics, optical communications and magnetometry.

This work was partially supported by RFBR (15-02-08377, 15-32-20330, 14-02-00712, 14-02-00939, 14-02-00680, 13-02-00283), Ministry of Education and Science of Russian Federation (gov. order no. 2014/139, project no. 825), Presidium of the Siberian Branch of Russian Academy of Sciences and by Russian Presidential Grants (MK-4680.2014.2 and NSh-4096.2014.2). M. Yu. Basalaev was also supported by the Dynasty Foundation.

References

- [1] G. Alzetta *et al.* Nuovo Cimento B **36**, 5-20 (1976)
- [2] E. Arimondo and G. Orriols Lett. Nuovo Cimento **17**, 333-338 (1976)
- [3] A.M. Akulshin, S. Barreiro and A. Lezama Phys. Rev. A **57**, 2996-3002 (1998)
- [4] Y. Dancheva *et al.* Opt. Commun. **178**, 103-110 (2000)
- [5] D.V. Brazhnikov *et al.* J. Exp. Theor. Phys. Lett. **91**, 625-629 (2010)
- [6] D.V. Brazhnikov *et al.* Eur. Phys. J. D **63**, 315-325 (2011)

High resolution spectroscopy of Cs atomic layers of nanometric and micrometric thickness

C. Andreeva¹, A. Krasteva¹, S. Cartaleva¹, A. Sargsyan², D. Sarkisyan², and K. Nasyrov³

¹*Institute of Electronics, Bulgarian Academy of Sciences, Sofia*

²*Institute for Physical Research, Academy of Sciences of Armenia, Ashtarak*

³*Institute of Automation and Electrometry, Russian Academy of Sciences, Novosibirsk*

Presenting Author: christina_andreeva@yahoo.com

The miniaturization of practical devices based on alkali atomic vapor confined in optical cells is of rising interest for development of photonic sensors. In this communication we present high resolution laser spectroscopy of Cs vapor confined in a unique optical cell with nanometric thickness (NTC) [1], where a strong spatial anisotropy is present for the time of interaction between the atoms and the laser radiation.

Extremely narrow velocity selective optical pumping (VSOP) resonances (~ 12 MHz) in the absorption and fluorescence profiles of the open optical transitions are demonstrated. The improved experimental system as compared to the used in [2] made possible the registration of a resonance in the fluorescence also of the closed transition.

A theoretical simulation is performed to analyze the physical processes behind the sub-doppler width (SDW) resonance sign reversal for the closed atomic transitions. The model involves elastic interactions between Cs atoms as well as elastic interaction of atom-cell windows, both resulting in depolarization of the excited state, which can lead to the new experimental observations.

We show that a small increase in the NTC thickness (from $L = \lambda$ to $L = 6\lambda$) allows reduction of light intensity and atomic source temperature needed for the narrow resonance formation, as can be seen in Fig.1.

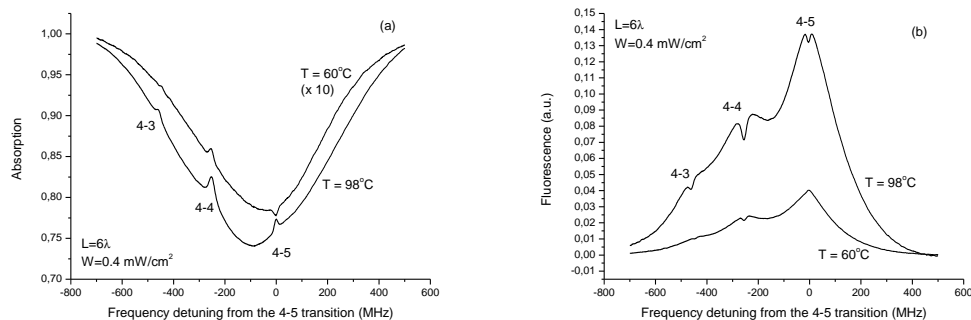


Figure 1: Transmission (a) and fluorescence (b) spectra at the $F_g = 4$ set of transitions, observed in the NTC with $L = 6\lambda$. For higher atomic concentration a narrow dip in the fluorescence occurs at the closed $F_g = 4 \rightarrow F_e = 5$ transition.

This makes it advantageous to use the narrow dips in the fluorescence profiles as frequency references for precise and significantly simplified stabilization of laser frequency, as well as for magnetometers with nanometric local spatial resolution and tunable atomic frequency references [3,4].

This work was partially supported by a Marie Curie International Research Staff Exchange Scheme Fellowship within the 7th European Community Framework Programme: “Coherent optics sensors for medical applications-COSMA” (Grant Agreement No: PIRSES-GA-2012-295264) and in the scope of the International Associated Laboratory IRMAS (CNRS-France & SCS-Armenia).

References

- [1] D. Sarkisyan *et al.* Opt. Commun. **200** 201 (2001)
- [2] C. Andreeva *et al.* Phys. Rev. A **76** 013837 (2007)
- [3] A. Sargsyan *et al.* Appl. Phys. Lett **93** 021119 (2007)
- [4] G. Hakhumyan *et al.* Opt. Commun **284** 4007 (2011)

Identifications of EUV transitions in promethium-like Pt, Ir, Os, and Re

H. Bekker¹, O. O. Versolato², A. Windberger¹, R. Schupp¹, P. O. Schmidt^{2,3}, J. Ullrich², and J. R. Crespo López-Urrutia¹

¹*Max-Planck-Institut für Kernphysik, Heidelberg, Germany*

²*Physikalisch-Technische Bundesanstalt, Braunschweig, Germany*

³*Institut für Quantenoptik, Leibniz Universität, Hannover, Germany*

Presenting Author: bekker@mpi-hd.mpg.de

Recent proposals to use highly charged ions (HCI) in next generation frequency standards, and for measurements of the variation of constants [1,2], has increased the need to understand the electronic structure of these ions. Specifically HCI near level crossings are of high interest, because they feature electric dipole transitions in the extreme ultra-violet (EUV) and optical regime, suitable for precision laser spectroscopy.

The existence of strong $5s - 5p$ EUV transitions in promethium(Pm)-like systems, which are near the $4f - 4s$ level crossing, was already predicted by Curtis and Ellis in 1980 [3]. Experimental observation of these transitions was never definitively confirmed due to the complexity of the spectra and deviations at the 1 %-level from atomic theory predictions.

We have experimentally investigated Pm-like Pt, Ir, Os, and Re ions to gain a better understanding of the electronic structure of these HCI [4]. The ions were produced and stored in an electron beam ion trap (EBIT) where the ions were excited through electron impact, the EUV fluorescence spectra were obtained using a grazing incidence flat-field spectrometer. The near mono-energetic electron beam of the EBIT ensured a well-defined charge state distribution, so that emission lines from different charge states could be separated. The resulting spectra were compared to synthetic spectra which were obtained using a collisional radiative model.

In this manner a number of characteristic transitions could be identified, and their wavelengths could be determined at the 50 ppm level. Even some of the $5s - 5p$ transitions, which appeared very weak in both observed and synthetic spectra, could be identified. Comparison to several state of the art calculations still shows deviations of up to 1 %, signaling the need for alternative, or new techniques in calculating the electronic structure of these complex HCI.

References

- [1] J. C. Berengut *et al.*, 2011 Phys. Rev. Lett. 106 210802
- [2] U. I. Safronova, V. V. Flambaum, M. S. Safronova, arXiv:1505.01019
- [3] L. J. Curtis and D. G. Ellis, 1980 Phys. Rev. Lett. 45 2099
- [4] H. Bekker *et al.* 2015 J. Phys. B: At. Mol. Opt. Phys. *in press*

Identifications of optical transitions in Ir¹⁷⁺ for investigations of variations of fundamental constants

A. Windberger¹, O. O. Versolato², H. Bekker¹, P. O. Schmidt^{2,3}, J. Ullrich², and
J. R. Crespo López-Urrutia¹

¹Max-Planck-Institut für Kernphysik, Heidelberg, Germany

²Physikalisch-Technische Bundesanstalt, Braunschweig, Germany

³Institut für Quantenoptik, Leibniz Universität, Hannover, Germany

Presenting Author: bekker@mpi-hd.mpg.de

Optical transitions in various highly charged ions (HCI) have been proposed for the investigation of a possible variation of fundamental constants, and for use in next generation frequency standards [1-3]. The atypical abundance of optical transitions in these HCI is due to a near degeneracy of electronic configurations near a level crossing. Enhanced relativistic effects make Nd-like Ir¹⁷⁺, which is near the $4f - 4s$ level crossing, highly sensitive to variations of the fine-structure constant α . Calculations for the electronic structure of Ir¹⁷⁺ are difficult and not accurate enough for precision laser spectroscopy, due to the complex correlations between the electrons in the open $4f$ -shell. To resolve this issue, we measured a number of optical transitions in Ir¹⁷⁺ with a precision of up to 1 ppm [4].

The ions were produced and stored in an electron beam ion trap (EBIT), where the ions were excited by electron impact. The subsequent emission light was observed using a Czerny-Turner type spectrometer. The Zeeman splitting, caused by the 8.00 T field in the EBIT, could be resolved and exploited to identify a number of magnetic dipole transitions. To further our understanding of Ir¹⁷⁺ we investigated Nd-like W¹⁴⁺, Re¹⁵⁺, Os¹⁶⁺, and Pt¹⁸⁺ in a similar manner. The identified transitions followed the predicted dependence on the atomic numbers, thereby confirming our identifications. By extrapolating the found scaling we were able to infer the wavelengths of proposed frequency standards in Hf¹²⁺ and W¹⁴⁺ [3].

In the measured Ir¹⁷⁺ transitions a search for closed optical cycles (Ritz combinations) was made. This resulted in two mutually exclusive candidates for the sought after transitions with highest sensitivity to α -variation. Recently performed improved measurements of these lines should establish which of the found cycles is correct, and thereby determine the energy splitting between the involved configurations.

References

- [1] J. C. Berengut *et al.*, 2011 Phys. Rev. Lett. 106, 210802
- [2] M. S. Safronova *et al.*, 2014 Phys. Rev. A 90, 042513
- [3] V.A. Dzuba, A. Derevianko, V.V. Flambaum, 2012 Phys. Rev. A 86, 054501
- [4] A. Windberger *et al.* 2015, Phys. Rev. Lett. 114, 150801

The $(2)^1\Pi$ state in KCs: Fourier-transform spectroscopy and potential construction

I. Birzniece¹, O. Nikolayeva¹, M. Tamanis¹, and R. Ferber¹

¹Laser Center, Department of Physics, University of Latvia, 19 Rainis blvd., LV-1586, Riga

Presenting Author: inese.birzniece@gmail.com

Spectroscopic information on the mixed excited states of heteronuclear alkali diatomics is of particular interest because of their application as an intermediate state for producing molecules in cold and ultracold conditions, preferably in the lowest $X^1\Sigma^+$ rovibronic state. The ultracold KCs molecules have not been produced yet, but optical schemes for its production are proposed in [1,2]. A different scheme which involves photoassociation via the mixed $(2)^1\Pi$ and $(2)^3\Pi$ states was used in [3] for RbCs. In present study we report on the first spectroscopic data and construction of the pointwise potential energy curve (PEC) for the $(2)^1\Pi$ state of KCs [4].

Similar to our previous KCs experiments [5,6], we recorded the back-scattered laser induced fluorescence (LIF) by Fourier-transform spectrometer Bruker IFS-125HR at a resolution of 0.03 cm^{-1} . KCs molecules were produced in a linear heat-pipe, filled with 10g of K and 7g of Cs, at about 300 °C temperature. For excitation we used the laser diodes (658 nm and 685 nm) and a Coherent CR 699 ring dye laser (Rh6G and DCM dyes). A Hamamatsu R928 photomultiplier was employed as a detector. The uncertainty of the line positions was estimated as 0.003 cm^{-1} .

From 180 recorded LIF spectra we obtained 2121 term values of e and f parity rovibronic levels. The assignment of quantum numbers v'' , J'' and J' for each LIF progression was based on the accurate ground state PEC [7]. The data set included vibrational $v' \in [0, 28]$ and rotational $J' \in [7, 274]$ levels. The experimental uncertainty of the term energy was estimated as 0.01 cm^{-1} . For systematically over J' data within $v' \in [0, 10]$ it was possible to determine the Λ -doubling constant, or q -factor. For $v' \in [0, 6]$ and $J' > 50$ the obtained q -factor values have not revealed significant perturbations. Therefore we averaged these values to $\bar{q} = (1.8 \pm 0.1) \times 10^{-6}\text{ cm}^{-1}$, being in excellent agreement with the $q = 1.84 \times 10^{-6}\text{ cm}^{-1}$ value calculated in [8].

The $(2)^1\Pi$ state PEC of KCs was constructed using the Inverted Perturbation Approach. The empirical PEC consists of 29 grid points in the internuclear distance range from 3.6 to 8.6 Å and describes the 67% of its well depth. The standard deviation (std) of the fit is 0.5 cm^{-1} , while for $v' \in [0, 7]$ the std is 0.008 cm^{-1} . The presented PEC obtained in one-state model can be used as the first step in further analysis of this state, which would require a more detailed spectroscopic information also on perturbing $(3)^3\Sigma^+$ and $(2)^3\Pi$ states.

The support from the Latvian Science Council Grant No. 119/2012 as well as from Latvian Ministry of Education and Science Grant No. 11-13/IZM14-12 is gratefully acknowledged.

References

- [1] H. J. Patel *et al.* Phys. Rev. A **90** 032716 (2014)
- [2] D. Borsalino *et al.* arXiv:1501.06276v2 (2015)
- [3] Z. Ji *et al.* Phys. Rev. A **85** 013401 (2012)
- [4] I. Birzniece *et al.* J. Chem. Phys. **142** 134309 (2015)
- [5] A. Kruzins *et al.* Phys. Rev. A **81** 042509 (2010)
- [6] I. Birzniece *et al.* J. Chem. Phys. **136** 064304 (2012)
- [7] R. Ferber *et al.* Phys. Rev. A **80** 062501 (2009)
- [8] J. T. Kim, Y. Lee, and A. V. Stolaryov J. Mol. Spectrosc. **256** 57-67 (2009)

Towards atomic anion laser cooling

G. Cerchiari¹, E. Jordan¹, and A. Kellerbauer¹

¹*Max-Planck-Institut für Kernphysik, Heidelberg*

Presenting Author: giovanni.cerchiari@mpi-hd.mpg.de

Laser cooling is an established technique used to create positive or neutral ensembles at sub-kelvin temperatures. This result has not yet been achieved for negative ions. We conduct experiments on the few atomic anions in which a strong electric-dipole transition has been predicted. Most atomic anions show only few, if any, bound excited states, strongly reducing the number of species theoretically suitable for laser cooling [1]. In addition to gathering information on these particular atomic species, our research pursues an appealing technique to cool any negative-ion species by sympathetic cooling in a shared trapping volume [2].

Starting from the preliminary results of other groups [3] we performed high-precision spectroscopic studies on Os^- and La^- [4,5]. We measured the transitions frequencies with vastly improved precision to address fundamental questions about hyperfine structure, cross-sections and the Zeeman effect, all with a view to laser cooling an atomic species in a Penning or a Paul trap. Our results indicate La^- as a promising candidate.

Currently we are modifying our apparatus to attempt the laser cooling of an ensemble of La^- ions in a linear Paul trap. In this talk, the spectroscopy results will be presented and an outlook on the cooling technique will be given.

References

- [1] O'Malley S. M. and Beck D. R., Phys. Rev. A **81** 032503 (2010)
- [2] Kellerbauer A. and Walz J., New J. Phys. **8** 45 (2006)
- [3] Walter C. W. et al., Phys. Rev. Lett. **113** 063001 (2014)
- [4] Warring U. et al., Phys. Rev. Lett. **102** 043001 (2009)
- [5] Kellerbauer A. Cerchiari G. Jordan E., Phys. Scr. **90** 054014 (2015)

The effect of the isomeric state ^{229m}Th on the observed hyperfine structure pattern

J. Dembczyński¹, M. Elantkowska², and J. Ruczkowski¹

¹*Institute of Control and Information Engineering, Faculty of Electrical Engineering, Poznań University of Technology, Piotrowo 3A, 60-965 Poznań, Poland*

²*Laboratory of Quantum Engineering and Metrology, Faculty of Technical Physics, Poznań University of Technology, Piotrowo 3, 60-965 Poznań, Poland*

Presenting Author: Jerzy.Dembczynski@put.poznan.pl

The study of the structure of ^{229}Th isotope is interesting both from the point of view of nuclear physics as well as its application to frequency standard, because the first excited isomeric state of the ^{229}Th nucleus exhibits the lowest known nuclear excitation energy which is about 8 eV.

The verification of the existence and determination of the energy of a low lying isomeric state can be easily done by a systematic study of the hyperfine structure for electronic levels of the ^{229}Th atom or ions by means of the LIF method in a Paul trap, in hollow cathode or on atomic beam.

The effects of the mixing of the wave functions for ground and isomeric nuclear states should be observed in the hyperfine structure patterns of spectral lines.

As an example we present the simulation for the transition $34543.556\text{ cm}^{-1} \rightarrow 17121.620\text{ cm}^{-1}$. The values of the hyperfine constants were taken from the paper of Kälber *et al.* [1]. The corresponding values for the isomeric state were calculated using the values of nuclear moments μ and Q equal $0.45\ \mu_N$ [2], 3.11 b [3] and $-0.08\ \mu_N$ [4], 1.74 b [4], for the ground and the isomeric nuclear states respectively. The same occupancy of the ground and isomeric states was assumed. The solid lines show the intensities of the line components, for the ground nuclear state, for the transitions $F' = 0 \rightarrow F = 1$ at the beginning to $F' = 5 \rightarrow F = 4$ at the end of x-axis. For the isomeric state, the dashed lines illustrate the line components for transitions $F' = 0 \rightarrow F = 1$ and $F' = 3 \rightarrow F = 4$, respectively.

Depending on the line width observed in the experiment, the existence of the isomeric state will be revealed in the middle of the hyperfine structure pattern as broadening and distortion of the line components or as additional line components. Therefore the hyperfine structure constants derived from the observed spectral line shape will differ from those determined in the absence of nuclear isomeric state admixture.

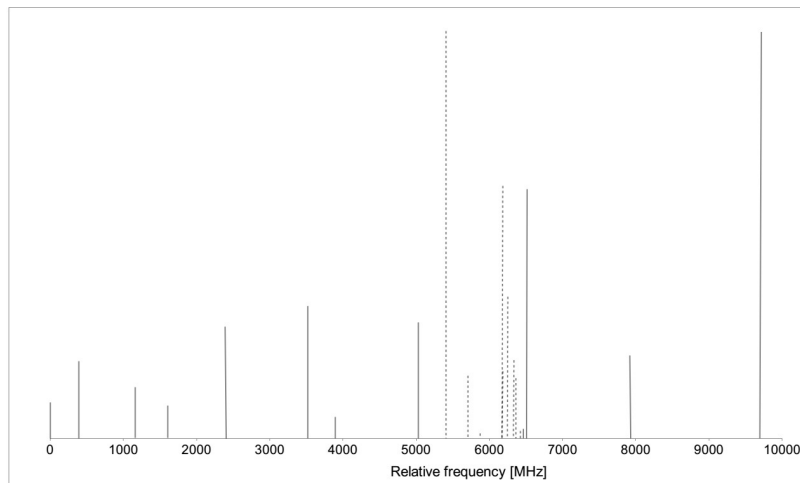


Figure 1: Simulation of the line structure for the transition $34543.556\text{ cm}^{-1} \rightarrow 17121.620\text{ cm}^{-1}$.

This work was supported by Poznań University of Technology within the project 04/45/DSPB/0135

References

- [1] W. Kälber *et al.* Z. Phys. A **334**, 103–108 (1989)
- [2] S. Gerstenkorn *et al.* J. Phys. **35**, 483–495 (1974)
- [3] C. J. Campbell, A. G. Radnaev, A. Kuzmich Phys. Rev. Lett. **106**, 223001 (2011)
- [4] E. V. Tkalya Phys. Rev. Lett. **106**, 162501 (2011)

Depletion spectroscopy and internal-state thermometry of buffer-gas-cooled polar molecules

T. Gantner¹, X. Wu¹, S. Chervenkov¹, M. Zeppenfeld¹, and G. Rempe¹

¹Max-Planck-Institute of Quantum Optics, Hans-Kopfermann-Str. 1, 85748 Garching, Germany

Presenting Author: thomas.gantner@mpq.mpg.de

We present a general technique for probing the internal-state distribution of electrically guided polar molecules [1]. Bright beams of buffer-gas cooled [2] molecules are guided by an electrostatic quadrupole guide and brought to a region with homogenous electric field. Here, a radio frequency field pumps molecules in a specific rotational state from guidable to non-guidable sublevels. Another bent piece of a quadrupole guide through a differential pumping section ensures that only molecules remaining in guidable states are detected by a quadrupole mass spectrometer. The population of the different rotational states can be derived from the depletion signal. This enables us to estimate the rotational temperature of the guided molecules.

Using this technique, we characterize our buffer-gas cell for different molecules, e.g. CH_3F , CF_3CCH ,... and for different regimes, effusive and hydrodynamic. As the scheme is extremely simple to implement in experiments using beams of guided molecules, we expect it to be well-suited for characterization in future experiments, e.g., with a centrifuge decelerator [3].

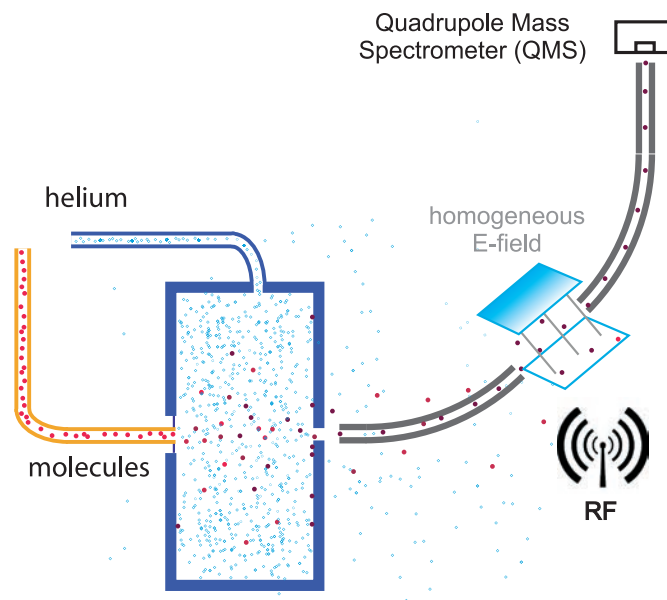


Figure 1: RF spectroscopy setup

References

- [1] S.A. Rangwala *et al.* Phys. Rev. A **67**, 043406 (2003)
- [2] L.D. van Buuren, *et al.* Phys. Rev. Lett. **102**, 033001 (2009)
- [3] S. Chervenkov, *et al.* Phys. Rev. Lett. **112**, 013001 (2014)

The Rayleigh and Raman scattering of light on metastable levels of diatomics: An advanced method and new data

A. Glushkov¹, O. Khetselius¹, A. Kvasikova¹, and E. Ponomarenko¹

¹Odessa State University - OSENU, Odessa

Presenting Author: dirac13@mail.ru

Laser action on molecules leads to different non-linear processes, including multi-photon ionization, excitation and dissociation, Raman scattering. The elementary two-photon processes are linear coherent and combinational scattering. The intensities and polarization of lines in these spectra are defined by polarizability and derivative on inter-nuclear distance. In this paper we study processes of the Rayleigh and Raman vibration scattering of a light on metastable levels of molecules (H₂, HD, D₂, Li₂, Rb₂, Cs₂, Fr₂). On the example of polarizability of metastable molecules it has been quantitatively studied an effect of nuclear motion in processes of the second order of the perturbation theory. An advanced numerical method for construction of the Green's functions for optical electrons and electron wave functions is developed within the model potential approach in the spheroid coordinates system that allows to take into account non-spherical character of molecular field. We have carried out computing an electron transition moment dependence upon the internuclear distance, molecular polarizability, its derivative on inter-nuclear distance, depolarization degree during the Rayleigh and Raman light scattering on the frequencies of the Rb, Nd lasers. Analysis of results of the calculation of a polarizability, its derivative on inter-nuclear distance, for excited triple metastable c_{3n}, states of the H₂, HD, D₂ molecules on the frequencies of the Rb (1,78eV) and Nd (1,18eV) lasers shows that the main contribution into polarization of the cited metastable molecules is provided by changing the electron shell under action of the external electromagnetic field. An influence of the nuclear motion effect has been also studied and found to be quite little. It is in a good agreement with simplified models estimates [3]. Relativistic generalization of proposed approach is carried out on the basis of many-body relativistic perturbation theory with account of the polarization and nuclear motion effects and generalized dynamical nuclear model with using the optimized one-quasiparticle representation [1,2].

References

- [1] A. Glushkov O. Khetselius, S. Malinovskaya *Frontiers in Quantum Systems in Chemistry and Physics Ser.: Progress in Theoretical Chemistry and Physics*, Eds. S. Wilson et al (Springer, Berlin, 2008) **18**, 523-545; A.V. Glushkov, O.Yu. Khetselius, A.A.Svinarenko, G.P. Prepelitsa *Coherence and Ultrashort Pulsed Emission*, Eds. F. Duarte (InTech, Vienna, 2011), 159-186
- [2] A. Glushkov et al. *Int. J. Quant. Chem.* **99**, 879–895 (2004); **99**, 936–940(2004); **109**, 3325–3329 (2009); A. Glushkov, O.Yu. Khetselius, L. Lovett *Frontiers in Quantum Systems in Chemistry and Physics Ser.: Progress in Theoretical Chemistry and Physics*, Eds. P. Peacuch et al (Springer, Berlin, 2009) **20**, 125-152
- [3] V. Davydkin, L.Rapoport *Sov.J.Quant.Electr.* **4**, 1123–1127 (1975); A. Glushkov *Opt. Spectr.* **66**, 1298–1301 (1989); *J. Phys. Chem.* **63**, 3072–3075 (1989)

Absolute absorption and dispersion in dense alkali-metal thermal vapours

I. G. Hughes¹, C. S. Adams¹, E. Bimbard¹, J. Keaveney¹, D. J. Whiting¹, M. A. Zentile¹, A. Sargsyan², and D. Sarkisyan²

¹Joint Quantum Centre Durham-Newcastle, Durham University Physics Department, Durham, UK

²Institute for Physical Research, National Academy of Sciences, Ashtarak-2 0203, Armenia

Presenting Author: i.g.hughes@durham.ac.uk

Many of the work-horse techniques of contemporary atomic physics experiments were first demonstrated in hot vapours. These media are ideally suited for quantum-optics experiments as they combine (I) a large resonant optical depth; (II) long coherence times; (III) well-understood atom-atom interactions. These features aid with the simplicity of both the experimental set up and the theoretical framework.

We have studied experimentally and theoretically the absorption and dispersion of alkali-metal atomic vapours [1-3]. Our model includes the effects of dipole-dipole interactions [4] and calculates the absolute susceptibility that enables quantitative predictions in the vicinity of the D lines. The model was a crucial component in our experimental measurement of the cooperative Lamb shift [5], the first measurement of this phenomenon, 40 years after its prediction. In a related experiment we measured the refractive index of high-density Rb vapour in a gaseous atomic nanolayer, thereby answering the question of what is the theoretical maximum refractive index of an atomic vapour [6]. We will present ideas and preliminary data of how to generate heralded single photons with a dense thermal ensemble.

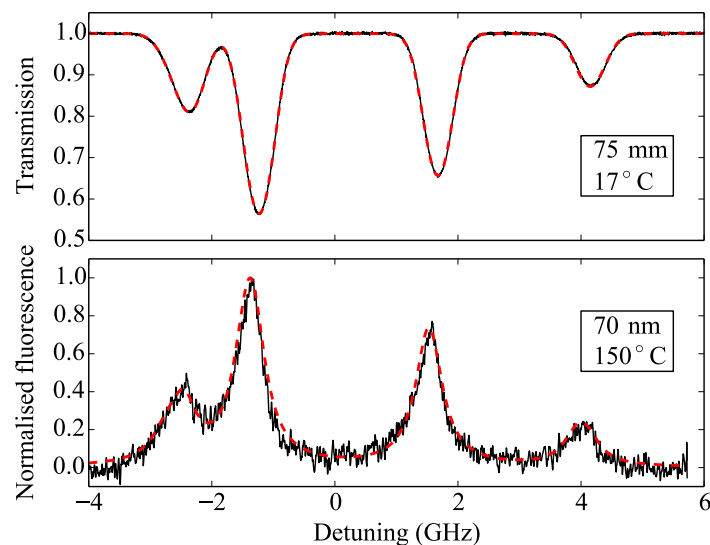


Figure 1: Experimental absorption (upper) and fluorescence (lower) spectra with theoretical models (red) taken on the Rb D2 line in cells differing in length by a factor of 10^6 .

References

- [1] P. Siddons *et al.* J. Phys. B **41** 155004 (2008)
- [2] P. Siddons *et al.* Nature Photonics **3** 225–229 (2009)
- [3] M. A. Zentile *et al.* Comp. Phys. Commun. **189** 162–174 (2015)
- [4] L. Weller *et al.* J. Phys. B **44** 195006 (2011)
- [5] J. Keaveney *et al.* Phys. Rev. Lett. **108** 173601 (2012)
- [6] J. Keaveney *et al.* Phys. Rev. Lett. **109** 233001 (2012)

Strontium optical lattice clocks

J. Lodewyck¹, J.-L. Robyr¹, S. Bilicki¹, E. Bookjans¹, and R. Le Targat¹

¹LNE-SYRTE, Observatoire de Paris, PSL Research University, CNRS, Sorbonne Universités, UPMC Univ. Paris 06, 61 avenue de l'Observatoire, 75014 Paris, France

Presenting Author: jerome.lodewyck@obspm.fr

Thanks to their large quality factor and the large number of simultaneously interrogated atoms, optical lattice clocks beat frequency stability and accuracy records [1–3].

Here, we propose the demonstration of a set of two operational lattice clocks using strontium atoms. They feature an uncertainty budget below 5×10^{-17} , mainly limited by the black-body radiation shift, and a frequency stability of 1.0×10^{-15} , after a 1 s integration time. The second clock has been operated during a full week, as part of the EMRP-funded project “International Timescales with Optical Clocks” (ITOC), with minimal human intervention. During this period, the clock, linked to a fiber-based frequency comb, provided integration points every second with an uptime larger than 93%. These developments are essential steps towards international comparisons of optical clocks, either by fiber links or via the PHARAO/ACES space clock project.

During this measurement campaign, the Sr clock has been compared to Cs and Rb microwave fountains, providing frequency ratio measurements with a statistical resolution below 10^{-16} , and an improved overall uncertainty over our previous measurement [4]. Moreover, these ratio measurements agree within the error bars with the results published in [4], reinforcing our confidence in the reproducibility of optical lattice clocks. Furthermore, these results bring improved constraints on a possible drift of fundamental constants.

Finally, we take profit from the reliability of the clock to investigate a pending issue that could have compromised the ultimate performances of OLCs. We propose a study of lattice induced effects by comparing various laser sources for the optical lattice: Semi-conductor tapered amplifiers, slaves lasers and a titanium-sapphire laser. We show that careful characterization of the light is necessary to ensure ultimate accuracy.

The EMRP is jointly funded by the EMRP participating countries within EURAMET and the European Union.

References

- [1] T.L. Nicholson *et al.* Nat. Commun. **6** 6896 (2015)
- [2] N. Hinkley *et al.* Science **341**, 1215 (2013)
- [3] I. Ushijima *et al.* Nature Photonics **9** 185 (2015)
- [4] R. Le Targat *et al.* Nat. Comm. **4**, 2109 (2013)

Study of $(3)^1\Pi$ and $(5)^1\Sigma^+$ states of RbCs based on $(3)^1\Pi \rightarrow (A - b)$ and $(5)^1\Sigma^+ \rightarrow (A - b)$ Fourier transform spectra analysis

K. Alps¹, A. Kruzins¹, O. Nikolayeva¹, M. Tamanis¹, R. Ferber¹, A. V. Stolyarov², and E. A. Pazyuk²

¹Laser Centre, Department of Physics, University of Latvia, 19 Rainis blvd., LV-1586, Riga,

²Department of Chemistry, Moscow State University, 119991, Moscow, Leninskie gory 1/3, Russia

Presenting Author: artis.kruzins@fizmat.lv

Recently observation and analysis of laser induced fluorescence (LIF) spectra to the $A^1\Sigma^+$ and $b^3\Pi$ states ($A - b$ complex for short) from $(3)^1\Pi$, $(4)^1\Sigma^+$ and $(5)^1\Sigma^+$ states in RbCs was reported [1]. It was shown that high accuracy of the $A - b$ complex description based on coupled-channels deperturbation treatment achieved in [1], allowed us to use the latter as an alternative to the ground state for the purpose to assign the observed $(3)^1\Pi \rightarrow A - b$ and $(5)^1\Sigma^+ \rightarrow A - b$ transitions and to determine the term values of the upper states with experimental accuracy 0.01 cm^{-1} . We report here of a continuation of the study of the $(3)^1\Pi$ and $(5)^1\Sigma^+$ states in RbCs. These states were first observed by REMPI method and partly described in [2, 3]. The aim of the present work was to obtain systematic term values data for the rovibronic levels and to construct the respective adiabatic potential energy curves.

In the experiment RbCs molecules were produced in a linear heat pipe at $310 \text{ }^\circ\text{C}$. The radiation of a single mode laser (CR 699-21) with Rhodamine 6G dye excited transitions from the ground state to the $(3)^1\Pi$ and $(5)^1\Sigma^+$ states. The LIF spectra to the $A - b$ complex were recorded by Fourier transform spectrometer (IFS 125-HR, Bruker) in the $6000\text{-}10000 \text{ cm}^{-1}$ spectral range. Excitation frequencies were selected within the range $16900 - 17700 \text{ cm}^{-1}$ by monitoring the LIF signal in the Preview Mode of the spectrometer. The recorded spectra contained also the $(4)^1\Sigma^+ \rightarrow A - b$ transitions excited accidentally by the same laser frequency. These transitions could be used as a test of assignment procedure, since the $(4)^1\Sigma^+$ state is very accurately described in [4]. The assignment of the LIF progressions allowed us to determine the energy and the rotational quantum number J' of the rovibronic levels of the $(3)^1\Pi$ and $(5)^1\Sigma^+$ states. Vibrational numbering v' of these states was based on the data from [2,3]. In several spectra rotational relaxation lines were observed around strong lines of the main progression, thus increasing the amount of term values data. The obtained term values of the $(3)^1\Pi$ and $(5)^1\Sigma^+$ states were included in the single potential fit using the Inverted Perturbation Approach to construct the point wise potentials.

The support from the Latvian Science Council Grant No. 119/2012 is gratefully acknowledged by Riga team and RFBR grant No. 13-03-00446-a by Moscow team.

References

- [1] A. Kruzins *et al.* J. Chem. Phys. **141**, 184309 (2014)
- [2] B. Kim and K. Yoshihara J. Chem. Phys. **100**, 1849 (1994)
- [3] Y. Yoon *et al.* J. Chem. Phys. **114**, 8926 (2001)
- [4] V. Zutters *et al.* Phys. Rev. A **87**, 022504 (2013)

Fourier transform spectroscopy and deperturbation analysis of the spin-orbit coupled $A^1\Sigma^+$ and $b^3\Pi$ states in RbCs

A. Kruzins¹, K. Alps¹, O. Docenko¹, I. Klincare¹, M. Tamanis¹, R. Ferber¹, E. A. Pazyuk², and A. V. Stolyarov²

¹Laser Centre, Department of Physics, University of Latvia, 19 Rainis blvd., LV-1586, Riga, Latvia

²Department of Chemistry, Moscow State University, 119991, Moscow, Leninskie gory 1/3, Russia

Presenting Author: artis.kruzins@fizmat.lv

We present an extended study of the strongly spin-orbit coupled singlet $A^1\Sigma^+$ and triplet $b^3\Pi$ states ($A - b$ complex for short) of the RbCs molecule, which provide an efficient optical path to transfer ultracold molecules to their rovibrational ground state, as demonstrated in [1]. Earlier several Fourier-transform (FT) studies were performed to obtain the term values of the $A - b$ complex in RbCs, and to describe this complicated system by deperturbation model based on four $A^1\Sigma^+ - b^3\Pi_{\Omega=0,1,2}$ coupled-channel (CC) approach [2,3]. However the achieved description of data have not reached the experimental accuracy. The goal of the present work was to obtain systematic term values data in the extended range of energy and quantum numbers of rovibronic levels, and to perform the CC deperturbation analysis allowing to reproduce the data with experimental accuracy. In the experiment the $A - b \rightarrow X$ and $(4)^1\Sigma^+ \rightarrow A - b$ laser induced fluorescence (LIF) FT spectra were recorded. RbCs molecules were produced in a heat pipe at 310 °C. A number of diode lasers covering the wavelength range from 830 nm to 1050 nm were used to excite directly the $A - b$ complex. In a different scheme, a single mode dye laser (Coherent 699-21) was used to excite the $(4)^1\Sigma^+$ state with subsequent observation of LIF signal to the $A - b$ complex. The latter scheme allowed us to observe "dark" levels of the triplet $b^3\Pi$ state far below the minimum of the singlet A state. Overall 8730 rovibronic term values of $A^1\Sigma^+$ and $b^3\Pi$ states of $^{85}\text{Rb}^{133}\text{Cs}$ and $^{87}\text{Rb}^{133}\text{Cs}$ isotopologues were determined with an uncertainty of 0.01 cm^{-1} in the energy range [9012, 14087] covering rotational quantum numbers $J \in [6, 324]$.

An energy-based deperturbation analysis performed in the framework of the four $A^1\Sigma^+ - b^3\Pi_{\Omega=0,1,2}$ coupled-channels approach reproduces 97% experimental term values of both isotopologues with a standard deviation of 0.0036 cm^{-1} . The reliability of the deperturbed mass-invariant potentials and spin-orbit coupling functions of the interacting $A^1\Sigma^+$ and $b^3\Pi$ states is additionally proved by a good reproduction of the $A - b \rightarrow X$ and $(4)^1\Sigma^+ \rightarrow A - b$ relative intensity distributions.

The support from the Latvian Science Council Grant No. 119/2012 is gratefully acknowledged by Riga team and RFBR grant No. 13-03-00446-a by Moscow team.

References

- [1] T. Takekoshi *et al.* Phys. Rev. Lett. **113**, 205301 (2014)
- [2] T. Bergeman *et al.* Phys. Rev. A **67**, 050501 (2003)
- [3] O. Docenko *et al.* Phys. Rev. A **81**, 042511 (2010)
- [4] A. Kruzins *et al.* J. Chem. Phys. **141**, 184309 (2014)

Alkali atoms in a strong transverse magnetic field: “guiding” transitions foretell behavior of all transitions of D_1 line

A. Papoyan¹, A. Sargsyan¹, G. Hakhumyan¹, and D. Sarkisyan¹

¹Institute for Physical Research, NAS of Armenia, Ashtarak-2, 0203, Armenia

Presenting Author: papoyan@ipr.sci.am

We report the existence of so-called “guiding” atomic transitions (GTs) in the system of transitions between magnetic sublevels of the hyperfine structure of D_1 lines of all alkali metal atoms in the case of linear (π) polarization. They allow predicting the probabilities of all atomic transitions in their group in strong transverse magnetic fields, as well as their frequency shifts with respect to magnetic field. In the case of the D_2 lines, GTs are absent. This effect was experimentally observed in rubidium vapor with the use of a half-wavelength cell ($\lambda/2$ -method) [1].

An experiment with a nanocell filled with Rb atomic vapor with a thickness of half the wavelength $L = \lambda/2 = 398$ nm for ensuring a sub-Doppler spectral resolution has completely confirmed the presence of guiding transitions shown in Fig.1. Two groups of six transitions for ^{85}Rb and two groups of four transitions for ^{87}Rb have been detected in the transmission spectra in magnetic fields above 4 kG. A guiding transition has been identified in each of four groups. Four transitions forbidden at $B = 0$ have been detected too; also their probabilities approach the probabilities of the guiding transitions with an increase in the magnetic field.

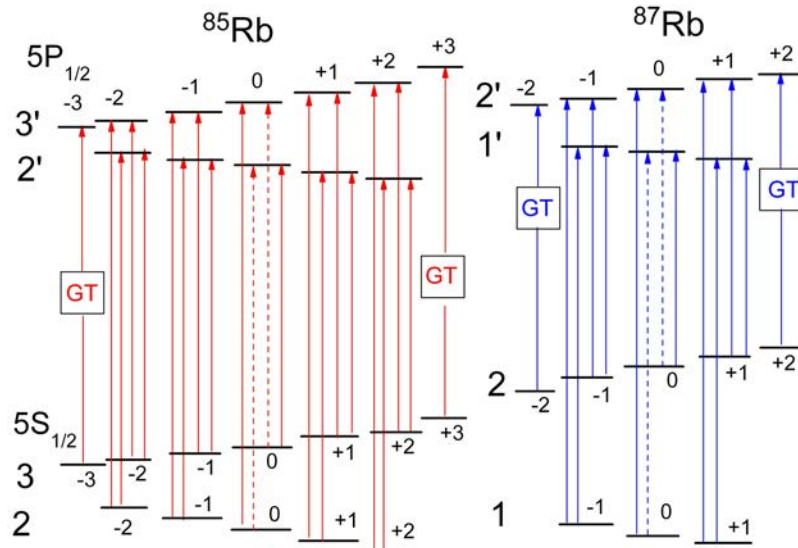


Figure 1: Diagram of the atomic transitions of D_1 line in ^{85}Rb (22 transitions) and in ^{87}Rb (14 transitions) in magnetic field $B \ll B_0$ ($B_0 = A_{hfs}/\mu_B \cong 0.7$ and 2 kG for ^{85}Rb and ^{87}Rb , respectively) in the case of π -polarized radiation ($\Delta F = 0, \pm 1$, $m_F = 0$, the dashed arrows indicate forbidden transitions). Squares mark GTs.

The good agreement of the experimentally measured spectra with the theoretical predictions proves that the $\lambda/2$ -method makes it possible to quantitatively trace the behavior of each individual atomic transition in the magnetic field. GTs exist for the D_1 lines of all alkali metal atoms.

References

- [1] A. Sargsyan, G. Akhumyan, A. Papoyan, D. Sarkisyan, JETP Lett. **101**, 303-307 (2015).

Selective reflection from dense Rb₂ molecular vapor

A. Papoyan¹, S. Shmavonyan¹, A. Khanbekyan¹, A. Gogyan¹, and M. Movsisyan¹

¹*Institute for Physical Research, NAS of Armenia, Ashtarak-2, 0203, Armenia*

Presenting Author: papoyan@ipr.sci.am

Selective reflection (SR) of light from an interface of a dielectric window and atomic vapor is known as a powerful spectroscopic tool for numerous applications [1]. Extension of this technique to molecular vapor is a challenge, mainly due to technical problems.

We report the first observation of SR from molecular vapor of Rb₂ dimers formed in all-sapphire sealed-off rubidium vapor cell at the temperature range of 455 – 515°C corresponding to number density of Rb₂ dimers $6.7 \times 10^{15} - 2.6 \times 10^{16} \text{ cm}^{-3}$. The selective reflection signals were recorded on various rovibronic components of $1(X)^1\Sigma_g^+ - 1(A)^1\Sigma_u^+$ bound-bound electronic transition of Rb₂ (left graph in Fig.1) by scanning a diode laser frequency in a spectral range of 851 – 854 nm ($11710 - 11750 \text{ cm}^{-1}$). Mainly selective reflection spectra corresponding to groups of several rovibronic transitions have been recorded, which is caused by high spectral density, large collisional broadening, and low oscillator strength of individual rovibronic transitions.

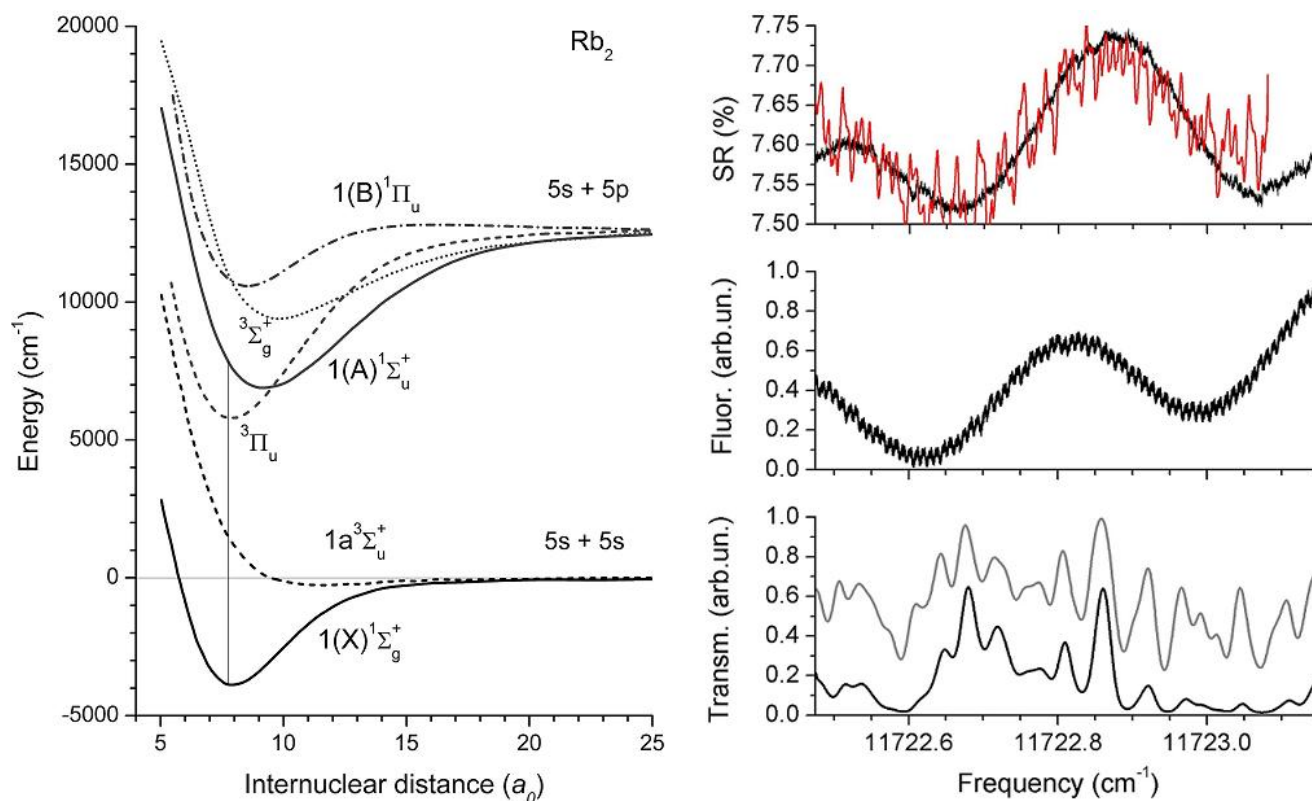


Figure 1: *Left:* Rb₂ potential curves for lower electronic states relevant for the present study. Vertical line indicates molecular electronic interstate transition with 852 nm wavelength. *Right:* Rb₂ selective reflection (upper graph) and fluorescence (middle graph) spectra recorded at $T = 461^\circ \text{C}$, $N_{\text{Rb}_2} = 9.3 \times 10^{15} \text{ cm}^{-3}$; transmission spectra (lower graph) recorded at $T = 310^\circ \text{C}$, $N_{\text{Rb}_2} = 7.0 \times 10^{13} \text{ cm}^{-3}$ (upper trace) and $T = 400^\circ \text{C}$, $N_{\text{Rb}_2} = 1.7 \times 10^{15} \text{ cm}^{-3}$ (lower trace). Colored noisy signal superimposed on measured SR spectrum presents the SR spectrum derived from fluorescence by data processing (see text).

We have proved that the recorded signals shall be attributed to selective reflection by careful alignment of the measurement setup, as well as by comparison of the experimentally recorded SR spectrum with the modeled one derived from the simultaneously measured fluorescence spectrum using Kramers-Kronig relation and Fresnel formula (right graph in Fig.1).

References

- [1] A. Badalyan *et al.*, Eur. Phys. J. D **37**, 157–162 (2006).

Precision isotope shift measurements of calcium ions using photon recoil spectroscopy

F. Gebert¹, Y. Wan¹, F. Wolf¹, J. C. Heip¹, J. Berengut², C. Shi¹, and P. O. Schmidt^{1,3}

¹*QUEST Institut, Physikalisch-Technische Bundesanstalt, Braunschweig, Germany*

²*School of Physics, University of New South Wales, Sydney, Australia*

³*Institut für Quantenoptik, Leibniz Universität Hannover, Germany*

Presenting Author: chunyan.shi@quantummetrology.de

Precision laser spectroscopy of trapped atoms is an important technique in fundamental physics. As a powerful tool, the laser induced fluorescence spectroscopy technique has been widely used. However, for non-closed broad transition, this technique is not well-suited. We present isotope shift measurements of the $^2D_{3/2} - ^2P_{1/2}$ and the $^2S_{1/2} - ^2P_{1/2}$ transitions in calcium ions by extending the photon recoil spectroscopy (PRS) technique to non-closed transition. In PRS, a spectroscopy ion is trapped and sympathetically cooled to the motional ground state by a co-trapped logic ion [1]. Photon recoil from absorption on the spectroscopy transition results in motional excitation, which is detected on the cooling ion using quantum logic techniques. In this way, we are able to detect around 10 scattered photons for the nearly-closed $^2S_{1/2} - ^2P_{1/2}$ transition of Ca^+ [2]. To achieve single-photon efficiency for the non-closed $^2D_{3/2} - ^2P_{1/2}$ transition, a new approach is employed, in which a single-photon repumping event is efficiently translated into the motion of the two ion crystal by amplifying the recoil from absorption of photons resonant with the $^2S_{1/2} - ^2P_{1/2}$ transition. The residual motional ground state population is then probed using a stimulated Raman adiabatic passage pulse driving a motional sideband on the cooling ion. Using the two techniques, we performed the first high precision absolute frequency measurement of the $^2D_{3/2} - ^2P_{1/2}$ and the $^2S_{1/2} - ^2P_{1/2}$ transitions for the isotopes $^{40}\text{Ca}^+$, $^{42}\text{Ca}^+$, $^{44}\text{Ca}^+$, $^{48}\text{Ca}^+$ with accuracy below 100 kHz [3]. Based on the precision isotope shift measurement we performed a multidimensional King's plot analysis and were able to significantly improve the uncertainty of changes in the mean square nuclear charge radii. Furthermore, we will present recent measurement results of the $^2S_{1/2} - ^2P_{3/2}$ transition in calcium ions.

References

- [1] Y. Wan *et al.* Phys. Rev. A **91**, 043425 (2015).
- [2] Y. Wan *et al.* Nat. Commun **5**, 4096 (2014).
- [3] F. Gebert *et al.* preprint arXiv:1504.03139 (2015).

**Energies and radiative properties
of the $A^1\Sigma^+ - b^3\Pi$ complex in KRb:
towards optimal ground-state transfer ultracold molecules**

K. Alps¹, A. Kruzins¹, M. Tamanis¹, R. Ferber¹, E. A. Pazyuk², and A. V. Stolyarov²

¹*Laser Center, Department of Physics, University of Latvia, 19 Rainis blvd., LV-1586, Riga*

²*Department of Chemistry, Lomonosov Moscow State University, 119991, Moscow, Leninskie gory 1/3,
Russia*

Presenting Author: avstol@phys.chem.msu.ru

Recently high resolution Fourier Transform (FT) spectroscopy and rigorous coupled-channel deperturbation analysis of the low-lying spin-orbit coupled $A^1\Sigma^+$ and $b^3\Pi$ states of KRb molecule have been performed [1]. The resulting mass-invariant deperturbed molecular parameters represent the termvalues of the $A - b$ complex of the different KRb isotopologues within accuracy of the measurements. A comparative study of the *ab initio* calculated $A^1\Sigma^+ - X^1\Sigma^+$ and $b^3\Pi - a^3\Sigma^+$ transition dipole moments demonstrate the remarkable agreement (with few percent) of the theoretical results obtained by the different quantum chemistry methods [2]. The highly accurate empirical adiabatic potential energy curves (PECs) for the ground singlet $X^1\Sigma^+$ and triplet $a^3\Sigma^+$ states of KRb up to their common dissociation limit became available as well [3]. This provides confidence that the energies and radiative properties of the KRb $A - b$ complex could be simulated at a high (close to experimental) level of accuracy in a wide range of the rovibronic excitation.

The goal of the present work is to perform a detailed theoretical analysis of the spectroscopic and radiative properties of KRb in order to identify the reasonable candidates for the stimulated Raman transitions between initial Feshbach resonance states (consist of the mutually mixed $X^1\Sigma^+$ and $a^3\Sigma^+$ levels due to hyperfine and magnetic external field perturbations), the spin-orbit coupled levels of the $A \sim b$ complex and absolute ground $X^1\Sigma^+$ ($v = 0, J = 0$) state [4]. We have used the brand new deperturbed molecular PECs, spin-orbit coupling functions and transition dipole moments to predict the rovibronic energies and radiative lifetimes of the $A - b$ complex along with transition probabilities from the complex to weakly bound levels of the both $X^1\Sigma^+$ and $a^3\Sigma^+$ states near dissociation threshold as well as absolute ground X -state. The calculated $A - b \rightarrow X$ spontaneous emission coefficients are in a good agreement with the relative intensity distributions measured for long laser-induced fluorescence progression on the well-bound levels of the X -state. The theoretical lifetime predicted for the metastable $b^3\Pi(v = 0)$ state $33.8 \mu\text{s}$ is remarkably close to its experimental counterpart [5]. The overall $A - b \leftrightarrow a$ transition probabilities are confirmed to be extremely weak due to the small $b - a$ transition moment [2,4]. At the same time the $A - b \leftrightarrow X$ transition probabilities from the highest vibrational levels of the X -state become comparable with the strength of the relevant transitions to the lowest $v_X = 0$ level of the ground X -state.

The support from the Latvian Science Council Grant No. 119/2012 as well as from Latvian Ministry of Education and Science Grant No. 11-13/IZM14-12 is gratefully acknowledged. Moscow team thanks for the support by the RFBR grant No. 13-03-00446a.

References

- [1] A. Kruzins *et al.* Abstracts of the EGAS47 (2015)
- [2] R. Beuc *et al.* J. Phys. B. **39**, S1191 (2006)
- [3] A. Pashov *et al.* Phys. Rev. A **76**, 022511 (2007)
- [4] D. Borsalino *et al.* Phys. Rev. A **90**, 033413 (2014)
- [5] J. Kobayashi *et al.* Phys. Rev. A **89**, 021401(R) (2014)

**Direct deperturbation analysis
of the $A^1\Sigma^+ \sim b^3\Pi$ complex in LiCs based on
polarization labelling spectroscopy
and *ab initio* calculation**

P. Kowalczyk¹, J. Szczepkowski², W. Jastrzebski², E. A. Pazyuk³, and A. V. Stoloyarov³

¹*Institute of Experimental Physics, Faculty of Physics, University of Warsaw, ul. Pasteura 5, 02-093
Warsaw, Poland*

²*Institute of Physics, Polish Academy of Sciences, Al. Lotników 32/46, 02-668 Warsaw, Poland*

³*Department of Chemistry, Lomonosov Moscow State University, 119991, Moscow, Leninskie gory 1/3,
Russia*

Presenting Author: avstol@phys.chem.msu.ru

For several years the mixed $A \sim b$ levels provided convenient windows to study the triplet manifold of excited states by perturbation-facilitated optical-optical double resonance transitions from the ground state of singlet symmetry $X^1\Sigma^+$ [1]. In more recent times the attention has been drawn to the fact that the same perturbation can facilitate transfer of ultracold molecules derived from Feshbach resonances to the absolute ground state (i.e. $v_X = 0$, $J_X = 0$) by a stimulated Raman process [2]. This motivates recent experimental efforts to characterize the $A \sim b$ complex in heavy (Rb and Cs) alkali atom molecules such as NaRb, NaCs, KCs, RbCs, Rb₂ or Cs₂.

The present analysis was undertaken to provide the rigorous coupled-channel (CC) deperturbation treatment of about 780 rovibronic term values of the strongly spin-orbit (SO) coupled $A^1\Sigma^+$ and $b^3\Pi$ states of the ⁷Li¹³³Cs molecule recorded by polarization labelling spectroscopy technique. The explicit $A^1\Sigma^+ \sim b^3\Pi_{\Omega=0,1,2}$ coupled-channels treatment allowed us to reproduce 95% experimental term values with a standard deviation of 0.05 cm⁻¹ which is close to the accuracy of the present experiment. The initial potential energy curves (PECs) of the mutually perturbed states and spin-orbit (SO) matrix elements were *ab initio* evaluated in the basis of the spin-averaged wave functions. Both interacting $A^1\Sigma^+$ and $b^3\Pi$ states are described by the analytical potentials defined by the "Expanded Morse Oscillator" (EMO) form. The direct SO coupling between the $b^3\Pi_0$ sub-state and $A^1\Sigma^+$ state as well as the spin-rotational mixing of different $b^3\Pi_{0,1,2}$ sub-states is explicitly taken into account using a semi-empirical, "morphed" form of the *ab initio* SO matrix elements.

The developed CC deperturbation model allowed us to assign more lines in the recorded spectra and to reproduce most of the experimental observations with an accuracy consistent with experimental uncertainties, thus considerably surpassing the accuracy of the previous study [3]. Furthermore, the achieved accuracy encouraged to imply the empirically refined PECs and SO functions as well as *ab initio* $A^1\Sigma^+ - X^1\Sigma^+$ and $b^3\Pi - a^3\Sigma^+$ transition moments to predict energy and radiative properties of the $A \sim b$ complex of both ^{6,7}LiCs isotopologues. The information could be useful for perturbation-facilitated double resonance experiments as well as to optimize formation and detection of ultracold LiCs molecules in their absolute ground state [4].

Moscow team thanks for the support by the RFBR grant No. 13-03-00446a.

References

- [1] P. Burns *et al.* J. Chem. Phys. **122**, 074306 (2005)
- [2] W. C. Stwalley Eur. Phys. J. D **31**, 221 (2004)
- [3] A. Grochola *et al.* J.Q.S.R.T. **145**, 147 (2014)
- [4] J. Deiglmayr *et al.* Phys. Rev. Lett. **101**, 133004 (2008)

High resolution study and deperturbation analysis of the $A^1\Sigma^+ - b^3\Pi$ complex in KRb

K. Alps¹, A. Kruzins¹, M. Tamanis¹, R. Ferber¹, A. V. Stolyarov², and E. A. Pazyuk²

¹Laser Centre, Department of Physics, University of Latvia, 19 Rainis blvd., LV-1586, Riga,

²Department of Chemistry, Moscow State University, 119991, Moscow, Leninskie gory 1/3, Russia

Presenting Author: tamanis@latnet.lv

In heavy heteronuclear alkali diatomic molecules containing Rb and Cs atoms the lowest excited $A^1\Sigma^+$ and $b^3\Pi$ states ($A - b$ complex for short) are strongly coupled by spin-orbit (SO) interaction. An accurate description of such systems is a challenging task, which imposes a detailed experimental study and elaboration of a powerful deperturbation procedure. Recently this problem was successfully solved for NaRb [1], NaCs [2], KCs [3], RbCs [4] and Rb₂ [5] molecules. In these studies the term values of the $A - b$ complex were determined from laser induced fluorescence (LIF) spectra recorded by high resolution Fourier Transform (FT) spectrometer. The coupled-channel deperturbation analysis allowed to reproduce the obtained data with experimental accuracy 0.01 cm⁻¹.

The goal of the present work is to apply this approach for the KRb $A - b$ complex. In the experiment KRb molecules were produced in a linear stainless steel heat pipe. The laser beam was sent into the heat pipe through a pierced mirror. The backwards LIF was collected by the same mirror and focused on the input aperture of the FT spectrometer Bruker IFS-125HR and recorded with a resolution of 0.03-0.05 cm⁻¹. We used a direct ($A^1\Sigma^+ - b^3\Pi$) ← $X^1\Sigma^+$ excitation by diode lasers (980 - 1020 nm) and by Ti:Sph laser (Coherent MBR-110) followed by observation of the ($A^1\Sigma^+ - b^3\Pi$) → $X^1\Sigma^+$ LIF. Overall more than 300 LIF spectra were recorded and 900 KRb progressions for ³⁹K⁸⁵Rb and ³⁹K⁸⁷Rb isotopologues were analyzed yielding more than 4000 term values of the $A - b$ complex, including the data from collisional rotational energy transfer. The data field contains rovibronic levels with rotational quantum numbers $J \in [3, 279]$ in the energy range $E \in [10927, 14250]$ cm⁻¹.

A direct deperturbation treatment of the experimental rovibronic term values of both isotopologues of the mutually perturbed $A^1\Sigma^+$ and $b^3\Pi$ states was accomplished in the framework of inverted coupled-channel approach by means of the 4x4 Hamiltonian constructed in Hund's (a) coupling case basis functions. The Expanded Morse Oscillator model was used to describe potential energy curves while for the SO coupling functions we adopted the "morphed" form of the relevant *ab initio* spin-orbit matrix elements. As a result, 44 mass-invariant fitting parameters of the corresponding functions have been required to reproduce 96% of experimental term values of the $A - b$ complex with a standard deviation of 0.004 cm⁻¹. The energy-based deperturbation analysis was additionally confirmed by a calculation of relative intensity distributions in the $A - b \rightarrow X$ LIF progressions.

The support from the Latvian Science Council Grant No. 119/2012 as well as from Latvian Ministry of Education and Science Grant No. 11-13/IZM14-12 is gratefully acknowledged. Moscow team thanks for the support by the RFBR grant No. 13-03-00446-a.

References

- [1] O. Docenko *et al.* Phys. Rev. A **75**, 042503 (2007)
- [2] J. Zaharova *et al.* Phys. Rev. A **79**, 012508 (2009)
- [3] A. Kruzins *et al.* J. Chem. Phys. **139**, 244301 (2013)
- [4] A. Kruzins *et al.* J. Chem. Phys. **141**, 184309 (2014)
- [5] A. N. Drozdova *et al.* Phys. Rev. A. **88**, 022504 (2013)

Progress in the classification of spectral lines of Praseodymium

Z. Uddin^{1,2}, I. A. Siddiqui^{1,2}, R. U. Reham², M. Jahangir², and L. Windholz¹

¹*Institute of Experimental Physics, Technical University Graz, Austria*

²*Department of Physics, University of Karachi, Pakistan*

Presenting Author: rizrehman@hotmail.com

In continuation of our work concerning fine structure levels of Praseodymium, we have found few new levels of Pr-I. Recently we discovered 11 new levels and were able to classify 49 spectral lines [1]. When investigating spectral lines of Pr in a Fourier transform spectrum of Pr [2] we found a new line of Pr with wavelength 9857.664 Å. This spectral line is reported first time here. Though the signal-to-noise ratio (SNR) of this line is not high, the hyperfine (hf) structure of the lines clearly indicates that it could be a transition between levels of low angular momenta. The simulation of this line tells us that it's a $J_o = 5/2$ to $J_u = 5/2$ transition. For the determination of the hyperfine constants, the line was fitted with $J_o = 5/2$ to $J_u = 5/2$, and we got 824.76 MHz and 1062.38 MHz. One of the known even lower levels of Pr, 14315.745 cm^{-1} , was then assumed to be the lower level of the transition, as it has $J_u = 5/2$ and an hf constant 1063.3 MHz. The addition of the wave number of the investigated spectral line to this level yields 24457.355 cm^{-1} (the energy of odd upper level of the transition). Further investigations confirmed the existence of this new upper level since it is classifying four more unclassified lines. These lines are presented in Table 1.

Wavelength Å	Upper level with odd parity			Lower level with even parity			Remarks
	J_o	Energy/ cm^{-1}	A_o/MHz	J_u	Energy/ cm^{-1}	A_u/MHz	
5552.302	2.5	24457.355	820(5)	2.5	6451.808	1191	New line
8054.486	2.5	24457.355	820(5)	1.5	12051.488	1071	New line
8503.789	2.5	24457.355	820(5)	1.5	12701.121	833	New line
8823.988	2.5	24457.355	820(5)	2.5	13127.722	156	New line
9857.664	2.5	24457.355	820(5)	2.5	14135.745	1063	New line

Table 1: Spectral lines of Pr - I classified by new upper level 24457.355 cm^{-1} .

References

- [1] Zaheer Uddin, Imran Siddiqui, Jaweria Tanweer, Saif Uddin Jilani and Laurentius Windholz J. Phys. B: At. Mol. Opt. Phys. **48**, 135001 (2015))
 [2] B. Gamper, Diploma Thesis , Graz 2007, Unpublished

Optical lattice atomic clocks as a reference for spectroscopy

M. Zawada¹, P. Morzyński¹, M. Bober¹, A. Cygan¹, S. Wójtewicz¹, K. Bielska¹, P. Masłowski¹, D. Lisak¹, and R. Ciuryło¹

¹*Institute of Physics, Faculty of Physics, Astronomy and Informatics, Nicolaus Copernicus University, Grudziądzka 5, PL-87-100, Toruń, Poland*

Presenting Author: zawada@fizyka.umk.pl

We report a system of two independent strontium optical lattice standards probed with a single shared ultra-narrow laser [1,2]. The two optical frequency standards (Sr1 and Sr2) are based on the $^1S_0 - ^3P_0$ transition in neutral strontium atoms. The Sr1 can operate with bosonic isotope ^{88}Sr while Sr2 can operate with either bosonic ^{88}Sr or fermionic ^{87}Sr isotope. Two clouds of atoms in Sr1 and Sr2 are independently probed by an ultra-stable laser with spectral width below 1 Hz. An Er:fiber optical frequency comb, with one tooth phase-locked to the ultra-stable laser allows performing spectroscopic measurements with accuracy of optical atomic clock. The absolute frequency of the clocks can be calibrated by a long distance stabilized fiber optic link with the UTC(AOS) and UTC(PL) via the OPTIME network [3].

As a demonstration of the accuracy of the system we plan to determine ratios of molecular oxygen B-band transition frequencies to the strontium optical atomic clock frequency. This will be realized by making optical heterodyne beat-notes of the clock laser and the CRDS spectrometer [4] probe laser with the same optical frequency comb at wavelengths of 698 nm and 690 nm, respectively. By referencing all measured frequencies to the same reference frequency, we will obtain frequency ratios free from uncertainties of the reference frequency. Such a technique allows for determination of frequency ratios with extreme accuracy and precision [5]. We also demonstrate the sub-Hz precision of measurements of relative positions of the optical cavity modes using novel CMDS technique [6].

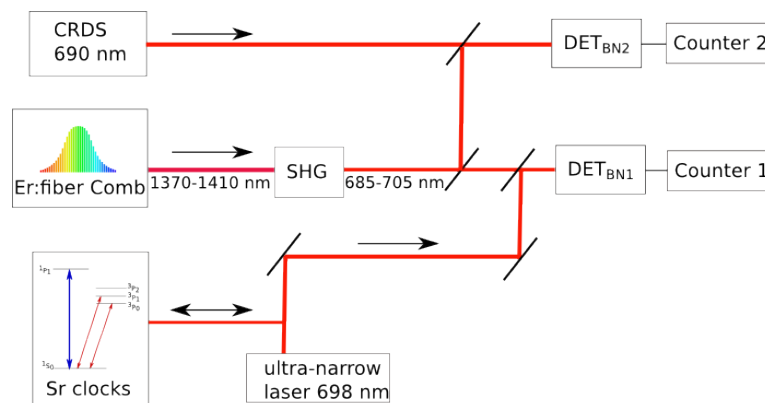


Figure 1: A simplified set-up of the measurement of ratios of molecular oxygen B-band transition frequencies in reference to the strontium optical atomic clock frequency.

References

- [1] T. Ido, H. Katori, Phys. Rev. Lett. **91**, 053001, (2003)
- [2] M. Bober *et al.* Meas. Sci. Technol. *in print* (2015)
- [3] Ł. Śliwczyński *et al.* Metrologia, **50**, 133 (2013)
- [4] S. Wójtewicz *et al.* J. Quant. Spectrosc. Radiat. Transfer **144**, 36–48 (2014)
- [5] T. Rosenband *et al.* Science **319**, 1808–1812 (2008)
- [6] A. Cygan *et al.* One-dimensional frequency-based spectroscopy, Opt. Express, *in print* (2015)

In-house XAS measurements using a von Hamos curved crystal spectrometer and an X-ray tube

F. Zeeshan¹, J. Hozzowska¹, L. Loperetti¹, and J.-Cl. Dousse¹

¹Department of Physics, University of Fribourg, Switzerland

Presenting Author: faisal.zeeshan@unifr.ch

X-Ray Absorption Spectroscopy (XAS) has become a routine technique at synchrotron radiation sources where the bright, coherent, energy tunable and monochromatic X-ray beams permit to investigate a variety of samples from different disciplines such as physics, chemistry, environmental sciences, geology, cultural heritage, archeology and biomedicine. For external users, however, the access to such advanced research facilities is not so easy and the available beam time is limited. In this context, a laboratory-based setup offers the advantages of lower costs and better accessibility. Such a setup based on a von Hamos curved crystal spectrometer [1] and a side-window X-ray tube was therefore developed at the University of Fribourg for in-house XAS measurements.

In the present setup the focal line of the electron beam on the X-ray tube anode, the sample and the center of the spectrometer crystal are aligned along the direction determined by the Bragg angle corresponding to the measured absorption edge (see Fig. 1). To preserve the energy resolution of the spectrometer, a narrow rectangular slit (width of 200 μm) is placed between the sample and the crystal. The X-ray tube is operated at low voltages in order to reduce the scattering background and the contributions from higher orders of diffraction.

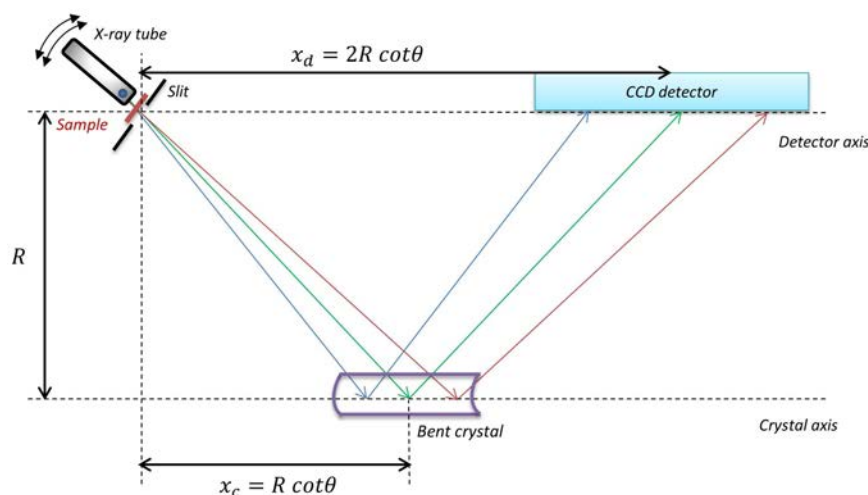


Figure 1: Schematic drawing of the laboratory-based XAS setup. R stands for the crystal radius of curvature and θ for the Bragg angle.

The K-edges of Ti, Fe, Cu and Ge and the L_3 -edges of Mo, Ag, Hf, Ta and Pt were measured. To probe the sensitivity of the setup, the less pronounced L_2 - and L_1 -edges were also measured but only for Mo and Ag. Precise edge energies could be determined and compared to existing experimental and theoretical values. The effect of the sample thickness on the experimental edge energy was carefully investigated. The L-edge energies corresponding to the first inflection point were found to be systematically lower than the values commonly used as references, the deviations being particularly pronounced for samples whose absorption edges are characterized by strong white lines.

References

[1] J. Hozzowska, J.-Cl. Dousse, J. Kern and Ch. Rhême, Nucl. Instrum. Meth. Phys. Res. A 376, 1996, 129

Mesoscopic quantum systems

Single-electron manipulation with resonant impurity states in silicon nanoelectronic circuits

J. Klocans¹, E. Potanina¹, G. Barinovs¹, and V. Kashcheyevs¹

¹*Department of Physics, University of Latvia, Riga*

Presenting Author: jevgenijsklocans@gmail.com elina.potanina@gmail.com

Steady decrease of the size of complementary metal-oxide-semiconductor devices entails the risk of failure for their future integration due to variability, which threatens the operation of circuits because of sample-to-sample fluctuations. The goal behind the project “Silicon at the Atomic and Molecular scale (SiAM)” is to turn this apparent limitation into an advantage by dopant implementation in a semiconductor host crystal, therefore bringing and consequently exploiting the benefits of the atomic and quantum nature of the quantum dot created. The main idea is to use the very sharp, deep and reproducible potential created by a dopant atom, resulting in a discrete level state system isolated from the noise coming from the surroundings, which opens doors for new profound functionalities to future information and communications technology systems.

In this study we present theoretical models developed to predict the overall current as a function of control voltage for different sets of the underlying physical parameters which will be measured experimentally within SiAM. The methods are based on solving the Master equation and illustrate the operation of a pure adiabatic electron pump [1] and the simulation of the output signal in a model with two atom impurities in series [2].

This work has been supported by European Commission through the Seventh Framework Programme (FP7) within project SiAM no. 610637.

References

- [1] S.J. Ray, P. Clapera, X. Jehl, T. Charron, S. Djordjevic, L. Devoille, E. Potanina, G. Barinovs, V. Kashcheyevs Precision Electromagnetic Measurements 446-447 (2014)
- [2] B. Roche, R.-P. Riwar, B. Voisin, E. Dupont-Ferrier, R. Wacquez, M. Vinet, M. Sanquer, J. Splettstoesser, X. Jehl Nature Communications 4 1581 (2013)

Photophysics of atoms and ions and AMO and FEL physics at large facilities

The photodetachment cross section of H^- : an animated-crossed-beam measurement

M. Génévriez¹, X. Urbain¹

¹*Institute of Condensed Matter and Nanosciences, Université catholique de Louvain, Louvain-la-Neuve B-1348, Belgium*

Presenting Author: matthieu.genevriez@uclouvain.be

The photodetachment of the negative hydrogen ion H^- has attracted numerous studies due to the ion's prototypical character and the importance of electron correlations in that weakly bound system. It has become a commonly used benchmark from atomic theories and numerical methods, which have, over the decades, reached an overall good agreement. On the experimental side fewer studies exist, and only one [1] provides absolute cross sections at various photon energies. Recently, Vandevraye *et al.* [2] have carried out an absolute measurement at 1064 nm (1.1653 eV), presented in Fig. 1.

In order to measure an absolute photodetachment cross section, it is necessary to disentangle the so-called volume effect. In our crossed beam setup, the finite size of the ion beam and of the laser beam defines an effective interaction volume, within which both the ion and the photon flux vary. The measured photodetachment signal is therefore an *average* over these local variations and the cross section is, in general, retrieved by assuming a certain distribution for both beams.

The animated-crossed-beam method, originally developed for electron-ion collisions [3], eliminates the need for the knowledge of the beams distributions. Instead of fully characterizing the interaction volume, it aims at *removing* its influence on the measured signal by repeatedly sweeping the laser beam across the ion beam, as realized by tilting a fused silica plate. After integration of the signal along the laser's vertical displacement, the cross section is expressed only in terms of easily measurable quantities, e.g., the laser power and the ion beam current.

The photodetachment cross section obtained in the range from 700 nm to 1064 nm [4] is in excellent agreement with previous experiments and compelling theoretical works, in particular the state-of-the-art calculation of Venuti and Decleva [5] shown in Fig. 1. We also confirm the commonly admitted value of $3.5 \times 10^{-21} \text{ m}^2$ at 1064 nm (1.1653 eV).

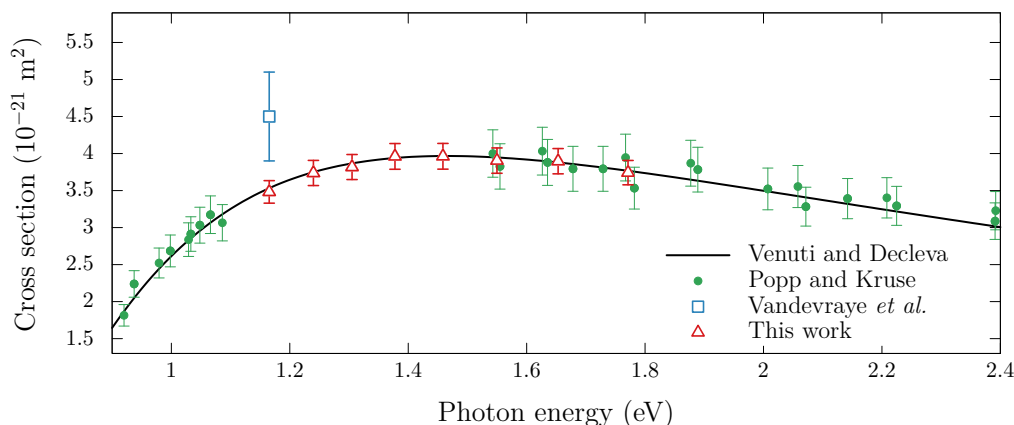


Figure 1: Photodetachment cross section of H^- versus photon energy.

References

- [1] H.-P. Popp, S. Kruse J. Quant. Spectroscop. Radiat. Transfer **16**, 683 (1976)
- [2] M. Vandevraye *et al.* Phys. Rev. A **90** 013411 (2014)
- [3] F. Brouillard, P. Defrance Phys. Scr. **1983**, 68 (1983)
- [4] M. Génévriez, X. Urbain Phys. Rev. A **91**, 033403 (2015)
- [5] M. Venuti, P. Decleva J. Phys. B: At. Mol. Opt. Phys. **30**, 4839 (1997)

Interference effects in one-photon and two-photon ionization by femtosecond VUV pulses due to an intermediate state

A. N. Grum-Grzhimailo¹, E. V. Gryzlova¹, E. I. Staroselskaya^{1,2}, J. Venzke³, and K. Bartschat³

¹*Skobeltsyn Institute of Nuclear Physics, Lomonosov Moscow State University, Russian Federation*

²*Faculty of Physics, Lomonosov Moscow State University, Russian Federation*

³*Department of Physics and Astronomy, Drake University, Des Moines, Iowa, USA*

Presenting Author: algrgr1492@yahoo.com

Two-pathway coherent control of photoionization and photodissociation has attracted much attention during the past two decades, from both experiment and theory alike. In experiments with X-ray free electron lasers (XFELs) a mixture of fundamental and higher harmonic frequencies is produced, which may be used in a coherent control scheme.

We theoretically studied interference effects in two-pathway ionization by the fundamental (two-photon ionization) and its second harmonic (one-photon ionization) when the two-photon channel is affected by an intermediate atomic resonance. While interference between the amplitudes of one- and two-photon ionization does not contribute to the total yield, an effect may appear in the photoelectron angular distribution (PAD) [1-3]. As an indicator for the two-pathway coherence, we use the asymmetry of the PAD with respect to the plane perpendicular to the electric field,

$$A(\theta) = [W(\theta) - W(\pi - \theta)] / [W(\theta) + W(\pi - \theta)] . \quad (1)$$

Here $W(\theta)$ is the intensity of the electron flux at an angle θ relative to the direction of the linear polarization of the XFEL. The asymmetry (1) depends on the XFEL parameters: the photon energy, the relative phase between the harmonics, their intensity, etc.

The process is exemplified by ionization from the hydrogen H(1s) state in the vicinity of the 1s-2p transition. Figure 1 shows the photon-energy dependence of the asymmetry $A(0)$ for different pulse durations, at a fixed peak laser intensity of 10^{12} W/cm² and the intensity of the second harmonic set to 5% of the fundamental. Predictions for other XFEL parameters, new analytical results, and those obtained by solving the time-dependent Schrödinger equation will be presented at the conference.

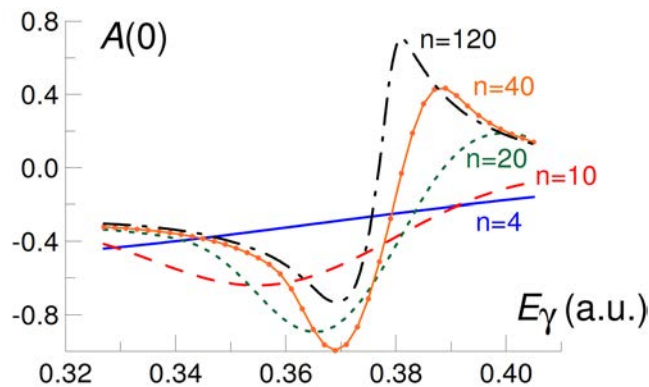


Figure 1: Asymmetry in the PAD for zero relative phase and time delay between the fundamental and second harmonics; n indicates the number of optical cycles in the laser pulse with a \sin^2 envelope. The above results were obtained by nonstationary perturbation theory.

References

- [1] N.A. Baranova *et al.*, JETP **55**, 4391 (1992)
- [2] Y.-Y. Yin, C. Chen, D.S. Elliott, and A.V. Smith, Phys. Rev. Lett. **69**, 2353 (1992)
- [3] R. Yamazaki and D.S. Elliott, Phys. Rev. Lett. **98**, 053001 (2007)

Photodissociation of oxygen molecules upon the absorption in Shumann-Runge bands in various environments: modeling study

A. Pelevkin¹, K. Miculis², A. Ubelis², N. S. Titova¹, and A. M. Starik¹

¹Central Institute of Aviation Motors, Aviamotornaya street 2, Moscow, 111116 Russia

²Institute of Atomic Physics and Spectroscopy, University of Latvia, Riga

Presenting Author: michulis@latnet.lv

Photodissociation of molecular oxygen plays an important role in the photochemistry of the atmosphere and can be used for the initiation of combustion in different combustible mixtures due to production of highly reactive atomic oxygen upon absorption of resonance laser radiation [1, 2]. For the analysis and modeling of photochemical processes both in the atmosphere and in the combustible mixtures it is needed to calculate the photodissociation rate with rather high accuracy upon the exposure of the mixture to solar radiation or to resonance laser radiation at given wavelength. As is known, O₂ molecules strongly absorb the ultraviolet radiation in the Shumann-Runge and Hertzberg systems.

In order to estimate the photodissociation rate it is necessary to reproduce the ultraviolet spectrum of O₂ molecules in different mixtures and at various values of temperature and pressure. This paper does address the calculations of the spectrum of Shumann-Runge bands in air and in H₂-O₂(air) mixture as well as the estimation of the photodissociation rate upon exposure of the mixture to ArF laser radiation at 193.3 nm wavelength. The variation of the composition of H₂-O₂(air) mixture with temperature $T_0 = 700 - 800$ K and pressure $P_0 = 0.5 - 1$ atm during the laser pulse duration ($\tau_p = 40$ ns) is also calculated. It should be emphasized that applied methodology for the calculation of O₂ spectrum in the Shumann-Runge bands allows us to reproduce with high accuracy the data on spectrum of Shumann-Runge system in the atmosphere reported elsewhere [3]. As an example Figure depicts the spectrum of O₂ molecule in the range of wavelength numbers $\nu = 51500 - 52000\text{cm}^{-1}$ for the stoichiometric H₂-air mixture at $T_0 = 800$ K and $P_0 = 1$ atm. On the basis of this methodology the values of photodissociation rate were calculated in the different sections of ArF laser beam propagating through the cell filled by the stoichiometric H₂-air mixture. The composition of the mixture in these sections was predicted by using the numerical simulation taking into account the detailed chemistry in the H₂-air system.

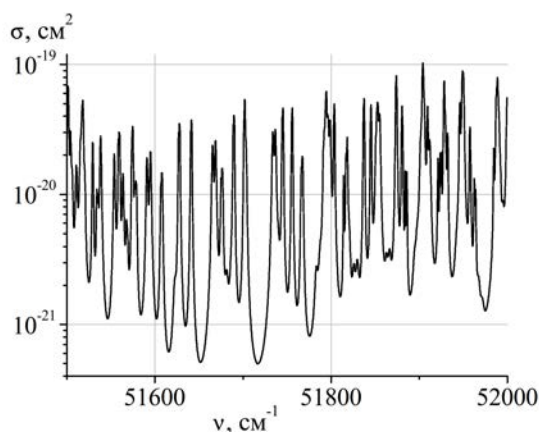


Figure 1: Absorption cross section of O₂ molecule in the range of wavelength $\nu = 51500 - 52000\text{cm}^{-1}$ for the stoichiometric H₂-air mixture at $T_0 = 800$ K and $P_0 = 1$ atm.

We acknowledge the support by the EU FP7 IRSES Project – NOCTURNAL ATMOSPHERE

References

- [1] M. Lavid, Y. Nachshon, S. K. Gulati, J. G. Stevens Sci. Technol. V 96, 231-245 (1994)
- [2] A. M. Starik, P. S. Kuleshov, N. S. Titova J. Phys. D 42, N 17, 175503 (2009)
- [3] M. Nicolet, S. Cleslik, R. Kennes Planet. Space Sci. V 31, N 4, 427-458 (1989)

Complete measurements of anisotropic x-ray emission following recombination of highly charged ions

C. Shah¹, P. Amaro¹, R. Steinbrügge², C. Beilmann^{1,2}, S. Bernitt², S. Fritzsche³, A. Surzhykov⁴, J. R. Crespo López-Urrutia², and S. Tashenov¹

¹Physikalisches Institut, Im Neuenheimer feld 226, 69120 Heidelberg, Germany

²Max-Planck-Institut für Kernphysik, Saupfercheckweg 1, 69117 Heidelberg, Germany

³Friedrich-Schiller-Universität Jena, Fürstengraben 1, 07743 Jena, Germany

⁴Helmholtz-Institut, Helmholtzweg 4, 07743 Jena, Germany

Presenting Author: tashenov@physi.uni-heidelberg.de

X-ray emission asymmetries following the resonant recombination into highly charged ions were studied using an electron beam ion trap (EBIT) of Max Planck Institute for Nuclear Physics in Heidelberg. Iron and krypton ions in the He-like through O-like charge states were populated in an EBIT and the K -shell dielectronic recombination (DR), trielectronic recombination (TR) and quadrolelectronic recombination (QR) resonances were systematically investigated. The x rays emitted in the decays of resonantly excited states were observed by two germanium detectors aligned along and perpendicular to the electron beam propagation direction and the corresponding intensities of the K -shell x-ray transition were recorded as a function of the electron collision energy. The x-ray emission asymmetries reveal the alignment of the intermediate excited states and, therefore, the polarization of the emitted x rays. Except for a few transitions, the experimental results are in excellent agreement with the theoretical calculations done with FAC and RATIP computer codes.

This measurement allows for a systematic modeling of the polarization of the prominent $K\alpha$ radiation emitted by hot anisotropic plasmas. Using the experimental data, we calculated the maximum polarization of the $K\alpha$ x rays emitted by an anisotropic plasma as a function of the plasma temperature, see Figure 1. Unexpectedly, we found that the degree of x-ray polarization is dominated by previously neglected trielectronic and quadrolelectronic recombination transitions. This information can be used for diagnostics of anisotropies in hot plasmas, in particular the experimental results should play an important role in diagnostics of hot astrophysical plasmas of solar flares and active galactic nuclei and laboratory fusion plasmas of tokamaks and stellarators.

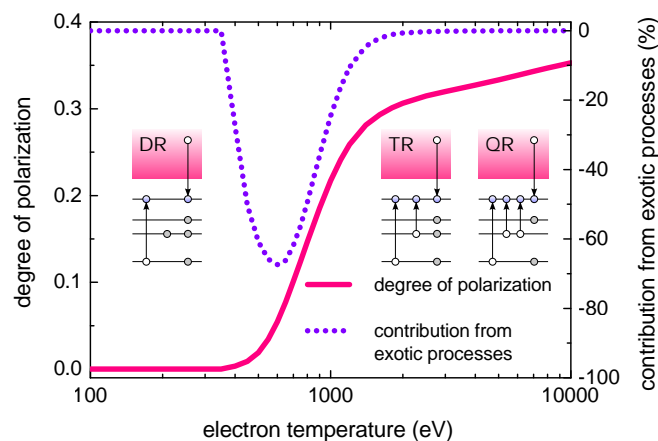


Figure 1: Maximum polarization of iron $K\alpha$ x rays due to resonant recombination as a function of the plasma temperature. Exotic trielectronic and quadrolelectronic recombination transitions dominate polarization in an intermediate range of plasma temperature.

Quantum optics/information including cold ions

Nonlinear optics and dynamics of atoms, molecules in an electromagnetic field and laser systems with elements of a chaos

V. Buyadzhi¹, A. Glushkov¹, G. Prepelitsa¹, and V. Ternovsky¹

¹Odessa State University - OSENU, Odessa

Presenting Author: vbuyad@mail.ru, dirac13@mail.ru

The paper is devoted to carrying out fundamentally new approaches to the universal quantum-dynamic and chaos-geometric modelling and analysis of the chaotic dynamics of nonlinear processes in atomic and molecular systems in intense electromagnetic fields and quantum-generator and laser systems and devices (including single-modal laser with an absorbing cell, a semiconductor laser coupled with feedback with delay, the system of semiconductor quantum generators, combined through a general cavity, fiber lasers). In order to make modelling chaotic dynamics it has been constructed improved complex system (with chaos-geometric, neural-network, forecasting, etc. blocks) that includes a set of new quantum-dynamic models and partially improved non-linear analysis methods including correlation (dimension D) integral, fractal analysis, average mutual information, false nearest neighbours, Lyapunov exponents (LE), Kolmogorov entropy (KE), power spectrum, surrogate data, nonlinear prediction, predicted trajectories, neural network methods etc [1-3].

It is carried out modelling of chaotic dynamics of the Li, Rb Rydberg states in ($n = 115, 125$; $m = 0$) in a static magnetic field $B = 4.5\text{T}$ and oscillating electric field with frequency $f=102\text{MHz}$) and shown that stochastic changing, fragmentation, extinction and again appearing of the peaks in power spectrum is occurred. There are firstly obtained original data on the LE, correlation, embedding, Kaplan-York D, KE and presented picture of the quantum fluctuations, stabilization, destabilization, delocalization, fractal properties and conditions for the KAM theorem. It has been presented a new approach to modelling the chaotic dynamics of diatomic molecules in intense electromagnetic field, which is, firstly, based on the numerical solution of the time-dependent Schrödinger equation and realistic model Simons-Parr-Finlan potential for diatomic molecules (quantum unit) and, secondly, the universal chaos-geometric nonlinear analysis unit, which includes the application of methods of correlational integral, LE and spectrum strength etc to analysing time series of populations, induced polarization. There are determined quantitative parameters of the GeO molecule chaotic dynamics in linear polarization field (intensity of 25 GW/cm^2), including, correlation D (2.73), embedding D, Kaplan-York D (2.51), LE (the first two are positive, +, +), KE etc. It is numerically investigated chaos dynamics generation in the erbium one-ring fibre laser (EDFL, 20.9mV strength, = 1550.190nm) with the control parameters: the modulation frequency f and dc bias voltage of the electro-optical modulator. It is shown that in depending upon f, V values there are realized 1-period ($f = 75\text{MHz}$, $V = 10\text{V}$ and $f = 60\text{MHz}$, $V = 4\text{V}$), 2-period ($f = 68\text{ MHz}$, $V = 10\text{V}$ or $f = 60\text{MHz}$, $V = 6\text{V}$), chaotic ($f = 64\text{MHz}$, $V = 10\text{ V}$ and $f = 60\text{MHz}$, $V = 10\text{V}$) regimes; there are calculated LE, correlation, embedding, Kaplan-York dimensions, Kolmogorov entropy and theoretically shown that chaos in the erbium fiber laser device is generated via intermittency by increasing the DC bias voltage and period-doubling bifurcation by reducing the frequency modulation computers in the full agreement with experiment [4].

References

- [1] A. Glushkov *et al.* Nonlin. Proc.in Geophys. **11**, 285–294 (2004); S. Kuznetsov, D. Trubetskov *Izv.Vuzov. Ser. Radiophys.* **XLVII**, 1–7 (2004)
- [2] A. Glushkov *et al.* *Atm. Environment.* **42**, 7284–7292 (2008); *Adv.in Space Res.* **42**, 1614–1618 (2008)
- [3] A. Glushkov A. Svinarenko, V. Buyadzhi *et al.*, *Adv. in Neural Networks, Fuzzy Systems and Artificial Intelligence, Ser.: Recent Adv. in Computer Engineering* (WSEAS, Gdansk, 2014) **21**, 143-160
- [4] T. Cheng *et al.* *Phys. Lett. A.* **265**, 384–390 (2000); C. Feng *et al.* *Chin. Phys. B.* **21**, 100504 (2013)

Transient switching of the Kerr nonlinearity and effect of Doppler broadening in a five- level Quantum system

H. R. Hamed¹, G. Juzeliūnas¹

¹*Institute of Theoretical Physics and Astronomy, Vilnius University, A. Goštauto 12, Vilnius LT-01108, Lithuania*

Presenting Author: hamid.r.hamedi@gmail.com

The third order susceptibility [1] is investigated in a five-level quantum scheme in which four strong laser components couple a pair of atomic internal states to another pair of states in all possible ways to form a closed loop configuration of the atom-light interaction.

First, a comparison is made between the Kerr nonlinear indices for the five-, four- and three- level systems. It is realized that the magnitude of the Kerr nonlinearity for the five- level system is larger than that of the three- and four- level counterparts.

Subsequently, the temporal evolution of the Kerr nonlinearity and the required optical switching time in the nonlinear regime is studied in this atomic system by using the density matrix equations of motion. It is demonstrated that such a medium can be employed as an optical switch in which the propagation of the laser pulse is controlled by another laser field. The results presented may be useful for understanding the switching feature of the EIT-based slow light Kerr nonlinearity, and be helpful for the realization of fast optical nonlinearities and optically controlled devices.

Finally, it is shown that effect of the Doppler broadening can lead to an enhanced Kerr nonlinearity while maintaining linear and nonlinear absorption [2].

References

- [1] R. W. Boyd, *Nonlinear Optics* (Academics, San Diego, 1992)
- [2] H. R. Hamed and G. Juzeliūnas. Accepted for publication in *Phys. Rev. A* (2015)

BEC of photons in a dye-filled microcavity: inhomogeneities, coherence and interactions

R. A. Nyman¹, J. Marelic¹

¹Centre for Cold Matter, Imperial College London, United Kingdom, SW7 2AZ

Presenting Author: jm3309@ic.ac.uk

Bose-Einstein condensation (BEC) is a universal phenomenon which occurs when a system of identical bosons at thermal equilibrium occupy the ground state in enormous numbers. By optically pumping a 1.5-micron long, dye-filled resonator, we can achieve both thermal equilibrium of photons and a well-defined ground state. Thus, the first room temperature BEC was demonstrated [1]. We have become only the second laboratory to create this quantum-fluid state of light.

There are many recent published theoretical models of photon BEC, some using rate equations, other fully quantised matter-light interactions. Some of our steady-state observations, such as the variation of critical pump power with pump spot size, contradict the predictions of these simple models, giving a challenge to our theory collaborators [2]. We will also present some of the results of a detailed comparison between our data and the model of Kirton and Keeling [3].

We have measurements of the first-order coherence, which show that the condensate has a longer coherence time than the thermal cloud. Our interferometer is capable of measuring the transverse coherence length, to give a full picture of $g^{(1)}(t - t', \mathbf{r}, \mathbf{r}')$. Dye-microcavity photons are thought to have the weakest particle-particle interactions of any system exhibiting BEC, although the mechanism and magnitude is currently undetermined. We have shown that even these interactions should be detectable in the momentum-resolved spectrum [4], and have begun experiments.

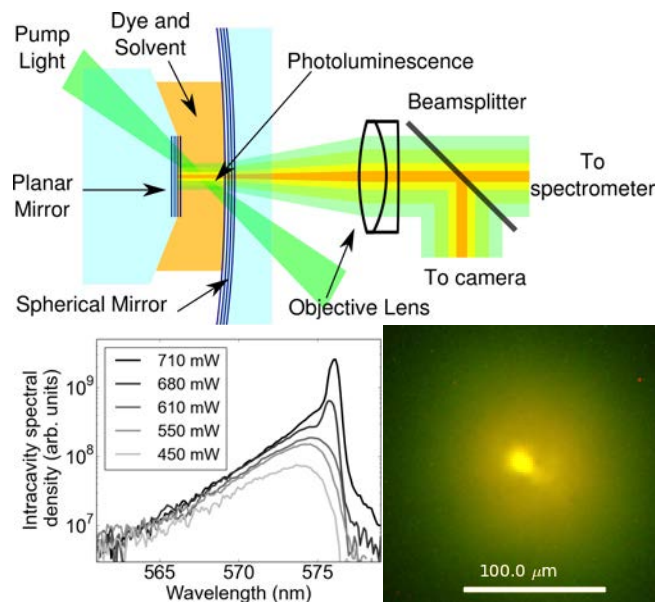


Figure 1: Top: experimental setup for demonstrating Bose-Einstein condensation of photons. Lower left: the intracavity spectrum, which is compatible with a Bose-Einstein distribution at room temperature, showing macroscopic occupation of the ground state. Lower right: a real-colour image.

References

- [1] J. Klaers et al, Nature, **468**, 545 (2010)
- [2] J. Marelic and R.A. Nyman, Phys. Rev. A. **91**, 033813 (2015)
- [3] P. Kirton and J. Keeling, Phys. Rev. Lett, **111**, 100404 (2013)
- [4] R.A. Nyman and M.H. Szymanska, Phys. Rev. A, **89**, 033844 (2014)

Ultrafast processes

Investigation of the H- (D-) loss from toluene's isotopologues in the fs timescale

Chr. Papadopoulou¹, S. Kaziannis¹, and C. Kosmidis¹

¹Department of Physics, University of Ioannina, GR 45110 Ioannina, Greece

Presenting Author: kkosmid@uoi.gr

The H-loss (or D-loss from the deuterated isotopologues) is the primary dissociation channel of toluene ($C_6H_5CH_3$). This dissociation channel is related to the radical [P-H] (P stands for the parent molecule) photo-isomerization, i.e. the six-membered (benzyl) to a seven-membered (tropyli) ring isomerization. The dynamics of this channel is studied in the fs timescale using a pump/probe excitation scheme in conjunction with a time-of-flight mass spectrometer. The 5th harmonic of a Ti:Sapphire femtosecond laser (160 nm) is used as the pump beam and a part of the fundamental laser beam (800 nm) serves as the probe.

Three isotopologues of toluene have been studied ($C_6H_5CH_3$, $C_6H_5CD_3$, $C_6D_5CD_3$). The dependence of the H- and D-loss on the delay time between the pump and the probe beams is presented for the first time. Furthermore, the influence of the isotopic effect versus that of the H-scrambling (Fig. 1), which attracted the researchers' interest in the past [1], is discussed.

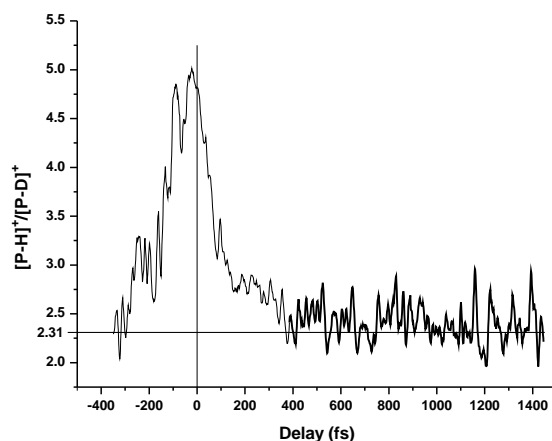


Figure 1: $[H\text{-loss}]/[D\text{-loss}]$ channel ratio in the case of $C_6H_5CD_3$.

Acknowledgement

We would like to thank Dr. E. M. Bennis for his contribution in the development of the experimental setup.

This research has been co-financed by the European Union (European Social Fund – ESF) and Greek national funds through the Operational Program "Education and Lifelong Learning" of the National Strategic Reference Framework (NSRF) - Research Funding Program: THALES (ISEPUMA). Investing in knowledge society through the European Social Fund.

References

- [1] T. A. Field *et al.* Chem. Phys. **250**, 81–110 (1999)

Applications of AMO Physics: Astrophysics, sensors, plasma physics, ...

Investigation of Hg resonance 184.9 nm line in a capillary low-pressure discharge

J. Alnis¹, Z. Gavare¹, A. Abola¹, V. Fyodorov¹, and E. Bogans¹

¹*Institute of Atomic Physics and Spectroscopy, University of Latvia, Riga*

Presenting Author: alnis@latnet.lv

In the last decade, growing interest has been directed to the capillary light sources. From a practical point of view, this interest is stimulated by their potential applications in various microsystems and portable devices, for instance, such light sources are used in portable LUMEX Mercury analyzer.

Most of the absorption spectrometers for Mercury determination in air are using spectral line of Hg at 253.7 nm, however the sensitivity of analyzer could be improved by using spectral line of Hg at 184.9 nm.

Data about structure of this resonance line in dependence on the cold spot temperature can be used not only for the lamp diagnostics but also for the validation of different type of calculations and models, considering radiation trapping. The radiation trapping effect plays an important role in light source devices using resonance radiation and it is important for the calculation of radiation efficiency and luminous output. The sensitivity of atomic absorption spectrometer is dependent both on intensity of emission source spectral line, as well as on profile of line, in particular self-absorption is of interest.

One of the investigation directions was targeted towards finding the optimal temperature regime for 184.9 nm light source. We produced a setup for thermostabilization of lamp “cold spot” and performed intensity measurements of Mercury 184.9 nm spectral line in temperature range from -5 to +40°C for lamps with different fillings.

The results of this investigation allows us to conclude that it will be necessary to thermostabilize the analyzer 184.9 nm light source at temperature at or below +15°C, though the final decision will be dependent on the overall thermal regime of the whole resulting device, when assembled.

Acknowledgement

EU FP7-ENV-2010 project “Global Mercury Observation System” (GMOS, Grant Agreement Number 265113)

Next-Generation Ion-Atom Hybrid Traps with Increased Control over Collision Energies

P. Eberle¹, A. Dörfler¹, R. Krishnamurthy¹, S. Willitsch¹, H. da Silva Jr.², M. Raoult², and O. Dulieu²

¹University of Basel, Switzerland

²Laboratoire Aime Cotton du CNRS, Paris, France

Presenting Author: p.eberle@unibas.ch

Recent studies of chemical reactions at low collision energies using laser-cooled, co-trapped ions and atoms in hybrid traps showed the ability of such systems to be used for investigation of the quantum character of reactive collisions [1-4]. Details of the mechanism of chemical reactions and the nature of molecular interaction potentials can be studied. But so far, insufficient control over the collision energy magnitude and distribution impeded the study of effects with narrow dependencies on collision energy, such as shape resonances [5]. Here, we present results from the extension of our hybrid trap setup with increased control over the collision energies.

Our hybrid trap consists of a linear Paul trap for atomic and molecular ions overlapped with a magneto-optical trap for neutral rubidium atoms. Initial experiments focused on interactions between $\text{Ca}^+ + \text{Rb}$ [1,2] and $\text{Ba}^+ + \text{Rb}$ [3], in which both systems have been laser cooled. Recently, chemical reactions of sympathetically cooled N_2^+ molecular ions with Rb atoms have been studied as well [4].

In the original setup, changing the number of ions and shape of the ion crystal was the only control over the energy of the ion-atom collisions. Heating of the ions due to micromotion lead to large spreads of the collision energies averaging out the effect of narrow resonances. In a new approach, we use a modified magneto-optical trap which allows the use of a dynamic atom cloud. Radiation pressure differences in the cooling laser beams along one axis create atom clouds in off-center positions. On-resonance push beams accelerate the atoms through the ion crystal after which the atoms are recaptured in the opposite off-center position from where they are pushed back through the crystal. By carefully tuning the cooling and push beam sequence and intensities we are able to produce moving atom clouds with well-defined velocities in the lab frame. Using this approach with ion strings on the rf null line of the ion trap, the collision energy resolution could be greatly improved.

References

- [1] F. H.J. Hall *et al.* Phys. Rev. Lett. **107**, 243202 (2011)
- [2] F. H.J. Hall, P. Eberle *et al.*; Mol. Phys., **111**, 14-15, 2020-2032 (2013)
- [3] F. H.J. Hall *et al.*; Mol. Phys. **111**, 12-13, 1683-1690 (2013)
- [4] F. H.J. Hall *et al.*; Phys. Rev. Lett. **109**, 233202 (2012)
- [5] H. da Silva Jr. *et al.*; New J. Phys. **17**, 045015 (2015)

Imaging the magnetic field distributions of chains of magnetic particles using nitrogen-vacancy centres in diamonds

A. Berzins¹, S. Lourette², J. Smits¹, K. Erglis³, A. Jarmola^{1,2}, F. Gahbauer¹, M. Auzinsh¹, D. Budker², A. Cebers³, and R. Ferber¹

¹Laser Centre, University of Latvia, Riga, Latvia

²Department of Physics, University of California, Berkeley, USA

³Laboratory of Magnetic Soft Matter, University of Latvia, Riga, Latvia

Presenting Author: andris.berzins@lu.lv

Nitrogen-vacancy (NV) centres in diamonds have proven to be very useful for measuring magnetic fields [1]. The NV centre has a triplet ground state with a zero-field splitting between the $m_s = 0$ and $m_s = \pm 1$ ground-state sublevels of 2.87 GHz. Moreover, in the presence of a local magnetic field the $m_s = \pm 1$ energies components are shifted by 2.8 MHz/G. Due to a non-radiative decay path via a singlet state that preferentially populates the $m_s = 0$ ground-state sublevel, the NV centre can be polarized optically, and the fluorescence from exciting $m_s = 0$ sublevel is more intense than the fluorescence from exciting the $m_s = \pm 1$ sublevels. As a result, the polarization state can be inferred from the fluorescence intensity. When a thin layer of NV centres is created close to the surface of a diamond, magnetic field distributions at the position of the NV layer can be imaged [2,3]. We have constructed a magnetic field microscope using a Leica DLM inverted microscope and are using it to study magnetic field distributions from magnetic spheres made from different materials and of different sizes. Chains of magnetic particles can be created by various methods. The simplest way is to dry a suspension of ferromagnetic particles in the presence of a magnetic field (see Fig. 1). We have also used strands of DNA to create flexible filaments of ferromagnetic particles coated with streptavidin. Magnetic field images have been made by the method of optically detected magnetic resonance (ODMR), in which the microwave frequency is scanned, and the fluorescence signal shows a minimum when the frequency is in resonance with a $m_s = 0 \rightarrow m_s = \pm 1$ transition. We report on our experiments to image the magnetic field distributions from these particles and to use the information to infer the magnetic properties of the particles.

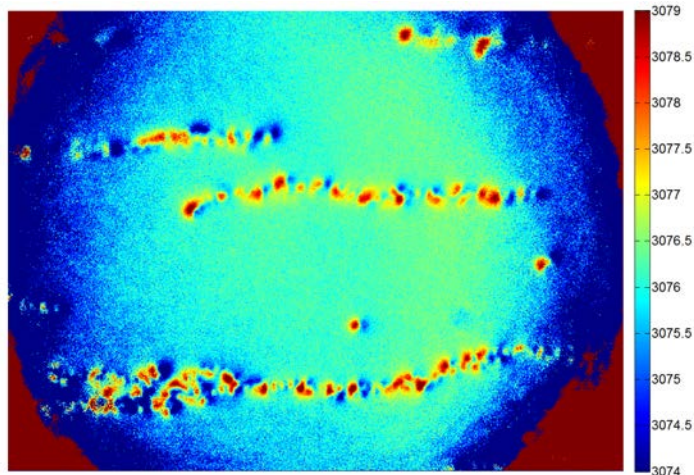


Figure 1: Image of magnetic field distribution of chains of 4 μm diameter ferromagnetic particles dried in the presence of a magnetic field. The color indicates the position of the ODMR peak for each pixel. A shift of 2.8 MHz corresponds to a magnetic field of one Gauss.

This work has received support from ESF Project Nr. 2013/0028/1DP/1.1.1.2.0/13/APIA/VIAA/054.

References

- [1] L. Rondin *et al.*, Rep. Prog. Phys. **77**, 056503 (2014)
- [2] L. M. Pham *et al.*, New Journal of Physics, **13**, 045021 (2011)
- [3] D. Le Sage *et al.*, Nature **496**, 486 (2013)

Hyperfine Structure, Lifetimes and Oscillator Strengths of V II

S. Bouazza¹, J. Ruczkowski², M. Elantkowska³, and J. Dembczyński²

¹*LISM, EA 4695, Université de Reims-Champagne, UFR SEN, BP 1039, F-51687 Reims Cedex 2*

²*Institute of Control and Information Engineering, Faculty of Electrical Engineering, Poznan University of Technology, Piotrowo 3A, 60-965 Poznan, Poland*

³*Laboratory of Quantum Engineering and Metrology, Faculty of Technical Physics, Poznan University of Technology, Piotrowo 3, 60-965 Poznan, Poland*

Presenting Author: safa.bouazza@univ-reims.fr

In First part of this work we confirmed the well-founded basis of new experimental data for some V II levels, recently published, through hyperfine structure constant values calculated for the first time,. Furthermore a good agreement is observed between single-step excitation and laser induced fluorescence V II radiative lifetimes found in literature data and our computed values recurring to ab-initio method.

In this study we also examined electric dipole transitions. We transformed angular coefficients of the transition matrix from SL coupling to intermediate one recurring to Racah algebra and using fine structure eigenvector amplitudes, previously determined. Transition integrals, treated as free in the least squares fit to experimental oscillator strength (gf) values [1-2] were then extracted; we give the two main deduced values: $\langle 3d^3 4p | r^1 | 3d^3 4s \rangle = -3.0346 \pm 0.0094$, $\langle 3d^3 4p | r^1 | 3d^4 \rangle = 0.8278 \pm 0.0026$ Finally, for a complete list of permitted transitions from depopulated odd-parity levels, gf values are predicted in a wide wavelength range: 2110-96000 Å.

References

- [1] J. Ruczkowski, , M. Elantkowska , J. Dembczynski J.Q.S.R.T. **145**, 20–42 (2014)
- [2] J. Ruczkowski, S. Bouazza , M. Elantkowska , J. Dembczynski J.Q.S.R.T.**155** 1–9 (2015)

Development of a Transportable Atom Gravimeter in HUST

Y.-Y. Xu¹, X.-C. Duan¹, M.-K. Zhou¹, J.-F. Cui¹, H.-B. Yao¹, X. Xiong¹, and Z.-K. Hu¹

¹*MOE Key Laboratory of Fundamental Physical Quantities Measurement, School of physics, Huazhong university of Science and technology, Wuhan 430074, China*

Presenting Author: xuyaoyaoleo@hust.edu.cn

We are developing a transportable atom gravimeter (TAG) in HUST, which is based on the work of our previous two laboratory-confined atom gravimeters. The vacuum system of our TAG is designed for an atomic fountain configuration, and the corresponding volume is only $0.75 \times 0.45 \times 1.4 \text{ m}^3$ including a two-dimensional magnetic-optical trap (2D-MOT) and an active vibration isolation. With regard to the laser system, two external-cavity diode lasers (ECDLs) are utilized as seed lasers, and two tapered amplifiers (TAs) are followed to provide required laser power. With the ECDLs and TAs included, the whole optical system can be accommodated by a $1 \times 0.7 \text{ m}^2$ breadboard. We have finished the construction of the optical system, and realized atoms loading as well as launching. And currently, we are working on atoms preparation and interfering. The aimed measurement uncertainty of our TAG is better than $5 \mu\text{Gal}$, and we expect to participate in the comparison of absolute gravimeters.

Large-momentum-transfer Bragg interferometer with Strontium atoms

X. Zhang^{1,2}, T. Mazzoni¹, R. Del Aguila¹, L. Salvi¹, N. Poli¹, and G. M. Tino¹

¹ *Dipartimento di Fisica e Astronomia and LENS - Università di Firenze, INFN - Sezione di Firenze, Via Sansone 1, 50019 Sesto Fiorentino, Italy*

² *The Abdus Salam International Centre for Theoretical Physics, Italy*

Presenting Author: zhang@lens.unifi.it

We report on the first atom interferometer with alkaline-earth atoms based on large-momentum-transfer (LMT) Bragg diffraction in a fountain. Alkaline-earth atoms have properties such as zero total spin in the ground state, narrow optical transitions, and low scattering cross section at ultra-low temperatures which promise unprecedented precision.

The atom we used for the interferometer is ^{88}Sr . The LMT up to $40 \hbar k$ is realized with composite pulses of two Bragg laser beams detuned about 8 GHz from the $^1S_0 - ^1P_1$ transition of Strontium at 460.862nm (here k is the wave vector of the Bragg laser beams). Typical interferometers are formed with two momentum states separated by $2 \hbar k$ to $6 \hbar k$ (1^{st} to 3^{rd} order Bragg diffraction). We have studied the performance of a gravity acceleration measurement with this interferometer, which are shown in Figure 1. A sensitivity of $4 \times 10^{-8}g$ is achieved at 2000 s of averaging. The dominant noise of the system now is the vibration on the retro-reflection mirror for Bragg beams.

This result opens the way to new experiments based on alkaline-earth atoms, for example the of Einstein Equivalence Principle (EEP) test using two kind of atoms such as one alkali atoms and one alkali-earth atoms[1,2], or a combination of a interferometer and Bloch oscillation in a optical lattice[3] to make use of the advantage of low scattering rate for Strontium atoms.

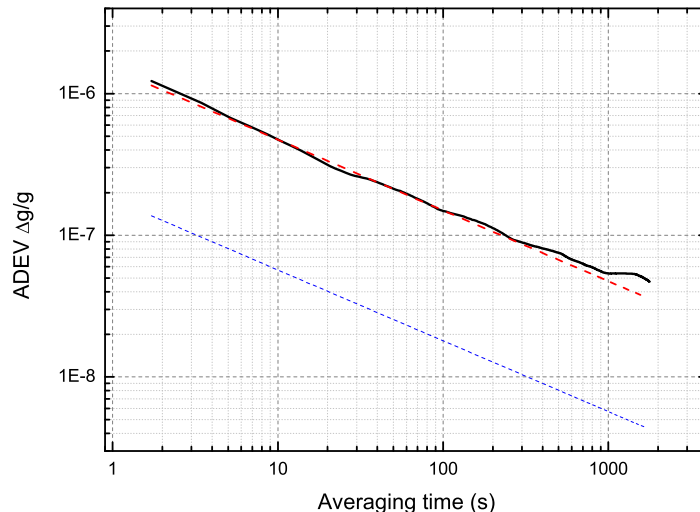


Figure 1: Allan deviation of the gravity acceleration measurement for a 1^{st} order Bragg interferometer with an interrogation time $T = 30$ ms (black straight line). Estimation of the residual acceleration noise of the retro-reflection mirror (dashed red line), and of the optical phase noise of Bragg beams (dash blue line).

References

- [1] M. G. Tarallo *et al.*, Phys. Rev. Lett. **113**, 023005 (2014)
- [2] J. Hartwig *et al.*, arXiv:1503.01213v1 [physics.atom-ph] (2015)
- [3] R. Charrière *et al.*, Phys. Rev. A **85**, 013639 (2012).

Other

X-ray spectroscopy as a tool to enlighten the growth of Van der Waals nanoparticles in a supersonic jet

L. Bernard Carlsson¹, C. Prigent¹, S. Cervera¹, A. Lévy¹, E. Lamour¹, S. Macé¹, J.-P. Rozet¹, S. Steydli¹, M. Trassinelli¹, and D. Vernhet¹

¹Sorbonne Universités, UPMC, Institut des NanoSciences de Paris (INSP), CNRS-UMR 7588, F-75005 Paris, France

Presenting Author: dominique.vernhet@insp.jussieu.fr

Since many decades, studies of collision processes of electrons, photons and heavy particles interacting with matter (from gaseous to solid) are an important tool in physics to understand the internal structure of matter at atomic level (or at nanoscale) as well as at very short time scale (down to fs). For example, recently, pump-probe experiments with IR and XFEL photons allowed probing the morphological structure of an isolated Van der Waals cluster by time resolved imaging [1].

Taking advantage of x-ray spectroscopy, which acts also as a very short time probe, we have investigated the μs temporal structure of the cluster condensation in high-density rare gas expansion (supersonic beams). Briefly summarized, we have previously demonstrated that the x-ray emission allows to determine: i) the absolute total atomic density when the cluster jet is submitted to keV electron impact; ii) the relative cluster density profile when interacting with an intense IR femtosecond laser pulse; iii) and finally the free atom density when irradiated by slow highly charged ions.

These first experiments led to the determination of a high degree of condensation (close to 100 %) of the clusters in the supersonic beam when using a skimmer [2]. These results have also paved the way towards new questions: what is the temporal evolution of the thermodynamic growing of clusters? What is the saturation time, needed for having stationary flow conditions in the beam?, etc. To obtain deeper information on the growth of Van der Waals nanoparticles in a supersonic jet, we are performing new experiments with our set-up at the SIMPA facility (French acronym for “Highly Charged Ion facility in Paris”) using Ne^{9+} of 90 keV on argon.

Figure 1 shows a comparison of the temporal x-ray signal when the supersonic jet interacts with 10 keV electrons and Ne^{9+} ions for a backing pressure of around 20 bar upstream a conical nozzle with a 300 μm aperture diameter and using a skimmer of 500 μm . Clearly, the x-ray signal starts before with HCIs compared to electron impact. It is a clear signature of the high sensitivity of HCIs to probe very low free atomic density when the cluster begins growing, i.e. at a time scale that is not reachable with “traditional” techniques (like optical measurements). More systematic measurements are under progress and a complete set of results varying the cluster size will be presented. They will provide new insights on the thermodynamics of a supersonic beam and on the cluster formation.

References

- [1] T. Möller *et al.*, PRL **108** (2012) 245005
- [2] M. Trassinelli *et al.*, J.Phys. Conf. Ser. **388** (2012) 082009

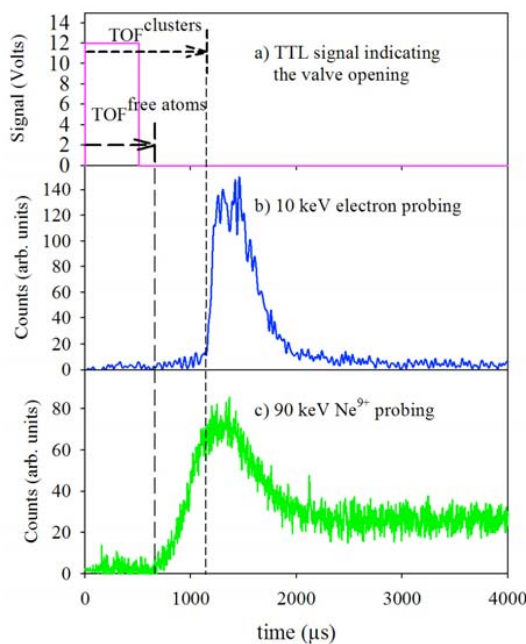


Figure 1: Preliminary results of temporal clusters' x-ray emission in case of b) 10 keV electrons and c) 90 keV Ne^{9+} ions

Vanadium Fine-Structure K-shell Electron Impact Ionization Cross Sections for Fast-Electron Diagnostic in Laser-Solid Experiments

P. Palmeri¹, P. Quinet^{1,2}, and D. Batani³

¹*Mécanique et Gravitation, Université de Mons – UMONS, B-7000 Mons, Belgium*

²*IPNAS, Université de Liège, B-4000 Liège, Belgium*

³*CELI, Université de Bordeaux, F-33400 Talence, France*

Presenting Author: patrick.palmeri@umons.ac.be

The K-shell electron impact ionization (EII) cross section, along with the K-shell fluorescence yield, is one of the key atomic parameters for fast-electron diagnostic in laser-solid experiments through the K-shell emission cross section. In addition, in a campaign dedicated to the modeling of the K lines of astrophysical interest [1], the K-shell fluorescence yields for the K-vacancy fine-structure atomic levels of all the vanadium isonuclear ions have been calculated.

In this study, the K-shell EII cross sections connecting the ground and the metastable levels of the parent vanadium ions to the daughter ions K-vacancy levels considered in Ref. [1] have been determined. The relativistic distorted-wave (DW) approximation implemented in the FAC atomic code has been used for the incident electron kinetic energies up to 20 times the K-shell threshold energies. Moreover, the resulting DW cross sections have been extrapolated at higher energies using the asymptotic behavior of the modified relativistic binary encounter Bethe model (MRBEB) of Guerra *et al.* [2] with the density-effect correction proposed by Davies *et al.* [3].

References

- [1] P. Palmeri *et al.* *Astron. Astrophys.* **543**, A44 (2012)
- [2] M. Guerra *et al.* *Int. J. Mass Spectrom.* **313**, 1 (2012)
- [3] J. R. Davies *et al.*, *Phys. Plasmas* **20**, 083118 (2013)

Semi-empirical studies of atomic transition probabilities, oscillator strengths and radiative lifetimes in Hf II

S. Bouazza¹, P. Quinet^{2,3}, and P. Palmeri³

¹LISM, E. A. 4695 Université de Reims-Champagne-Ardenne, UFR SEN, BP 1039, F-51687 Reims Cedex 2, France

²IPNAS, Université de Liège, B-4000 Liège, Belgium

³Mécanique et Gravitation, Université de Mons – UMONS, B-7000 Mons, Belgium

Presenting Author: patrick.palmeri@umons.ac.be

Over the past few years, laser induced fluorescence and Fourier Transform techniques have been applied to measure radiative lifetimes and branching fractions in Hf II in order to derive oscillator strengths and transition probabilities [1,2]. In the present work, we propose to compare for the first time these experimental data to computed values obtained by two different semi-empirical approaches, respectively based on a parametrization of the oscillator strengths [3] and on a pseudo-relativistic Hartree-Fock model [4] including core-polarization effects [5]. The overall agreement between all sets of data is found to be good. We furthermore give radial integrals of the main atomic transitions in this study: $\langle 5d6s6p|r^1|5d^26s \rangle = 0.1504$ (0.0064), $\langle 6s^26p|r^1|5d6s^2 \rangle = 1.299$ (0.012), $\langle 5d^26p|r^1|5d^26s \rangle = -0.298$ (0.013), $\langle 5d^26p|r^1|5d^3 \rangle = 2.025$ (0.027). Finally a new set of oscillator strengths and transition probabilities is reported for many transitions in Hf II.

References

- [1] M. Lundqvist *et al.* *Astron. Astrophys.* **450**, 407 (2006)
- [2] J. E. Lawler *et al.* *Astrophys. J. Suppl. Ser.* **169**, 120 (2007)
- [3] J. Ruczkowski, M. Elantkowska, J. Dembczynski *J. Quant. Spec. Radiat. Transf.* **145**, 20 (2014)
- [4] R. D. Cowan, *The Theory of Atomic Structure and Spectra* (University of California Press, Berkeley, 1981)
- [5] P. Quinet *et al.* *Mon. Not. R. Astr. Soc.* **307**, 934 (1999)

List of Authors

A

A Quinto, M., 111
Abola, A., 160
Adams, C. S., 59, 133
Aitelhadjali, Z., 111
Akulshin, A., 85
Ali Khan, M., 49
Alibert, J., 66
Allmendinger, F., 96
Almond, J. R., **42**
Alnis, J., **123, 160**
Alps, K., 135, 136, 140, 142
Amaro, P., 152
Amiryan, A., **107**
Andreeva, C., **64, 125**
Andreeva, Ch., 123, **124**
Andrijauskas, T., **65**
Aoki, M., 117
Aouchiche, H., 99
Apfelbeck, F., 45
Apsitis, A., 84
Araujo-Ferreira, A. G., 81
Arimondo, E., 68
Arndt, M., 55
Arnold, C., 36
Asvany, O., 20
Auccaise, R., **81**
Auzinsh, M., 83, 85, 105, 162

B

Böll, O., 90
Bäckström, E., 46
Bücking, T. M., 110
Bade, S., 78
Barillot, T., 88
Barinova, G., 147
Barker, P. F., 52, 54
Barontini, G., 114
Barr, I. J. M., 114
Barredo, D., **51**
Bartschat, K., 150
Basalaev, M. Yu., 124
Batani, D., 168
Bateman, J., 69
Baumann, T. M., 62
Baye, D., 93
Beilmann, C., 152
Bekker, H., 47, **126, 127**
Belov, N. A., **82**
Bengtsson, S., 37
Berengut, J., 139
Bernard Carlsson, L., 167
Bernitt, S., 110, 152
Berry, M., **14**
Berzins, A., **83, 162**
Berzins, U., 84

Beterov, I., 64
Bezuglov, N. N., 80
Bianchi, G., 108
Bielska, K., 144
Bilicki, S., 134
Bimbard, E., 59, 133
Birzniece, I., **128**
Björkhage, M., 46
Blackley, C. L., 50
Blagoev, K., 103
Blahins, J., **84**
Blaum, K., 32
Blessenohl, M. A., 47
Bloch, D., **30**
Blom, M., 46
Blondel, C., 33
Bober, M., 144
Bogans, E., 160
Bolpasi, V., 74
Bonagamba, T. J., 81
Bookjans, E., 134
Bordas, C., 88
Bouazza, S., **115, 163, 169**
Brünken, S., 20
Brazhnikov, D. V., 124
Breteau, D., **33**
Brice, I., 123
Browaeyns, A., 51, 53
Brune, M., 15
Buchauer, L. F., 110
Buchet, M.-A., 78
Budker, D., **21, 85, 162**
Bumby, J. S., 42
Burchianti, A., **48**
Busaite, L., **85**
Buyadzhi, V., **86, 154**
Bylicka, B., 29

C

Cabrera-Gutiérrez, C., 75
Calabrese, R., 108
Cantat-Moltrecht, T., 15
Capon, A., 43
Caradonna, P., 43
Carlström, S., **37**
Cartaleva, S., 105, 125
Caruso, F., 49
Cataliotti, F. S., 49
Catani, J., 70
Cebers, A., 162
Cederquist, H., 46
Celestrino Teixeira, R., 15
Cerchiarì, G., **129**
Cervera, S., 167
Champenois, C., 44, 101
Champion, C., 99, 111

Chaves de Souza Segundo, P., 30
 Cheinet, P., 68
 Chen, L.-L., 39
 Cherukattil, M. S., **49**
 Chervenkov, S., 131
 Chruściński, D., 29
 Cinins, A., 64
 Ciuryło, R., 144
 Clos, G., 28
 Cohen, S., **87, 88**
 Colombo, S., **60**
 Cornish, S. L., 50
 Corradi, L., 108
 Crespo López-Urrutia, J. R., 44, 47, 62, 110,
 126, 127, **152**
 Cui, J.-F., 164
 Cygan, A., 144
 Cyr, A., 38

D

Dörre, N., 55
 Dörfler, A., 161
 Décamps, B., **66**
 da Silva Jr., H., 161
 Dainelli, A., 108
 de Moraes Neto, G. D., 81
 de Aquino Carvalho, J. C., 30
 Del Aguila, R., 165
 Del Bino, L., 70
 Delande, D., 40
 Dembczyński, J., **130, 163**
 Deng, X.-B., **89**
 Diermaier, M., 43
 Dijck, E. A., **90**
 Dimitriou, A., 87
 Docenko, O., 136
 Dolgovskiy, V., 60
 Dong, G., **67**
 Dotsenko, I., 15
 Dousse, J.-Cl., 145
 Drag, C., 33
 Drewsen, M., 62
 Duan, X.-C., 39, 89, 164
 Ducloy, M., 30
 Dulieu, O., 73, 161
 Dunning, A., 69
 Dunseath, K. M., 38
 Dupré, P., 34
 Dutta, I., 57

E

Eberle, P., **161**
 Edmunds, P. D., **52**
 Efimov, D. K., **80**
 Ekers, A., 64
 Ekman, J., 94
 Elantkowska, M., 130, 163
 Enderlein, M., 28
 Engström, L., **103, 104**

Entin, V. M., 64, 124
 Erglis, K., 162

F

Fang, B., **57**
 Faoro, R., **68**
 Ferber, R., 83, 128, 135, 136, 140, 142, 162
 Ferlino, F., **19**
 Fescenko, I., **92, 123**
 Feuchtenbeiner, S., 62
 Fiedler, J., **100**
 Filippin, L., **93, 94**
 Fioretti, A., 70
 Fitch, N. J., 42
 Florko, T., 86
 Fonseca, P. Z. G., **54**
 Franke, K., 32
 Freegarde, T., **69**
 Fritzsche, S., 47, 94, 152
 Froese Fischer, Ch., 112
 Fujiwara, Y., 117
 Fukao, Y., 117
 Fyodorov, V., 160

G

Génévriez, M., **38, 149**
 Gabbanini, C., **70**
 Gahbauer, F., 83, 162
 Gaigalas, G., 112, 113
 Gantner, T., **131**
 Garrido Alzar, C. L., 57, **78**
 Gauguet, A., 66
 Gavare, Z., 160
 Gebert, F., 139
 Geiger, R., 57
 Germann, M., 27
 Geyer, P., 55
 Glöckner, R., 77
 Gleyzes, S., 15
 Glushkov, A., **95, 132, 154**
 Godefroid, M., 93, 94, 112
 Gogyan, A., 138
 Gorceix, O., 76
 Gozzini, S., 70
 Grasdijk, J. O., 90, **96**
 Greffet, J.-J., 53
 Gregory, P. D., 50
 Gregory, R., 69
 Gribakin, G. F., **97**
 Grier, A. T., 45, 90
 Grujić, Z. D., 60, **98**
 Grum-Grzhimailo, A. N., **150**
 Gryzlova, E. V., 150
 Guo, C., 36
 Guyomarc'h, D., 101

H

Häfner, S., 41
 Hakhumyan, G., 106, 137

Hamed, H. R., **155**
 Hansen, A. K., 62
 Hanstorp, D., 46, 84
 Harman, Z., 82
 Haroche, S., 15
 Harries, J., 110
 Harth, A., 36
 Hartman, H., 103, 104
 Haslinger, P., 55
 Hegi, G., 27
 Heil, W., 96
 Heip, J. C., 139
 Hermann-Avigliano, C., 15
 Heyl, C. M., 37
 Higaki, H., 34
 Higashi, Y., 117
 Higuchi, T., 32, 117
 Himsworth, M., 69
 Hinds, E. A., 42, 114
 Hoekstra, S., 90, 121
 Hole, O. M., 46
 Hollain, D., 47
 Horst, B., 34
 Hoszowska, J., 145
 Houssin, M., 101
 Hu, Z.-K., **39**, 47, 89, 164
 Hughes, I. G., 59, **133**
 Hutson, J. M., 50

I

Ibrügger, M., 77
 Ichimura, A., 109
 Ignatovich, S. M., 124
 Inuma, H., 117
 Ikedo, Y., 117
 Imadouchene, N., **99**
 Inguscio, M., 48, 70
 Ishida, K., 117
 Iwasaki, M., 117
 Iwata, G. Z., 45

J

Jönsson, P., 94, 112, 113
 Jacquy, M., 75
 Jahangir, M., 143
 Jarmola, A., 162
 Jastrzebski, W., 141
 Jennewein, S., 53
 Ji, Z., 50
 Joerg, H., **47**
 Jordan, E., 129
 Jungmann, K., 90, 96
 Jusko, P., 20
 Juzeliūnas, G., 65, 80, 155

K

Källberg, A., 46
 Köppinger, M. P., 50
 Kühn, S., 110

Kadono, R., 117
 Kalaitzis, P., 88
 Kalnins, U., 83
 Kamigaito, O., 117
 Kaminska, M., 46
 Kamsap, M. R., **101**
 Kanai, Y., 34
 Kanda, S., 117
 Karpuk, S., 96
 Kashcheyevs, V., 147
 Kasprzak, M., **58**
 Kato, D., 113
 Kawall, D., 117
 Kawamura, N., 117
 Kaziannis, S., 158
 Keaveney, J., **59**, 133
 Kellerbauer, A., 129
 Khanbekyan, A., 108, 138
 Khetselius, O., 86, 132
 Klincare, I., 136
 Klocans, J., **147**
 Knoop, M., 44, 101
 Koda, A., 117
 Kohnen, M., 62
 Kojima, K. M., 117
 Kolbinger, B., 43
 Konovalova, E. A., **102**
 Kosmidis, C., **158**
 Koss, P. A., 98
 Kowalczyk, P., 141
 Kozlov, M. G., **23**, 102, 118
 Krasteva, A., 125
 Krausse, H.-J., 96
 Krishnamurthy, R., 161
 Kruzins, A., **135**, **136**, 140, 142
 Kubo, K., 117
 Kuhnle, E. D., 41
 Kumar, A., 50
 Kuraptsev, A. S., **71**
 Kuroda, N., 34
 Kvasikova, A., 132
 Kwela, J., 115
 Kwong, C. C., **40**

L

L'Huillier, A., 37
 Löfgren, P., 46
 Lévy, A., 167
 Lépine, F., 88
 L'Huillier, A., 36
 Labuhn, H., 51
 Laburthe-Tolra, B., 76
 Lahaye, T., 51
 Laliotis, A., 30
 Lamour, E., 91, 167
 Landragin, A., 57, 78
 Larsen, E. W., 37
 Le Targat, R., 134
 Lebedev, V., 60

Leefer, N., 32, 85
 Lehner, S., 43
 Leibfried, D., 28
 Leopold, T., 62, 84
 Lepers, M., **73**
 Leroy, C., **105–107**
 Lien, Y.-H., 114
 Lim, J., 42
 Lisak, D., 144
 Lodewyck, J., **134**
 Loperetti, L., 145
 Lorek, E., **36**, 37
 Losquin, A., 36
 Lourette, S., 162
 Lovecchio, C., 49
 Lu, B., 50
 Lucioni, E., 70
 Lundberg, H., 103, 104
 Luo, Q., 39

M

Mårsell, E., 36
 Macé, S., 167
 Majewska, I., 45
 Malbrunot, C., 43
 Malcheva, G., 103
 Maniscalco, S., **29**
 Mannervik, S., **46**
 Maréchal, E., 76
 Marciniak, A., 88
 Marelic, J., **156**
 Marinelli, C., 108
 Mariotti, E., **108**
 Markovski, A., 64
 Marmugi, L., 108
 Mas, H., **74**
 Masłowski, P., 144
 Massiczek, O., 43
 Mathavan, S. C., 121
 Matsuda, Y., 32, 34, 117
 Maurin, I., 30
 Mauritsson, J., 36, 37
 Mavrogordatos, T., 54
 Mazzoni, T., 165
 McDonald, M., **45**
 McGuyer, B. H., 26, 45
 Meinema, C., 121
 Mibe, T., 117
 Micke, P., 62, **110**
 Miculis, K., **151**
 Mikkelsen, A., 36
 Millen, J., 54
 Miranda, M., 36
 Miyake, Y., 117
 Mizutani, T., 117
 Modugno, G., 70
 Mohanty, A., 90
 Molony, P. K., **50**
 Monteiro, T. S., 54

Mooser, A., **32**
 Morzyński, P., 144
 Moszynski, R., **26**, 45
 Moussa, M. H. Y., 81
 Movsisyan, M., 138
 Murtagh, D. J., 34

N

Nagahama, H., 32
 Nagamine, K., 117
 Nagata, Y., 34
 Najafian, K., 27
 Nakamura, M., **109**
 Nascimento, R. F., 46
 Nasyrov, K., 125
 nEDM collaboration, the, 58
 Neri, E., 48
 Nguyen, T. L., 15
 Nikolayeva, O., 128, 135
 Nilsson, H., 103, 104
 Nishiyama, K., 117
 Notermans, R. P. M. J. W., **61**
 Nuñez Portela, M., 90
 Nyman, R. A., 156

O

Offenhauser, A., 96
 Ogitsu, T., 117
 Okubo, T., 117
 Onderwater, C. J. G., 90
 Oubaziz, D., **111**

P

Pachucki, K., 35, 119
 Paleček, D., 37
 Palmeri, P., 103, **168**, **169**
 Pandey, S., 74
 Papadopoulou, Chr., 158
 Papoyan, A., **137**, **138**
 Pashayan-Leroy, Y., **105–107**
 Passerat de Silans, T., 30
 Patkóš, V., 116
 Pavlou, E., 88
 Pazyuk, E. A., 135, 136, 140–142
 Pedregosa, J., 62
 Pedregosa-Gutierrez, J., **44**, 101
 Pelevkin, A., 151
 Pelle, B., 68
 Pierrat, R., 40
 Piest, B., 62
 Piilo, J., 29
 Pillet, P., 68
 Pires, R., 41
 Poli, N., 165
 Ponomarenko, E., 132
 Potanina, E., **147**
 Poullos, K., 74
 Preclíková, J., 37
 Prehn, A., 77

Prepelitsa, G., 154
 Prigent, C., 91, 167
 Pruvost, L., **75**
 Pustelny, S., 85

Q

Quinet, P., 103, 168, 169
 Quint, W., 32

R

Radžiūtė, L., 113
 Radics, B., 34
 Raimond, J. M., **15**
 Ramillon, J.-M., 91
 Raoult, M., 161
 Ravets, S., 51
 Rehann, R. U., **143**
 Reinherd, P., 46
 Rempe, G., 77, 131
 Rengelink, R. J., 61
 Ricci, L., 108
 Roati, G., 48
 Robert-de-Saint-Vincent, M., **76**
 Robyr, J.-L., 134
 Rodewald, J., **55**
 Rohlén, J., 84
 Rosèn, S., 46
 Rozet, J.-P., 91, 167
 Ruauudel, J., 75
 Ruczkowski, J., 130, 163
 Ruth Le Sueur, C., 50
 Rutkis, J., 123
 Ryabtsev, I. I., 64, 124
 Rynkun, P., **112, 113**

S

Sabulsky, D. O., **114**
 Safronova, M. S., **17**
 Saito, N., 117
 Sakamoto, N., 117
 Salvi, L., 165
 Sargsyan, A., 105–107, 125, 133, 137
 Sarkisyan, D., 105–107, 125, 133, 137
 Sasaki, K., 117
 Sauer, B. E., 42
 Sauerzopf, C., 43
 Savoie, D., 57
 Schaetz, T., **28**
 Schafer, K. J., 37
 Scheel, S., 100
 Scheider, G., 32
 Schilder, N., 53
 Schlemmer, S., **20**
 Schmöger, L., 44, **62**
 Schmidt, H. T., 46
 Schmidt, P. O., 62, 110, 126, 127, 139
 Schmidt, U., 96
 Schupp, R., 126
 Schwarz, M., 62

Sezer, U., 55
 Shah, C., 47, **152**
 Shao, C.-G., 89
 Shi, C., **139**
 Shimomura, K., 117
 Shmavonyan, S., 138
 Siddiqui, I. A., 143
 Silberberg, Y., **18**
 Simon, M., **16**
 Simon, M. C., 43
 Simonsson, A., 46
 Skomorowski, W., 26, 45
 Smerzi, A., 48
 Smits, J., 162
 Smorra, C., 32
 Sobolev, Y., 96
 Sobolewski, L. M., 115
 Sokolov, I. M., 71
 Sortais, Y. R. P., **53**
 Spielman, I., 65
 Starik, A. M., 151
 Staroselskaya, E. I., 150
 Steinbrügge, R., 152
 Steydli, S., 91, 167
 Stolyarov, A. V., 135, 136, **140, 141, 142**
 Strasser, P., 117
 Sugano, M., 117
 Surzhykov, A., 47, 152
 Svärd, R., 36
 Svinarenko, A., 86
 Swann, A. R., 97
 Szczepkowski, J., 141

Š

Šimsa, D., **116**

T

Taichenachev, A. V., 124
 Tajima, M., **34, 117**
 Tamanis, M., 128, 135, 136, 140, **142**
 Tanaka, K. S., **117**
 Tarallo, M. G., 45
 Tarbutt, M. R., 42
 Tashenov, S., 47, **152**
 Terao-Dunseath, M., 38
 Ternovsky, V., 154
 Thomas, R. D., 46
 Tino, G. M., **22, 165**
 Titova, N. S., 151
 Tomassetti, L., 108
 Tomono, D., 117
 Tong, X., 27
 Tonoyan, A., 106, 107
 Torii, H. A., 34, 117
 Torikai, E., 117
 Toyoda, A., 117
 Trassinelli, M., 91, 167
 Tretyakov, D., 64
 Trombettoni, A., 48

Tukiainen, M., 29
Tullney, K., 96

U

Ubelis, A., 84, 151
Uddin, Z., 143
Ueno, K., 117
Ueno, Y., 117
Ulbricht, H., **56**
Ullrich, J., 62, 126, 127
Ulmanis, J., **41**
Ulmer, S., 32, 34
Urbain, X., 38, 149

V

Valappol, N., 90
Valtolina, G., 48
van den Berg, J. E., 121
Van Gorp, S., 34
Vanella, A., 108
Vassen, W., 61
Venzke, J., 150
Vernac, L., 76
Vernhet, D., **91**, **167**
Versolato, O. O., 62, 126, 127
Viaris de Lesegno, B., 75
Viatkina, A. V., **118**
von Klitzing, W., 74

W

Wójtewicz, S., 144
Walz, J., 32
Wan, Y., 139
Warring, U., 28
Weidemüller, M., 41
Weis, A., 60, 92, 98
Whiting, D. J., 59, 133
Widmann, E., **43**
Wienczek, A., **119**
Wilkowski, D., 40
Willitsch, S., **27**, 161
Willmann, L., 90, 96
Wilschut, H. W., 90
Wilson-Gordon, A. D., **105**
Windberger, A., 62, 126, 127
Windholz, L., 143
Wolf, F., 139
Wolf, M., 43
Wu, X., 131
Wyart, J.-F., 73

X

Khani, K., 48
Xiong, X., 164
Xu, Y.-Y., **164**

Y

Yakshina, E., 64
Yamamoto, A., 117

Yamazaki, Y., 32, 34
Yan, W., 78
Yang, T., 40
Yao, H.-B., 89, 164
Yoshida, M., 117
Yousif Al-Mulla, S. Y., **120**
Yudin, V. I., 124

Z

Zaccanti, M., 48
Zamastil, J., 116
Zapara, A., **121**
Zawada, M., **144**
Zeeshan, F., **145**
Zelevinsky, T., 26, 45
Zentile, M. A., 59, 133
Zeppenfeld, M., **77**, 131
Zhang, X., **165**
Zhou, M.-K., 39, 89, 164
Zientkiewicz, M., **35**
Zigmantas, D., 37
Zimmer, S., 96
Zmeskal, J., 43
Zuliani, A., 68

List of Participants

James Almond	CT-11	jra13@c.ac.uk
Janis Alnis	P-56, P-57	janis.alnis@lu.lv
Christina Andreeva	P-1, P-58, P-59	christina.andreeva@lu.lv
Tomas Andrijauskas	P-2	tomas.andrijauskas@tfai.vu.lt
Ruben Aucaise	P-15	raestrada@uepg.br
Marcis Auzins		marcis.auzins@lu.lv
Henri Bachau		bachau@celia.u-bordeaux1.fr
Daniel Barredo	CT-20	daniel.barredo@institutoptique.fr
Hendrik Bekker	P-60, P-61	bekker@mpi-hd.mpg.de
Nikolay Belov	P-16	belov@mpi-hd.mpg.de
Klaas Bergmann		bergmann@rhrk.uni-kl.de
Michael Berry	PL-1	asymptotico@bristol.ac.uk
Andris Berzins	P-17	andris.berzins@lu.lv
Uldis Berzins		uldis@micronic.se
Inese Birzniece	P-62	inese.birzniece@gmail.com
Jānis Blahins	P-18	JANIS_59@inbox.lv
Decamps Boris	P-3	decamps@irsamc.ups-tlse.fr
Dmitry Budker	PL-8	budker@berkeley.edu
Alessia Burchianti	CT-17	burchianti@lens.unifi.it
Laima Bušaite	P-19	laima.busaite@lu.lv
Vasily Buyadzhi	P-20, P-85	vbuyad@mail.ru
Stefanos Carlström	CT-6	stefanos.carlstrom@fysik.lth.se
Francesco Cataliotti		fsc@lens.unifi.it
Giovanni Cerchiari	P-63	giovanni@mpi-hd.mpg.de
Mohamed Shahid Cherukattil	CT-18	shahid@lens.unifi.it
Samuel Cohen	P-21, P-22	scohen@uoi.gr
Simone Colombo	CT-29	simone.colombo@unifr.ch
Andra Damberga		andra.damberga@lu.lv
Bloch Daniel	IT-5	daniel.bloch@univ-paris13.fr
Hennequin Daniel		daniel.hennequin@univ-lille1.fr
Breseau David	CT-2	david.breseau@u-psud.fr
Jerzy Dembczyński	P-64	jerzy.dembczynski@put.poznan.pl
Xiaobing Deng	P-23	xiaobingdeng@hust.edu.cn
Elwin Dijck	P-24	e.a.dijck@rug.nl
Vernhet Dominique	P-25, P-95	dominique.vernhet@insp.jussieu.fr
Guangjiong Dong	P-4	gj.dong@qq.com
Xiaochun Duan		duanxiaochun2011@hust.edu.cn
Pascal Eberle	P-90	p.eberle@unibas.ch
Peter Edmunds	CT-21	p.edmunds@ucl.ac.uk
Dmitry Efimov	P-14	dmitry.efimov@de29866.spb.edu
Mohamed Elnagar		ah.anani@yahoo.com
Bess Fang	CT-26	bess.fang@quantumlah.org
Riccardo Faoro	P-5	riccardo.faoro@u-psud.fr
Ruvins Ferber		ruvins.ferbers@lu.lv
Francesca Ferlaino	PL-6	francesca-ferlaino-group@uibk.ac.at
Ilja Fescenko	P-26	iliafes@gmail.com
Livio Filippin	P-27, P-28	lifilipp@ulb.ac.be
Robert Flack		r.flack@ucl.ac.uk
Tim Freearde	P-6	timf@soton.ac.uk
Carlo Gabbanini	P-7	carlo.gabbanini@ino.it
Florian Gahbauer	P-91	florian.gahbauer@lu.lv
Thomas Gantner	P-65	Thomas.Gantner@mpq.mpg.de
Carlos L. Garrido Alzar	P-87	carlos.garrido@obspm.fr

Matthieu Genevriez	CT-7, P-81	matthieu.genevriez@uclouvain.be
Dmitry Glazov		glazov.d.a@gmail.com
Aleksander Glushkov	P-29, P-66	dirac13@mail.ru
Olivier Grasdijk	P-30	j.o.grasdijk@rug.nl
Gleb Gribakin	P-31	g.gribakin@qub.ac.uk
Zoran Grujic	P-32	zoran.grujic@unifr.ch
Alexei Grum-Grzhimailo	P-82	algrgr1492@yahoo.com
Hamid Reza Hamedi	P-86	hamid.r.hamedi@gmail.com
Helm Hanspeter		helm@physik.uni-freiburg.de
Dag Hanstorp		dag.hanstorp@gu.se
Joerg Holger	CT-16	hjoerg@physi.uni-heidelberg.de
Zhong-Kun HU	CT-8	zkhu@hust.edu.cn
Ifan Hughes	P-67	i.g.hughes@durham.ac.uk
Noura Imadouchene	P-33	nora.imady@gmail.com
Raimond Jean-Michel	PL-2	jmr@lkb.ens.fr
Lodewck Jérôme	P-68	jerome.lodewyck@obsmp.fr
Fiedler Johannes	P-34	johannes.fiedler@uni-rostock.de
Muhamadou Kamaso		gingerly_809@hotmail.com
Marius Romuald Kamsap	P-35	marius.kamsap@univ-amu.fr
Malgorzata Kasprzak	CT-27	malgorzata.kasprzak@fys.kuleuven.be
James Keaveney	CT-28	james.keaveney@durham.ac.uk
Janis Klavins		jklavins@latnet.lv
Ilze Klincare		ilze.klincare@lu.lv
Jevgenijs Klocans	P-80	jevgenijsklocans@gmail.com
Elena Konovalova	P-36	lenaakonvalova@gmail.com
Artem Korobitsin		koroaa@mail.ru
Constantine Kosmidis	P-89	kkosmid@uoi.gr
Mikhail Kozlov	PL-10	mgk@mf1309.spb.edu
Artis Kruzins	P-69, P-70	artis.kruzins@fizmati.lv
Alexey Kuraptsev	P-8	aleksej-kurapcev@yandex.ru
Chang Chi Kwong	CT-9	kwon0009@e.ntu.edu.sg
Engström Lars	P-37, P-38	lars.engstrom@fysik.lth.se
Reinis Lazda		lazdareinis@gmail.com
Maxence Lepers	P-9	maxence.lepers@u-psud.fr
Claude Leroy	P-39, P-40, P-41	claudelero@u-bourgogne.fr
Eleonora Lorek	CT-5	eleonora.lorek@fysik.lth.se
Sabrina Maniscalco	IT-4	smanis@utu.fi
Sven Mannervik	CT-15	mannervik@fysik.su.se
Simon Marc	PL-3	marc.simon@upmc.fr
Jakov Marelic	P-88	jm3309@ic.ac.uk
Emilio Mariotti	P-42	mariotti@unisi.it
Hector Mas Peris	P-10	hector.mas@iesl.forth.gr
Nakamura Masato	P-43	mooming@phys.ge.cst.nihon-u.ac.jp
Mickey McDonald	CT-14	mpm2153@columbia.edu
Frans Meijer		frans.meijer@os.put.poznan.pl
Peter Micke	P-44	peter.micke@quantummetrology.de
Kaspars Miculis	P-83	michulis@latnet.lv
Peter Molony	CT-19	p.k.molony@dur.ac.uk
Vincenzo Monachello		vincenzo.monachello.14@ucl.ac.uk
Andreas Mooser	CT-1	andreas.mooser@cern.ch
Joel Morley		joel.morley.14@ucl.ac.uk
Robert Moszynski	IT-1	robert.moszynski@tiger.chem.uw.edu.pl
Artūrs Mozers		art.mozers@gmail.com
Remy Notermans	CT-30	r.p.m.j.w.notermans@vu.nl
Dahbia Oubaziz	P-45	oubaziz_dahbia@yahoo.fr

Patrick Palmeri	P-96, P-97	patrick.palmeri@umons.ac.be
Aram Papoyan	P-71, P-72	aram.papoyan@gmail.com
Nick Parker		nick.parker@ncl.ac.uk
Yevgenya Pashayan-Leroy		yevgenya.pashayan-leroy@u-bourgogne.fr
Jofre Pedregosa Gutierrez	CT-13	jofre.pedregosa@univ-amu.fr
Elina Potanina		elina.potanina@gmail.com
Serg Pozdneev		pozdneev@sci.lebedev.ru
Laurence Pruvost	P-11	laurence.pruvost@u-psud.fr
Martin Robert-de-Saint-Vincent	P-12	martin.rdsv@univ-paris13.fr
Jonas Rodewald	CT-24	jonas.rodewald@univie.ac.at
Pavel Rynkun	P-46, P-47	pavel.rynkun@tfai.vu.lt
Dylan Sabulsky	P-48	d.sabulsky@imperial.ac.uk
Bouazza Safa	P-49, P-92	safa.bouazza@univ-reims.fr
Marianna Safronova	PL-4	msafrono@udel.edu
Stephan Schlemmer	PL-7	schlemmer@ph1.uni-koeln.de
Lisa Schmöger	CT-31	lisa.schmoeger@mpi-hd.mpg.de
Chintan Shah	P-84	chintan@physi.uni-heidelberg.de
Chunyan Shi	P-73	chunyan.shi@quantummetrology.de
Yaron Silberberg	PL-5	yaron.silberberg@weizmann.ac.il
Vanessa Simon		vsimon@physi.uni-heidelberg.de
Daniel Simsa	P-50	simsadan@gmail.com
Janis Smits		smitsjanis@gmail.com
Ewa Stachowska		ewa.stachowska@put.poznan.pl
Andrey Stolyarov	P-74, P-75	avstol@gmail.com
Janis Stonis		Janis.Stonis@lu.lv
Minori Tajima	CT-3	minor.tajima@cern.ch
Maris Tamanis	P-76	maris.tamanis@lu.lv
Kazuo Tanaka	P-51	tanaka@kaduo.jp
Guglielmo M. Tino	PL-9	tino@fi.infn.it
Schaetz Tobias	IT-3	tobias.schaetz@physik.uni-freiburg.de
Hendrik Ulbricht	CT-25	h.ulbricht@soton.ac.uk
Juris Ulmanis	CT-10	ulmanis@physi.uni-heidelberg.de
Rizwan Ur Rehman	P-77	rizrehman@hotmail.com
Xavier Urbain		xavier.urbain@uclouvain.be
Anna Viatkina	P-52	anna.viatkine@gmail.com
Manuel Vogel		m.vogel@gsi.de
Antoine Weis		antoine.weis@unifr.ch
Roland Wester		ingeborg.rauter@uibk.ac.at
Eberhard Widmann	CT-12	eberhard.widmann@oeaw.ac.at
Albert Wienczek	P-53	albert.wienczek@fuw.edu.pl
Stefan Willitsch	IT-2	stefan.willitsch@unibas.ch
Arlene Wilson-Gordon		arlene.gordon@biu.ac.il
Yaoyao Xu	P-93	xuyaoyaoleo@hust.edu.cn
Samir Yousif Al-Mulla	P-54	samir.al-mulla@hb.se
Cem Yuçe		cyuce@anadolu.edu.tr
Sortais Yvan	CT-22	yvan.sortais@institutoptique.fr
Artem Zapara	P-55	a.zapara@rug.nl
Michal Zawada	P-78	zawada@fizyka.umk.pl
Faisal Zeeshan	P-79	faisal.zeeshan@unifr.ch
Martin Zeppenfeld	P-13	martin.zeppenfeld@mpq.mpg.de
Xian Zhang	P-94	zhang@lens.unifi.it
Min-Kang Zhou		zmk@hust.edu.cn
Magdalena Zientkiewicz	CT-4	magz@fuw.edu.pl
Piergiacomo Zucconi Galli Fonseca	CT-23	ucappzu@ucl.ac.uk

